REPUBLIC OF TÜRKİYE

ALTINBAŞ UNIVERSITY

Institute of Graduate Studies

Electrical and Computer Engineering

IS-OWC SYSTEM USING OFDM WITH HYBRID MDM-PDM INCORPORATING DWDM TOWARD TPBS DATE RATE BASED 5G (LEO-GEO) SATELLITE COMMUNICATION

Maan Muataz Abdulwahid ALMANTHOR

Doctor of Philosophy

Supervisor

Assoc. Prof. Dr. Sefer KURNAZ

İstanbul, 2024

IS-OWC SYSTEM USING OFDM WITH HYBRID MDM-PDM INCORPORATING DWDM TOWARD TPBS DATE RATE BASED 5G (LEO-GEO) SATELLITE COMMUNICATION

Maan Muataz Abdulwahid ALMANTHOR

Department of Electrical and Computer Engineering

Doctor of Philosophy

ALTINBAŞ UNIVERSITY

2024

The dissertation titled IS-OWC SYSTEM USING OFDM WITH HYBRID MDM-PDM INCORPORATING DWDM TOWARD TPBS DATE RATE BASED 5G (LEO-GEO) SATELLITE COMMUNICATION prepared by MAAN MUATAZ ABDULWAHID ALMANTHOR and submitted on 15/01/2024 has been **accepted unanimously** for the degree of Ph.D. in Electrical and Computer Engineering.

Assoc. Prof. Dr. Sefer KURNAZ

Supervisor

Thesis Defense Committee Members:

Assoc. Prof. Dr. Sefer KURNAZ	Department of Computer Engineering, Altınbaş University	_____
Asst. Prof. Dr. Abdullahi Abdu IBRAHIM	Department of Computer Engineering, Altınbaş University	_____
Asst. Prof. Dr. Serdar KARGIN	Department of Biomedical Engineering, Istanbul Arel University	_____
Asst. Prof. Dr. Oğuz KARAN	Department of Software Engineering, Altınbaş University	_____
Asst. Prof. Dr. Zeynep ALTAN	Department of Software Engineering, Istanbul Beykent University	_____

I hereby declare that this dissertation meets all format and submission requirements of a Ph.D. dissertation.

I hereby declare that all information presented in this graduation project has been obtained in full accordance with academic rules and ethical conduct. I also declare all unoriginal materials and conclusions have been cited in the text and all references mentioned in the Reference List have been cited in the text, and vice versa as required by the abovementioned rules and conduct.

Maan Muataz Abdulwahid ALMANTHOR

Signature

DEDICATION

I dedicate this dissertation to ….

To my father, my mother, and all those who helped and encouraged me, and to my family and friends. I have a special feeling of gratitude for my loving parents, whose words of encouragement and push for tenacity ring in my ears. My wife, who has never left my side and is very special, I am truly thankful for having you in my life. Finally, I dedicate this work to my second father and advisor, Dr. Sefer KURNAZ, for the kindness and white heart he had.

ABSTRACT

IS-OWC SYSTEM USING OFDM WITH HYBRID MDM-PDM INCORPORATING DWDM TOWARD TPBS DATE RATE BASED 5G (LEO-GEO) SATELLITE COMMUNICATION

ALMANTHOR, Maan Muataz Abdulwahid

Ph.D., Electrical and Computer Engineering, Altınbaş University,

Supervisor: Assoc. Prof. Dr. Sefer KURNAZ

Date: January/2024

Pages: 202

Long-distance transmission to handle Geostationary Earth Orbit (GEO)-based transmission and high data rates and enhancing the scalability of Pointing error (Pe) for Tx and Rx antennas are satellite communication difficulties. This thesis develops a new Intersatellite Optical Wireless Communication (Is-OWC) system employing hybrid division methods of Mode Division Multiplexing (MDM) with two Hermite-Gaussian modes (HG00 and HG01) and Polarization Division Multiplexing (PDM) with two polarizations. 5.12 Tbps, 48,000 km transmission, 8-channel system Results demonstrate reliable system performance over the planned distance and data rate, with an average log BER of (HG00 = -5.02 and HG01 = -5.32) for p1 and (HG00 = -4.83 and HG01 = -5.16) for p2 at 48,000 km, beyond the BER FEC threshold of -2.42. Distance-OSNR inverse relation the recommended system's OSNR tolerance was < 50.5 dB with Tx and Rx Pe of 1 mrad. When transmission distance rises, HG00's EVM parameter is bigger than HG01's due to maximum mode power. However, received power and distance implies a considerable receiver sensitivity at a Pe of 1 milliradian for both the Tx/Rx. A two-coding scheme DP-DQPSK system was built, examined, and compared to the specified system capacity to test the revolutionary system's reliability. OSNR varied by 3 dB for Rx Pe up to 2 mrad and 5 dB for higher pe values due to significant antenna misalignment. Up to 40,000 km, the technique works. Distance enabled Tx Pe up to 4 mrad. As Tx/Rx aperture diameters grow, geometrical losses and attenuation are eliminated, lowering expected channel log BER. The recommended method

discovered that 5 cm Tx diameter operated well up to 40,000 km, while 10 cm may enable specific channels reach the needed distance. 15 cm diameter works. 20 cm may increase system performance, but it needs a Tx/Rx diameter trade-off to minimize transmission losses. The recommended method transfers data up to 30,000 km with a 10 cm Rx diameter. 20 cm diameter transmission ranges to 40,000 km. 30 cm are appropriate for 48,000 km transmission. Thus, increasing the Rx aperture diameter above the Tx aperture diameter reduces geometrical losses and attenuation, which impact antenna gain.

Keywords: Inter Satellite Link, MDM, PDM, Pointing Error, Satellite Communication.

TABLE OF CONTENTS

Pages

ABSTRACT ..... **vi**

LIST OF TABLES ..... **xii**

LIST OF FIGURES ..... **xv**

ABBREVIATIONS ..... **xix**

1. INTRODUCTION **1**

1.1 MOTIVATION 1

1.2 EARLY HISTORY OF SATELLITE COMMUNICATIONS 2

1.3 OPTICAL WIRELESS COMMUNICATION (OWC) 8

1.4 SATELLITE COMMUNICATIONS 10

1.5 ELEMENTS OF SATELLITE COMMUNICATION SYSTEM 12

1.5.1 Space Segment 13

1.5.2 Ground Segment 14

1.6 SATELLITE ORBITS 15

1.6.1 Geostationary Earth Orbit (GEO) 16

1.6.2 Medium Earth Orbit (MEO) 18

1.6.3 Low Earth Orbit (LEO) 19

1.7 ADVANTAGES OF SATELLITE COMMUNICATION 22

1.8 FREQUENCY SELECTION OF SATELLITE COMMUNICATION 22

1.9 APPLICATIONS OF SATELLITE COMMUNICATIONS 23

1.10 PROBLEM STATEMENT 25

1.11 SIGNEFICNACE OF THIS STUDY 26

1.12 THESIS OBJECTIVES 27

1.13 THESIS OUTLINES 27

2. LITERATURE REVIEW **29**

3. METHODOLOGY **36**

3.1 INTRODUCTION 36

3.2 OPTISYSTEM PROGRAM 36
3.3 WAVELENGTH DIVISION MULTIPLEXING (WDM) 38
3.3.1 WDM Overview 38
3.3.2 Type of WDM 39
3.3.3 Components of The WDM System 40
3.4 ORTHOGONAL FREQUENCY DIVISION MULTIPLEXING (OFDM) 41
3.4.1 OFDM Overview 41
3.4.2 OFDM Principle 43
3.4.3 OFDM Advantages and Disadvantages 45
3.5 QUADRATURE AMPLITUDE MODULATION (QAM) 46
3.5.1 QAM Overview 46
3.5.2 QAM Concept of Work 48
3.5.3 QAM Advantage and Disadvantage 49
3.5.4 QAM Order Schemes 50
3.6 MODE DIVISION MULTIPLEXING (MDM) 51
3.6.1 MDM Overview 51
3.6.2 MDM Concept of Work 51
3.6.3 MDM Components 53
3.6.4 MDM Types 54
3.7 POLARIZATION DIVISION MULTIPLEXING (PDM) 57
3.8 THE PROPOSED SYSTEM 59
3.8.1 Transmitter Part (Tx) 59
3.8.2 OWC Transmission Part 68
3.8.3 Receiver Part (Rx) 69
3.9 METHODOLOGY OF THE PROPOSED SYSTEM 73
3.10ATMOSPHERIC EFFECTS ON OWC 77
3.10.1Atmospheric Attenuation 77
3.10.2 Misalignment Fading 78

3.11 STUDIED PARAMETERS 79
3.11.1 Bit Error Rate (BER) 79
3.11.2 Receiver Sensitivity 80
3.11.3 Optical Signal-to-Noise Ratio (OSNR) 81
3.11.4 Error Vector Magnitude (EVM) 82
3.12 APERTURE DIAMETER 84
3.13 ALTERNATIVE SYSTEM DESIGN 85
4. RESULTS AND DISCUSSIONS 88
4.1 INTRODUCTION 88
4.2 RESULTS BASED FIRST OBJECTIVE 88
4.2.1 Results Based Bit Error Rate (BER) 88
4.2.2 Results Based Min BER 92
4.2.3 Results Based OSNR 94
4.2.4 Results Based EVM 97
4.2.5 Results Based Received Power 100
4.2.6 Results Based Constellation Diagram 104
4.2.7 Results of Comparison with Alternative Satellite System 111
4.3 RESULTS BASED SECOND OBJECTIVE 119
4.3.1 Results-Based Rx Pointing Error 119
4.3.1.1 Log BER-based results 119
4.3.1.2 OSNR-based results 133
4.3.2 Results-Based Tx Pointing Error 141
4.3.2.1 Log BER-based results 141
4.3.2.2 OSNR-based results 151
4.4 RESULTS BASED THIRD OBJECTIVE 154
4.4.1 Results Based Tx Aperture Diameter 154
4.4.2 Results Based Rx Aperture Diameter 157
5. CONCLUSIONS 161

5.1 CONCLUSIONS BASED FIRST OBJECTIVE 161
5.2 CONCLUSIONS BASED SECOND OBJECTIVE 162
5.3 CONCLUSIONS BASED THIRD OBJECTIVE 162
5.4 FURURE WORK 163
REFERENCES 164
APPENDIX A 174
APPENDIX B 179
APPENDIX C 182
APPENDIX D 184

LIST OF TABLES

Pages

Table 1.1: Frequency Band Allocation For Satellite Communication 23

Table 2.1: Summarization Of The Literature Studies 33

Table 3.1: Comparison Between CWDM And DWDM..... 40

Table 3.2: Capacity Achieved By Different QAM Schemes..... 50

Table 3.3: Components Selected For The Tx Part Of The Proposed System 67

Table 3.4: Component Parameters For The OWC Part Of The Proposed System..... 68

Table 3.5: Components Selected For The Rx Part Of The Proposed System 72

Table 4.1: Log BER Results For The Proposed System With Polarization 1 (P1) 89

Table 4.2: Log BER Results For The Proposed System With Polarization 2 (P2) 90

Table 4.3: Averaged Log BER Vs. Different Distances For The Two Polarizations..... 92

Table 4.4: Min BER Results For The Proposed System With P1 93

Table 4.5: Min BER Results For The Proposed System With P2 93

Table 4.6: Averaged Min BER Vs. Different Distances For The Two Polarizations 94

Table 4.7: OSNR Values For Different Distances And The Two Polarizations 94

Table 4.8: EVM Values Obtained From System For The Two Modes Of P1 98

Table 4.9: EVM Values Obtained From System For The Two Modes Of P2 98

Table 4.10: Received Power Vs. Transmission Distances For P1 ……..100

Table 4.11: Received Power Vs. Different Transmission Distances For P2 ……..…...100

Table 4.12: Log BER Parameter Of DPSK Precoder Under Different Distance ……....112

Table 4.13: Log BER Parameter For Duobinary Precoder Under Different Distance …... 112

Table 4.14: Averaged Log BER For Two-Polarization System Using DPSK Precoder ….115

Table 4.15: Averaged Log BER For The Two-Polarization System Using Duobinary Precoder……..115

Table 4.16: Comparison Of Average Log BER Between The Two Proposed Systems.... 116

Table 4.17: Comparison Between The Performance Of The Proposed Is-OWC MDM-PDM System And Is-OWC DP-DQPSK System 117

Table 4.18: Log BER Vs. Rx Pe At Distance Of 10,000 Km 121

Table 4.19: Log BER Vs. Rx Pe At Distance Of 20,000 Km 123

Table 4.20: Log BER Vs. Rx Pe At Distance Of 30,000 Km 125

Table 4.21: Log BER Vs. Rx Pe At Distance Of 40,000 Km 127

Table 4.22: Log BER Vs. Rx Pe At Distance Of 48,000 Km 129

Table 4.23: Averaged Log BER Under Influence Of Pe And Transmission Distances…...131

Table 4.24: The Final Averaged Log BER Values Over Different Distances 132

Table 4.25: OSNR From Different Channels Vs. Different Rx Pe At Different Distances..133

Table 4.26: Log BER Vs. Different Tx Pe At 10,000 Km 142

Table 4.27: Log BER Vs. Different Tx Pe At 20,000 Km 143

Table 4.28: Log BER Vs. Different Tx Pe At 30,000 Km 144

Table 4.29: Log BER Vs. Different Tx Pe At 40,000 Km 145

Table 4.30: Log BER Vs. Different Tx Pe At 48,000 Km 146

Table 4.31: Averaged Log BER Vs. Different Tx Pe And Transmission Distances..... 150

Table 4.32: Total Averaged Log BER Vs. Tx Pe And Transmission Distances..... 151

Table 4.33: OSNR From Different Channels Vs. Tx Pe At Different Distances..... 152

Table 4.34: Log BER Values At Tx Aperture Diameter Of 5 Cm 155

Table 4.35: Log BER Values At Tx Aperture Diameter Of 10 Cm 156

Table 4.36: Log BER Values At Tx Aperture Diameter Of 15 Cm 156

Table 4.37: Log BER Values At Tx Aperture Diameter Of 20 Cm 157

Table 4.38: Averaged Log BER At Various Tx Aperture Diameters 157

Table 4.39: Log BER Values At Rx Aperture Diameter Of 30 Cm..... 159

Table 4.40: Log BER Values At Rx Aperture Diameter Of 20 Cm 159

Table 4.41: Log BER Values At Rx Aperture Diameter Of 10 Cm 160

Table 4.42: Averaged Log BER At Various Rx Aperture Diameters 160

LIST OF FIGURES

Pages

Figure 1.1: Classification Of The Electromagnetic Spectrum [27] 9

Figure 1.2: Classification Of The OWC System [3] 10

Figure 1.3: General Concept Behind The Passive Satellite [28] 11

Figure 1.4: General Concept Behind The Active Satellite [28] 12

Figure 1.5: General Diagram Of Satellite Communications [28]..... 13

Figure 1.6: The Space Segment [28] 14

Figure 1.7: Ground Segment [28]..... 15

Figure 1.8: GEO Concept [29] 17

Figure 1.9: Galileo Constellation [29] 19

Figure 1.10: LEO Concept [29] 21

Figure 1.11 : Space Communication With Different Earth Orbits [29] 21

Figure 1.12: Applications Of Satellite Communications [34]..... 25

Figure 3.1: Optisystem General Methodology 37

Figure 3.2: Main Window Of The Optisystem Program 37

Figure 3.3: Spectrum Comparison Between The CWDM And DWDM [47]..... 39

Figure 3.4: The WDM System [50]..... 41

Figure 3.5: General Diagram Of The OFDM Transmitter [51]..... 42

Figure 3.6: Spectrum Modulation In The a) Single Carrier, b) Multiple Carriers With Guard Band, And c) OFDM Multiple Carriers [56] 43

Figure 3.7: Three Subcarriers With The OFDM Symbol [57] 44

Figure 3.8: 16 QAM Constellation Diagram [63] 47

Figure 3.9: Waveform Allocation For The 16 Combined Symbols Represented In The 16 QAM [63] 47

Figure 3.10: Internal Circuit Of The QAM Modulator [63] 48
Figure 3.11: Internal Circuit Of The QAM Demodulator [63] 49
Figure 3.12: MDM Principle For Multiple Stream Data [72]. 52
Figure 3.13: The Distribution Of Fields In MDM [73] 52
Figure 3.14: MDM Utilization In The Transmission System [73] 53
Figure 3.15: HG Mode Distribution Of Intensity [75] 55
Figure 3.16: LG Mode Distribution Of Intensity [79] 55
Figure 3.17: LG Mode Distribution Of Intensity [79] 56
Figure 3.18: PDM-Based System [82] 57
Figure 3.19: PDM With Dual Polarization [83] 59
Figure 3.20: The Overall Design Of The Proposed System 61
Figure 3.21: Schematic View Of The Proposed System 62
Figure 3.22: Subsystem Design Of The Tx Part Using Optisystem 64
Figure 3.23: A Schematic Design For The Tx Subsystem Of The Proposed System 65
Figure 3.24: Excited Modes Of HG a) Represent HG 00 And b) Represents HG 01 66
Figure 3.25: A Schematic Design For The Rx Subsystem Of The Proposed System 70
Figure 3.26: Subsystem Design Of The Rx Part Using Optisystem. 71
Figure 3.27: Flowchart Describing The Methodology Of The Proposed System 75
Figure 3.28: Demonstration Of Pointing Error In Satellite Communication [90] 78
Figure 3.29: OSNR From The Variation Of Optical Power And Frequency [97] 81
Figure 3.30: EVM Concept [98] 82
Figure 3.31: The Visualization Of EVM In IQ Plane [99] 83
Figure 3.32: Layout Design Of The Alternative DP-DQPSK 8 Channel System 87
Figure 4.1: Log BER Vs. Different Wavelengths For The Proposed System With P1 91
Figure 4.2: Log BER Vs. Different Wavelengths For The Proposed System With P2 91

Figure 4.3: Averaged Log BER Vs. Different Distances For The Two Polarizations 92

Figure 4.4: OSNR Vs. Different Transmission Distances For P1 95

Figure 4.5: OSNR Vs. Different Transmission Distances For P2 95

Figure 4.6: Log BER Vs. OSNR For Two Modes At A Distance a)10,000 Km, b) 20,000 Km, c) 30,000 Km, d) 40,000 Km, And e) 48,000 Km 96

Figure 4.7: EVM Vs. Wavelengths Of The Proposed System With Different Distances For a) HG00-P1, b) HG01-P1, c) HG00-P2, And d) HG01-P2 99

Figure 4.8: Received Power Vs. Different Distances For a) P1, And b) P2 101

Figure 4.9: Log BER Vs. Receiver Sensitivity For Two Modes At Distance Of a) 10,000 Km, b) 20,000 Km, c) 30,000 Km, d) 40,000 Km And e) 48,000 Km 102

Figure 4.10: EVM% Vs. Receiver Sensitivity For Two Modes At Distance Of a) 10,000 Km, b) 20,000 Km, c) 30,000 Km, d) 40,000 Km And e) 48,000 Km 103

Figure 4.11: Constellation Diagram For P1 And Two Modes Where: (Left) Before CE, (Middle) After CE, And (Right) After CPE 105

Figure 4.12: Constellation Diagram For P2 And Two Modes Where: (Left) Before CE, (Middle) After CE, And (Right) After CPE 108

Figure 4.13: Log BER Vs. Different Distances For DPSK Precoder a) P1 And b) P2 113

Figure 4.14: Log BER Vs. Different Distances For Duobinary Precoder a) P1 And b) P2..114

Figure 4.15: Average Log BER Vs. Different Satellite Systems And Distances ……..116

Figure 4.16: Log BER Vs. Rx Pe At 10,000 Km With a) HG00-P1, b) HG01-P1, c) HG00-P2, And d) HG01-P2 122

Figure 4.17: Log BER Vs. Rx Pe At 20,000 Km With a) HG00-P1, b) HG01-P1, c) HG00-P2, And d) HG01-P2 124

Figure 4.18: Log BER Vs. Rx Pe At 30,000 Km With a) HG00-P1, b) HG01-P1, c) HG00-P2, And d) HG01-P2 126

Figure 4.19: Log BER Vs. Rx Pe At 40,000 Km With a) HG00-P1, b) HG01-P1, c) HG00-P2, And d) HG01-P2 128

Figure 4.20: Log BER Vs. Rx Pe At 48,000 Km With a) HG00-P1, b) HG00-P2, c) HG01-P1, And d) HG01-P2 130

Figure 4.21: Averaged Log BER Vs. Different Pe For All Studied Distances 132

Figure 4.22: OSNR Vs. Wavelengths At Different Rx Pe For a) 10,000 Km, b) 20,000 Km, c) 30,000 Km, d) 40,000 Km, And e) 48,000 Km..... 135

Figure 4.23: Log BER Vs. OSNR With Different Rx Pe At 10,000 Km Distance..... 137

Figure 4.24: Log BER Vs. OSNR With Different Rx Pe At 20,000 Km Distance..... 137

Figure 4.25: Log BER Vs. OSNR With Different Rx Pe At 30,000 Km Distance..... 138

Figure 4.26: Log BER Vs. OSNR With Different Rx Pe At 40,000 Km Distance..... 138

Figure 4.27: Log BER Vs. OSNR With Different Rx Pe At 48,000 Km Distance..... 139

Figure 4.28: Average Log BER Vs. OSNR For Different Rx Pe..... 140

Figure 4.29: Log BER Vs. Different Tx Pe At 10,000 Km..... 147

Figure 4.30: Log BER Vs. Different Tx Pe At 20,000 Km..... 147

Figure 4.31: Log BER Vs. Different Tx Pe At 30,000 Km..... 148

Figure 4.32: Log BER Vs. Different Tx Pe At 40,000 Km..... 148

Figure 4.33: Log BER Vs. Different Tx Pe At 48,000 Km..... 149

Figure 4.34: Average Log BER Vs. OSNR For Different Tx Pe..... 153

ABBREVIATIONS

3G	:	Third Generation
4G	:	Fourth Generation
5G	:	Fifth Generation
AMI	:	Alternate Mark Inversion
AMPS	:	Advanced Mobile Phone System
AT&T	:	American Telephone and Telegraph Company
ATS-1	:	Applications Technology Satellite
BER	:	Bit Error Rate
BSS	:	Broadcast Satellite Service
CE	:	Channel Estimation
CPE	:	Carrier Phase Estimation
CDMA	:	Carrier Division Multiple Access
CTS	:	Communications Technology Satellite
CWDM	:	Coarse Wavelength Division Multiplexing
DMGD	:	Differential Modal Group Delay
DP-QPSK	:	Dual polarization Quadratic Phase Shift Keying
DSP	:	Digital Signal Processing
DWDM	:	Dense Wavelength Division Multiplexing
EVM	:	Error Vector Magnitude
EDFA	:	Erbium-Doped Fiber Amplifier
EPON	:	Ethernet PON
FoC	:	Fiber Over Copper

FSK	:	Frequency Shift Keying
FSO	:	Free Space Optic
FSS	:	Fixed Satellite Services
FTTB	:	Fiber To the Building
FTTH	:	Fiber To the Home
FMF	:	Few Mode Fiber
Gbps	:	Giga bit Per Second
GEO	:	Geostationary Earth Orbit
GO	:	Geostationary Orbit
GPON	:	Gigabit PON
GPS	:	Global Positioning System
GSM	:	Global System for Mobile Communication
GSO	:	Geosynchronous Orbit
GUI	:	Graphical User Interface
HG	:	Hermite Gaussian
HyG	:	Hypergeometric-Gaussian
ICI	:	Intercarrier Interference
IEEE	:	The Institute of Electrical and Electronics Engineers
IG	:	Ince-Gaussian
IM/DD	:	Intensity Modulation/Direct Detection
IoT	:	Internet of Things
IR	:	Infrared
ISI	:	Inter Symbol Interference
Is-OWC	:	Intersatellite Optical Wireless Communication

ITU	:	International Telecommunication Union
LEO	:	Low Earth Orbit
LG	:	Laguerre-Gaussian
LO	:	Local Oscillator
LoS	:	Line of Sight
MDM	:	Mode Division Multiplexing
MEO	:	Medium Earth orbit
M-MIMO	:	Massive Multiple Input Multiple Output
Mm-wave	:	Millimeter Wave
MZM	:	Mack Zandar Modulator
NASA	:	National Aeronautics and Space Administration
NGN	:	Next Generation Network
NGO	:	Non-Geostationary Orbit
NLoS	:	Non-Line of Sight
NRZ	:	Non-Return to Zero
OFDM	:	Orthogonal Frequency Division Multiplexing
OWC	:	Optical Wireless Communication
Pe	:	Pointing Error
P/S	:	Parallel to Serial
PDM	:	Polarization Division Multiplexing
P1	:	First Polarization
P2	:	Second Polarization
PON	:	Passive Optical Network
QAM	:	Quadratic Amplitude Modulation

QF	:	Quality Factor
RF	:	Radio Frequency
RFID	:	Radio Frequency Identifier
RZ	:	Return to Zero
S/P	:	Serial to Parallel
SCORE	:	Signal Communicating by Orbiting Relay Equipment
SCPC	:	Single Channel Per Carrier
SGN	:	Satellite News Gathering
SMUX	:	Spatial Multiplexer
SNR	:	Signal to Noise Ratio
TDM	:	Time Division Multiplexing
TT&C	:	Tracking, Telemetry, Command
TTC&M	:	Tracking, Telemetry, Command, and Monitoring
TWT	:	Traveling Wave Tube
UAVs	:	Unmanned Aerial Vehicles
US	:	United State
UV	:	Ultra Violate
UWB	:	Ultra-Wide Band
VB	:	Visual Basic
VHF	:	Very High Frequency
VL	:	Visible Light
VSATs	:	Very Small Aperture Terminal
WDM	:	Wavelength Division Multiplexing
Wi-Fi	:	Wireless Fidelity

WLAN : Wireless Local Area Networks

WiMAX : Worldwide Interoperability for Microwave Access

XGPON : Ten X Gigabit PON

1. INTRODUCTION

1.1 MOTIVATION

The Internet is undergoing rapid expansion due to the proliferation of several mobile apps that make heavy use of bandwidth on an unprecedented scale. One of the probable explanations for the rise is the Internet of Things (IoT) technologies that have introduced unprecedented revolutions in the number of devices in the network. A fundamental aspect of IoT is the pervasiveness of a wide range of devices, including mobile phones, sensors, actuators, and Radio-Frequency Identification (RFID) tags, amongst others. Using a one-of-a-kind addressing system, these entities are able to communicate with one another and collaborate with the entities in their immediate environment in order to achieve their shared objectives [1]. Since 2020, there has been a view that the Internet will be linked to billions of devices, with an average of six to seven devices per person [2]. The millimeter wave (mm-wave) and Massive Multiple-Input Multiple-Output (M-MIMO) antenna technologies are projected to be incorporated into the Fifth Generation (5G) wireless communication systems, which are promising solutions for supporting the enormous quantity of devices that are predicted. However, the transmission rates of Radio Frequency (RF)-based wireless mobile technologies are restricted to controlled RF spectrums because there is a finite amount of accessible RF spectrum. This is because of the proliferation of different cutting-edge wireless technologies and standards, such as WiMAX (IEEE 802.16), Ultra-Wide Band (UWB) (IEEE 802.15), Wireless Fidelity (Wi-Fi) (IEEE 802.11), iBurst (IEEE 802.20), and the cellular based Third Generation (3G) and Fourth Generation (4G) [3]. In addition, major improvements have been made in optical system capacity, network reach, and the ability to serve more customers as a result of the adoption of cutting-edge technology in optical communications. Passive Optical Network (PON) technologies, such as Gigabit PON (GPON), 10Gbps PON (XG-PON), and Ethernet PON (EPON), are one example of a broadband network based on optical fiber that provides useful solutions to communication problems by bringing services closer to customers. Fiber over Copper (FoC) and wireless LAN (WLAN) are two more types of network architecture. One of the most pressing problems today is how to cater to varying needs for services in order to set up adaptable and extensive networks. The Next Generation Network's (NGN) cost-effectiveness and expansive network coverage can only be realized via the convergence of wireless and optical

networks. By combining the flexibility of wireless networking with the bandwidth of optical infrastructure, NGN can more easily reach its capacity and efficiency targets. In addition, Optical Wireless Communication's (OWC) fast data transfer rates and expanded capacity make it an attractive technology for broadband network access. As a result, OWC is well-suited to meeting the low-cost, yet stringent bandwidth requirements of the many services and applications deployed over NGNs.

1.2 EARLY HISTORY OF SATELLITE COMMUNICATIONS

Scientists from several countries developed various space communication ideas due to breakthroughs in various scientific fields. Konstantin Tsiolkovsky (1857-1935) invented the Rocket Equation in 1879, which is still used to build rockets. He pioneered space flight science. He also described the first human-made satellite and identified a Geosynchronous Orbit (GSO). He gave no real-world instances of GSO. In 1923, German rocket scientist Hermann Oberth proposed that orbiting rocket crews might indicate distant earth locations using mirrors. Rocketeer Hermann Oberth. In 1928, Austrian physicist Hermann Noordung proposed a manned spaceship in Geostationary Orbit (GO). Russian scientists suggested reflecting TV pictures of moving spacecraft in 1937. George O. Smith wrote a series of essays for Astounding Science Fictions on Venus Equilateral in 1942 and 1943. This planet relayed communication between Venus Station and earth Station when the Sun blocked it. However, Arthur C. Clarke, an electrical engineer and science fiction writer, is credited for inventing satellite communications. Science fiction author Clarke [6-8].

The year 1945 offered a satellite communication technology overview. Clarke supported earth-orbiting space stations. These stations would act as repeaters to provide communication between any two places on the surface below. He calculated that if the space station's orbit had a radius of 42,000 Km, it would match the planet's axis rotation and seem stationary from any earthly position. He also suggested that three synchronous stations above the equator at 120 degrees apart may provide global communications coverage. The notion may become a one-billion-dollar communications company after additional examination. Clarke did not submit a patent application for what would become the most commercially successful invention of the 20th century because he felt satellites would not be technically and economically feasible until the 21st century [6-10].

The Soviet Union launched the first artificial satellite, Sputnik-1, in October 1957. National Aeronautics and Space Administration (NASA) launched the first geosynchronous satellite, SYNCOM, in 1963, realizing Clark's idea. Many technological breakthroughs and the practical realization of devices and systems during and after World War II made satellite communications possible. During the cold war, worldwide military rivalry pushed scientific and technological research and development to a considerably larger size and quicker speed than it would have been if employed for peaceful purposes. A communications satellite was put into earth orbit due to considerable interest from certain organizations and advances in other disciplines of science and technology [11,12].

Russia's International Geophysical Year project launched Sputnik-1 on October 4, 1957. Sputnik launched the space age and brought artificial satellites to the globe. Sputnik weighed 184 pounds in its 560-mile orbit. Two radio transmitters—20.005 MHz and 40.002 MHz—were installed. This spaceship was more than simply scientific and technical. It had a major psychological and political influence on the US, leading to technical rivalry with Russia, long-term space research planning, and NASA [13].

The US Air Force launched SCORE, short for "Signal Communicating by Orbiting Relay Equipment," into low orbit in December 1958. 160 by 1280 Km. SCORE pioneered artificial satellite communications. SCORE sent pre-recorded audio messages between earth stations via a time lag. President Eisenhower's SCORE-transmitted message to stations worldwide was the first hint of satellites' impact on point-to-point communications. The relay's uplink frequency was 150MHz and its downlink frequency was 108MHz. Its longest message lasted four minutes. SCORE ran on its batteries for 12 days before dying. The satellite descended 22 days after launch [13-15].

ECHO satellites 1 and 2, launched by NASA in August 1960 and January 1964, respectively, were the first of six passive communications relay evaluations. The following experiments used these satellites. ECHO satellites were gigantic, aluminized Mylar spheres that orbited the globe. They passively reflected signals from ground stations. They caught people's attention because they could be seen from earth with the naked eye under the right lighting conditions, usually shortly before sunrise or sunset. This contributed to their popularity. ECHO relays operated from 162 to 2390 MHz and needed enormous ground terminal

antennas with 10 kW transmit capabilities. These antennas typically measured 18 meters. ECHO 1 and 2 orbited for about 8 and 5 years, respectively [13-15].

The October 1960 COURIER mission investigated low-orbiting satellite store-and-forward and real-time capabilities. SCORE delayed repeater technology extended this mission. COURIER operated at 1.7 to 1.8 GHz for its downlink and 1.8 to 1.9 GHz for its uplink. The first artificial satellite powered by solar cells used solid-state components except for 2-watt power tubes. A command system issue ended the satellite's operations after 17 days [14,15].

WESTFORD was the second passive communications relay testing technique. The US Army successfully launched it in May 1963. WESTFORD consisted of small resonant copper dipoles spanning an orbital belt. Dipole reflectors reflected signals for communications. The relay frequency, 8350 MHz, scaled the dipole length. California and Massachusetts ground stations successfully transmitted voice and Frequency Shift Keying (FSK) up to 20 kbps. When the belt separated, the connection capacity dropped to less than 100 bps. Passive communications declined as active satellites developed rapidly, and ECHO and WESTFORD stopped passive technology trials [16]. NASA launched the first active wideband communications satellites, TELSTAR Satellites 1 and 2, for AT&T/Bell Telephone Laboratories in July 1962 and May 1963, respectively. These satellites were AT&T/Bell Telephone Laboratories. TELSTAR relayed analog FM communications, had a bandwidth of 50 MHz, and operated at 6.4 GHz uplink and 4.2 GHz downlink. These frequencies enabled the 6/4 GHz C-band, which provides most Fixed Satellite Services (FSS) worldwide. TELSTAR 1 transmitted multichannel telephone, telegraph, fax, and television transmissions to US and French stations until November 1962, when radiation from the Van Allen belt destroyed the command subsystem. TELSTAR 2, upgraded with radiation-resistant electronics and flown into a higher orbit to avoid the VanAllen belts, operated properly for two years [17-19].

In December 1962, RCA debuted RELAY 1, which operated for 14 months. RELAY has two redundant repeaters with one 25 MHz and two 2 MHz channels. Its 10-watt Traveling Wave Tube (TWT) output amplifier operated at uplink frequencies of 1725MHz and downlink frequencies of 4160MHz. US, Europe, and Japan successfully transmitted a lot of telephone and network television. RELAY 2, launched in January 1964, ran for 14 months like its predecessor. Satellites can reliably communicate, as shown by RELAY and

TELSTAR. They also proposed sharing frequencies without interference between satellite and terrestrial systems [17-21].

The first commercially functional synchronous communications satellite EARLYBIRD was renamed INTELSAT I. NASA launched INTELSAT's COMSAT-designed satellite in April 1965. The C-band communications subsystem included two 25MHz transponders with uplinks at 6.3 GHz and downlinks at 4.1 GHz. The architecture resembled SYNCOM 3. It could accommodate 240 voices or one television circuit in both directions. TWT output 6 watts. Commercial satellite communications began on June 28, 1965, when US-Europe operations began. INTELSAT III succeeded EARLYBIRD in August 1969 [19-22].

The first of NASA's successful satellites was Applications Technology Satellite (ATS-1). In December 1966, a second one demonstrated considerable satellite communications numbers. The ATS-1's electric despond antenna had an 18-decibel gain and 17-degree beamwidth. It used two 25MHz repeaters on C-band with an uplink of 6.3 GHz and a downlink of 4.1 GHz. ATS-1 delivered the first multiple access communications from synchronous orbit. ATS-1 tested satellite-based air-to-ground communications with 149 MHz uplink and 136 MHz downlink lines. ATS-1's high-resolution camera took the world's first orbital photos. ATS-1 provided Pacific basin Very High Frequency (VHF) communications until 1985 when the station retaining control was lost [17,18].

The ATS-3, launched in November 1967, also experimented in the C and VHF bands using multiple access communications and orbit control methods. The first system to do a 'cross-strap' operation at both C-band and VHF frequencies was the ATS-3. C-band might transmit VHF signals to the ground. ATS-3 took the first high-resolution colour photographs of the "blue marble" earth from a synchronous orbit. ATS-3, like ATS-1, offered public service VHF communications throughout the US and the Pacific Ocean for almost a decade [17]. This exceeds the system's designed lifespan.

The ATS-5 used the C-band communications subsystem of its predecessors but not the VHF band. Instead, it examined air-to-ground navigation and air traffic control communications using an L-band subsystem with uplink and downlink frequencies of 1650 MHz and 1550 MHz. ATS-5 carried a millimeter wave experiment package that provided propagation data on the impact of the atmosphere on earth-space communications at 31.65 GHz (uplink) and

15.3 GHz (downlink). The experiment package used a 31.65 GHz uplink and a 15.3 GHz downlink. The spin-stabilized ATS-1 and -3 spacecraft were replaced by the gravity gradient-stabilized ATS-5. The satellite was launched into synchronous orbit in August 1969, but its spin prevented the gravity stabilization boom from being deployed. After being spin-stabilized, ATS-5's satellite antennas circle around the earth every 860 milliseconds to view new regions. In this unexpected "pulsed" mode, most communications experiments were only partly effective. The 15.3 GHz millimeter wave experiment downlink worked following ground terminal receiver tweaks. Over a dozen US and Canadian stations obtained propagation data [12-19].

In November 1972, NASA launched Telsat Canada's ANIK A satellite. The first privately produced commercial communications satellite. Two more ANIK A orbited between April 1973 and May 1975. Hughes Aircraft Company's C-band satellites featured 12 36MHz-wide transponders. TV distribution, SCPC telephone, and data services were the main offerings. One beam spanned the northern US and Canada at 5 watts [21]. ANIK A's antenna plan was optimized for Canada, but it also covered the northern US, allowing US communications companies to lease its services for domestic operations before US satellites were operational. ANIK D satellites replaced ANIK A satellites in 1985 [21,22].

NASA's second-generation uses the Technology Satellite program's ATS-6 spacecraft advanced communications satellite technology and demonstrated new uses [21]. ATS-6 had a 9-meter deployable parabolic antenna, an earth-observing module, two sun-seeking solar arrays, and supporting components. It orbited around 94 degrees West for a year in May 1974. In July 1975, educational television experiments in India moved it to 35 degrees East longitude. After a year, it was moved again to 140 degrees west, where it participated in many experimental programs until 1979, when it was removed from synchronous orbit. Eight ATS-6 communications and propagation tests spanning 860 MHz to 30 GHz. ATS-6 communications subsystems have four receivers. These receivers were 1650MHz (L-band), 2253MHz (S-band), 5925–6425 (C-band), and 13/18 GHz (K-band). The transmitters utilized 860, 2063, 3953–4153, and 20/30 GHz frequencies. Cross-strapping at Intermediate Frequency (IF) between any receiver and any transmitter (excluding the 13/18 GHz receiver, which only worked with a 4150MHz transmitter) allowed the ATS-6 to support several communication modalities [22-24].

The Communications Technology Satellite (CTS) program, a collaboration between NASA and the Canadian Department of Communications, evaluated high-power satellite technology for Ku-band Broadcast Satellite Service (BSS) applications. NASA used a TWT on CTS at 12 GHz and 200 watts to receive TV and two-way talk with ground terminal antennas as small as 120 cm [13-19]. In addition, a propagation beacon operating at 11.7 GHz was added, and 36-month propagation data was collected for many US locations [22-25]. From January 1976 through November 1979, the CTS conducted significant experimental testing and demonstrations in the US and Canada [13].

Due to the steep decline in satellite technology and service prices, terrestrial satellite communications (satellites within a country) were introduced in the 1970s. Regional satellite communications were initially conceivable using 1970s technology. These communications featured antennal coverage zones spanning many adjacent countries with comparable communications interests. New satellite services and participants began in the 1980s. About 100 nations offered satellite systems or services. Lease/buy alternatives, private networks, Very Small Aperture Terminal (VSATs), and private launch services were also introduced this decade to finance pricey satellite systems and services. Satellite-based mobile and personal communications started in the 1990s. During this time, higher RF was used to manage rising data rates as capacity in lower assigned frequency bands reached saturation. "Smart satellites" permitted on-board processing and other cutting-edge technology. The satellite became a major communications processing center in the sky from a data relay. Mobile cellular satellite communications networks and direct-to-home video and audio transmission have emerged quickly in the new century. Communications satellites often employ the GSO. Low-orbit non-GSO networks are taking over, especially for global cellular mobile communications [13-22].

Satellite communications have grown rapidly to new industries and applications that make use of satellite connections and provide cost-effective alternatives to conventional telecommunications transmission. To maximize satellite connection benefits, this expansion has occurred.

1.3 OPTICAL WIRELESS COMMUNICATION (OWC)

The OWC can possibly be an innovation that is either an option for or an enhancement to the current remote RF arrangements. For instance, OWC gear that works in the 350–1550 nm frequency district can give a high information speed of around 30 GB/s. Due to this advantage, it is an engaging choice for managing the predominant "last mile" and "last leg" challenges in the entrance organization. Moreover, the reusing of assets is a fundamental essential for portable correspondence frameworks to expand the organization's ability and work on its inclusion. This model might be fulfilled by OWC innovation through the joining of spatial varieties [13, 23]. The OWC association might be of various setups, for example,

a. Line of Sight (LoS)
b. Non-Line of Sight (NLoS)
c. Diffuse
d. Quasi diffuses.
e. Multispot LoS

The LoS connections are the ones with the greatest data speeds, the lowest Bit Error Rate (BER) performance, and the least complicated protocol out of these many setups. Because of these advantages, LoS links are the most popular arrangement for use in outdoor applications. Despite this, the most significant drawbacks of the LoS connection are its immobility and its susceptibility to obstruction. On the other hand, configurations with diffuse and nondirected LoS offer better mobility advantages and are less susceptible to shading. Nevertheless, path loss, noise, and multipath-induced dispersion significantly slow down the achievable data rate for high-speed links. The method known as Intensity Modulation/Direct Detection, or (IM/DD) for short, is the one that is used the most often in OWC systems. In addition, the use of coherent schemes is another option for increasing channel use. While the implementation of a coherent strategy could significantly improve system performance, doing so might also contribute to an increase in system complexity. This may be explained by the fact that accurate wave-front matching between the incoming signal and the Local Oscillator (LO) is essential to ensure that efficient coherent reception is achieved. In addition, the usage of DD is not complex since it just requires low-cost transceiver components; unlike coherent systems, which need intricate high-frequency

circuit designs, DD does not require these kinds of designs [23-26]. Research interests in the OWC system as a potential option to cater to the network needs in cost-effective ways have been developing over the last several years. Indoor and outdoor optical wireless communications are the two categories that make up the OWC umbrella term. The infinite bandwidth given by the OWC can be ascribed to several bands such as Infrared (IR), Visible Light (VL), and Ultra Violate (UV) being utilized for communication reasons [27]. The electromagnetic spectrum is broken down into its constituent parts as shown in Figure 1.1.

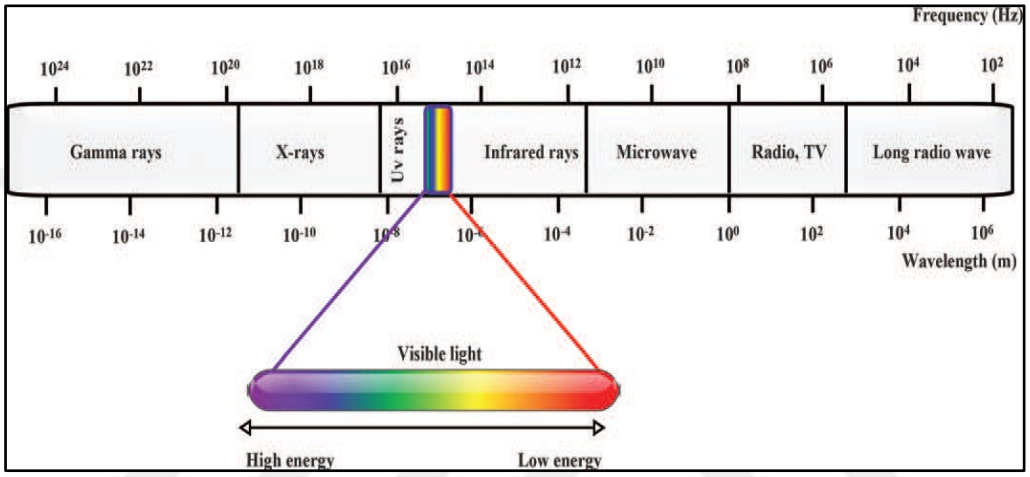

Figure 1.1: Classification Of The Electromagnetic Spectrum [27].

In addition to this, the spectrum illustrates the frequency and wavelength ranges that are now being occupied by the bands in OWC. For a wireless connection within the building, the OWC makes use of infrared or visible-light technology. It is of utmost significance, in circumstances in which there is a low possibility of providing network access via physically connected connections. In addition, the indoor OWC systems can be arranged into one of four primary configurations, including tracked, diffused, nondirected LoS, and directed LoS. In addition, the outdoor OWC makes use of an optical carrier to transmit data from one location to another through an unguided channel, which may be an atmosphere or open space. This channel may be any of these two locations. Therefore, another name for this OWC technology is a Free-Space Optical (FSO) communication system. The FSO communication systems function at frequencies in the near-infrared range and may be divided into two categories: terrestrial and space optical communications. These include building-to-building communications, satellite-to-ground communications, ground-to-satellite communications, satellite-to-satellite communications, and satellite-to-airborne

platform communications such as the Unmanned Aerial Vehicles (UAVs) [22-26]. The OWC system categorization may be seen shown as a tree diagram in Figure 1.2.

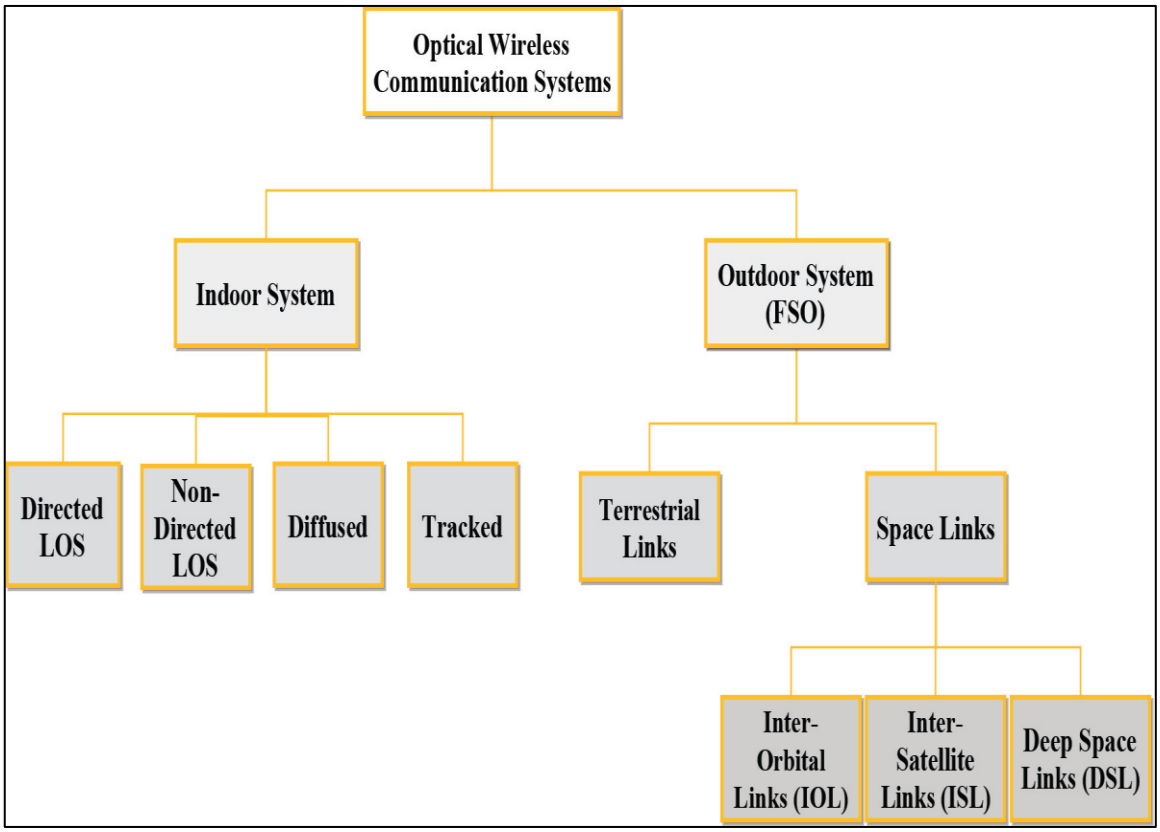

Figure 1.2: Classification Of The OWC System [3].

1.4 SATELLITE COMMUNICATIONS

The purpose of a communication satellite, an artificial satellite in Earth's orbit, is to receive communications signals transmitted from ground stations, amplify them, and potentially process them before sending them back to Earth. This allows one or more ground stations to receive the signals. The data sent via communications does not originate from or end at the satellite. In the same way as ground-based microwave relay towers facilitate communication, the satellite also acts as an active transmission relay. Both active and passive satellites were being considered as possible solutions for the purpose of creating long-distance communications in the early 1950s. On the other hand, active satellites have mainly replaced passive ones because of technological developments, even if passive ones were useful for communications [28,29].

The term "passive satellite" refers to a satellite that does nothing more than reflect signals sent from one earth station to another or from many earth stations to still others. It does neither modify nor amplify the electromagnetic energy that is incident on it, but rather it reflects it. It is unable to create electricity; rather, it only reflects the power that is already present. In August of 1960, NASA successfully launched the first artificial, passive satellite in their ECHO-I series. The notion of the overall view is demonstrated in Figure 1.3, which is behind the passive satellite concept.

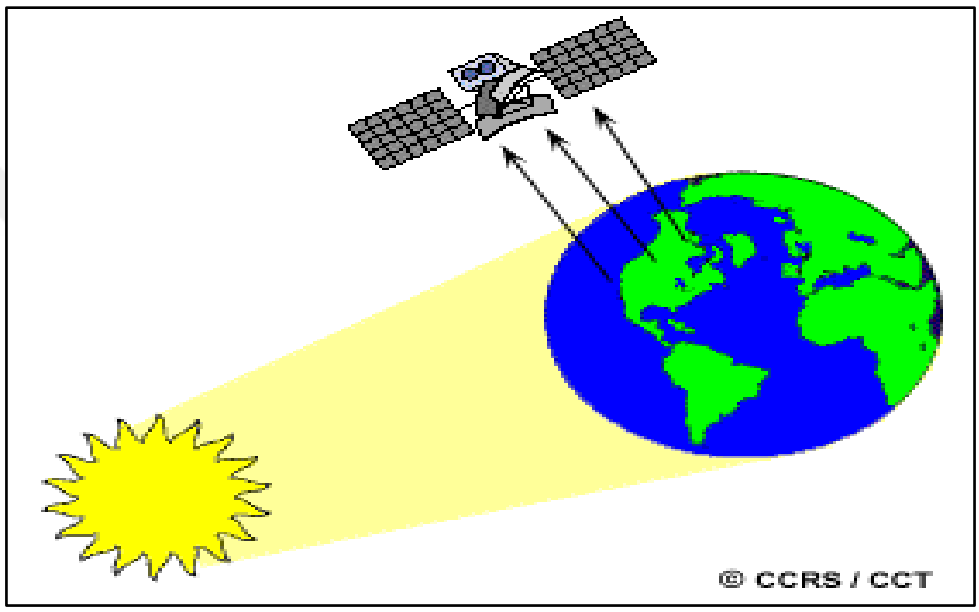

Figure 1.3: General Concept Behind The Passive Satellite [28].

A worldwide system would have required a huge number of passive satellites that were accessible randomly by different users. Control of satellites was not practicable from the ground. And lastly, one of the most significant issues was the significant loss of signal that occurred as a result of the long distance that the signal had to travel to get from the transmitter to the receiver through the satellite.

On the other hand, an active satellite processes the signal it receives from the earth by either amplifying or modifying it before retransmitting it. Satellites that are capable of transmitting electricity are referred to as active satellites. Have several benefits in comparison to passive satellites, such as the requirement of a lower-power earth station, the fact that they are not open to arbitrary usage, and the fact that they are directly controlled by operators from the ground [28-30]. The operation of such a satellite is depicted straightforwardly in Figure 1.4.

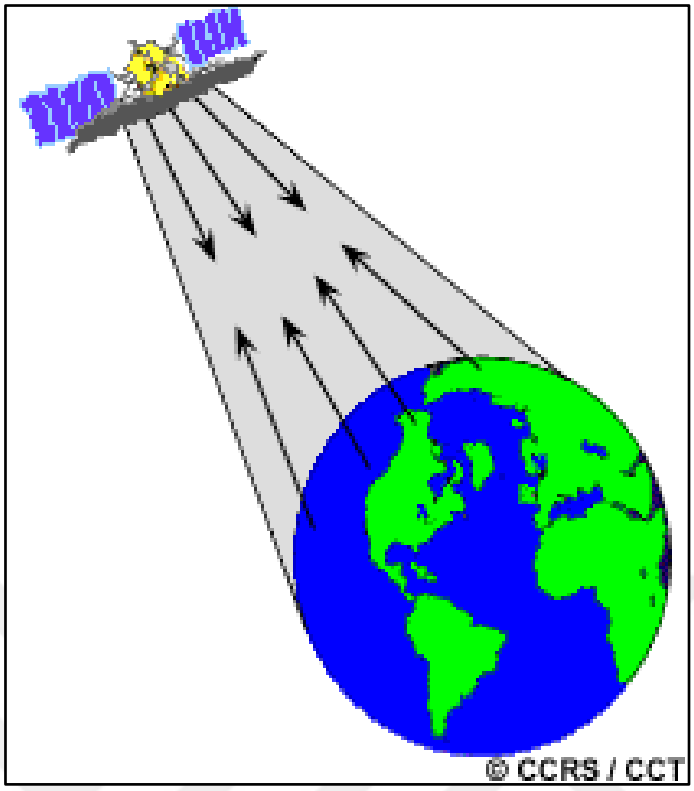

Figure 1.4: General Concept Behind The Active Satellite [28].

To launch greater satellites into orbit, however, requires rockets that are both larger and more powerful than those used for lighter satellites. This is one of the drawbacks of such a design. Another precondition for the necessary presence of an onboard power source. In addition to that, there was a disruption in service because of the malfunction of several electrical components.

1.5 ELEMENTS OF SATELLITE COMMUNICATION SYSTEM

The space segment and the ground (or earth) segment are the two portions or segments that make up the satellite communications section. These segments are respectively known as the space segment and the ground segment. These portions were divided according to the overarching principle of the satellite communication design, which may be seen in Figure 1.5.

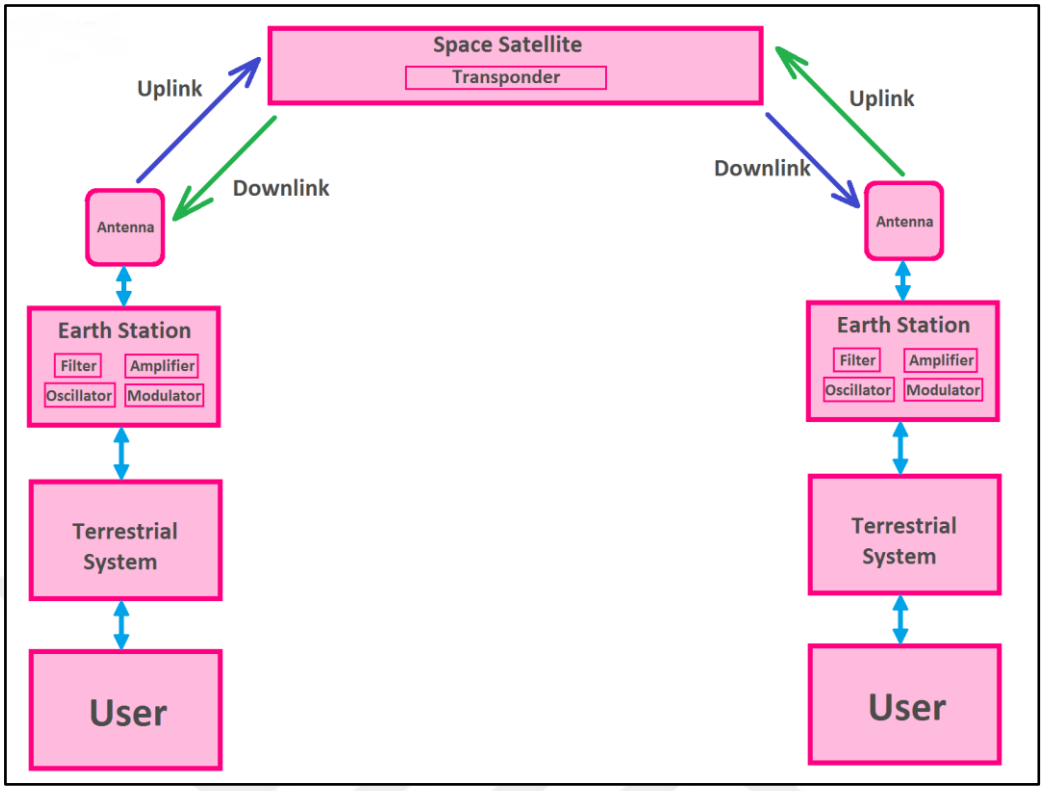

Figure 1.5: General Diagram Of Satellite Communications [28].

1.5.1 Space Segment

The space segment is the part of the system that is in outer space. The many components that make up the space segment of a communications satellite system are depicted in Figure 1.6. The satellite in orbit inside the system and the ground station that controls the operational aspects of the satellite in orbit make up what is known as the space segment of the system. The ground station is also known as the Tracking, Telemetry, Command (TT&C) station and the Tracking, Telemetry, Command, and Monitoring (TTC&M) station. Both names are used interchangeably. The TTC&M station is responsible for important spacecraft management and control activities, which ensure that the satellite can continue functioning normally while it is in orbit. In most cases, the user communications links and the TTC&M links that connect the spacecraft to the ground are kept distinct from one another. TTC&M connections may operate in the same frequency bands as other bands or in bands entirely different from those other bands. TTC&M is often carried out in a separate earth terminal facility that has been purpose-built to handle the complicated activities that are necessary to keep a spacecraft in orbit [30,31].

Figure 1.6: The Space Segments [28].

1.5.2 Ground Segment

In this segment, the terminals that are situated on the earth's surface and make use of the communications capabilities provided by the space segment are what make up the ground segment of the communications satellite system and as seen in Figure 1.7. The TTC&M ground stations are not considered part of the ground section. The ground segment terminals may be broken down into three primary categories, which are as follows [30,31]:

a. Fixed-based terminal.
b. Mobile-based terminal.
c. Transportable-based terminal.

Fixed terminals are built to allow users to access the satellite from a stationary position on the ground. They may offer a variety of services, but what sets them apart is the fact that they remain stationary during the communication process with the satellite. Fixed terminals include things like the VSATs that are used in private networks, as well as the terminals that are put on residential buildings and are used to receive broadcast satellite signals. Transportable terminals are intended to be mobile, but once they have been placed at their final destination, they are intended to stay stationary for the duration of the transmission process to the satellite. Satellite News Gathering (SGN) trucks are one example of a transportable terminal. These trucks go to different areas, halt in one spot, and then erect an

antenna to establish linkages with satellites. Meanwhile, the mobile terminals were developed specifically to maintain communication with a satellite even when the user is moving. They can be further classified as either land mobile, aeronautical mobile, or marine mobile, according to whether they are located on the earth's surface or near it [30,31].

Figure 1.7: Ground Segment [28].

1.6 SATELLITE ORBITS

The route that a satellite takes as it travels around the surface of a planet is known as its orbit. Orbits of satellites may be divided into two categories: Geostationary Orbit and Non-Geostationary Orbit, abbreviated as (GO) and (NGO) respectively. Because of the many problems that are associated with NGOs, their use was severely restricted. These disadvantages are indicated by the complicated difficulty of transmitting a signal from one satellite to another, the shorter estimated lifespan of satellites at NGOs, and the requirement for more frequent satellite replacements compared to those in GO. On the other hand, there is only one GO that can be achieved around the planet when playing GO, and it lies on the plane that is perpendicular to the equator. The speed of the satellite's orbit around the planet is equal to the speed at which the earth spins on its axis. Because of this, GO possesses several benefits, the most notable of which are the ease with which ground stations may be tracked, the practically constant range, and the extremely tiny frequency change. On the other hand, GO, much like NGO, has several shortcomings, which are indicated by the transmission latency of the order of 250 milliseconds, the significant loss in free space, and

the absence of polar coverage. It is important to point out that a GSO can also take on the form of a geostationary orbit. A GSO can be any orbit, such as one with an elliptical route, that has a period that is equal to the period of the earth's rotation. On the other hand, a GO must be in a circular orbit that is also located above the equator to be considered geostationary. GO can be classified into three categories from the prospect of the height and far from the earth, these categories are listed and clarified as [28-31].

1.6.1 Geostationary Earth Orbit (GEO)

The orbital periods of GEO satellites are perfectly timed about the earth. When viewed from a steady location on earth, these satellites give the impression of being motionless. Because of the manner that these satellites are positioned in space, only three satellites are required to offer connectivity throughout the whole surface of the earth (that is, their footprint covers almost one-third of the earth). These satellites travel in a continuous circle because of their orbit. Three requirements must be met before satellites may achieve geostationary orbit. These satellites are expected to have a lifespan of fifteen years [28-31]. The GEO idea is shown here in Figure 1.8.

a. The satellite ought to be positioned at 35,786 km, which is about equivalent to 36,000 Km, above the surface of the globe.

b. These satellites are required to move at the same pace as the earth's rotation and in the same direction as the earth's motion, which is toward the east.

c. The angle of the satellite about the earth must be completely horizontal. When put into practice, a geostationary satellite is more accurately referred to as a geosynchronous satellite. This is because various causes cause these spacecrafts to deviate from the ideal geostationary condition which are:

d. The gravitational tug of both the sun and the moon causes these satellites to veer off course from their orbit. They have struggled during the length of time. (Because of their great distance from the surface of the earth, these satellites are completely unaffected by the gravitational pull of the earth.)

e. Because of the rotation of the earth, these satellites are subjected to centrifugal force, which causes them to depart from the orbit in which they were originally placed.

f. Because the earth is not shaped like a perfect circle, the speed of satellites has to be continuously adjusted by earth stations. In addition to their use in television and radio broadcasting, weather forecasting, and the operation of telephone networks, these satellites also serve as the backbones of the Internet.

There is a small Doppler shift when a satellite is placed in GEO, making it excellent for satellite transmission and other multipoint applications. Additionally, GEO satellites have a view of a given location that is uninterrupted during the day and night. Finally, the GEO satellite is located at a great distance from the globe, which enables it to cover a vast area—nearly a quarter of the surface of the world.

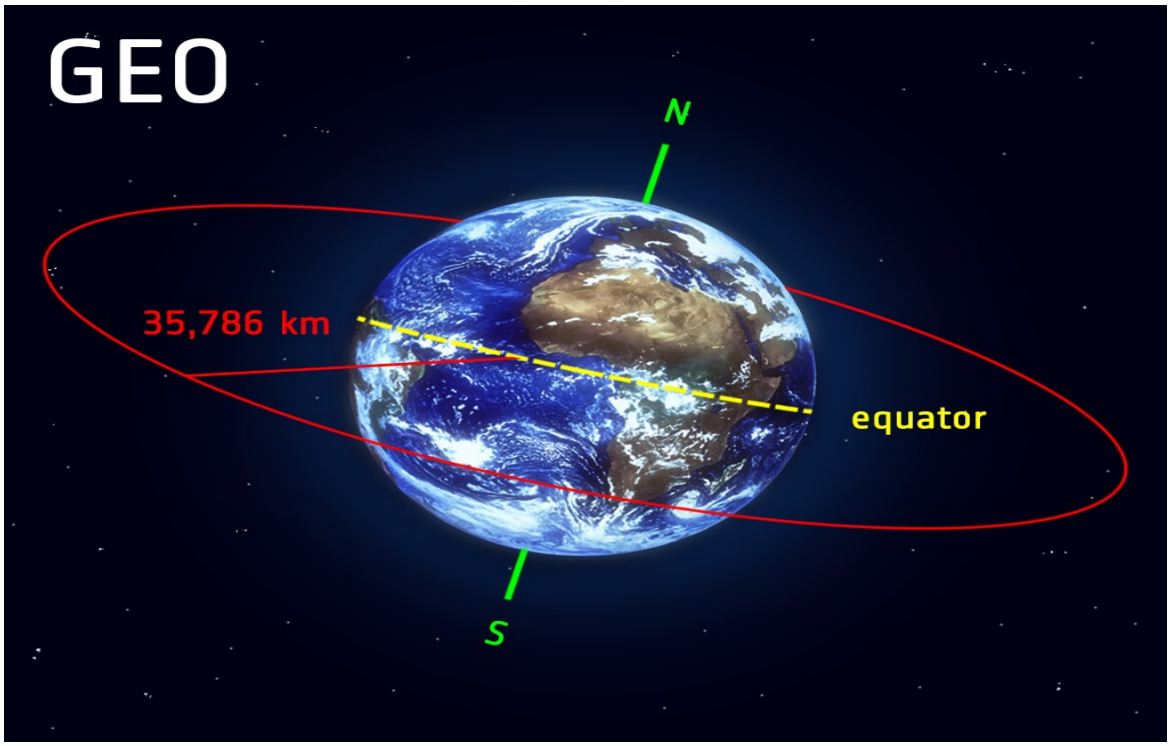

Figure 1.8: GEO Concept [29].

On the other side, GEO has a few drawbacks, which should include the following: Because of the low elevation above a latitude of 60 degrees, receiving signals from these satellites is more difficult in the polar areas of the earth (the poles). As a result, bigger antennas are required in this scenario. The towering structures in cities, along with the low elevation that comes with being further from the equator, cause shading of the signals. Because of the relatively high transmit power that is required, devices that are powered by batteries might run into issues. These satellites are not suitable for use with mobile phones of this size. The

high latency is the most significant challenge for voice and data communication since the signal must travel at least 72,000 Km without any handoffs, which is a significant distance. Either the frequencies will not be able to be utilized because of the vast footprint, or the GEO satellite will require specialized antennas that focus on a smaller region. It is an extremely costly endeavour to transfer a GEO into orbit [28-31].

1.6.2 Medium Earth Orbit (MEO)

MEOs may be placed in the middle between Low Earth Orbits (LEOs) and GEOs, not only in terms of their orbit but also in terms of the benefits and drawbacks that come along with them. The system only needs a dozen satellites since it uses orbits that are around 20,000 Km in diameter. This is more than a GEO system but far less than a LEO system. Because these satellites rotate more slowly in comparison to the earth, the system that controls them may be designed in a more straightforward manner (satellite periods are about six hours). It is possible for a MEO to cover greater populations, which would result in the need for fewer handovers if this were done.

On the other hand, the disadvantages carried from the MEO based satellite placement because of the greater distance to the earth, which causes the delay to rise to roughly 70–80 ms. To have a smaller footprint, the satellites require a higher transmit power and specialized antennas. Another consideration is that an MEO satellite's greater orbital altitude results in a longer time delay and a poorer signal than an LEO satellite does, although the MEO satellite's signal is not as degraded as that of a GEO satellite.

In the meanwhile, the fact that an MEO satellite has a longer length of visibility and a broader footprint than a LEO satellite implies that a MEO network requires fewer satellites than a LEO network does. It is utilized in a widespread manner by satellite navigation systems, such as the Galileo program in Europe. Galileo is the European satellite navigation system that drives navigation communications throughout the continent. It is used for a variety of navigational purposes, from tracking huge jumbo planes to providing navigational instructions to your smartphone. Galileo can give coverage across huge swaths of the earth at the same time because it is comprised of a constellation of many satellites. Figure 1.9 depicts the Galileo constellation for your viewing pleasure [28-31].

Figure 1.9: Galileo Constellation [29].

1.6.3 Low Earth Orbit (LEO)

These satellites have been positioned between (500 -1500) Km above the earth's surface. As a result of their lower orbital altitude, LEOs have a significantly shorter duration than geostationary satellites, which range from (95 to 120) minutes. LEO systems work hard to achieve a high height at every location on earth so that they can provide a communication link of the highest possible quality. Around 10 minutes is the maximum amount of time that any given LEO satellite will be visible from Earth. Transmission rates of around 2,400 bps are sufficient for voice communication when modern compression techniques are utilized. Even mobile terminals equipped with omnidirectional antennas and transmitting power in the region of 1 watt can make use of the bandwidth made available by LEOs. The delay that is experienced by packets that are sent using an LEO is not very high (approx. 10 ms). The latency is equivalent to that of wired connections over large distances (about 5–10 ms). Because of their smaller footprints, LEOs allow for improved frequency reuse, which is conceptually similar to how cellular networks are designed. LEOs have the potential to deliver a significantly greater elevation in polar regions and, as a result, improved worldwide coverage. Primary applications for these satellites include remote sensing as well as the provision of mobile communication services (due to lower latency). The requirement for many satellites to provide worldwide coverage is the most significant shortcoming of the LEO concept.

There are a few different ideas that include fifty to two hundred or even more satellites in orbit. Due to the limited amount of time that one can see while they are at a high elevation, extra methods are required for connection handovers between the various satellites. Because of the large number of satellites and the rapid movement of those spacecraft, the whole satellite system has a high degree of complexity. Because to air drag and radiation from the inner Van Allen belt, the average lifespan of LEO objects is only approximately five to eight years. This is one of the main issues with LEOs. If each satellite had a lifespan of eight years and there were 48 of them, then every two months a new satellite would have to be launched. The reduced latency achieved with the use of a single LEO is just one aspect of the overall picture [28-31].

Other considerations include the requirement for the routing of data packets from satellite if a user desires to communicate with people all over the world. A GEO often does not require this kind of routing because of its huge footprint, which means that senders and recipients are most likely located inside the same footprint. The use of satellites in LEO comes with several potential drawbacks, the most significant of which are the requirements for a network of LEO satellites, which can be prohibitively expensive, and the necessity for LEO satellites to make up for Doppler shifts brought on by their own relative motion [28-31].

In addition, the drag caused by the atmosphere has an influence on LEO satellites, leading their orbits to degrade with time. In the meanwhile, a significant advantage of employing LEO satellites is that, in comparison to GEO satellites, they are closer to the ground, which results in increased signal strength and a reduced amount of time delay. This makes them more suitable for point-to-point communication [28-31].

Furthermore, LEO satellites have a more limited region of coverage, which leads to a lower capacity and more wasted bandwidth [28-31]. The concept of LEO can be seen in Figure 1.10, which shows the limited region that the satellite can cover because of its distance from the earth and the small footprint achieved from satellite placement in this region.

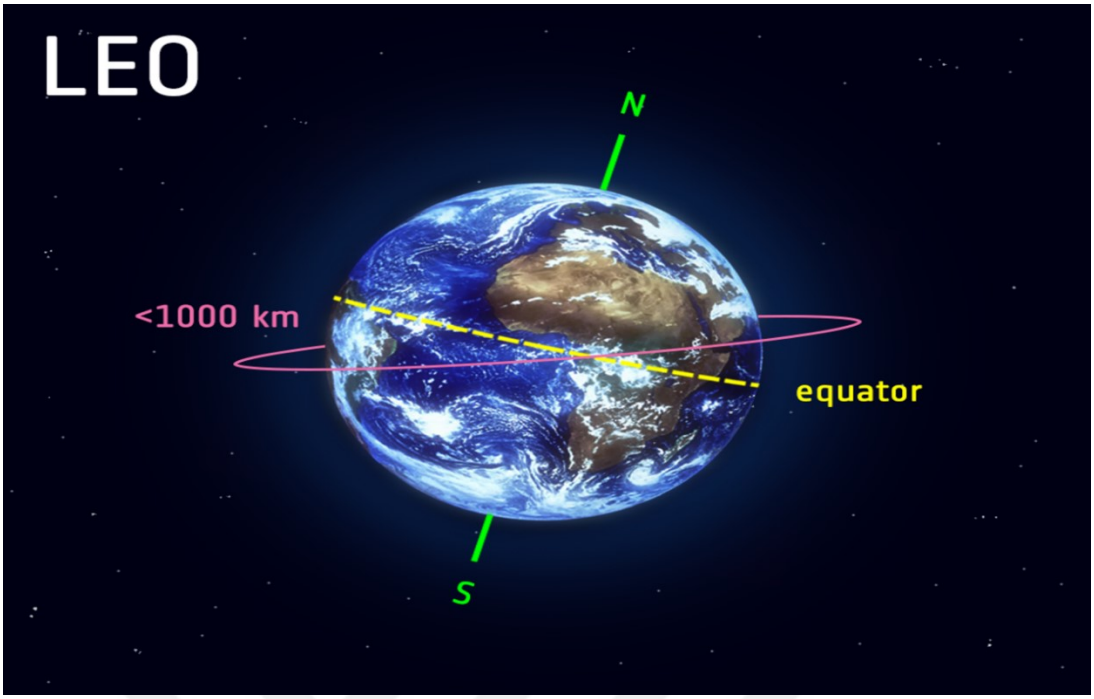

Figure 1.10: LEO Concept [29].

A summarization of optical space communication that includes the function of all the three mentioned earth orbits can be seen in Figure 1.11

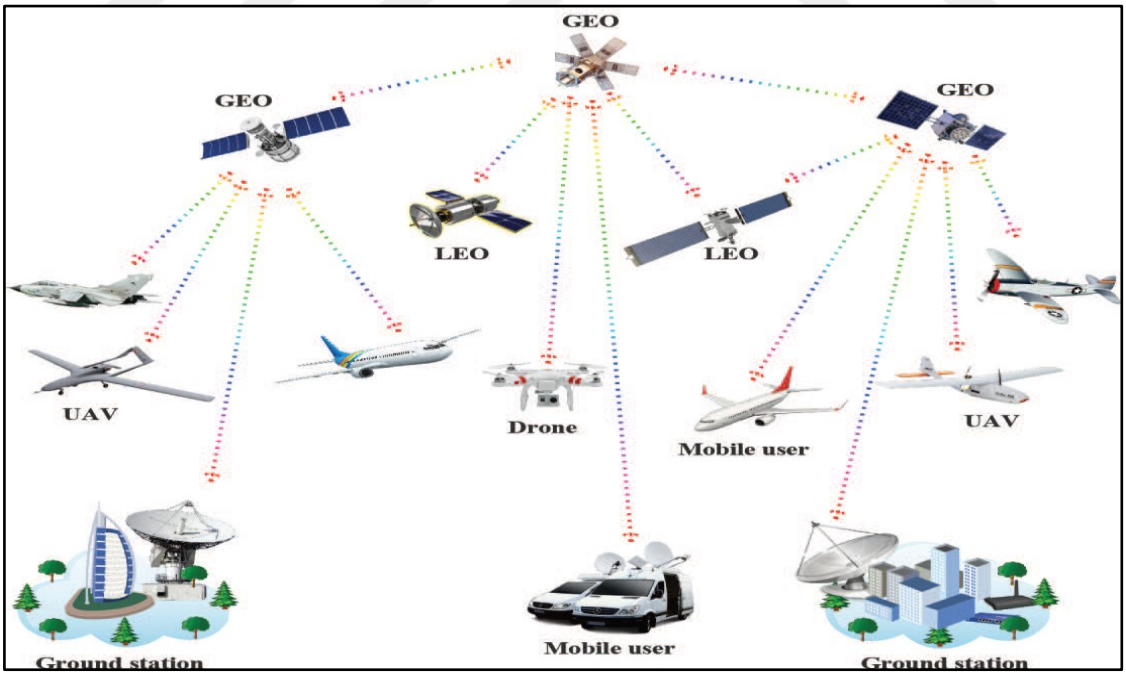

Figure 1.11: Space Communication With Different Earth Orbits [29].

1.7 ADVANTAGES OF SATELLITE COMMUNICATION

The significance behind using satellite communication is listed below [15, 16, 32, 33]

a. The geographical region that may be covered via satellite transmission is large, and this is especially true for locations that have a low population density.
b. A wide range of frequencies.
c. Applications for wireless and mobile communication may be simply set up using satellite communication regardless of location.
d. It can be used for a variety of things, including international mobile communication, private business networks, distant communication telephone distribution, weather forecasting, radio, and TV signal broadcasting, gathering military intelligence, guiding ships and aircraft, tying together remote regions, and distributing television, to name just a few.
e. The coding and decoding equipment is often responsible for providing security during the satellite transmission process.
f. It is straightforward to acquire service from a single source, and standardized assistance is readily available.
g. Because the installation and maintenance of satellite communication systems are simple and inexpensive, they offer the ideal solution.
h. If a serious situation arises, each earth station may be removed from its current position in a reasonably short amount of time and then reinstalled somewhere else.
i. Ground station locations are simple to set up and take care of.

1.8 FREQUENCY SELECTION OF SATELLITE COMMUNICATION

The process of allocating frequencies to satellite services is a complex one that involves collaboration and preparation on a global scale. The International Telecommunication Union (ITU) mandated that this practice be carried out. To carry out this frequency planning, the world has been split up into three distinct regions [28,29,33]:
Europe, Africa, and Mongolia make up the first region.
North and South America, as well as Greenland, make up the second region.
The portions of Asia that are not included in region 1 make up the third region, together with Australia and the south-west Pacific. The frequency bands are parcelled out to the numerous

satellite services that operate within these regions. Table 1.1 presents the frequency band assignments that have been made for the purpose of satellite communication.

This thesis will demonstrate the proposed novel Wavelength Division Multiplexing (WDM) Intersatellite Optical Wireless Communication (Is-OWC) system with a hybrid division multiplexing method based on the Ka-band of frequency. Because Ka-band-based satellite communication is a proven technology and can achieve high-speed service to customers beyond the reach of terrestrial networks. Also, several companies demonstrate a commercial satellite and use the Ka-band as a frequency allocation. Listing these companies has been mentioned as seen in Appendix A.

Table 1.1: Frequency Band Allocation For Satellite Communication.

Band	Frequency (GHz)	BW	Applications
L	2-1	1	MSS
S	2-4	2	MSS,NASA, Searching satellite
C	4-8	4	FSS
X	8-12.5	2.5	FSS
Ka	26.5-40	13.5	FSS

1.9 APPLICATIONS OF SATELLITE COMMUNICATIONS

a. Accurate Weather Predictions: Satellites were created for the express purpose of observing the climatic conditions of the globe. They keep a constant watch over the allotted regions of the planet and provide forecasts on the weather conditions in certain places. Taking pictures of the world from a satellite allows for the completion of this task. These photos are transmitted to the Earth station using the radio frequency that has been allotted to it. An earth station is a radio station that is situated on the surface of the planet and is responsible for transmitting signals received from satellites. These satellites monitor the changes in the earth's flora, sea status, ocean colour, and ice fields, and are extremely helpful in the prediction of natural disasters such as hurricanes [28,33].

b. Radio and Television Broadcasting: These specialized satellites are what is responsible for making hundreds of channels from all over the world accessible to people all over the

world. They are also in charge of broadcasting live matches, as well as news and services provided by radio stations all around the world. To receive these channels from these satellites, a dish of between 30 and 40 cm in diameter is required [28,33].

c. Military Satellites: These satellites are frequently employed for a variety of objectives, including the collecting of intelligence, serving as a communications satellite for military purposes, or even as a military weapon. By itself, a satellite does not belong to either the military or the civilian sphere. It is possible to determine whether it has a military or civilian purpose based on the type of payload that it transports [28,33].

d. Navigation Satellites: This technology enables accurate localization in any part of the world, and with the use of a few supplementary methods, the accuracy may go into the range of a few meters. Global Positioning System (GPS) is used in conjunction with other types of navigational systems to aid in the navigation of airplanes and ships. GPS receivers are now standard equipment in many newer automobiles. This technology may also be utilized, for instance, for the administration of truck fleets or for the geolocation of vehicles in the event that they are stolen [28,33].

e. Global Telephone: The construction of worldwide telephone backbones was one of the first applications of satellites for the purpose of communication. This was one of the first applications of satellites. It was often quicker to launch a new satellite as opposed to utilizing cables to transmit data. However, fiber optic cables are still replacing satellite communication over long distances. This is because, with fiber optic cables, light rather than radio frequency is utilized for transmission; as a result, the speed of the communication is significantly increased (and of course, reducing the delay caused due to the amount of distance a signal needs to travel before reaching the destination.). When using satellites, the signal needs to travel roughly 72,000 Km in order to reach a distance of around 10,000 Kms distant. This involves transmitting data from the ground to the satellite and then (mainly) from the satellite to another point on Earth. This results in a sizeable degree of latency, which is made more noticeable to consumers while they are on voice call [28,33].

f. Establishing Connections in Isolated Regions: In many parts of the world, including Antarctica, researchers, for example, do not have a direct wired connection to the telephone network or the internet. This may be since a country's infrastructure is not yet developed

enough, or it may be because of the location of the area. In this instance, the satellite offers comprehensive coverage, and (in most cases) there is at least one satellite that can always be seen beyond the horizon [28,33].

g. Worldwide Mobile Communication: The primary function of satellites in the context of mobile communication is to broaden the region that is covered by the network. The coverage area of cellular phone systems like AMPS and Global System for Mobile Communication (GSM) (as well as their descendants) does not extend to every portion of a country. The areas that are not covered often have a low population and are in places where it would be financially prohibitive to deploy base stations. However, due to the incorporation of satellite communication, a mobile phone user may now move between satellites and terrestrial networks, giving them access to global connections [28,33]. Figure 1.12, summarize the different aspect that uses of satellite communication.

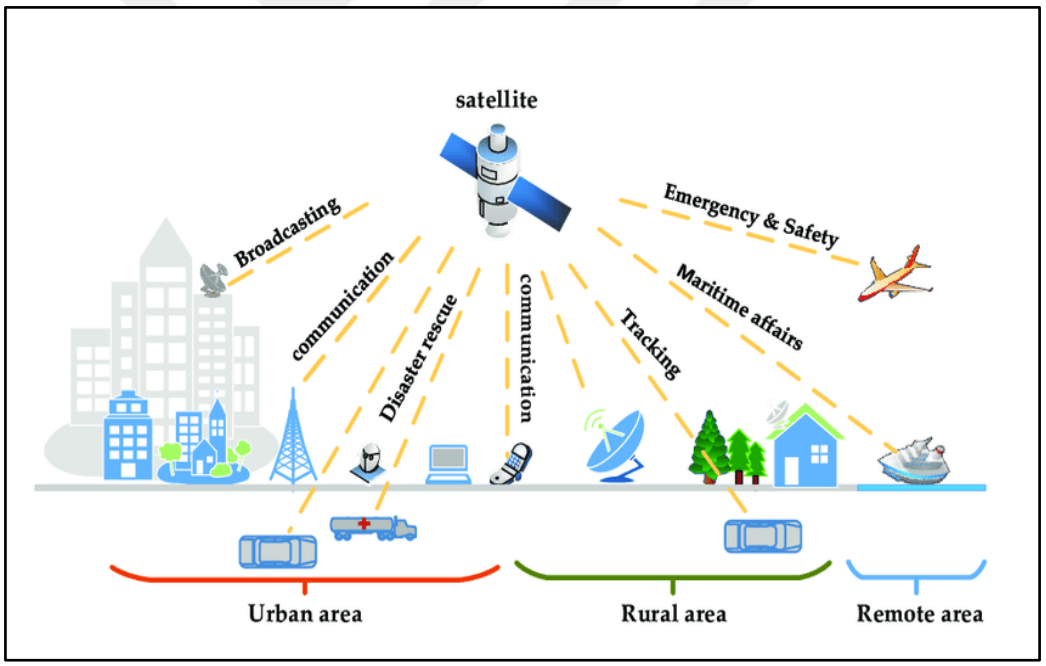

Figure 1.12: Applications Of Satellite Communications [34].

1.10 PROBLEM STATEMENT

The proliferation of artificial satellites can be attributed to the internet's contribution to a rise in the interconnectivity of global communications. People are more connected than they have ever been, and there are presently an estimated 35 billion devices that are part of the IoT. It is anticipated that this number would approach 50 billion devices by the year 2030. Satellites

have played an extremely important part in the advancement of this connectivity. There are many different types of satellites, and each one serves a specific purpose, such as data acquisition, research, telecommunications, safety, navigation, business insights, environmental monitoring, and defence. Only in the past couple of years has there been a significant rise in the number of satellites that have been launched. The primary objective of the satellite firms was to find a balance between the amount of data that could be acquired and the amount of distance that could be sent. As a direct consequence of this, the development of a revolutionary satellite system that is capable of dependable transmission and can reach GEO ranges was an essential component in the process of enhancing satellite communication fields. In addition, making use of the correct modulation format to accomplish a reliable system design might result in a greater data rate with fewer errors during transmission. This is a potential benefit. In addition, making use of contemporary mode approaches for profile intensity, such as Mode Division Multiplexing (MDM), was an additional topic that garnered a significant amount of attention in recent years. Therefore, developing a dependable system that can perform effectively for Tbps satellite communication was an essential issue that needed to be handled to suit future demands and applications based on 5G.

1.11 SIGNIFICANCE OF THIS STUDY

This thesis proposes to study the significance of using Orthogonal Frequency Division Multiplexing (OFDM) to design a novel higher data rate satellite system for the Is-OWC prospect, where OFDM uses many closely spaced orthogonal subcarriers that are transmitted in parallel to handle the large impact of data rate. Each subcarrier is modulated using 16 Quadratic Amplitude Modulation (16 QAM), a commonplace digital modulation method. Since the subchannels of OFDM are so tightly spaced, it is more resistant to electromagnetic interference and makes better use of the total available bandwidth. In addition to that, using hybrid trends of division multiplexing techniques of MDM and Polarization Division Multiplexing (PDM) was another important issue related to the proposed work which can make the major key for raising the transmission data rate, where in this thesis a novel methodology for combing these techniques will be proposed to achieve a reliable system with GEO based transmission distance, and with Tera bit data rate.

1.12 THESIS OBJECTIVES

The objectives of the proposed thesis can be listed below:

a. Design, model, and implement a spectrum efficient, high capacity, long-distance WDM Is-OWC system that uses the OFDM as a modulation technique and with novel utilization of hybrid division techniques of MDM and PDM. Which can increase the performance of the proposed system by using different modes and polarization.
b. Achieve higher data rate transmission reaching up to 5.12 Tbps at cost-effectiveness and lower complexity implementation for achieving advanced satellite functions.
c. Investigate the performance of the proposed system concerning different space turbulence represented by the pointing error (pe) for the transmitter (Tx) and the receiver (Rx) antenna to achieve the optimum reliability of the proposed system.
d. Investigate the impact of different antennas diameter for both the Tx and Rx sides of the proposed system to quantify with the system optimum requirements of antenna size for cost effectiveness and power consumption issues.

1.13 THESIS OUTLINE

The outline carried in this thesis are as follows:

a. Chapter one includes a general introduction related to the topics that the proposed thesis aims to cover that is clarified, and a brief history of satellite communication is explored from more than 50 years ago. After that, the classification of orbits, satellite elements, and OWC is mentioned in detail. Also, this chapter mentions the problem statement related to the motivation to select the thesis topic and methodology. Additionally, the significance of the proposed methodology and the objectives are explained to highlight the significance of the presented thesis. Finally, the frequency allocation and bands are the last important issue to be considered with satellite communication and are supported by mentioning the applications that the satellite can be enforced for.

b. Chapter two will demonstrate the most relevant previous publications and contributions from other researchers and industries in the field of Is-OWC, where a large impact of studies was proposed and tries to handle the objective mentioned in the first chapter. Additionally,

a support table summarizes the most important aspects of each study to show the pros and cons of each study.

c. Chapter three will present the methodology related to the proposed system, beginning with a demonstration of the dedicated simulation software that has been used for the system. Then the proposed system, including its three main parts, will be mentioned, and clarified in detail. After that, all the utilized modulation techniques and hybrid division multiplexing will be highlighted. Finally, the parameters to be used in analyzing the performance of the proposed system will be listed and clarified in detail.

d. Chapter four will present the results of the proposed system performance by using the hybrid scheme of MDM and PDM with OFDM for Is-OWC with the WDM technique. The results will be classified into sections. The first section will demonstrate the overall system's results in achieving the data rate required and the targeted distance of transmission. Then, the different values of pe for the Tx and Rx will be analyzed to indicate the reliability of the proposed system. Finally, the variation impact of antenna diameter for both Tx and Rx are included in investigating the performance of the proposed system.

e. Chapter Five will mention and list the conclusions explored from the proposed satellite system and will mention the future scopes to be considered in future studies.

2. LITERATURE REVIEW

a. In [35], a 32-channel based Is-OWC Dense WDM (DWDM) system was designed and implemented by using the powerful software of Optisystem. The demonstrated system can transmit data rate of 320 Giga bit per second (Gbps) and for 5000 km. In addition, it has been studying the impact of raising input power on the proposed system performance where it has set the values of 10, 20, and 30 dBm for the input power. Also, it has been tested two modulation formats of Non-Return to Zero (NRZ) and Returns to Zero (RZ). The achieved results indicate that using NRZ gives better results than RZ for the studied parameters of Quality Factor (QF) and BER. Moreover, the obtained results recommended using a power of 20 dBm as an optimum power for lancing the 320 Gbps of data rate. In contrast, the drawback with the proposed system was related to the small amount of data rate achieved which needs to be further improved to satisfy recent applications. Also, the distance achieved of only 5000 km is very short to satisfy with satellite communication and needs to be further increased.

b. In [36], authors proposed a 64-channel-based Is-OWC DWDM system with a different modulation format. The proposed system is designed to carry a data rate of 2.56 Tbps for distances up to 2500 km. The launch power selected for the laser source was 30 dBm and the power of the Erbium Doped Fiber Amplifier (EDFA) was 30 dB. Results obtained indicate that using Alternate Mark Inversion (AMI) -based modulation gives the best overall results among the other two methods of modulation. However, the utilization of AMI with a high data rate would affect synchronization. Also, the distance achieved needs to be further improved as there must be a trade-off between the achieved data rate and the distance.

c. In [37], authors proposed a 16-channel Is-OWC system by using the Dual Polarization Quadratic Phase Shift Keying (DP-QPSK) with a data rate transmitted of 1.6 Tbps and for a significant distance of 15,600 km. The utilization of coherent detection for the proposed system indicates higher performance for the proposed system as compared with the utilization of QPSK and DP-DQPSK-based modulation format. The achieved log BER was -2.42, the channel spacing selected was 100 GHz, the input power used was 30 dBm, and the selected diameter for both Tx and Rx was 15 cm. Even with the significant improvement achieved with the proposed methodology which is represented by the higher data rate and

transmission distance, however, using the coherent detection would increase the complexity impact for the demonstrated system. For instance, attaching more channels would require many line coding techniques and may not be considered a cost-effective system.

d. In [38], researchers proposed a 64-channel Is-OWC DWDM utilizing the MDM technique and three cases of modulation techniques, these techniques are represented by the DPSK, DQPSK, and Manchester. The selected input power for launching the Continuous Wave (CW) laser was 30 dBm. The investigation results indicate that using the DQPSK gives the best overall results with a QF result of 32,01 dBm as compared to the other two methods. Thereby, the system could achieve a total data rate of 2.56 Tbps and a transmission distance of up to 3750 km. The results obtained confirmed the efficiency of the spectral when handling the WDM technique. However, the utilization of the MDM technique to create 64-linear polarization modes would increase the mode dispersion between these channels and reduce the capacity of the individual channels. Also, the achieved distance needs to be further improved to satisfy satellite-based applications.

e. In [39], authors proposed a single channel Is-OWC based on using the ODFM and DPSK as the modulation technique. The proposed system investigates three cases of Pe which is the 1, 3 and 5 milliradian (mrad) respectively. The selected input power for the proposed system was -4 dBm and the set frequency was 7.5 GHz. Additionally, two cases of bandwidth values were included represented by 850 nm and 1550 nm were included in the proposed system investigation. Results were obtained to give a good Signal Noise Ratio (SNR) indication which was 24.81 dB for 20,000 km. Also, results demonstrate that using the bandwidth of 850 nm gives a better overall performance as it raises the SNR value by 5 dB when compared to 1550 nm. The demonstrated results give a lower cost system with less affecting by nonlinearity impairments. However, the achieved data rate still needs to be further raised and tested over very long distances.

f. In [40], authors proposed a 2-channel MDM-based Is-OWC system with a total data rate of only 80 Gbps. The distance achieved by their system was only 6000 km and the selected input power was 30 dBm. The utilization of the MDM for the proposed system was a major contribution to the proposed system which could be further considered to raise the transmission distance and data rate by adding intensity profiles to the transmitted signals. However, the system implemented didn’t consider the future requirement of satellite

communication which is represented by the higher transmission distance and higher individual data rate per channel. In addition, using the Pe of value equal to 2 mrad only would reduce the capability of the proposed system, where the authors must investigate different values of it to demonstrate the system with optimum performance.

g. In [41], another 2-channel Is-OWC system is designed, modelled, and implemented using the powerful technique of MDM that is represented by using the Laguerre-Gaussian (LG00) and LG01. In addition, the proposed system uses OFDM as a modulation technique. The data rate achieved by the system was only 20 Gbps and the distance performed was 1600 km only. Two modulation techniques of NRZ and RZ are tested for the proposed system. Results obtained indicate that using NRZ could achieve better results than using the RZ for OWC. The drawback of the proposed system is that it selects the Pe of 5 mrad only and the achieved data rate and distance would not satisfy the requirements of 5G requirements and satellite-based applications.

h. In [42], authors proposed a 4-channel WDM with OFDM modulation technique to handle transmission for an FSO-based medium. The proposed system could achieve a data rate of 80 Gbps for a distance of only 2700 m. The modes utilized are distinct spatial modes of the Hermite Gaussian (HG) and LG. The tested environments are represented by the fog case of weather. The significant part of the proposed system is represented by the ability to transmit higher data rates for different channels individually. However, the achieved data rate and distance need to be improved to meet the recent applications of 5G communication networks and what comes behind.

i. In [43], authors proposed a 10-channel WDM system that uses the MDM and DP-QPSK techniques together with the ability to transmit 4 Tbps of data rate. The proposed system could achieve a transmission distance of over 40,000 km. the laser power selected was -10 dBm, with various ranges of Pe ranging between 1 to 5 mrad and the laser line width equal to 10 MHz which is considered as a large value selected. Very small diameters for Tx and Rx antennae were set which is equal to 150 mm. The significance behind the proposed method was the ability of each channel to transmit 400 Gbps of data rate. Additionally, the achieved distance was satisfactory to meet the GEO-based satellite applications. However, the proposed system uses the coherent-based detection method which increases the complexity of the proposed system where it will require the utilization of Digital Signal

Processing (DSP) tools to handle the dual polarization issue. Additionally, the proposed system didn't consider the different impacts of nonlinearity on the proposed system which may reduce the performance of the proposed system.

j. In [44], authors proposed a multiple-channel WDM system for the Is-OWC system by utilizing the techniques of MDM with two modes of HG00 and HG01 and Tx diversity. The latter technique includes the utilization of hybrid NRZ-RZ and NRZ-AMI and is compared with the non-Tx diversity case. The distance studied was about 5000 km, and each channel was capable to transmit a data rate of 40 Gbps per mode. The study has included the investigation of different Pe values and distances. Results obtained were based on the studied parameter of log BER which indicates that using the combination of the NRZ-AMI has achieved the best overall results as compared with the other two methods. However, the proposed system has not met the requirement of the latest applications of 5G where the data rate and distance should be further improved.

Table 2.1 presents a summary table for the literatures that have been mentioned, highlighting the benefits and drawbacks of each research. This table is intended to serve as a comparison for the purpose of highlighting the contribution that has been carried out in this thesis. Its purpose is to provide a more in-depth look at the literature that is associated with this thesis subject. In addition to that, showcasing the contribution that a large number of writers have made from a few of years ago to the current day. Furthermore, to provide clarity on the development of a satellite system with the objective of increasing both the data rate and the distance of transmission.

Table 2.1: Summarization Of The Literature Studies.

Ref.	Methodology	Distance	Data Rate	Pros.	Cons.
[35]	32-channel Is-OWC DWDM system	5000 km	320 Gbps	1-investigate the impact of raising input power on system transmission 2- NRZ modulation format gives better results than using the RZ. 3- recommended using the power of 20 dBm with NRZ to achieve the required data rate	1- the data rate achieved needs to be further improved and raised to satisfy 5 G-based requirements 2- the distance of 5000 km is very low for satellite communication and needs to improve.
[36]	64 channel Is-OWC WDM using a different modulation format	Up to 2500 km	2.65 Tbps	1- based on observation AMI modulation format gives better results as compared to others 2- achieving an acceptable data rate	1- data rate needs to be improved 2- transmission distance needs to be improved 3- using AMI based modulation format with a higher data rate would affect synchronization
[37]	16 channel DP-QPSK Coherent OFDM	15,600 km	1.6 Tbps	using Co-DP-QPSK indicates best results than using the QPSK and DP-DQPSK for higher data rate and higher transmission distance	1- using coherent detection increases the impact of complexity for the proposed system. 2- adding more channels requires using many lines coding techniques 3- using a higher aperture diameter for Tx and Rx of 15 cm
[38]	64 channel MDM Is-OWC using modulation technique of DPSK, DQPSK, and Manchester	Up to 3750 km	2.56 Tbps	1- Using the DQPSK gives the best overall results as compared to other studied methods. 2- achieving a significant data rate	1 - Employing the method of mode division to produce a 64-mode channel would result in an increase in the mode dispersion between these channels

Table 2.1: Summarization Of The Literature Studies "Table Continued".

					of the individual channels. 2- The distance needs to be further improved to satisfy application-based Is-OWC
[39]	Single-channel IS-OWC system that uses the DPSK and OFDM techniques	20,000 km	10 Gbps	1-The utilization of ODFM with DPSK was the major contribution of the proposed study. 2- using the bandwidth of 850 nm gives improvement ins SNR with 5 dB as compared to 1550 nm. 3- using OFDM with DPSK can reduce the nonlinearity effects.	1- The data rate needs to be further improved to satisfy recent 5G applications. 2- The detection method utilized has not been mentioned 3- Needs further improvement in several channels attached.
[40]	2 channel MDM Is-OWC	6000 km	80 Gbps	investigating the significance of using the Mode of channel for transmission and raising the data rate per each channel	1- using a large Pe angle equal to 2 2- transmission distance needs to be raised 3- data rate needs to be improved
[41]	2 channel Is-OWC MDM OFDM system	1600 km	20 Gbps	Results obtained indicate that using NRZ giver better results than using RZ in OWC	1- low data rate 2- a low distance of transmission 3- higher Pe for Rx equal to 5 mrad
[43]	DP-QPSK MDM 10 channel WDM Is-OWC system	40,000 km	4 Tbps	Designing a hybrid MDM WDM system could boost the transmission capability and overall distance	1- using a very large Pe value reach to 5 mrad 2- using coherent detection makes the system complex and expensive

Table 2.1: Summarization Of The Literature Studies "Table Continued".

[42]	4-channel MDM OFDM FSO-based system	2700 m	80 Gbps	Significant results for the proposed system in sending higher data rates per each channel individually.	1- data rate needs to be improved 2- transmission needs to be improved
[Proposed]	8 channel WDM Is-OWC with 2 HG Modes	48,000 km	5.12 Tbps	1- Higher data rate with 2- proposed a novel methodology to raise the data rate per channel by using the power of hybrid MDM and PDM techniques 3- study the impact of the different Pes on the proposed system performance	Another technique could be tested for future studies.

3. METHODOLOGIES

3.1 INTRODUCTION

This chapter will present the theoretical concepts for the proposed methodology related to this thesis. To start with, the software used by Optisystem to design, model, and test the proposed Is-OWC WDM MDM PDM system will be clarified. After that, the theoretical aspects related to the utilized techniques that form the major contribution of the thesis topic will be listed, clarified, and supported with equations. Then, the proposed novel system will be withdrawn with all details related to its parts and components. Finally, the studied parameters to be utilized to analyze the performance of the proposed system will be illustrated in detail to give a view of the significance of each parameter.

3.2 OPTISYSTEM PROGRAM

The level of sophistication of a system used for optical communications is always increasing. The design and testing of these optical communication systems, which often include nonlinear devices and non-Gaussian noise sources, are quite complex and need a significant amount of time to complete because of the complexity of the systems and the noise sources they use. In addition, the need for cost-effective tools to handle the scenarios of fiber optical network design was an important issue. Among many solutions provided the Optiwave Corporation's Optisystem is a strong piece of software that can simulate optical communication networks at the physical layer [45]. This simulation is done using Optisystem. The most recent release of this program is Optisystem 19, which has several different tools and components that facilitate the process of designing and modelling the desired suggested system of this thesis. Users can plan, test, and simulate nearly every kind of optical link that exists in the transmission layer of a wide variety of optical networks with the help of Optisystem, which is a cutting-edge software design tool that is constantly being improved upon and possesses a great deal of power. Optisystem provides many features which can simplify the design process for the end user and among these features is the easy arrange of the utilized tools as libraries. In addition, Optisystem provides an easy way to build the desired network by using drag and drop and with Graphical User Interface (GUI) user control. The methodological steps of the Optisystem program can be viewed in Figure 3.1. The simple main screen of the software can be seen in Figure 3.2.

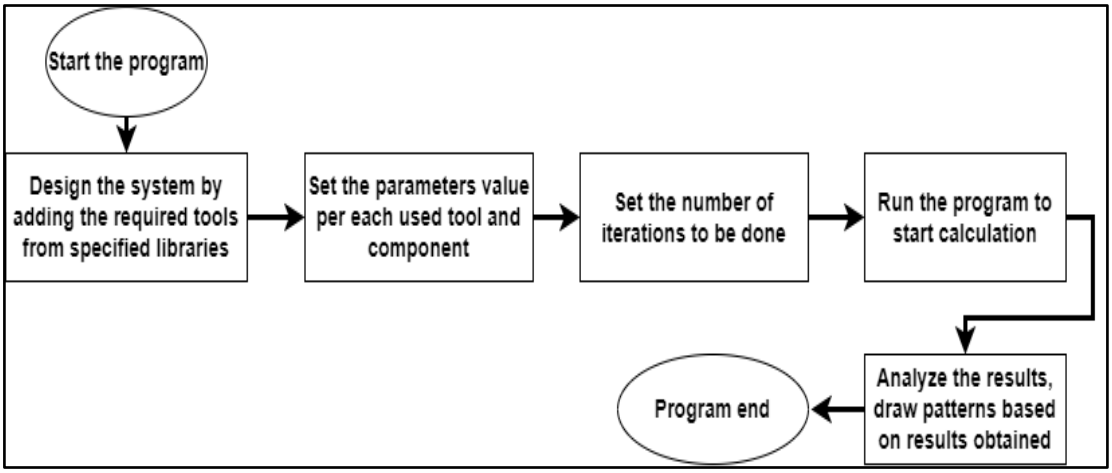

Figure 3.1: Optisystem General Methodology.

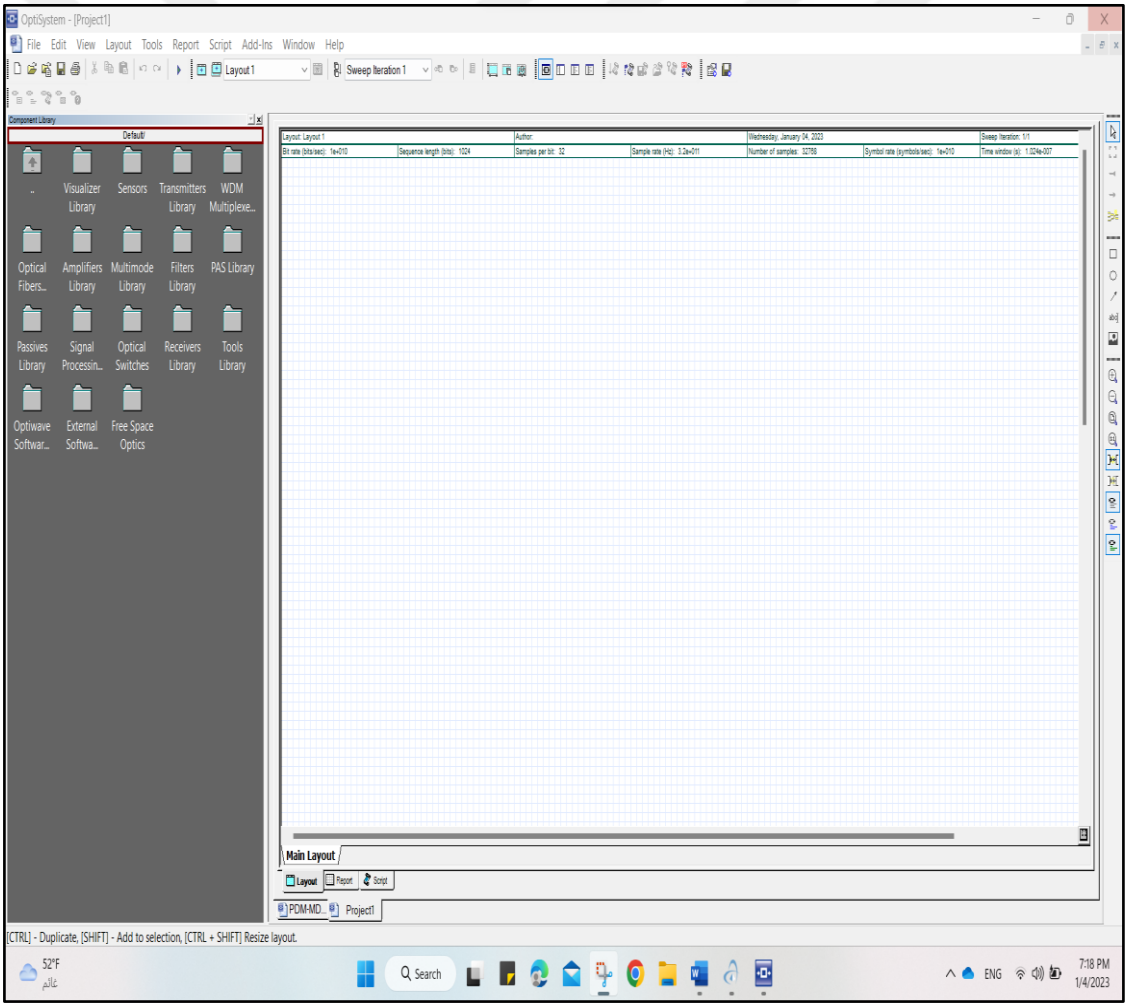

Figure 3.2: Main Window Of The Optisystem Program.

3.3 WAVELENGTH DIVISION MULTIPLEXING (WDM)

The technique of WDM will be demonstrated by clarifying its definition, types, and components of its system.

3.3.1 WDM Overview

WDM is a technology that is used in fiber-optic communications that multiplexes multiple optical carrier signals on a single optical fiber. This is accomplished by using laser light with varying wavelengths (colors) to transmit the respective messages. This not only enables bidirectional communications over a single strand of fiber but also provides for a multiplication in capacity over that same strand of fiber. However, the term WDM is more generally used to refer to this technique [46].

When referring to a radio carrier, the word FDM is often used, but the term WDM is typically used when referring to an optical carrier (which is normally characterized by its wavelength) (which is more often described by frequency). On the other hand, given that the ratio of wavelength to frequency is inverse, and as light and radio waves are both types of electromagnetic radiation, we may consider these two words to be interchangeable in the context of this discussion [46].

In a WDM system, the signals are combined by a multiplexer located at the Tx and then separated into their parts by a demultiplexer located at the receiver. It is feasible to have a device that can do both concurrently and may operate as an optical add-drop multiplexer if the appropriate kind of fiber is used [46].

The idea was initially presented in a paper that was published in 1970, and by 1978, researchers had successfully implemented WDM systems in the lab. In the beginning, WDM systems could only combine a maximum of two signals. Modern systems can manage up to 160 signals, which allows them to grow a fundamental 10 Gbit/s fiber system to a potential total capacity of more than 1.6 Tbit/s across a single fiber pair [46].

Because they enable telecommunications firms to increase the capacity of their networks without the need to lay more fiber, WDM systems are quite popular among these businesses. As a result, in this thesis, the technique of WDM will be used for attaching multiple channels and combining them to be transmitted over Is-OWC-based space transmission [46].

3.3.2 Type of WDM

WDM systems may be classified according to one of three distinct wavelength patterns: conventional, coarse, or dense WDM. Up to 16 channels may be provided by conventional WDM systems that operate in the third transmission window (C-band) of silica fibers at around 1550 nm [47]. DWDM makes use of the same transmission window as Time Division Multiplexing (TDM), but the channel spacing is much closer together. A Cores WDM (CWDM) system is intended for short-range communications and typically supports 8 wavelengths per fiber. This system makes use of wide-range frequencies and wavelengths that are spaced very far apart. In most cases, CWDM is used for applications that need a lower cost, a lesser capacity (sub-10G), and shorter distances, all of which place a significant emphasis on cost. A comparison between the two types concerning spectrum utilization can be seen in Figure 3.3 [47]. Because DWDM utilizes closer wavelength spacing to pack more channels onto a single fiber, the number of multiplexed channels is much higher in DWDM systems than in CWDM systems. CWDM systems, on the other hand, have a substantially lower channel density. In addition to being able to support a greater number of wavelengths than CWDM platforms, DWDM systems are also capable of dealing with higher-speed protocols. This is because most companies that sell optical transport equipment today support 100G or 200G per wavelength, while new technologies are making it possible to support speeds of 400G and even higher. A comparison between the two types of WDM can be formed as seen in Table 3.1.

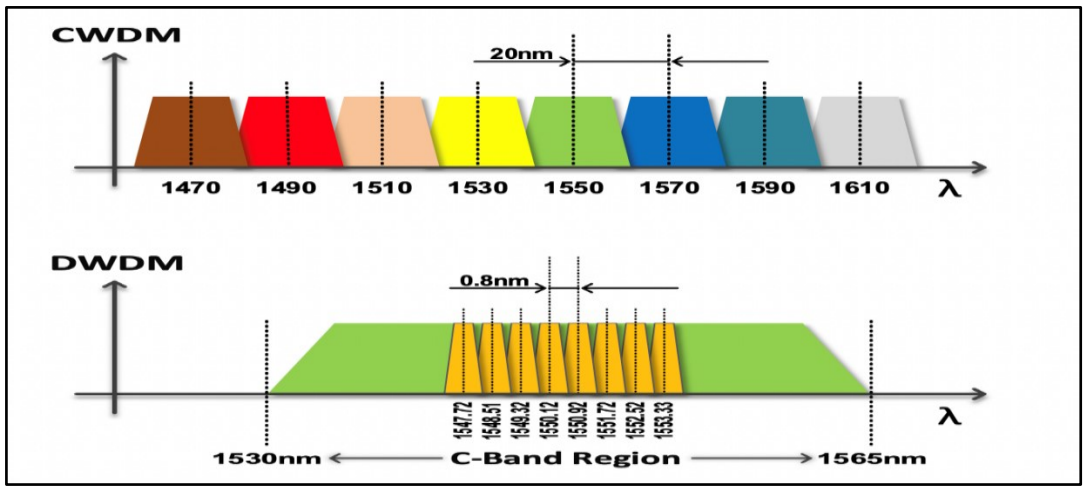

Figure 3.3: Spectrum Comparison Between The CWDM And DWDM [47].

Table 3.1: Comparison Between CWDM And DWDM [48].

Specification	**CWDM**	**DWDM**
Characteristics	identified by wavelength	identified by frequency
Capacity	Low	High
Cost	Low	High
Distance	Short distance	Long distance
Frequency	wide range	narrow range
Spacing between wavelength	More	Less
Amplification	no need amplification	need amplification.
Number of wavelength per fiber	less than or equal to 8	more than 8

3.3.3 Components of The WDM System

The WDM system consists of three components and as seen in Figure 3.4 which are.

a. Multiplexer terminal: In essence, the wavelength multiplexer at the terminal has one wavelength-converting transponder for every wavelength signal that it will transport. The input optical signal is received by the wavelength-converting transponders, and then that signal is converted into the electrical domain before the signal is retransmitted using a 1550-nm band laser. (In the middle of the 1990s, early DWDM systems consisted of 4 or 8 transponders that could convert wavelengths. Around the year 2000, commercially accessible systems with the capacity to transport 128 signals were available) [49].

b. Transmission medium: This component includes the use of regular fiber optical cable or using other media such as the FSO or OWC or it could include a hybrid medium-based system. The most important issue to be considered in this part are the transmission distance and selecting the appropriate amplifier [49].

c. Demultiplexer terminal: The client-layer devices can identify the individual signals because the terminal demultiplexer splits the multi-wavelength signal back into its component signals and outputs them on separate fibers. In the beginning, this demultiplexing

process was carried out passively, except for certain telemetry. Before being relayed to respective client-layer systems, however, such demultiplexed signals are often routed to optical and electrical output transponders to enable transmission to faraway client-layer systems (and to allow for digital domain signal integrity assessment) [49].

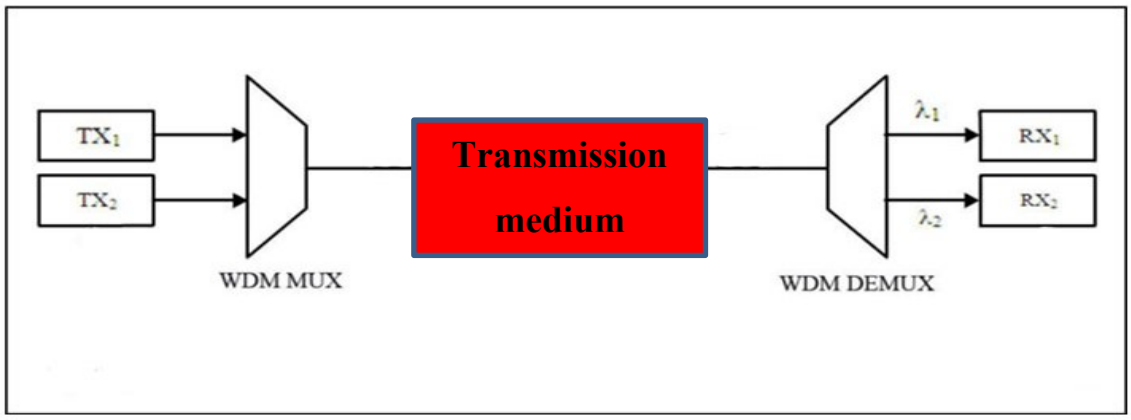

Figure 3.4: The WDM System [50].

3.4 ORTHOGONAL FREQUENCY DIVISION MULTIPLEXING (OFDM)

A broad overview of OFDM's guiding principles is presented in this subsection so that readers may better understand the impetus for the use of OFDM strategies in optical communication systems.

3.4.1 OFDM Overview

Modulation is used in modern communication systems, and there are often two different approaches to choose from. There is also something called multi-carrier modulation in addition to single-carrier modulation. The information is modulated onto a single carrier in the process known as single-carrier modulation, which involves modifying either the amplitude, frequency, or phase of the carrier. This information can be in the form of bits or symbols when dealing with digital systems (collection of bits) [51]. The signalling interval in a single-carrier modulation system is identical to the symbol duration, and the modulated carrier takes up the full available bandwidth. The symbol duration T_S will decrease in proportion to the rise in the data rate. If the T_S is less than the channel delay spread, there will be high Inter Symbol Interference (ISI) as a result of the memory of the dispersive channel, and an error floor will rapidly form [52]. Because of this, the system is put in a

position where it is more likely to suffer information loss as a result of unfavourable conditions such as frequency selective fading as a result of multipath, interference from other sources, and impulsive noise [52-54].

The modulated carrier, on the other hand, uses up just a small portion of the available bandwidth in multi-carrier modulation systems like FDM systems. In these types of systems, the information that is being communicated at a high data rate is split up into N parallel streams operating at a lower rate, with each of these streams modulating a distinct subcarrier at the same time. If the overall data rate is R_S, then the data rate for each parallel stream would be equal to R_S divided by the number of streams. Because of this, it can be deduced that the symbol duration of each parallel stream is N times longer than the symbol duration of the serial stream; and it is significantly more than the channel delay spread. These systems are resistant to ISI and are thus finding growing application in contemporary communication systems, particularly those that make use of high data rates and place a premium on conserving the limited available spectrum [55]. The general diagram for the FDM Tx can be seen in Figure 3.5, where C0, C1, C2, and C3 are the labelled subcarrier, N represents the number of subcarriers, and T_S represents the symbol duration.

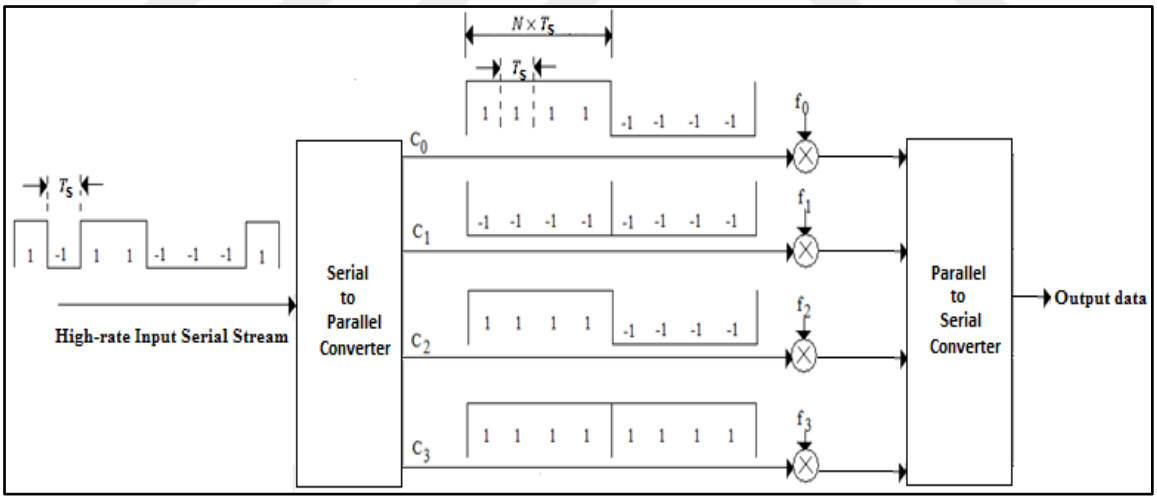

Figure 3.5: General Diagram Of The OFDM Transmitter [51].

The demonstration of the single and multi-carrier modulation concerning spectrum view can be seen in Figure 3.6 (a) and (b) respectively. FDM system needs a guard frequency band between the modulated subcarriers, as shown in Figure 3.6 (b). These guard bands are there to prevent the spectrum of one subcarrier from interfering with the spectrum of another

subcarrier and to ensure accurate independent demodulation of subcarriers using filters. The utilization of these guard bands leads to inefficient utilization of the spectrum [56]. OFDM is a kind of FDM that employs orthogonal subcarriers, and it was developed from FDM. Figure 3.6 (c) presents the OFDM signal in the frequency domain. The overlapping of the spectra of the subcarriers in OFDM, as can be seen in Figure 3.6 (c), results in a reduction in the amount of bandwidth required. Each subcarrier's spectrum has a sin-shaped distribution, and the peaks of one subcarrier's spectrum correspond to the zero-crossings of the spectra of the other subcarriers. There is no incidence of Intercarrier Interference (ICI) so long as the orthogonality between the subcarriers is preserved. This is because the energy from one subcarrier does not influence the energy of the subcarriers that are nearby [56].

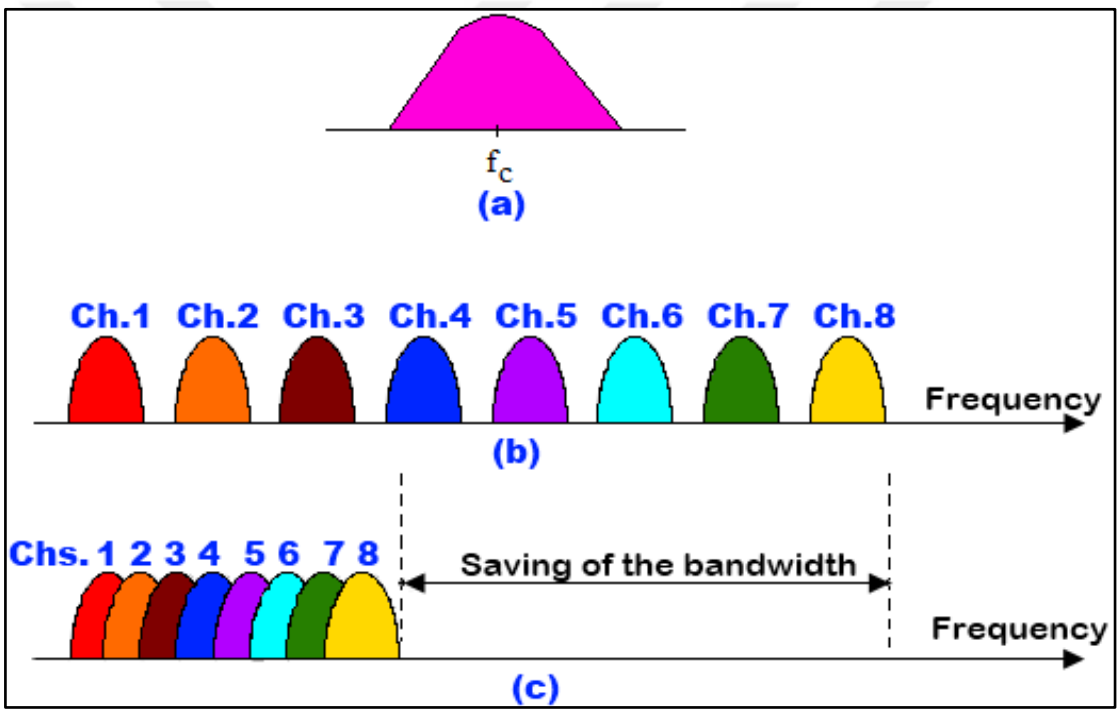

Figure 3.6: Spectrum Modulation In The a) Single Carrier, b) Multiple Carriers With Guard Band, And c) OFDM Multiple Carriers [56].

3.4.2 OFDM Principle

The principle behind the OFDM technology was carried out for several years, which is based on the orthogonality of the subcarrier. A set of subcarriers $Sn(t)$ can be represented by equation 3.1 and can be said to be orthogonal in the time domain as expressed in equation 3.2 [57].

$$Sn(t) = e^{j(2\pi fnt)} \tag{3.1}$$

$$< Sk(t), Sl(t) >_0^T = \int k(t).Sl(t).dt \tag{3.2}$$

$$= \int_0^T e^{j2n(fk-fl)t}.dt$$

$$= \int_0^T e^{j2n(k-l)\Delta ft}.dt$$

$$= T\delta_{k,l} = \begin{cases} 1, if\ k = 1 \\ 0, if\ k \neq 1 \end{cases}$$

Where $\delta_{k,l}$ represents the delta symbol of Kronecker.

Two factors should keep in mind as conditions for the orthogonality property between the subchannels which are [57-59]:

a. The frequency of each subcarrier must be selected in such a way that there is an integer number of cycles for that subcarrier inside the period of the OFDM symbol.

b. The difference in the number of cycles per OFDM symbol that exists between neighbouring subcarriers is required to be one.

As a clarification for the above two conditions, Figure 3.7 can confirm that.

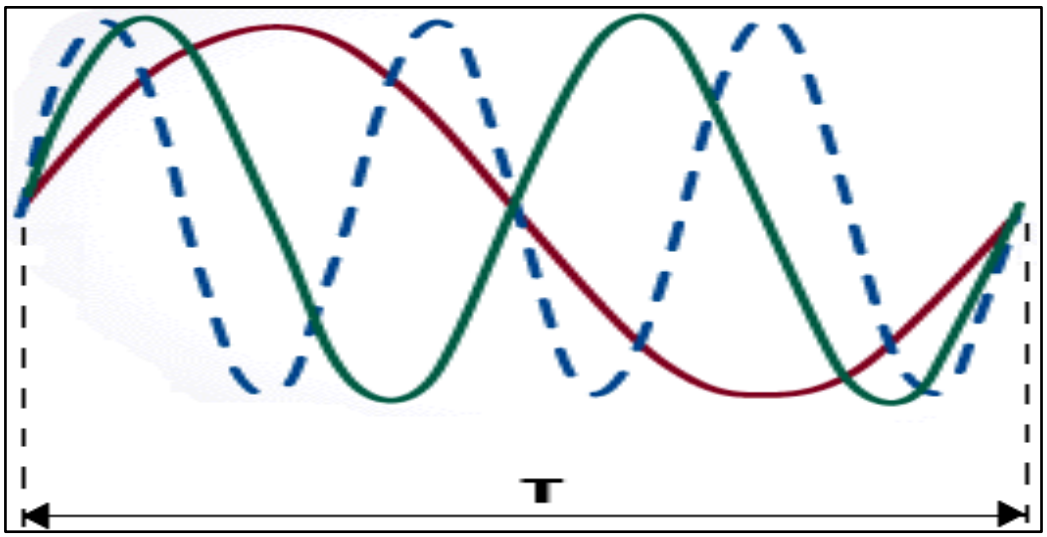

Figure 3.7: Three Subcarriers With The OFDM Symbol [57].

3.4.3 OFDM Advantages and Disadvantages

a. One of the key advantages of OFDM is that, in comparison to single carrier systems, it has a higher level of resistance to frequency-selective fading, making it one of its most advantageous characteristics. This is since OFDM splits the overall channel into many narrowband signals. These signals are then impacted separately as flat fading subchannels. Because of this, OFDM is more robust to frequency-selective fading than systems with a single carrier [60-62].

b. Resistance to interference: Interference that appears on a channel could have a restricted bandwidth, which means that it might not impact all of the subchannels. This is known as interference resilience. This indicates that not all the data has been deleted [60-62].

c. Efficient use of the spectrum: One of the most notable benefits offered by OFDM is that it allows for more effective use of the spectrum by using close-spaced and overlapping sub-carriers [60-62].

d. OFDM has several benefits, one of which is that it is resistant to ISI. This is a direct consequence of the slow data rate that is sent on each of the subchannels.

e. Resistant to the impacts of narrow bands: By using appropriate channel coding and interleaving, it is possible to recover symbols that were lost because of the frequency selectivity of the channel and narrowband interference [60-62].

On the other hand, the drawbacks of OFDM may be summed up by the issues that are listed below:

a. A high peak-to-average power ratio: An OFDM signal has an amplitude fluctuation that is like that of noise, and it also has a comparatively high broad dynamic range, also known as a peak-to-average power ratio. This affects the efficiency of the RF amplifier since the amplifiers need to be linear and be able to accept significant amplitude changes [60-62].

b. susceptible to carrier frequency offset and drift: Another drawback is that OFDM is sensitive to carrier frequency offset. Single carrier systems are less sensitive [60-62].

3.5 QUADRATURE AMPLITUDE MODULATION (QAM)

In the digital modulation system known as QAM, information is sent across the channel by altering both the amplitude and phase of the high-frequency carrier signal. This is done to maximize data transmission efficiency. The signal that is sent is shown as a constellation on a plot that has two axes, which are labelled in-phase and quadrature respectively. The in-phase and quadrature axes may be distinguished from one another by a phase difference of 90 degrees. As a result, these two axes cannot be rotated around each other since they are orthogonal [63].

3.5.1 QAM Overview

The QAM system involves combining two or more bits into a single sign, which then locates itself on the constellation plot. Each symbol, which is also known as a state, has a one-of-a-kind amplitude and phase level that allows it to be distinguished from one another across the various places in the constellation. Given that the modulation technique makes use of binary data, equation 3.3 is used to obtain the number of transmitted bits [63-65].

$$M = 2^N \tag{3.3}$$

where N is the number of bits and M is the number of potential combinations matching any given number of bits N. Because 2N's value is likewise an integer, the total number of bits that may be transferred, as shown in equation 3.4 [63-65].

$$N = \log_2 M \tag{3.4}$$

A carrier wave with a constant frequency and sixteen distinct possible states may be said to be modulated using the QAM technique known as 16-QAM. This may be shown in a graphic called a constellation can be seen in Figure 3.8, where each state is represented by a symbol that represents one of 16 distinct amplitude and phase levels. The in-phase (X-axis) and quadrature (Y-axis) axes make up the constellation plot. These axes are orthogonal to one another, which means that they are separated by a phase that is exactly 90 degrees from each other [63-65].

In a 16-QAM system, each symbol in the constellation may hold a maximum of four bits (0s and 1s). As a result, the number of feasible options when employing 4 binary bits is 24, which equals 16, with each state or symbol carrying a value ranging from 0000 to 1111.

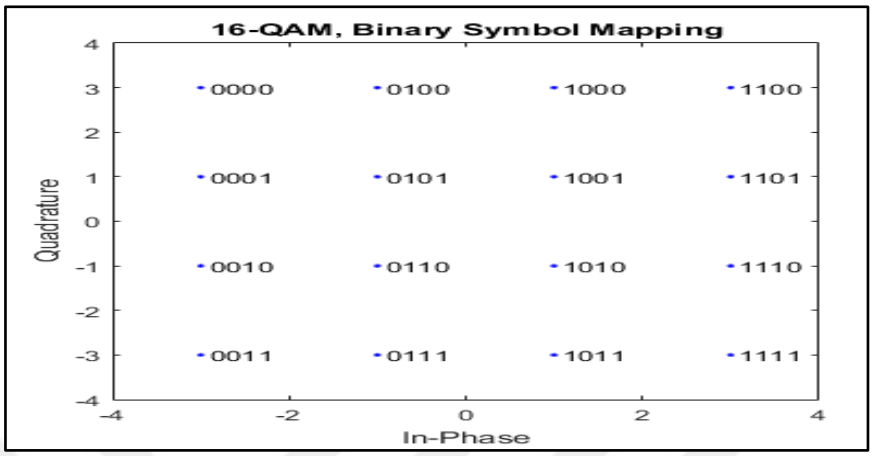

Figure 3.8:16 QAM Constellation Diagram [63].

Waveforms for four-bit symbols may be seen in the graphic below; each symbol has its distinct amplitude and phase level. For instance, the symbols 0000 and 0001 both have the same amount of amplitude but differing amounts of phase. As a result, they are located on opposite sides of the quadrature axis. Similarly, the symbols 1001 and 1101 both carry the same phase level but differing amplitude values. As a result, to make it possible to differentiate between the two, they will be split apart along the axis of in-phase [63-65]. Waveform representation can be seen in Figure 3.9 [63].

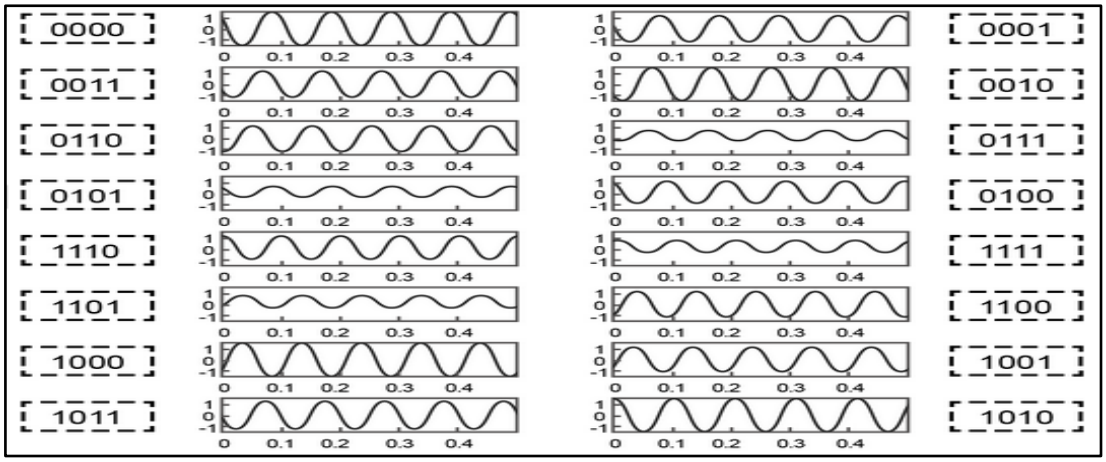

Figure 3.9: Waveform Allocation For The 16 Combined Symbols Represented In The 16 QAM [63].

3.5.2 QAM Concept of Work

To understand the concept of work for the QAM, first, it's necessary to mention that QAM consists of two parts, the first used in the Tx part and known as the modulator, and the second used in the Rx part and known as the demodulator.

As shown in Figure 3.10, a simple QAM modulator circuit comprises a mixer, local oscillator, 90-degree phase shifter, and summer block at the output port. The I and Q components of the circuit receive the signal input. A local oscillator produces a clear sinusoidal signal with a set frequency and amplitude. To create a high-frequency carrier signal, the mixer circuit multiplies the incoming signal with the oscillator signal. While the oscillator signal and incoming signal are simply mixed to create the in-phase signal, the oscillator signal is phase-shifted by 90 degrees to create the quadrature waveform, which is then mixed with the data signal. A QAM-modulated signal is produced by combining the resultant two waveforms, the in-phase, and quadrature, at the summer circuit [63,66,67].

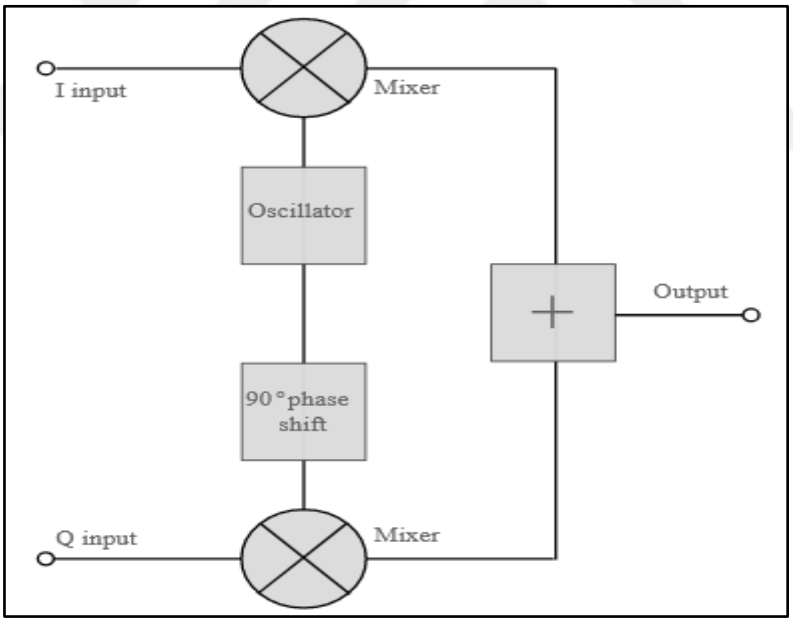

Figure 3.10: Internal Circuit Of The QAM Modulator [63].

A splitter device is used in the QAM demodulation process to separate the incoming modulated signal into its in-phase and quadrature components and as seen in Figure 3.11. The two components being orthogonal to one another allows for coherent signal extraction. The in-phase and quadrature signals may be separated using a low-pass filter. The received signal is multiplied by a cosine signal and then fed through a low-pass filter to isolate the in-

phase signal. To extract the quadrature component, a sine wave is multiplied by the received waveform and then sent through a lowpass filter [66,67].

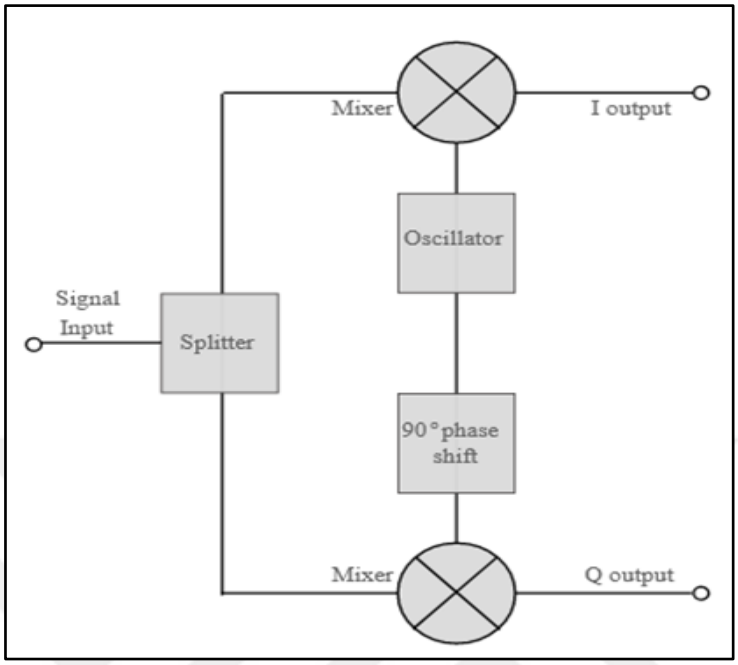

Figure 3.11: Internal Circuit Of The QAM Demodulator [63].

3.5.3 QAM Advantage and Disadvantage

The advantage of using the QAM modulation are [58,69]:

a. The major advantage is to increase the number of transmitted bits per carrier which can be considered a bandwidth-efficient utilization technique.
b. QAM uses the variation of phase and amplitude to boost the efficient transmission of the radio frequency.

On the other hand, the disadvantages of using QAM modulation are :

a. Noise is more likely to affect QAM. This is due to the proximity of the transmission states, which results in less noise being needed to transmit the signal from one location to another.
b. The utilization of the phase and amplitude in QAM would require maintaining linearity and such requirements would reduce the efficiency of the system and can consume more power.

3.5.4 QAM Order Schemes

M-ary QAM is another name for QAM modulation, where M could represent the number of bits shown in the constellation diagram. 16-QAM, 32-QAM, 64-QAM, 256-QAM, 1024-QAM, and 4096-QAM are other QAM schemes. Each of these encourages larger data rates. The efficiency behind each QAM scheme can be listed in Table 3.2. Increasing the order of the QAM scheme generally results in a higher link capacity for fixed channel sizes. The incremental capacity improvements begin to slow down when complexity increases beyond a certain point [63].

Table 3.2: Capacity Achieved By Different QAM Schemes [63].

Modulation Scheme	Bits/Symbol	Capacity Gain
BPSK	1	
4-QAM	2	
8-QAM	3	50%
16-QAM	4	33%
32-QAM	5	25%
64-QAM	6	20%
128-QAM	7	17%
256-QAM	8	14%
512-QAM	9	13%
1024-QAM	10	11%
2048-QAM	11	10%
4096-QAM	12	9.77%

Greater QAM modulation techniques provide higher signal bandwidths and data speeds, as shown in the table above. The space between two constellation points, however, diminishes as we go up the M-ary QAM modulation scheme to keep the mean constellation energy constant for a given square grid. The likelihood of two points (noisy) overlapping is thereby increased, making it difficult to tell one point from the other. As a result, there is more interference and noise, which decreases the SNR, which in turn raises BER. To boost the SNR, decrease BER, and increase the likelihood of detecting signals with low-bit errors in noisy situations, lower-order QAM techniques may be utilized [63].

Hardware complexity is a further crucial factor. In the M-ary QAM method, the constellation size grows while the point-to-point constellation distance shrinks as we go higher. As a result, higher-order QAMs present a more difficult detection problem at the receiver. When there is noise present, it is possible to intelligently differentiate various constellation points using a reliable signal processing approach. Nevertheless, the expense and complexity of the technology needed to support the expanding constellation size will rise in line with it [63].

3.6 MODE DIVISION MULTIPLEXING (MDM)

is a method used in several commercial optical fiber communication networks to increase data capacity. In essence, the concept involves employing several guided modes of multimode fiber for various transmission channels. The demonstration for the MDM technique will be as follows.

3.6.1 MDM Overview

Each supported mode in the waveguide may be utilized as a transmission channel to boost the capabilities of fiber optic cable. Figure 3.12 demonstrates that with the right optical setup, information may be modulated using the available modes. High data transmission speeds may be attained for silicon photonics and optical fibers using this method [70,71].

3.6.2 MDM Concept of Work

As illustrated in Figure 3.13, optical fibers are cylindrical waveguides made up of a high refractive index (n1) core and a low index (n2) cladding. Except for a change in its overall scale and phase, the distribution of the electromagnetic field as described by the guided mode wave equation propagates invariantly down the fiber as seen in Figure 3.13 (a). The normalized frequency determines the number of guided modes in an optical cable (v), which can be expressed as seen in equation 3.5 [72,73].

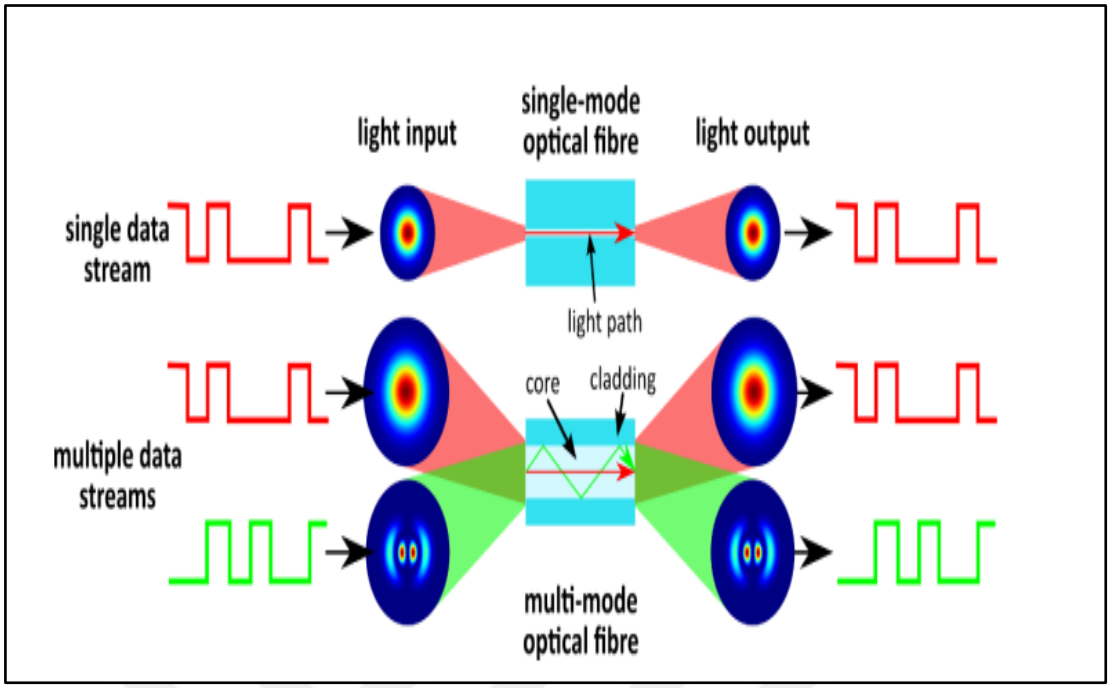

Figure 3.12: MDM Principle For Multiple Stream Data [72].

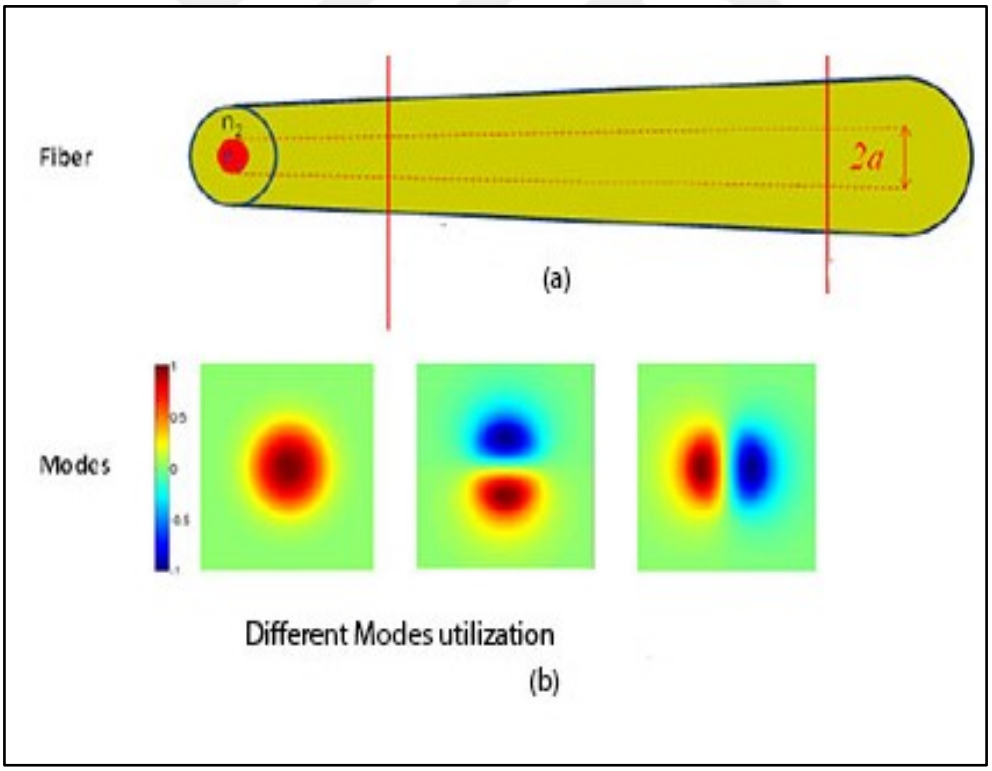

Figure 3.13: The Distribution Of Fields In MDM [73].

$$v = \frac{2\pi}{\lambda} a \sqrt{n1^2 - n2^2} \quad (3.5)$$

Where a represents the radius of the core, λ is the wavelength. So, when v is small it will not support only one mode, but when v raised above 2.405, the fiber can support two modes as seen in Figure 3.13 (b) [73].

3.6.3 MDM Components

Typically, MDM uses the components listed below and as clarified in Figure 3.14 [73]:

a. The commonly used multimode fibers are referred to as Few-Mode Fibers (FMF) because they typically have a limited number of guided modes. Although they might theoretically be step-index fibers, graded-index fibers designed for minimal Differential Modal Group Delay (DMGD) are often used because they enable the employment of less complex Rx technology [74].

b. Specific Spatial Multiplexers (SMUX) are needed to (a) inject signals from many single-mode fibers into the core of a FMF and (b) separate the signals after transmission to deliver them to various photodetectors. Spatial multiplexers come in a variety of varieties.

c. There are specialized fiber amplifiers such as the EDFA for FMF that are designed for the least amount of modal gain fluctuation to sustain adequately high signal strengths over long distances [74].

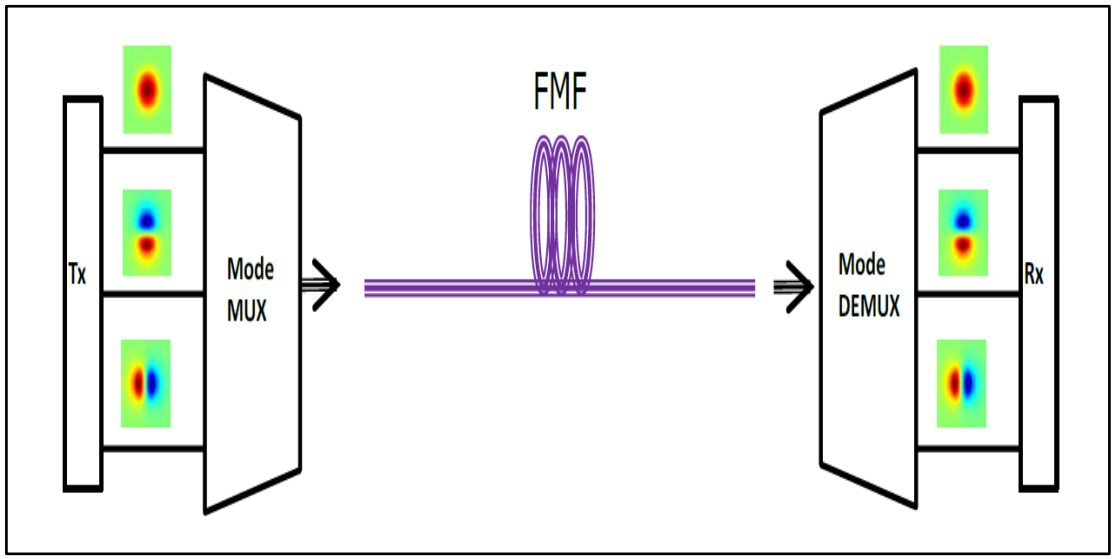

Figure 3.14: MDM Utilization In The Transmission System [73].

3.6.4 MDM Types

is a technique used in optical communication systems to increase the data-carrying capacity of an optical fiber by utilizing multiple spatial modes within the fiber and classified as below:

a. Hermite-Gaussian (HG) modes

The intensity profile of light will typically alter throughout propagation whether it is traveling through open space or a homogenous optical medium. This is not the case, however, for certain types of electric field amplitude distributions known as modes. In these cases, the form of the amplitude profile stays constant despite possible changes to the optical phase, scaling, and overall optical power. Modes of HG can be expressed as in equation 3.6 [75]. In addition, the process of phase transformation that is used for the transverse mode profiles is carried out by making use of the vortex lens, which, as illustrated by equation 3.7, will alter the focus of the output beam. This is done to accommodate the requirements of the transverse mode profiles.

$$\Psi_{m,n}(r,\varphi) = H_m\left(\frac{\sqrt{2}x}{w_{0x}}\right)\exp\left(-\frac{x^2}{{w_{0x}}^2}\right)\exp\left(j\frac{\pi x^2}{\lambda {R_{0x}}^2}\right)H_n\left(\frac{\sqrt{2}y}{w_{0y}}\right)\exp\left(-\frac{y^2}{{w_{0y}}^2}\right)\exp\left(j\frac{\pi y^2}{\lambda {R_{0y}}^2}\right) \quad (3.6)$$

Where m and n represent the x and y index for mode dependencies for the x and y-axis respectively. R is the radius of curvature and w_0 is the spot size. H_m and $H_n$are the Hermite polynomials.

$$T(x,y) = -exp\left[-j\frac{\pi n\left(x^2+y^2\right)}{2\lambda f} + matan\left(\frac{x}{y}\right)\right] \quad (3.7)$$

where f refers to the length, m is the parameter of the vortex and n refers to the refractive index.

Such a mode has n nodes in the horizontal direction and m nodes in the vertical direction in its intensity distribution. Figure 3.15 shows a sample of HG mode intensity dispersion. The radial profile of HG modes follows a Gaussian distribution, while the angular variation is determined by Hermite polynomials. HG modes are labelled using two indices (p and q) that indicate the number of times the Hermite polynomial is applied along the x and y directions, respectively. These indices determine the shape and size of the mode [76].

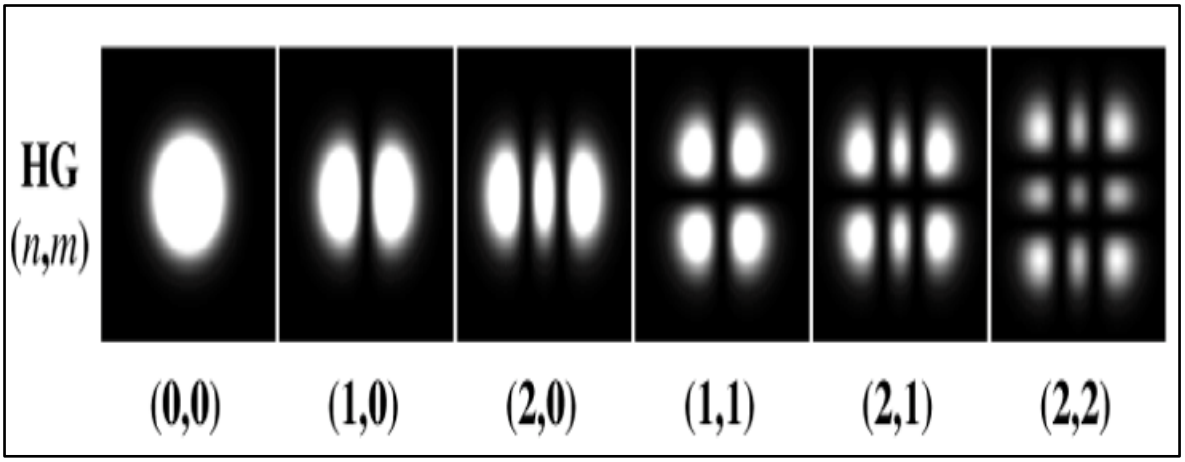

Figure 3.15: HG Mode Distribution Of Intensity [75].

b. Laguerre-Gaussian (LG) modes

are a type of solution that describes the spatial intensity distribution of light in optical systems. These modes have unique azimuthal and radial characteristics. LG modes also have a radial distribution that follows a Laguerre polynomial multiplied by a Gaussian function. This radial profile determines the mode's size and intensity distribution [77, 78]. An example of the LG mode for intensity distribution can be seen in Figure 3.16.

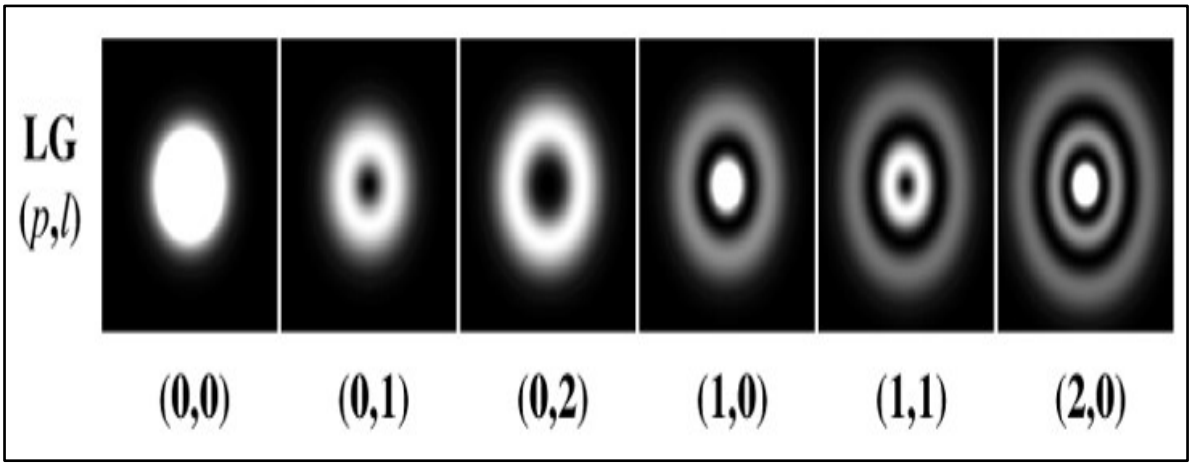

Figure 3.16: LG Mode Distribution Of Intensity [79].

c. Ince Gaussian (IG) modes

are a family of solutions that describe the spatial intensity distribution of light. They are named after the mathematician Edward Lindsay Ince. They have elliptical symmetry in their transverse intensity profiles. This elliptical symmetry distinguishes them from the circular

symmetry of LG modes and the rectangular symmetry of HG modes. The radial distribution of IG modes is characterized by a product of parabolic cylinder functions and a Gaussian factor [80]. An example of IG mode for intensity distribution can be seen in Figure 3.17

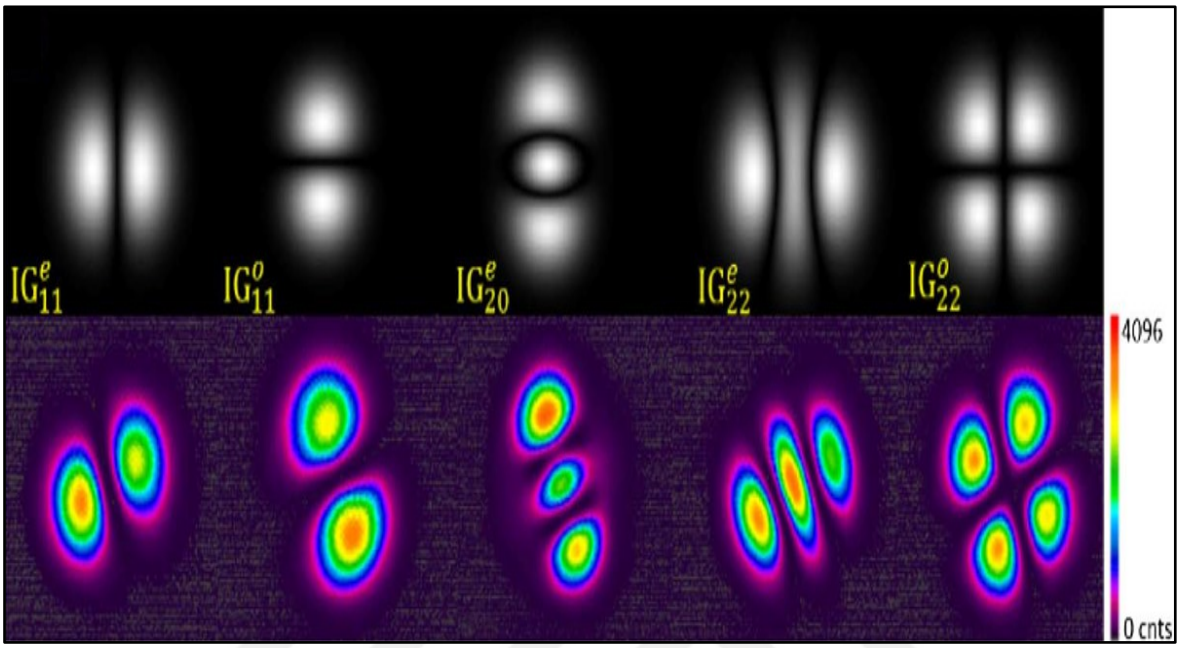

Figure 3.17: LG Mode Distribution Of Intensity [79].

the significance of HG modes over LG and IG modes often depends on the application. HG modes are particularly useful for beam shaping, laser resonators, and orthogonal analysis of modes. The choice between these modes depends on factors such as symmetry, spatial distribution, and the unique properties required by the application at hand. As a result, in this thesis, it has been selecting the HG Mode instead of other types due to the below reasons:

a. HG mode can reduce the diffraction spreading.

b. HG mode provides higher intensity at the center.

c. HG mode provides higher compatibility with certain optical elements.

d. HG mode provides better resilience to mode crosstalk.

e. HG modes have simpler spatial structure.

3.7 POLARIZATION DIVISION MULTIPLEXING (PDM)

is a technique used in optical communication systems to increase data transmission capacity by leveraging different polarization states of light. The challenge of PDM requires precise control of the polarization states throughout the optical communication system to prevent interference between the polarizations and maintain signal quality is one method that may be used to either double the capacity of the system or increase the spectral efficiency [81, 82]. Two data channels, each of which is modulated in its own unique way, are sent down a single fiber at the same time using this method. These data channels have the same wavelength, but orthogonal polarization states. When it reaches the receiver, the signal is split into its two polarization channels, which are then separately detected. The general system diagram for PDM can be seen in Figure 3.18, where it can be noticed that the system consists of a WDM system with multiple channels, polarization MUX and DEMUX, and some types of amplifiers to amplify the transmitted signals.

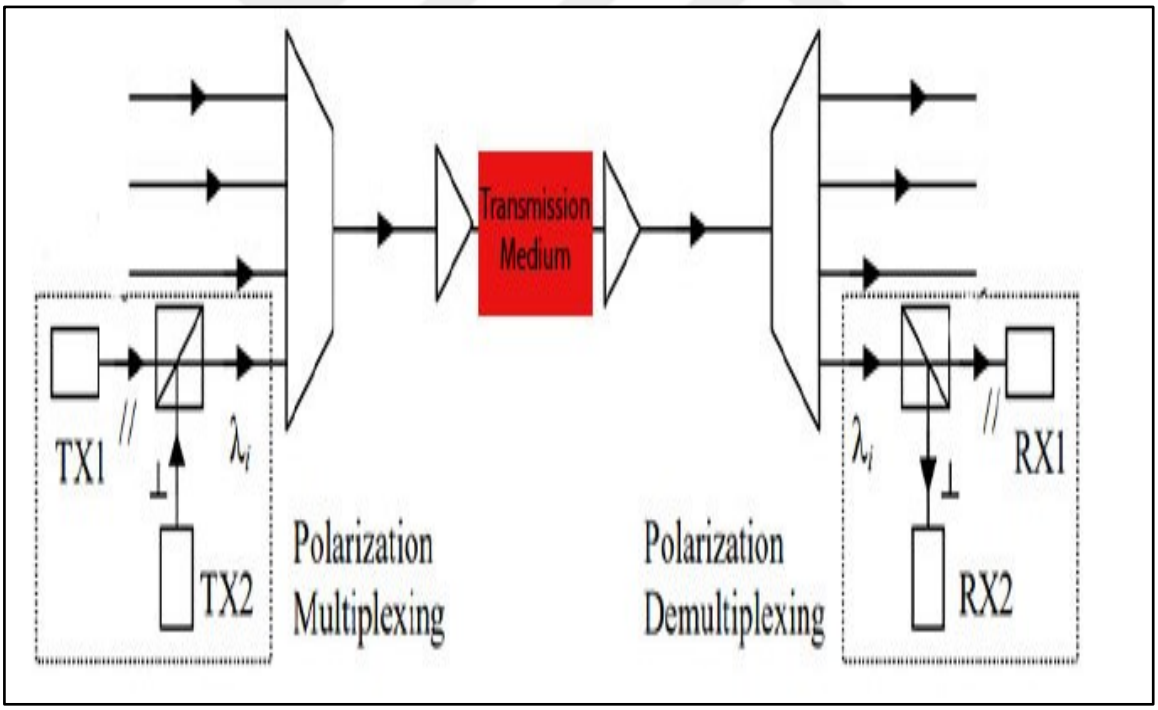

Figure 3.18: PDM-Based System [82].

PDM, which can be defined as a physical layer method for multiplexing signals carried on electromagnetic waves and allowing the transmission of two channels of information on the same carrier frequency by using waves of two orthogonal polarization states, was one of the

most significant polarization technologies. It allowed for the transmission of two channels of information on the same carrier frequency by using waves of two orthogonal polarization states. It is possible to double the bandwidth of microwave communications, such as satellite television downlinks, by equipping satellite dishes with two feed antennas that are orthogonally polarized and using them simultaneously. It is also used in fiber optic communication, which involves the transmitting of distinct light beams with left and right circularly polarized circular polarization via the same optical cable. Figure 3.19 illustrates the principle behind PDM. The polarization angle of each data channel is completely unique to itself. If it is a system with two separate data channels, then the angles of polarization for each data channel will be 0 degrees and 90 degrees, respectively. If it is a three-channel system, the angles of polarization for the data channels will be 0 degrees, 60 degrees, and 120 degrees, respectively. If it is a four-channel system, the angles of polarization for the data channels will be as follows: 0 degrees, 45 degrees, 90 degrees, and 135 degrees [83, 84].

This thesis will use the PDM technique along using the OFDM due to the following reasons:

a. increase the data rate transmitted by considering two polarizations of 0° and 90°.

b. Also, the utilization of PDM will be used with an advanced coding method of 16 QAM which can be used to increase the system performance and reduce the problem of drifting the polarization which will occur due to the physical changes that occur due to transmission for longer distances.

c. Additionally, the use of PDM makes it possible to increase the user capacity while simultaneously raising the level of spectral efficiency.

d. Furthermore, the optical transmission data rate may be increased to its maximum capabilities by combining PDM with OFDM modulation.

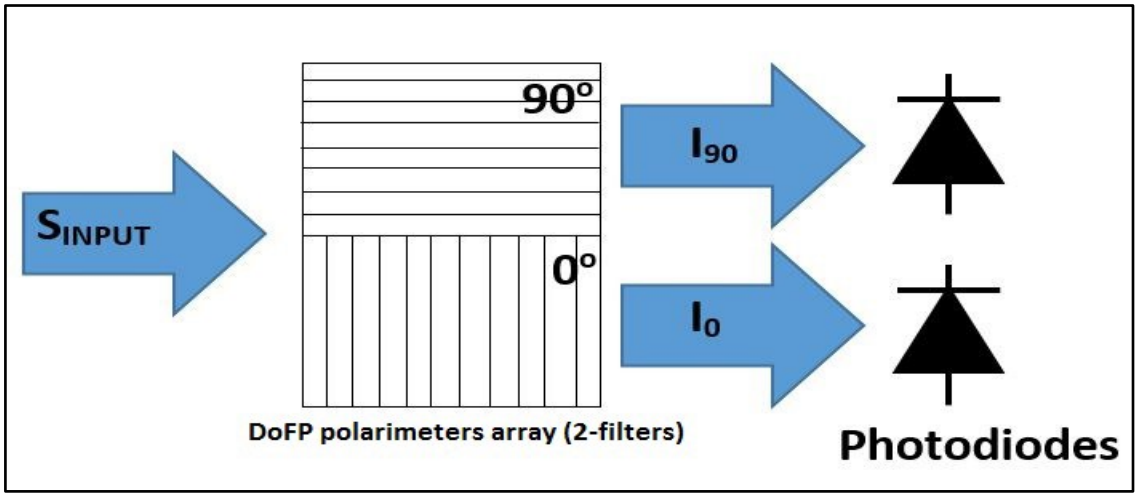

Figure 3.19: PDM With Dual Polarization [83].

3.8 THE PROPOSED SYSTEM

This section presents the modelling of the proposed Is-OWC WDM system incorporating MDM and PDM techniques, which have been carried out by using the Optisystem simulator. Figure 3.20 shows the designed system using Optisystem. To start with, the demonstration of proposed system parts will be demonstrated to describe all the components and tools utilized to form each part. Figure 3.21 clarify the three parts of the proposed system with the schematic view. Then, the parameters selected for each part will be demonstrated in detail to give a justified view of the proposed system. It is worth mentioning, that the design of the proposed system using Optisystem includes a subsystem block which is used to reduce the complexity of the design and give a better view of the proposed system.

3.8.1 Transmitter Part (Tx)

To handle the data for the Tx portion, a QAM sequence generator took care of it after the binary data was generated. This allowed it to construct two parallel M-ary symbol sequences from the binary signals, which required the usage of a Serial to Parallel (S/P) converter beforehand. As was illustrated previously in section 3.5, to generate a 16 QAM, it needs a 4-bit per sequence and a total of 4 potential sequences of binary data. After that, OFDM converts the incoming serial data stream into a parallel stream of OFDM symbols and then assigns OFDM symbols to orthogonal subcarriers in the signal. For there to be optical transmission, each OFDM symbol must have its frequency domain information converted

into its time domain equivalent. An inverse Fourier transform is performed on each OFDM symbol, and a guard extension helps to mitigate the influence of ISI.

At long last, the information that is being modulated will be processed as an electrical component of the Mack Zander Modulator's (MZM) two arms. At that time, the electrical component of the signal will be complete. The transmission of the optical signal, on the other hand, begins with the light wave that is produced by the CW laser source and is then managed by several components that are installed inside each Tx subsystem. Figure 3.22 and Figure 3.23, respectively, illustrate the internal component structure and schematic design of the Tx subsystem. Both figures are in the same file. First, the laser signal is separated into two parts, which distribute the power in an equal manner across the two output ports, as shown in equation 3.8. Equation 3.9 shows the mathematical representation of a two-dimensional optical field to describe the spatial distribution of an optical beam in terms of Hermite-Gaussian modes, provided is a product of Hermite-Gaussian functions in both the x and y directions, modulated by exponential terms that describe the curvature of the wavefronts in the x and y directions. Next, the transverse mode profiles (HG00 and HG01) are applied to each individual component to transform single-mode signals into multimode signals. The process of phase transformation that is used for the transverse mode profiles is done by utilizing the vortex lens, which will change the focus of the output beam and as demonstrated by equation 3.10 and as seen in Figure 3.24 [86].

$$Ex, y\ out = \frac{E_{in(t)} 10^{\frac{-\alpha}{20}}}{\sqrt{2}} \tag{3.8}$$

Where α represents the attenuated factor for output power.

$$\Psi_{m,n}(r, \varphi) = H_m\left(\frac{\sqrt{2}x}{w_{0x}}\right). e^{\left(-\frac{x^2}{{w_{0x}}^2}\right)}. e^{\left(j\frac{\pi x^2}{\lambda {R_{0x}}^2}\right)}. H_n\left(\frac{\sqrt{2}y}{w_{0y}}\right). e^{\left(-\frac{y^2}{{w_{0y}}^2}\right)}\ \mathrm{e}^{\left(j\frac{\pi y^2}{\lambda {R_{0y}}^2}\right)} \tag{3.9}$$

Where m and n represent the x and y index for mode dependencies for the x and y-axis respectively. R is the radius of curvature and $w_{0\mathrm{x}}$ and $w_{0\mathrm{y}}$ are the beam waist width in the x and y coordination respectively, $R_{0\mathrm{x}}$ and $R_{0\mathrm{y}}$ are the radii curvature of wavefront in x and y coordinates respectively. H_m and $H_n$are the Hermite polynomials.

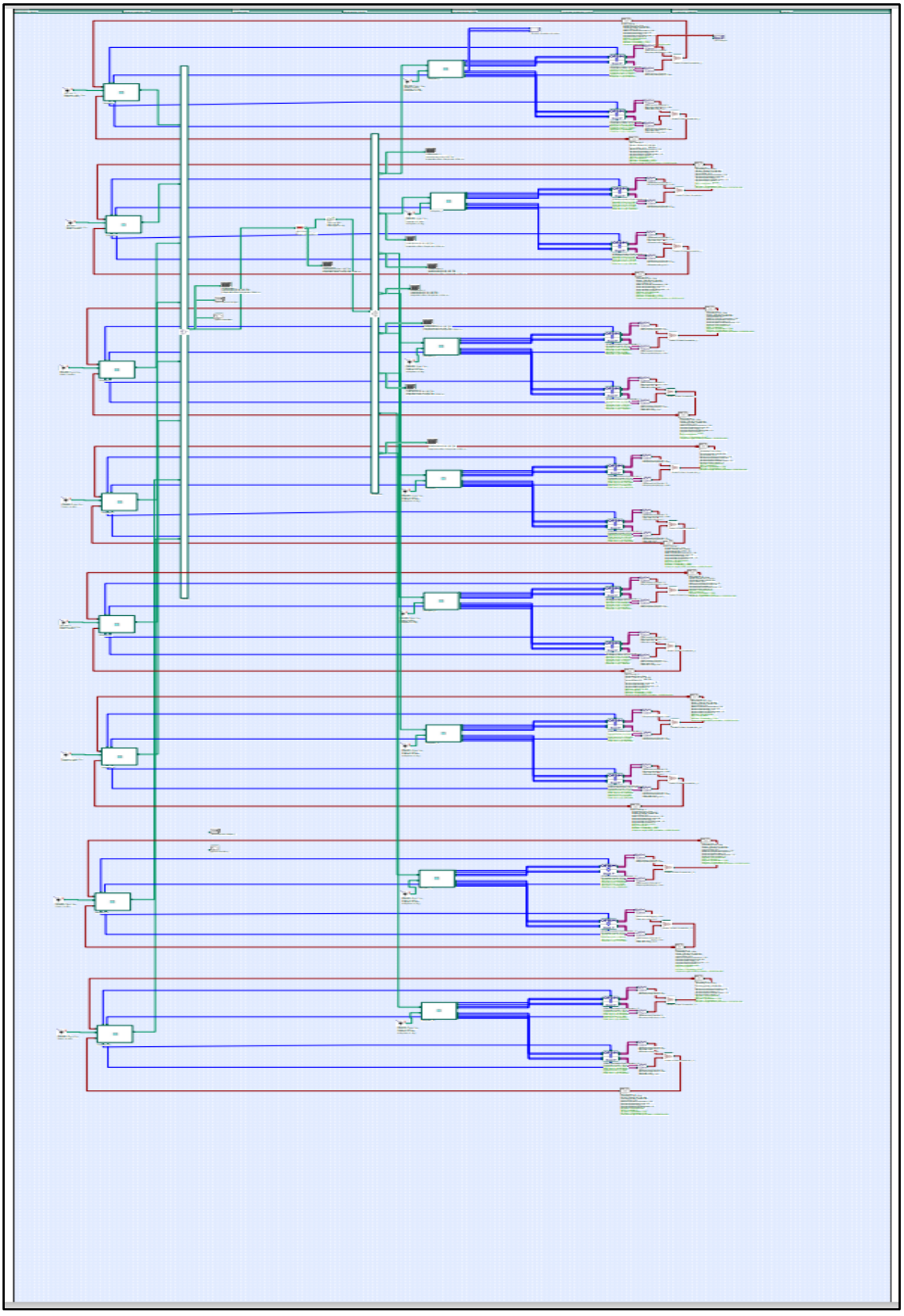

Figure 3.20: The Overall Design Of The Proposed System.

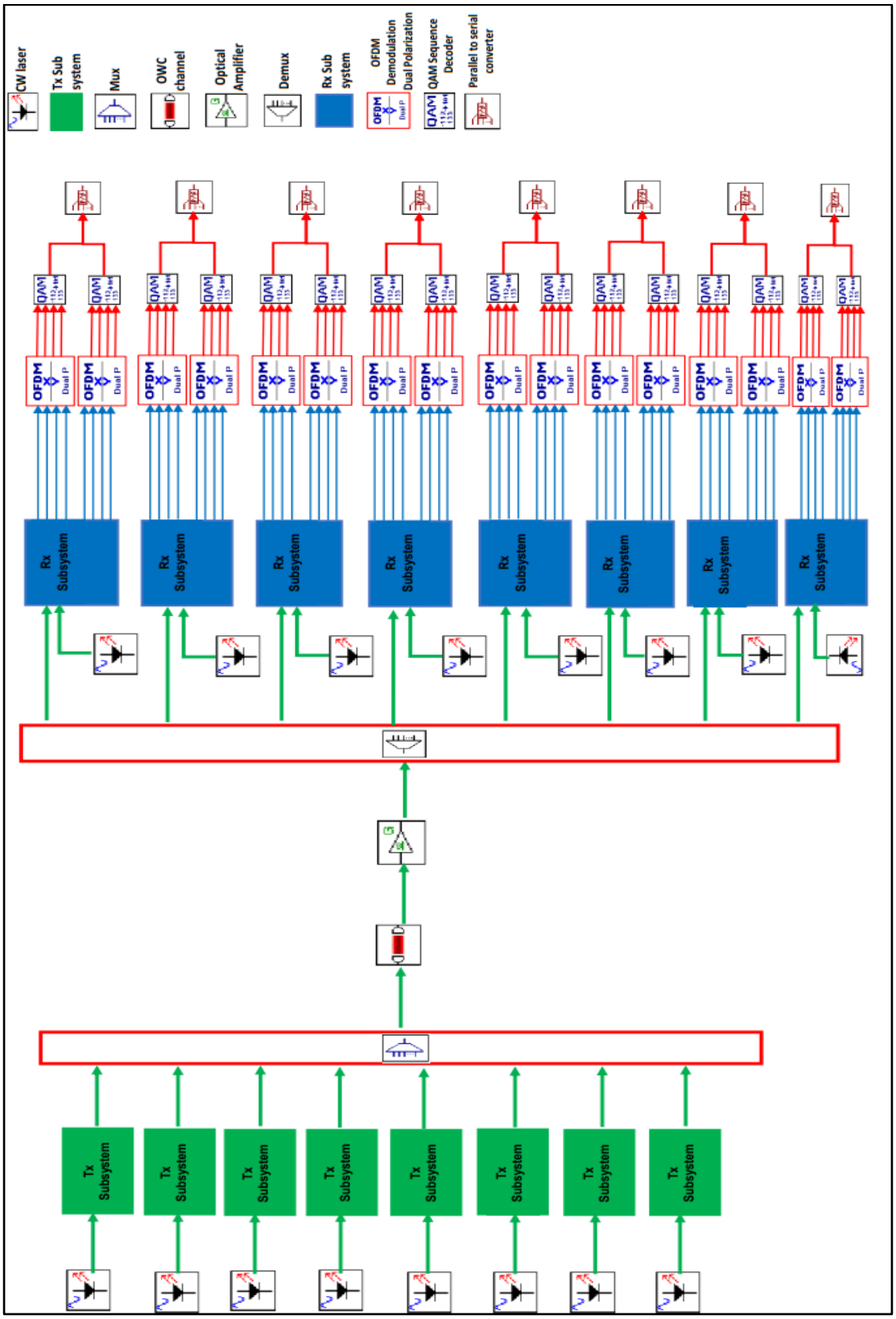

Figure 3.21: Schematic View Of The Proposed System.

Then every mode is taken care of with two polarization splitters at 90° to shape the optical info arm of the used double-port MZM. The result power for the MZM can be communicated as in condition 3.10 [87]. For each set of the result signal from MZM, one result will be taken care of with a stage shifter of 90° to give a period stage postponement to the result MZM signal for every polarization per mode, as exhibited in condition 3.11.

$$E_0(t) = \frac{E_{in}(t)}{10^{(\frac{IL}{20})}} \cdot \left[\left(\frac{\left(1 - \frac{1}{\sqrt{10^{ExRatio/10}}}\right)}{2} \right) . e^{(\frac{j\pi v2(t)}{V_{\pi RF}} + \frac{j\pi vbias2}{V_{\pi DC}})} + (1 - \left(\frac{\left(1 - \frac{1}{\sqrt{10^{ExRatio/10}}}\right)}{2} \right) . e^{\left(\frac{j\pi v1(t)}{V_{\pi RF}} + \frac{j\pi vbias1}{V_{\pi DC}}\right)} \right] \quad (3.10)$$

Where $E_{in}(t)$ represents the optical input signal from the ODFM modulator, IL is the loss of insertion, $v1(t)\ and\ v2(t)$ are the electrical voltage entered for the two side arms of the MZM, $vbias1\ and\ vbias2$ represents the voltage v1 and v2 bias respectively, $V_{\pi RF}$ and $V_{\pi DC}$ are the switching voltage for modulation and bias respectively and $ExRatio$ represents the Extension Ration set for the MZM [87].

$$E\ out\ (t) = E\ in\ (t) * exp(j\Delta\Phi) \quad (3.11)$$

Where $E\ in\ (t)$ represents the outputted optical power, and Φ is the amount of the phase shift.

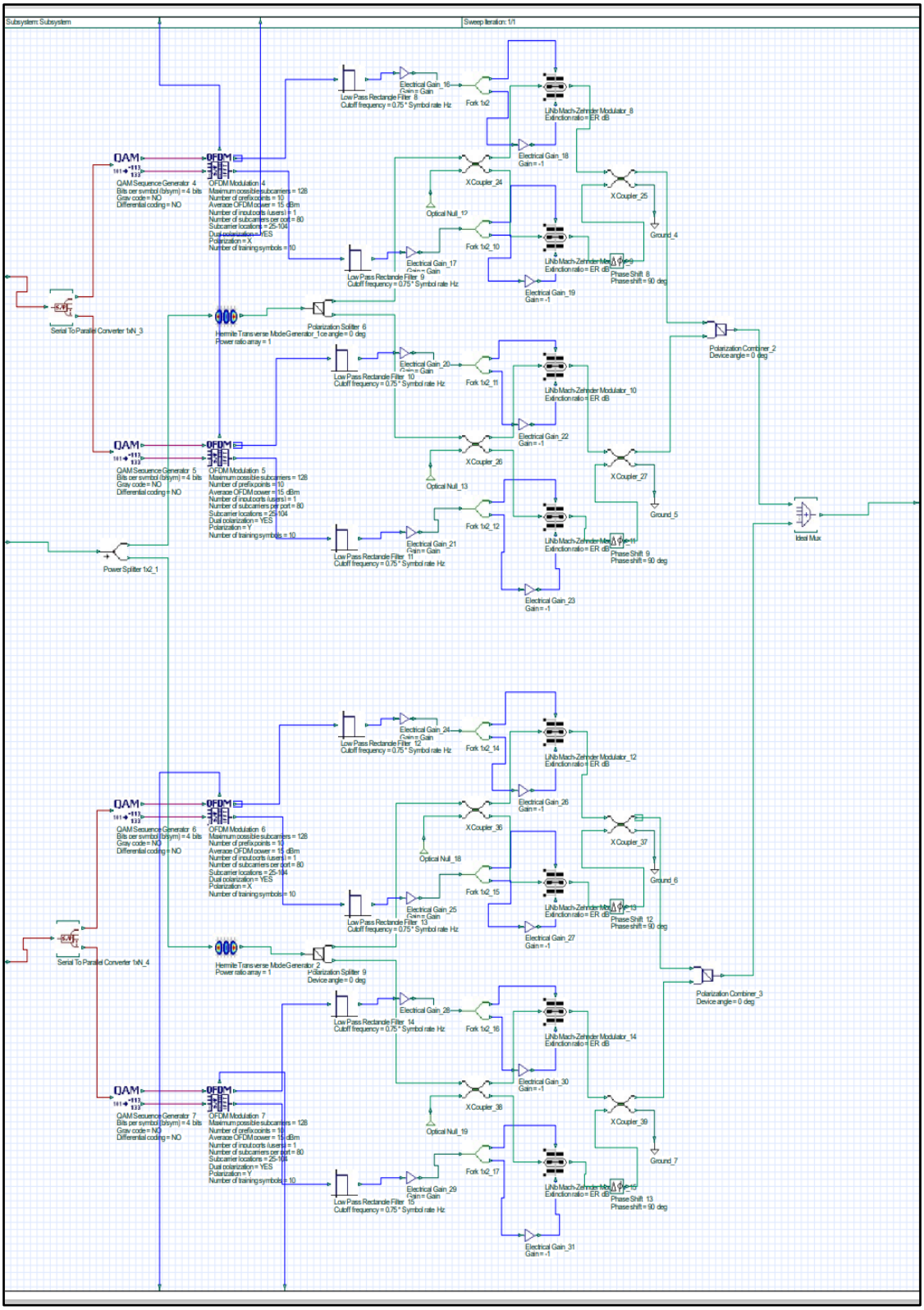

Figure 3.22: Subsystem Design Of The Tx Part Using Optisystem.

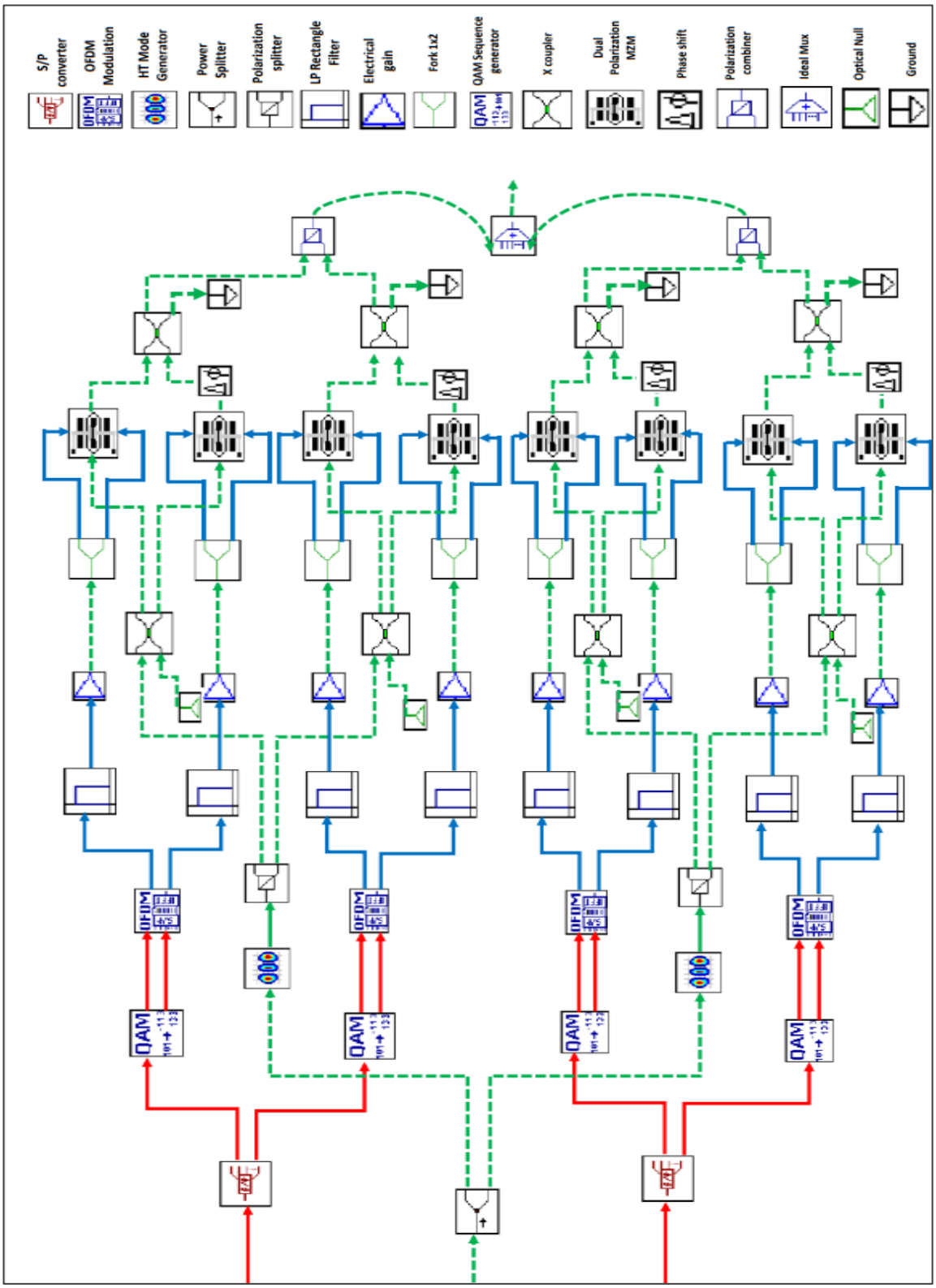

Figure 3.23: A Schematic Design For The Tx Subsystem Of The Proposed System.

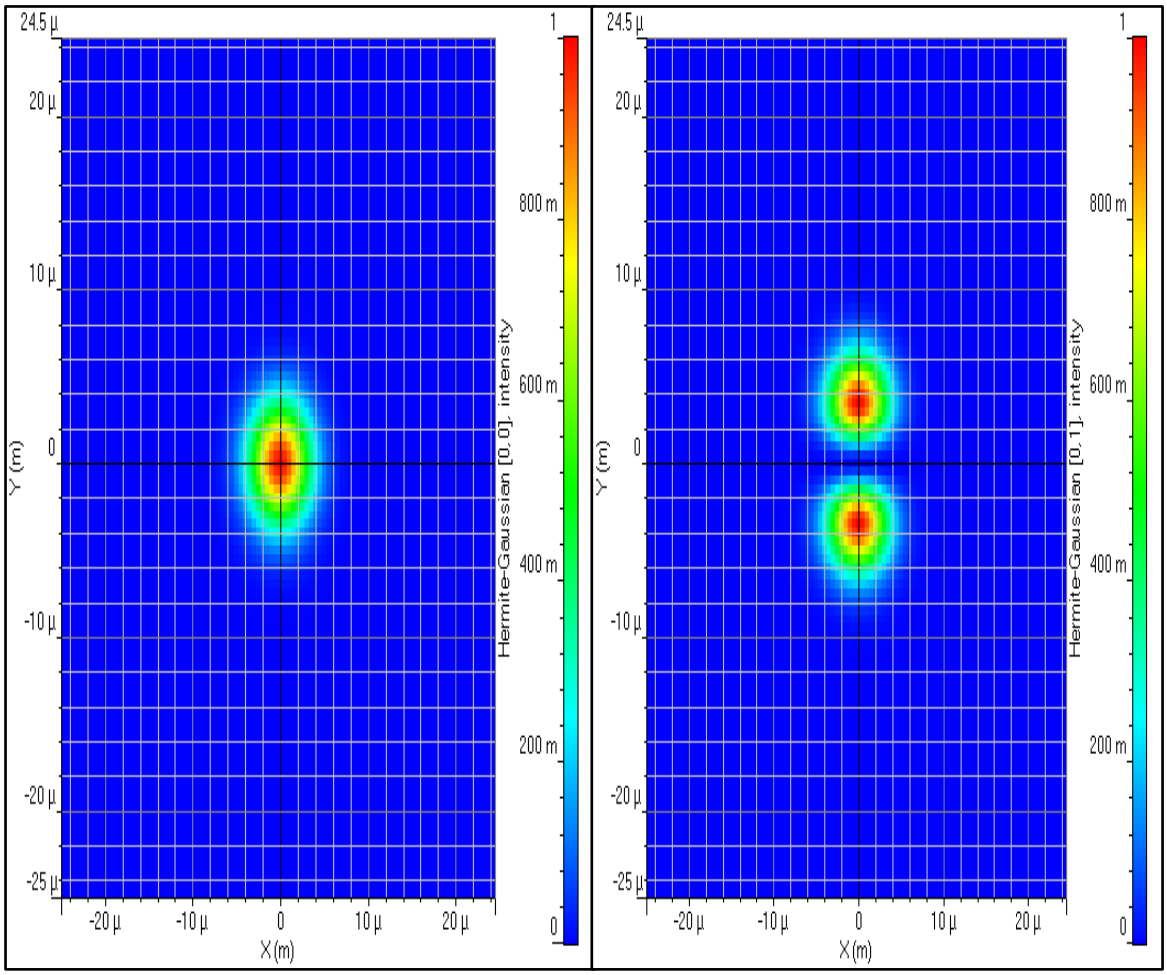

Figure 3.24: Excited Modes Of HG a) Represent HG 00 And b) Represents HG 01.

To wrap things up, a MUX is utilized to blend the sign that was delivered by the two ports. From that point forward, the result from every ideal MUX for every one of the eight channels is thought about as a contribution for the WDM MUX. This MUX will total every one of the channels into a solitary connection that will be designed for transmission by means of Is-OWC. Recorded in Table 3.3 is the boundary set that relates to the boundaries that were utilized in this segment.

Table 3.3: Components Selected For The Tx Part Of The Proposed System.

Component	Parameter	Value
CW Laser	Frequency	193.1-193.8
	Power	14
	Linewidth	0.1
S/P Converter	Number of output ports	2
QAM sequence generator	Bits per symbol (b/sym)	4
	Constellation type	Square/Rectangular
OFDM Modulation	Maximum possible subcarriers	128
	Symmetric spectrum	0
	Number of prefix points	10
	Average OFDM power	15
	Number of input ports (users)	1
	Number of subcarriers per port	80
	Subcarrier locations	25-104
LP Rectangle Filter	Cutoff frequency	0.75 * Symbol rate
Hermite Transverse Mode Generator	Power ratio array	1
	Mode polarization	X and Y
	Pol. X m, the n index array	0 0, 0 1
	Pol. X spot size X	5
	Pol. X spot size Y	5
	Pol. Y m,n index array	0 0, 0 1
LiNb Mach-Zehnder Modulator	Extinction ratio	ER
	Switching bias voltage	4
	Switching RF voltage	4
	Insertion loss	1
Ideal MUX	Number of input ports	2
	Loss	5
Simulation window	Bit rate	3.20E+11
	Time window	2.05E-07
	Sample rate	3.20E+11
	Sequence length	65536
	Symbol rate	4.00E+10
	Number of samples	65536
	Reference wavelength	193.1
	MDM pol Spot size	5
	Gain	2
	Electrical Gain	18
	ER	40
WDM MUX	Number of input ports	8
	Bandwidth	70

3.8.2 OWC Transmission Part

The part of the OWC medium makes up the transmission segment, which is then trailed by an optical speaker that enhances the sign that is being conveyed. Inequation 3.12 [88] might be utilized to give explanation about the displaying of the Is-OWC medium.

$$P_R = P_T \eta_T \eta_R \left(\frac{\lambda}{4\pi Z}\right)^2 . G_T G_R . \exp(-G_T . \theta_{T^2}) . \exp(-G_R . \theta_{R^2}) \quad (3.12)$$

Where P_R and P_T are the optical power for Rx and Tx respectively, $\eta_T \; and \; \eta_R$ are the optical efficiency for the Tx and Rx accordingly, Z represents the range, λ is the wavelength, $. G_T \; and \; G_R$ are the gains for Tx and Rx antenna which are given by 3.13 and 3.14 respectively. And $\theta_T \; and \; \theta_R$ are the Pe for the Tx and Rx respectively, which are considered as Pe factors [88]:

$$G_T = \frac{\pi D_T}{\lambda^2} \quad (3.13)$$

$$G_R = \frac{\pi D_R}{\lambda^2} \quad (3.14)$$

Where D_T and D_R represents the Tx and Rx antenna diameter for the telescope. The parameters set for this part component are listed in Table 3.4.

Table 3.4: Component parameters for the OWC part of the proposed system.

Component	Parameter	Value
Is-OWC channel medium	Frequency	193.1
	Range	varied
	Free space path loss	included
	Geometrical gain	included
	Transmitter aperture diameter	15
	Receiver aperture diameter	30
	Transmitter telescope gain	120
	Receiver telescope gain	100
	Transmitter optics efficiency	included
	Receiver optics efficiency	included
	Transmitter Pe angle	varied
	Receiver Pe angle	varied
Optical Amplifier	Operation mode	Gain Control
	Gain	36

3.8.3 Receiver Part (Rx)

The multiplexed signal that was sent over the OWC channel is demultiplexed with a 1x8 DEMUX, and afterward each channel is demonstrated with a Rx subsystem that starts with a spatial DEMUX part that isolates a client determined number of WDM spatial sign channels prior to removing all spatial modes that are related with each channel. This interaction is rehashed for each channel. With regards to the Rx part, this is finished. From that point onward, every mode is moved to a polarization Splitter, what parts the mode into a symmetrical polarization for every one of the two-channel port and four-connect per port, separately, to address the 16 QAM's four pieces. This cycle is rehashed until the mode is finished. Furthermore, a photodetector is responsible for dealing with each port. This piece of equipment is responsible for the errand of changing over optical motivations into electrical driving forces. In the last phase of the demodulation cycle, each four associations for each port and each channel are projected to a double polarization OFDM demodulator. This is finished to forestall any impedance. The OFDM signal is consequently changed over into a computerized M-ary signal with the utilization of this procedure. Because of the way that it was grown exclusively for OFDM frameworks that utilization double polarization multiplexing, its application is restricted exclusively to those frameworks who utilize this strategy.

A QAM grouping decoder gets the result of the last option, and it is liable for changing over the two simultaneous QAM M-ary image successions into a double sign. Unravelling the result of the last option is made conceivable subsequently. The double sign that is moving from the two ports that are shared by each channel is associated with the Lined up with Sequential (P/S) converter since it is associated with the sign. Delineations 3.25 and 3.26, separately, represent the association that exists between the interior schematic demonstrating of the Rx subsystem and the displaying that depends on the Optisystem. Inside the Rx subsystem, you will find both associations. It is likewise essential to take note of that Table 3.5 incorporates an outline of the boundaries that were utilized in the assessment of this part.

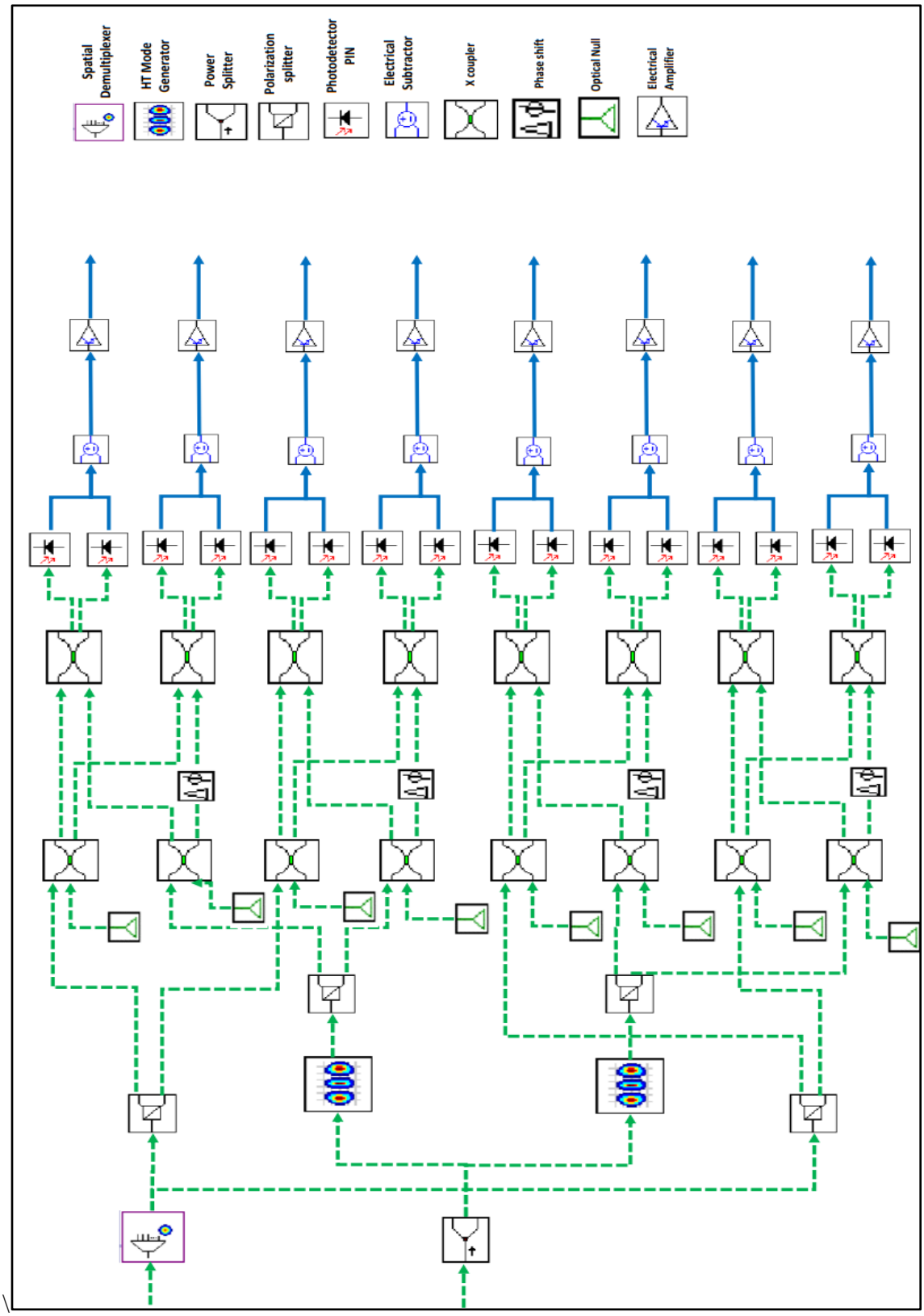

Figure 3.25: A Schematic Design For The Rx Subsystem Of The Proposed System.

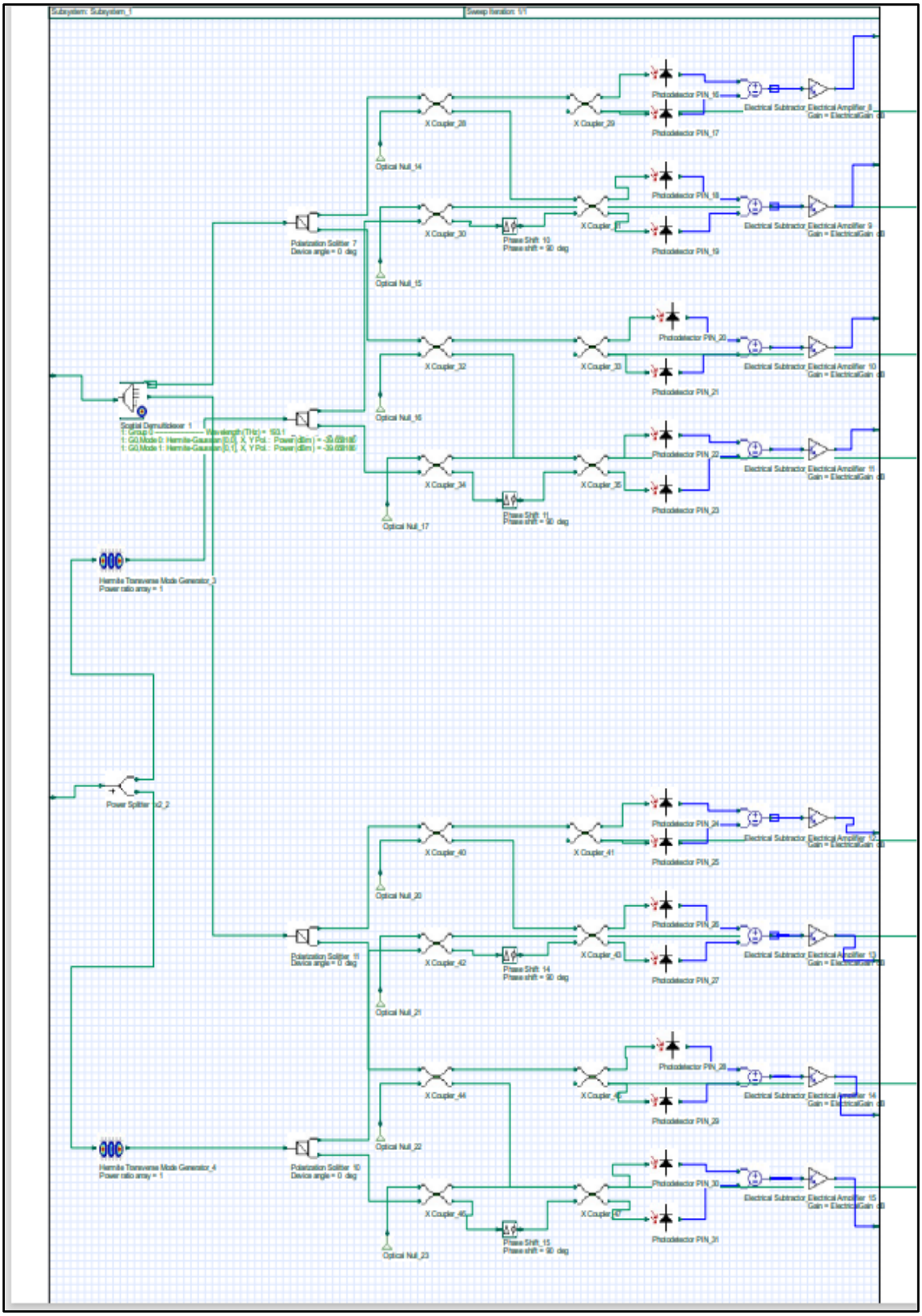

Figure 3.26: Subsystem Design Of The Rx Part Using Optisystem.

Table 3.5: Components Selected For The Rx Part Of The Proposed System.

Component	Parameter	Value
WDM DEMUX	Number of output ports	8
	Bandwidth	90
Spatial DEMUX	Number of wavelengths	1
	Bandwidth	60
	Insertion loss	0
	Depth	100
	Filter type	Bessel
	Filter order	2
	Number of spatial modes	2
X coupler	Coupling coefficient	0.5
	Additional loss	0
	Conjugate	included
Phase shift	Phase shift	90
PIN Photodetector	Responsivity type	Constant
	Responsivity	1
	Dark current	10
	Noise calculation type	Numerical
Electrical Amplifier	Gain	Electrical Gain
	Include noise	1
	PSD	0
	Average noise power	-80
	Noise power spectral density	-60
	Maximum possible subcarriers	128
	Enable Dispersion Compensation	1
	Number of training symbols	10
	Location of pilot symbols: X	25,44,64,65,84,104
	Location of pilot symbols: Y	25,44,64,65,84,104
	Number of output ports (users): X	1
	Number of subcarriers per port: X	80
	Subcarrier locations: X	25-104
	Subcarrier phases: X	0
	Modulation type per port: X	16QAM
	Constellation type (if QAM) per port: X	Square
	Channel Wavelength	193.1
	DC Reference Wavelength	193.1
	Dispersion Coefficient	16.75
	Residual Dispersion Slope	0.075
	Propagation Length	0.5
QAM Sequence Decoder	Bits per symbol (b/sym)	4
	Constellation type	Square

It is worth mentioning, that the Optisystem-based simulator provides the capability to convert and work with the script as well as Graphical User Interface (GUI) window design. As a result of that, in Appendix B, the code script for the designed system mentioned in this section has been formulated to give brief details of the tools utilized, components, and the parameter values set for each component. The code script for the proposed WDM Is-OWC OFDM with hybrid MDM and PDM was generated in Visual Basic (VB) language, which can be easily studied and followed. In addition, the targeted code script only represents the code generation for a single channel of the proposed 8-channel WDM system.

3.9 METHODOLOGY OF THE PROPOSED SYSTEM

This section will demonstrate the methodology of the proposed topic in this thesis to meet the objectives mentioned in chapter one and to give a sky-view look at the novel method proposed in this thesis. Thus, the methodology carried out for the WDM-Is-OWC OFDM with 16 QAM modulation and hybrid MDM & PDM can be summarized in the below points and further clarified as seen in the flowchart in Figure 3.27.

a. The first step is to design the proposed system with 8 channels by using the Optisystem program and using the techniques of OFDM and 16 QAM modulation techniques, which have been shown in the previous section. The utilization of OFDM is to modulate the digital data created into 128 orthogonal subcarriers.
b. The following step includes using the MDM technique that has been clarified earlier in this chapter, which will send the data by using two intensity profiles of higher order modes known as the HG modes, where two modes of HG00 and HG01 will duplicate the transmitted channel per each polarization to be transmitted by using two modes.
c. After that, involve the utilization of the PDM components from the Optisystem program to separate the transmission line into two lines, where the first line has a polarization of 0 degrees and the second of 90 degrees. This method has been used to improve the capacity of the proposed system, where it can double the total data rate transmitted.
d. By using the required MUX components to combine the generated lines from the previous two steps to appropriate it for transmission.
e. In this step, the out data from the MUX will be transmitted via the dedicated Is-OWC medium.

f. At the Rx side, the first step considered is to recombine the transmitted 8 channels by using the WDM DEMUX. Then each channel will handle a few steps individually for handling the separation of modes and polarization. For the two generated modes, the received data from the individual channels will be handled by using a special spatial demultiplexer to separate the modes.
g. The next step will handle the separation of the PDM technique per each generated mode and by using the required tools to further convert the optical to electrical signal form by using the PIN photodetector.
h. Then prepare the transmitted data for the OFDM dual polarization demodulation procedure and the demodulated signal will be handled by a 16 QAM decoder.
i. Run the Optisystem program for performing the calculations and to achieve the objectives of the proposed thesis. These objectives are as follows:

The first objective: is to design a novel system by using incorporating hybrid division techniques to boost the data rate to achieve a higher impact. And achieve transmission for higher distances to satisfy GEO-based ranges. This objective will be evaluated in the next chapter based on the different performance metrics.

Second objective: is to study the impact of different space turbulence on the performance of the proposed system such as the Pe to quantify the reliability of the proposed novel system of this thesis. It is worth mentioning that the description of each component to demonstrate its terminology were listed in Appendix C.

Third Objective: to study the impact of antenna diameter variation on the Tx and Rx satellite concerning the utilization of the proposed system methodology mentioned earlier in this section. This objective aims to highlight the impact of change in the antenna size will affect the usage of hybrid techniques of MDM & PDM.

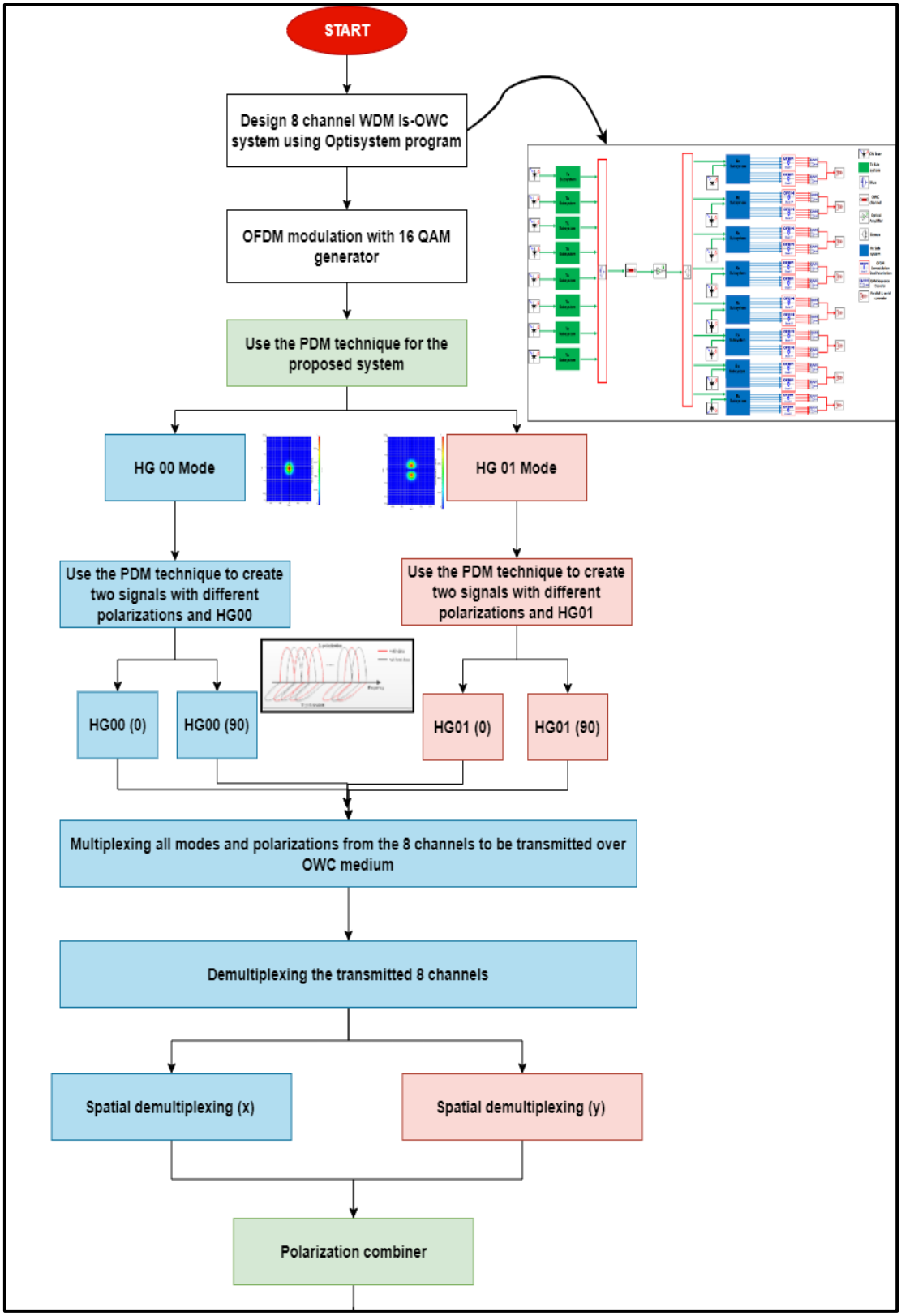

Figure 3.27: Flowchart Describing The Methodology Of The Proposed System.

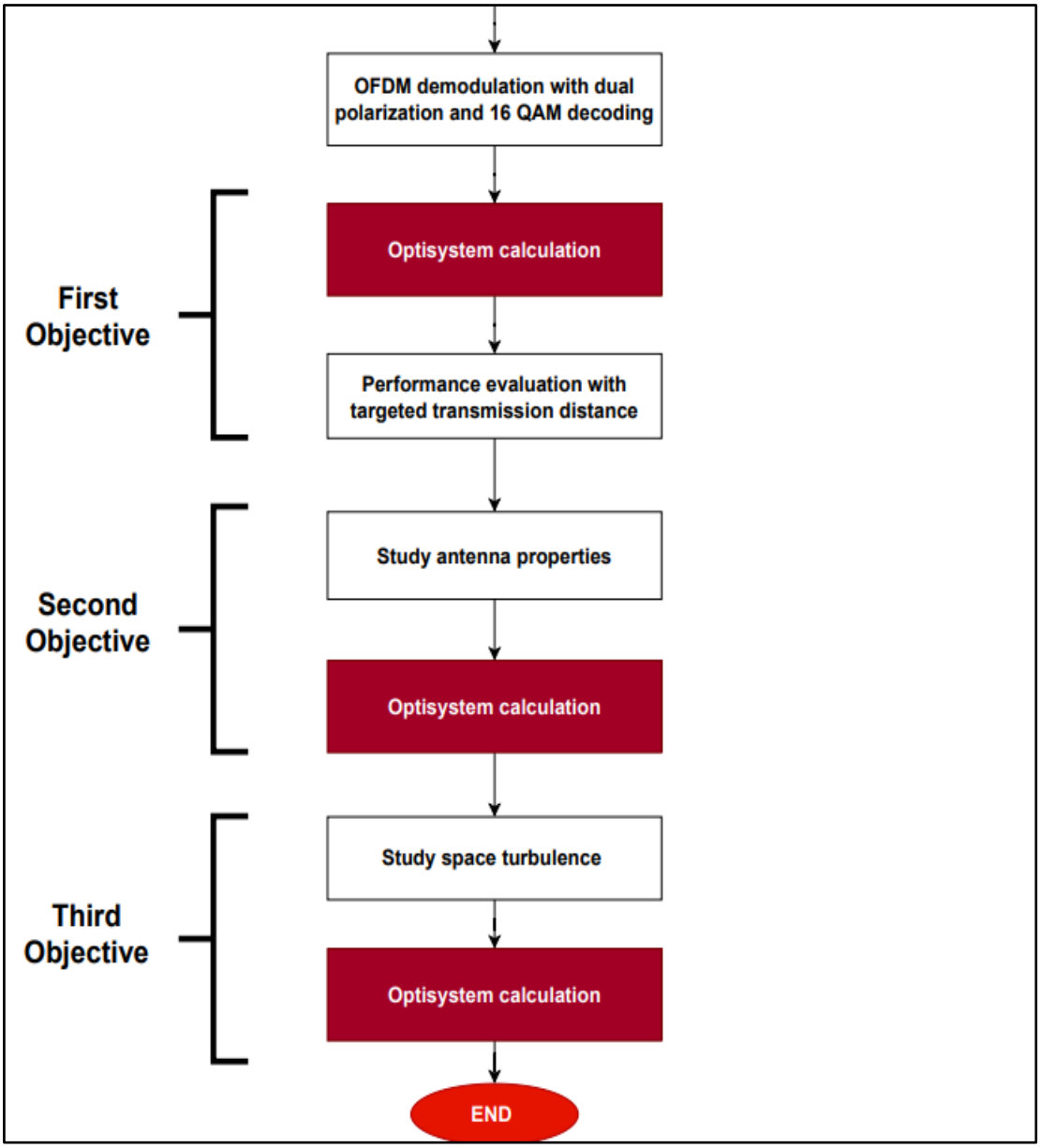

Figure 3.27: Flowchart Describing The Methodology Of The Proposed System "Figure Continued".

3.10 ATMOSPHERIC EFFECTS ON OWC

This section will discuss and highlight all the effects that are related to the atmosphere and can have a serious effect on the OWC between satellites.

3.10.1 Atmospheric Attenuation

When the signals are travelled across the atmosphere, it suffers from different losses. First to start with the impact of attenuation suffered by signal power can be obtained according to Beers law and as expressed in equation 3.15 [89].

$$h(z,\lambda) = \frac{P(z,\lambda)}{P(0,\lambda)} = \exp\,(-\Phi(\lambda)z) \tag{3.15}$$

where $h(z,\lambda)$ represents the loss that depends on the path length of the propagated signal (z) and the wavelength, $P(z,\lambda)$ and $P(0,\lambda)$ is the signal power and emitted power at z distance respectively, $\Phi(\lambda)$ represents the attenuation coefficient and can be calculated as seen in equation 3.16 [89].

$$(-\Phi(\lambda) = \Phi\mathrm{m}(\lambda) + \Phi\mathrm{a}(\lambda) + \beta\mathrm{m}(\lambda) + \beta\mathrm{a}(\lambda) \tag{3.16}$$

Where Φm and Φa represent the coefficient of absorption for molecular and aerosol respectively, and the βm and βa are the scattering coefficient for the same set mentioned above respectively. When performing a transmission distance over a long range, the attenuation would be assumed to be constant. Thereby, the attenuation factor $\Phi(\lambda)$ can be calculated as in equation 3.17 [89].

$$\Phi(\lambda) = \frac{3.912}{v}\left(\frac{\lambda}{550}\right)^{-q} \tag{3.17}$$

$$q = \begin{cases} 1.6\ when\ v\ is\ greater\ than\ 50\ km \\ 1.3\ when\ v\ between\ 6\ km\ to\ 50\ km \\ 0.585 * v^{\frac{1}{3}}\ when\ v\ is\ less\ than\ 6\ km \end{cases}$$

Where q represents the parameter dependency on particle size as expressed by the Kruse model and v is the visibility measured in km.

3.10.2 Misalignment Fading

This is also known as the Pe, when the signal is travelled between a satellite in space it would require higher accuracy in beamwidth pointing. As a result, it will affect the performance and reliability of the satellite system. Pe essentially happened on the Rx side due to many reasons that will affect the antenna of the Rx and make it move from its location. Also, another reason for Pes is the movement of the earth and its impact on the accuracy of the received signal. The demonstration of Pes can be seen in Figure 3.28 [90].

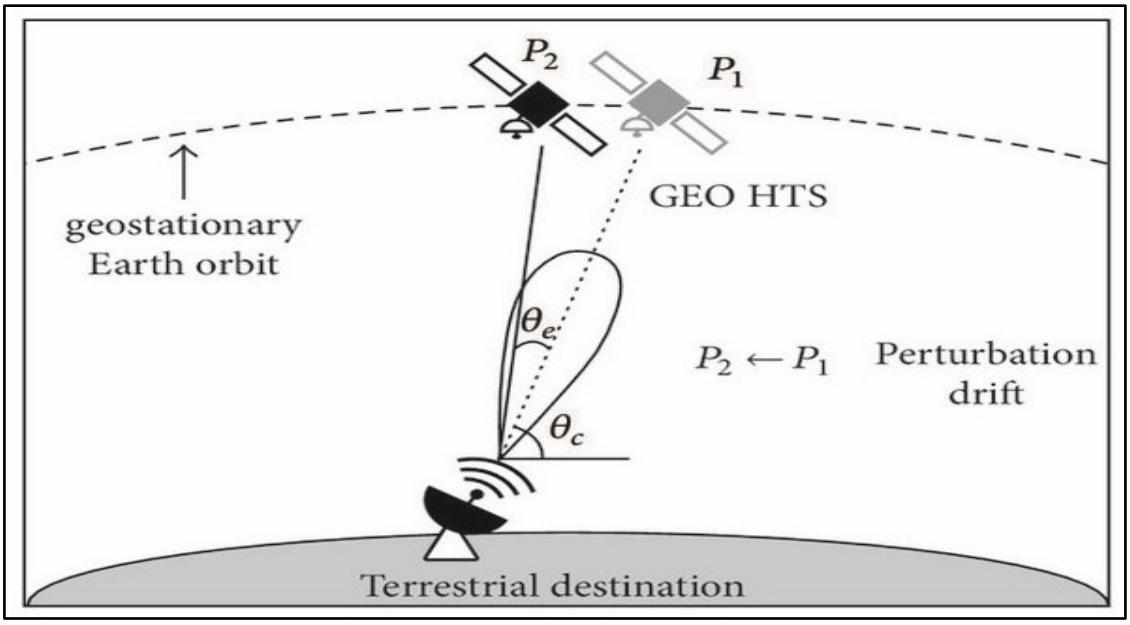

Figure 3.28: Demonstration Of Pointing Error In Satellite Communication [90].

By considering the θ equal to the summation of the θc and θe which represents the satellite elevation and the elevation error respectively. θe lies between the starting angle of the beam transmitted from P1 and the drifted actual satellite location P2. As a result, θ and θc can be calculated from equation 3.18 and equation 3.19 respectively [90].

$$\theta = \arctan\left[\frac{sin\Delta\varphi \sin\Phi + cos\Delta\varphi \cos\Phi cos(\lambda+\Delta\lambda) - 0.151}{\cos\left[\arcsin\left[sin\Delta\varphi \sin\Phi + cos\Delta\varphi \cos\Phi cos(\lambda+\Delta\lambda)\right]\right]}\right] \quad (3.18)$$

$$\theta c = \arctan\left[\frac{cos\Phi cos\lambda - 0.151}{\cos\left[\arcsin\left(cos\Phi cos\lambda\right)\right]}\right] \quad where\ \Delta\varphi = 0 \quad (3.19)$$

Where Φ is the destination latitude, $\lambda = \lambda tx - \lambda rx$ is the difference in latitude between the Tx point and the Rx point, $\Delta\varphi$ is the amount of drifting for the satellite in the north-south direction, $\Delta\lambda$ is the amount of drifting in the east-west direction.

Hence, now it become relatively easy to calculate the θe by subtracting θ from θc. It is worth mentioning, that λrx can be obtained generally from the six elements of the satellite's elliptical orbits, where it is important to obtain the latitude and longitude angels of the satellite that are denoted as $l_{lat}\ and\ l_{lon}$ and as expressed in equation 3.20 and equation 3.21 respectively [90].

$$l_{lat} = \arcsin\left\{\sin i\,.\sin\left[w + 2arctan\left(\sqrt{\frac{1+e}{1-e}}\tan\frac{E}{2}\right)\right]\right\} \tag{3.20}$$

$$l_{lon} = r + \arctan\left\{\cos i\,.\tan\left[w + 2arctan\left(\sqrt{\frac{1+e}{1-e}}\tan\frac{E}{2}\right)\right]\right\} - w_e(t - tn) \tag{3.21}$$

where *i* represents the orbit indication, *E* is the eccentric anomaly, w_e is the average angular velocity of the earth, t is the time, tn is the time of the satellite when passes the ascending node. And by obtaining the $l_{lat}\ and\ l_{lon}$ for the case of with and without Pe then it will become easy to obtain the $\Delta\varphi$ and $\Delta\lambda$ by considering the difference between the two values.

3.11 STUDIED PARAMETERS

This section will present the parameters to be studied to evaluate the performance of the proposed system as follows:

3.11.1 Bit Error Rate (BER)

The BER is the level of pieces got in a transmission that remember botches for correlation with the complete number of pieces got. In the space of transmission for broadcast communications, this rate is frequently communicated as "ten to the power less a number," which is likewise one of its not unexpected documentations. The BER means that the times a bundle or different information unit must be dislike considering an error. Assuming the BER is excessively high, it might infer that a lower information rate will further develop the complete transmission time for a given measure of information that was moved. This is on

the grounds that the BER might be brought down by utilizing a slower information rate, which will bring about fewer bundles that should be despise. If the BER is exceptionally high, this might be the outcome. Condition 3.22 might be utilized to decide BER when only one polarization is utilized. While it is feasible to work out the BER for the double polarization framework as it is depicted utilizing condition 3.23, individual computations for the two ports of each channel that are addressed by either the x side or the y side can be gotten utilizing condition 3.24. These conditions can be found underneath. [91-94].

$$BER = \frac{Error\ Bit}{Sequence\ length - 2.Guardbits} \tag{3.22}$$

$$BER = \frac{x\ Error\ Bit + y\ Error\ Bit}{Sequence\ length - 2.Guardbits} \tag{3.23}$$

$$BERx|y = \frac{x|y\ \ Error\ Bit}{(Sequence\ length - 2.Guardbits)/2} \tag{3.24}$$

3.11.2 Receiver Sensitivity

In the back-to-back setup, receiver sensitivity is defined as the minimal amount of optical signal power that is received at a certain BER. This is the standard way of measuring Rx performance. This value gives an indication of how well the Rx was designed. When the receiver's sensitivity is increased, the system's performance in terms of longer transmission distance and increased tolerance to fiber impairments also improves [95].

On the other hand, receiver sensitivity is not the most important metric to consider for long-haul systems that include a large number of optical amplifiers. The receiver sensitivity is replaced by the Optical Signal-to-Noise Ratio (OSNR) as the foundation for performance comparison in the optically amplified long-haul system. In spite of this, back-to-back receiver sensitivity remains an effective performance metric for high-speed receiver design. The sensitivity of the optical receiver is one of the parameters of optical receivers that are utilized most often in fiber-optic networks. It is defined as the minimal amount of signal optical power that must be present at the receiver in order to accomplish a desired degree of BER performance. For the BER to be less than 10^{-12} in a particular optical system, the minimum signal optical power that must reach the receiver must be no less than 35 dBm; as a result, the receiver sensitivity is 35 dBm [96].

3.11.3 Optical Signal-to-Noise Ratio (OSNR)

Quantifying the amount of optical noise that interferes with optical signals is accomplished with its help. After passing via an optical network, a channel's OSNR is determined by calculating the ratio of the signal power to the noise power in that channel. It provides an evaluation of the extent to which the signal power has been influenced by the noise power. The value of the OSNR should be increased according to how beneficial it is for the system. The OSNR is a key criterion for assessing how effectively the proposed system will perform, and its value may be computed by applying equation 3.25 to the data provided [36]. The concept of obtaining the OSNR can be seen in Figure 3.29 [94].

$$OSNR = 10.\log_{10}\frac{Signal\ power}{Noise\ Power} \tag{3.25}$$

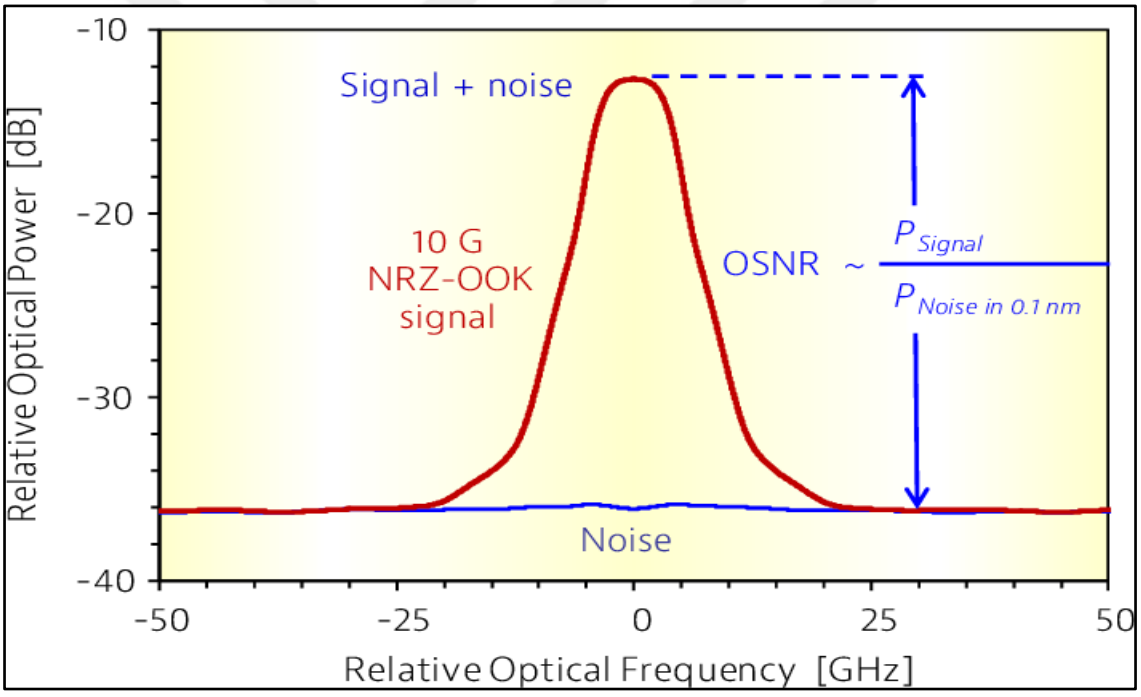

Figure 3.29: OSNR From The Variation Of Optical Power And Frequency [97].

The OSNR is significant because it indicates the level of degradation that occurs when an optical signal is sent using an optical transmission system that has optical amplifiers. optical signals are susceptible to a wide variety of disturbances, including a decrease in power as well as polarization and dispersion. Therefore, leading to random noise, which in turn causes misalignments, jitter, and other disturbances, which ultimately result in erroneous bits at a rate known as BER.

3.11.4 Error Vector Magnitude (EVM)

is a well-known system-level performance statistic that serves as a compliance test for several communication standards, including Wireless Local Area Networks (WLAN 802.11), mobile communications (4G LTE, 5G), and a lot of other communication standards. In addition to this, it is an immensely important system-level statistic that can quantify the cumulative effect of all the possible impairments in a system via a single and simple to comprehend number. This may be done by calculating the system's overall availability. In addition to this, the EVM is the Root Mean Square (RMS) of the error vectors that have been calculated and represented as a percentage of the EVM Normalization Reference. EVM is the length of the vector that links the I/Q reference-signal vector to the I/Q measured-signal vector. This length is measured at the position where the symbol was detected. Figure 3.30 presents an illustration of the computation of the EVM metric, as well as a diagram illustrating the process of calculating a single error vector [98].

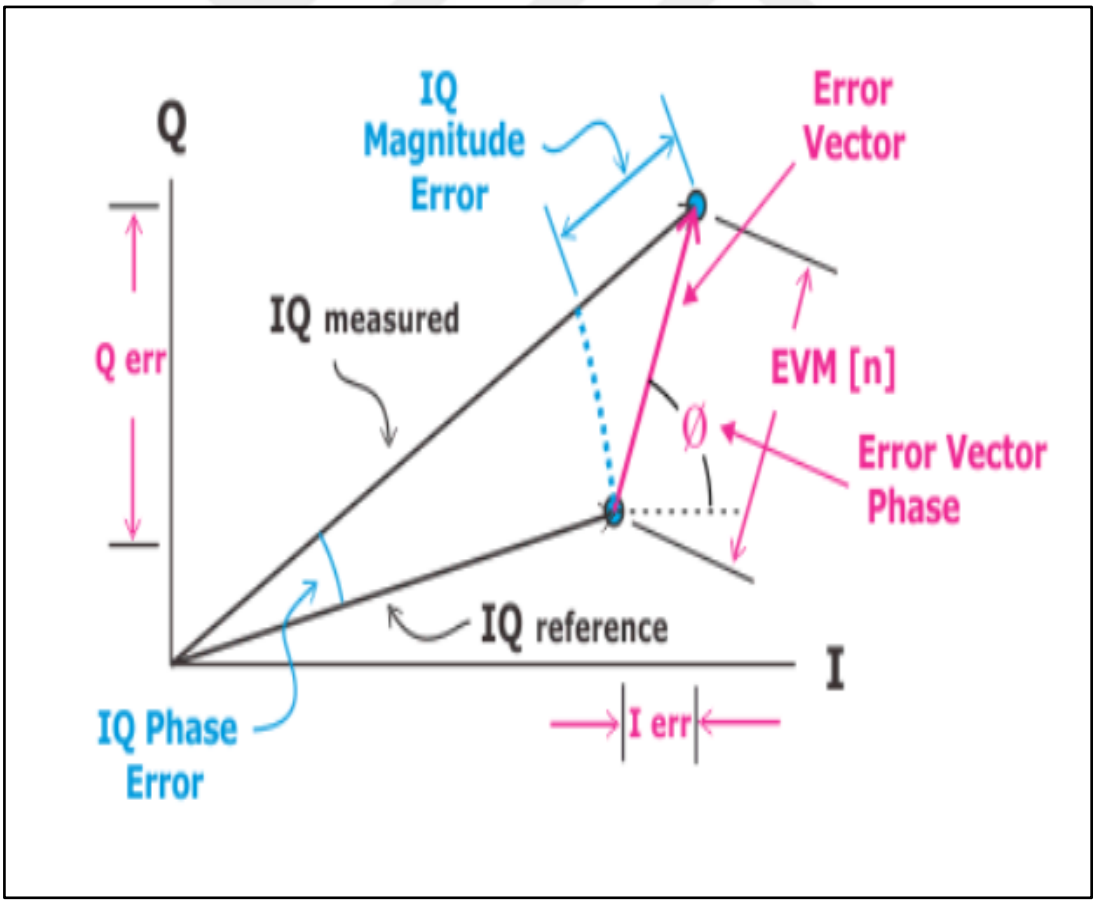

Figure 3.30: EVM Concept [98].

When handling the OFDM for system implementation, the EVM can be calculated with respect to the total number of OFDM subchannels N and as seen in equation 3.26 and as clarified in Figure 3.31 [99].

$$EVM\ rms = \sqrt{\frac{\frac{1}{N}\sum_{n=1}^{N}|Z_n - S_n|^2}{\frac{1}{N}\sum_{n=1}^{N}|Z_n|^2}} \tag{3.26}$$

Where Z_n is the reference symbol, and S_n is the nth received symbol. When handling M-ary square QAM, the BER can be calculated with respect to the error function and SNR as in equation 3.27.

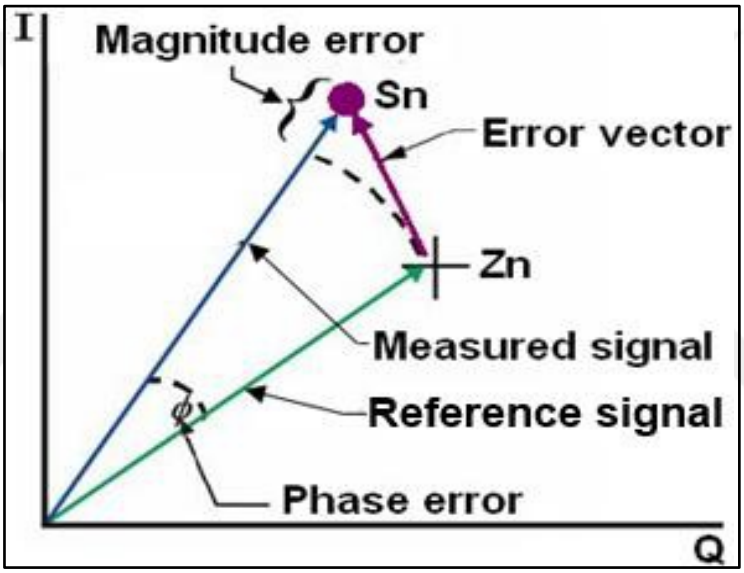

Figure 3.31: The Visualization Of EVM In IQ Plane [99].

$$BER \cong \frac{\sqrt{M}-1}{\sqrt{M}\log_2\sqrt{M}}\ .erfc\left[\sqrt{\frac{3\log_2 M.\gamma}{2(M-1)}}\right] \tag{3.27}$$

Where $erfc$ (x) is the error function and γ is the SNR value. It is worth mentioning that there is a reverse relation with respect to the SNR value as expressed in equation (3.28) [99].

$$BER \cong \frac{1}{\sqrt{\gamma}} \tag{3.28}$$

As a result, BER can be obtained with respect to EVM for an M-ary square QAM as in equation (3.29) [99].

$$BER \cong \frac{2\sqrt{M}-1}{\sqrt{M}\log_2\sqrt{M}} \cdot Q\left[\frac{\sqrt{2}}{EVM}\sqrt{\frac{3\log_2 M}{2(M-1)}}\right] \quad (3.29)$$

Where Q is the quality factor for the received signal.

3.12 APERTURE DIAMETER

The region around an antenna in which power may be extracted by exploiting the effects of an electromagnetic field is known as the antenna aperture. The effective aperture of an antenna takes the form of a circular region around the antenna. This region is also referred to as the capture area. It is dependent on several elements, one of which is the density of the electromagnetic field that is present surrounding the antenna. Another component is the available voltage. The intensity of the signal being sent in a single direction determines the size of the antenna aperture in that direction. The gain will be stronger for apertures that are wider, whereas apertures that are smaller will only support a gain that is lesser. The effectiveness of an antenna aperture may be determined in a few different ways, one of which is by comparing the apertures of one antenna to those of another antenna. In order to characterize the antenna's aperture, a professional may take a measurement of the gain as well as the power in watts and then utilize mathematical calculations to do so. When compared to smaller devices, antennas that are larger in size often have larger apertures. However, the effective aperture of an antenna does not necessarily have a one-to-one correlation with the physical size of the antenna. Small antennas may now have apertures that are comparable in size to those of physically larger systems because of advancements in design components like shape, antenna type, polarization, and power [100].

The antenna acts as the connection point between the "guided wave" (which may be traveling over a coaxial cable, for instance) and the electromagnetic wave that is moving through free space. It is possible for an antenna to both broadcast and receive signals at the same time. The behaviour of antennas is the same regardless of whether they are operating as a transmitter or a receiver. The aperture antenna is the kind of antenna that is easiest to see in one's mind. An excellent example of an aperture antenna is the parabolic dish, which may be used for either microwave communications or ground stations for satellites. Gain of an aperture antenna grows with increasing antenna size and grows with rising frequency. Gain

also grows with increasing frequency. An estimated formula may be used to determine the gain of an antenna using a circular parabolic dish type of aperture [101].

$$Gain\ (dBi) \approx 18 + 20 \log D + 20 \log f \tag{3.30}$$

Where D represent the diameter of the antenna and f is the frequency.

The collimated beam of light is transmitted by the optical transmitter. The connection distance causes an increase in the width of the beam that is being broadcast. A lower link margin at the receiver side is caused by a wider beam width, which in turn leads to signal loss, a lower OSNR, and an increase in BER. On the receiver side, the diameter of the reception aperture must be bigger in size in order to receive all of the information that is conveyed by the optical carrier; yet, at the same time, a larger receiver aperture results in noise from the ambient light [102].

Hence, this thesis will include the investigation of the different values for the Tx and Rx aperture diameter as a third objective by studying their influence on the performance of the proposed system considering various distances up to 48,000 km.

3.13 ALTERNATIVE SYSTEM DESIGN

In this section, the alternative system designed by using other modulation technique of Dual Polarization-Differential Quadratic Phase Shift Keying (DP-DQPSK) and handled by using direct detection technique. The proposed system designed in Optisystem as seen in Figure 3.32, and the steps summarizing the alternative system design and methodology are lists below:

a. An 8 channel DP-DQPSK with direct detection method is designed.

b. Using the DP-DQPSK which is a method of modulation that may be found in digital communication systems, most notably optical communication systems. Digital Phase Shift Keying (DPSK) is a method for transmitting digital data that works by encoding information in the phase difference between successive symbols. In DP-DQPSK, the use of differential encoding is the most important innovation. It does this by recording the phase difference between the current symbol and the symbol that came before it rather than simply encoding the data bits onto the phase of the carrier signal. This encoding significantly lessens the

signal's susceptibility to any absolute phase changes that may take place inside the transmission channel. DP-DQPSK makes use of a 4-phase constellation diagram, which indicates that it provides a total of four distinct phase values for each symbol. There are four possible phase values: 0 degrees, 90 degrees, 180 degrees, and 270 degrees. Each distinct combination of two bits that make up the input data stands in for one of these phase values.

c. Direct detection refers to a method of extracting information from an optical signal without the need of keeping the phase information of the signal intact. This method is used to recover information.

d. In the context of communication systems, the manipulation of the data to be broadcast prior to its modulation into the carrier signal is performed by a precoder, which is a kind of digital signal processing. This thesis uses two precoding techniques called DPSK and Duobinary precoder to be used for the transmitter side of the alternative system and to be investigated over same tested distances towards 48,000 km. The primary goal of a precoder is to optimize the signal for transmission through a particular communication channel, taking into consideration factors like channel characteristics. The goal of modifying the broadcast signal using duobinary precoding is to do it in such a manner that it lowers the level of ISI without needing an extremely sophisticated receiver.

e. The comparison would be carried based on two precoding methods to quantify with the optimum and then compare the performance with the proposed novel system carried in this thesis. The aim of this work is to test more than one system and provide comprehensive analysis and evaluation of the proposed OFDM 16 QAM with hybrid MDM and PDM based system.

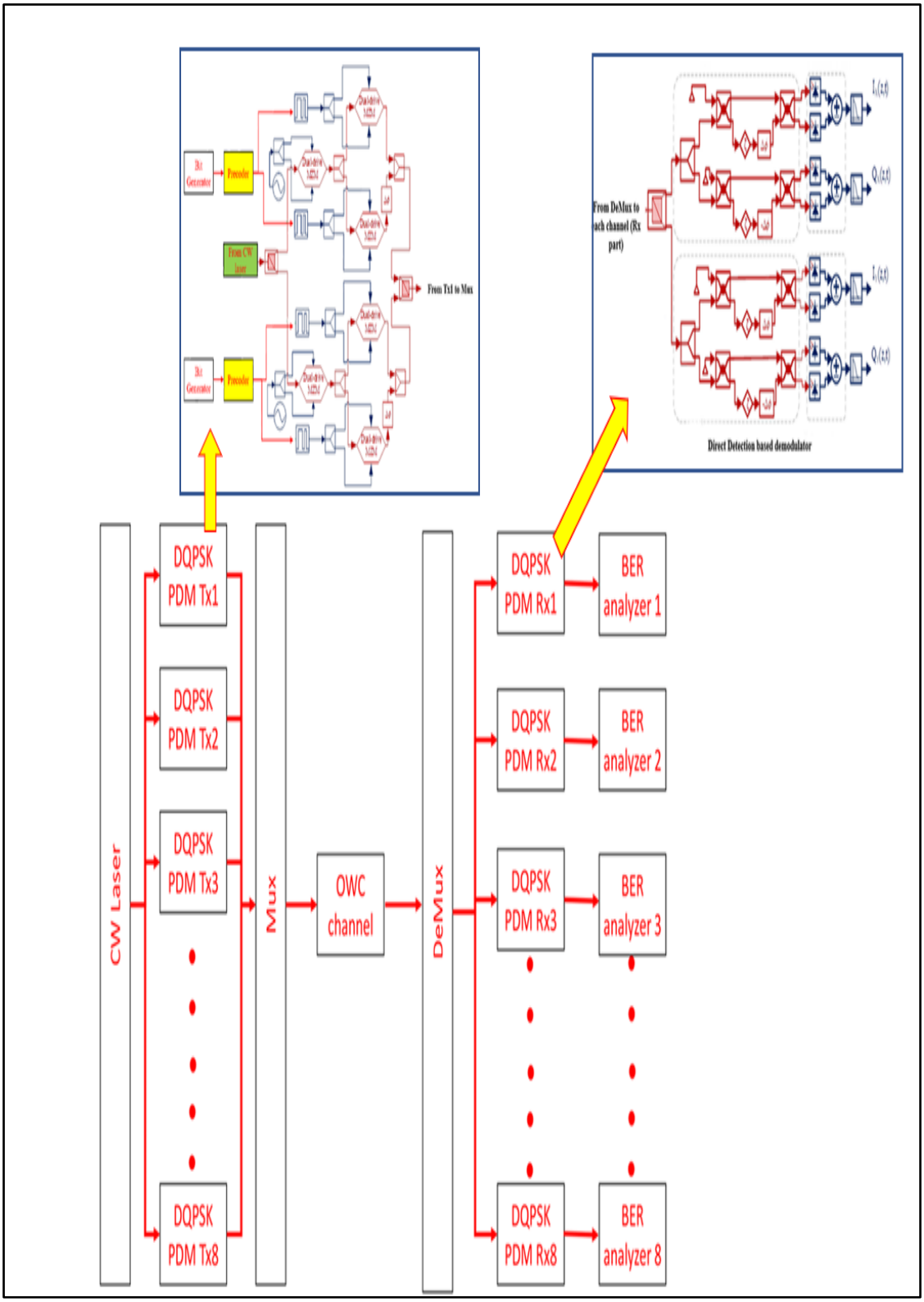

Figure 3.32: Layout Design Of The Alternative DP-DQPSK 8 Channel System.

4. RESULTS AND DISCUSSIONS

4.1 INTRODUCTION

This chapter will demonstrate the results obtained from the novel satellite system proposed in this thesis. The results analysis and evaluation would be based on the three selected objectives to be satisfied. System evaluation will be based on the wide range of studied parameters concerning the selected range of the investigated transmission distances to meet the GEO-based applications.

4.2 RESULTS BASED FIRST OBJECTIVE

This part will demonstrate the results of the first objective mentioned in the first chapter of this thesis, where it will include the result of the proposed novel satellite system which will be evaluated based on different parameters and different transmission distances.

4.2.1 Results Based Bit Error Rate (BER)

The first parameter to evaluate the performance of the proposed 8-channel WDM Is-OWC system with MDM-PDM techniques was the log BER which can indicate the amount of error related to the data transmitted. This parameter will be studied concerning the range of the investigated distances between (10,000 km – 48,000 km) and with MDM technique based on the utilized two modes of (HG00 and HG01) and based on the utilized PDM technique represented by the utilization of two polarizations (p1 and p2). All the obtained results of the log BER parameter are listed in Table 4.1 and Table 4.2 for the two polarizations respectively.

The BER is a key statistic that is used to evaluate the performance of communication systems. It gives a measurable assessment of the quality of the data transfer that is being done. Engineers and academics utilize BER to evaluate how effectively a system is functioning and to evaluate and compare various communication technologies and modulation methods.

Table 4.1: Log BER Results For The Proposed System With Polarization 1 (P1).

Channel	WDM Is-OWC system with (HG00 and HG01) modes and polarization 1 (p1)									
	10,000 km		20,000 km		30,000 km		40,000 km		48,000 km	
	HG00	HG01	HG00	HG01	HG00	HG01	HG00	HG01	HG00	HG01
193.1	-17.3888	-18.0365	-14.3548	-14.6925	-11.2978	-11.5675	-8.1778	-8.3175	-5.9778	-6.0175
193.2	-17.1655	-17.9033	-14.1315	-14.5593	-11.0745	-11.4343	-7.9545	-8.1843	-5.8545	-5.9843
193.3	-16.9274	-17.9687	-13.8934	-14.6247	-10.8364	-11.4997	-7.7164	-8.2497	-5.6164	-5.9497
193.4	-16.6595	-17.8895	-13.6255	-14.5455	-10.4685	-11.4205	-7.3485	-8.1705	-5.2485	-5.8705
193.5	-16.3905	-17.5288	-13.3565	-14.1848	-10.2995	-11.0598	-7.1795	-7.8098	-5.0795	-5.5098
193.6	-15.8394	-16.5857	-12.8054	-13.5417	-9.7484	-10.4167	-6.6284	-7.1667	-4.5284	-4.8667
193.7	-15.6559	-16.1993	-12.6219	-13.1553	-9.5649	-10.0303	-6.4449	-6.7803	-4.2449	-4.4803
193.8	-14.9450	-15.4182	-11.9110	-12.3742	-8.8540	-9.2492	-5.7340	-5.9992	-3.6340	-3.8492

Table 4.2: Log BER Results For The Proposed System With Polarization 2 (P2).

Channel	WDM Is-OWC system with (HG00 and HG01) modes and polarization 2 (p2)									
	10,000 km		20,000 km		30,000 km		40,000 km		48,000 km	
	HG00	HG01	HG00	HG01	HG00	HG01	HG00	HG01	HG00	HG01
193.1	-17.3306	-18.0114	-14.2966	-14.6674	-11.2396	-11.5424	-8.1196	-8.2924	-5.9196	-5.9924
193.2	-17.0748	-17.9035	-14.0408	-14.5595	-10.9838	-11.4345	-7.8638	-8.1845	-5.7638	-5.9695
193.3	-16.7097	-17.9337	-13.6757	-14.5897	-10.6187	-11.4647	-7.4987	-8.2147	-5.3987	-5.9147
193.4	-16.6441	-17.8105	-13.6101	-14.4665	-10.3531	-11.3415	-7.2331	-8.0915	-5.1331	-5.7915
193.5	-16.0836	-16.9611	-13.0496	-13.9171	-9.9926	-10.7921	-6.8726	-7.5421	-4.7726	-5.2421
193.6	-15.7177	-16.4162	-12.6837	-13.3722	-9.6267	-10.2472	-6.5067	-6.9972	-4.4067	-4.6172
193.7	-15.3667	-15.8796	-12.3327	-12.8356	-9.2757	-9.7106	-6.1557	-6.4606	-3.9057	-4.1506
193.8	-14.7453	-15.1393	-11.7113	-12.0953	-8.6543	-8.9703	-5.5343	-5.7203	-3.3343	-3.5803

The analysis of the log BER results can be handled as shown in Figure 4.1 and Figure 4.2 for p1 and p2 respectively. It can be noticed that log BER has a direct relation with raising

distances, which indicates an increasing impact of error in the transmitted bit when handling longer distances. Also, from the same figures it can be noticed that using the HG01-based mode can achieve better results as compared to HG00. Moreover, this difference between the two modes is less variation when handling the second polarization of the utilized PDM technique.

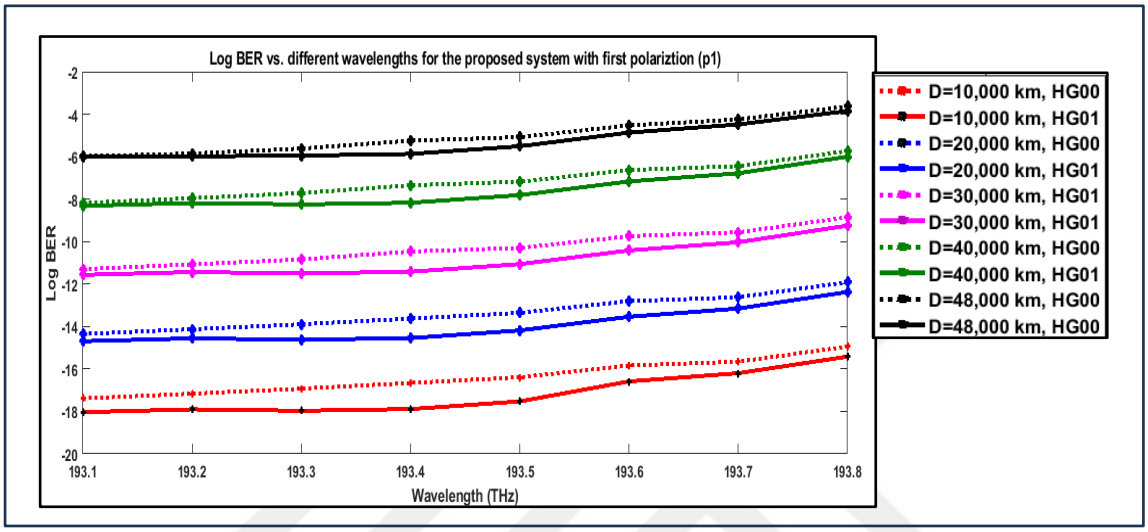

Figure 4.1: Log BER Vs. Different Wavelengths For The Proposed System With P1.

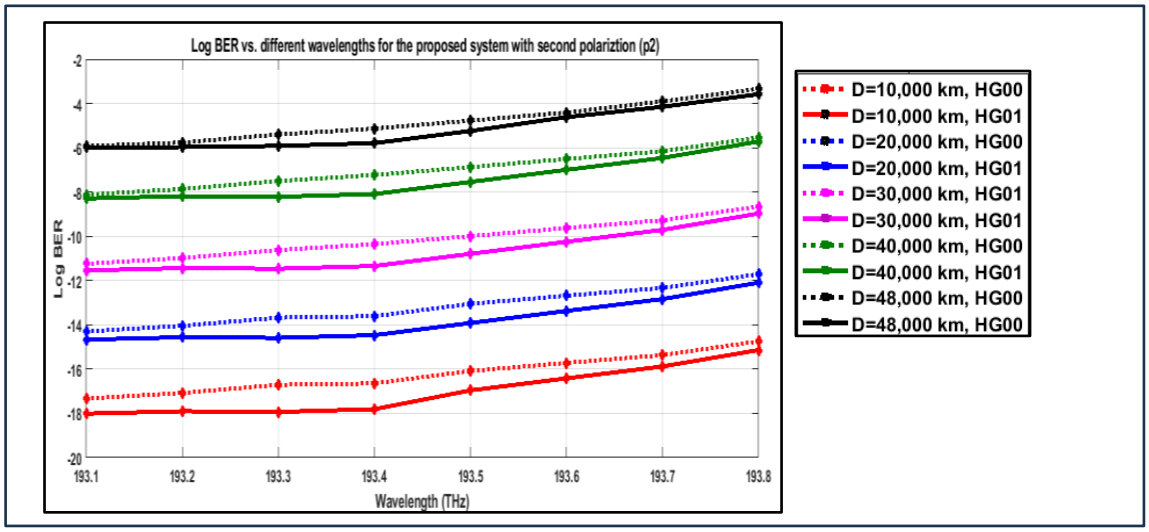

Figure 4.2: Log BER Vs. Different Wavelengths For The Proposed System With P2.

To get a closer view of the obtained results, these results will be averaged from each mode case and per each polarization as it lists in Table 4.3. These results confirm the reliability of the proposed novel method in handling 5.12 Tbps of data rate for distances reaches to 48,000

km to satisfy recent GEO-based applications. Additionally, their results were drawn in Figure 4.3 concerning the log BER FEC threshold of -2.42 which is reported by many previous publications, which confirms the adaptability of the proposed system in and being less than the FEC threshold.

Table 4.3: Averaged Log BER Vs. Different Distances For The Two Polarizations.

Channel	10,000 km		20,000 km		30,000 km		40,000 km		48,000 km	
	HG00	HG01	HG00	HG01	HG00	HG01	HG00	HG01	HG00	HG01
p1	-16.37	-17.19	-13.34	-13.96	-10.27	-10.83	-7.15	-7.58	-5.02	-5.32
p2	-16.21	-17.01	-13.18	-13.81	-10.09	-10.69	-6.97	-7.44	-4.83	-5.16

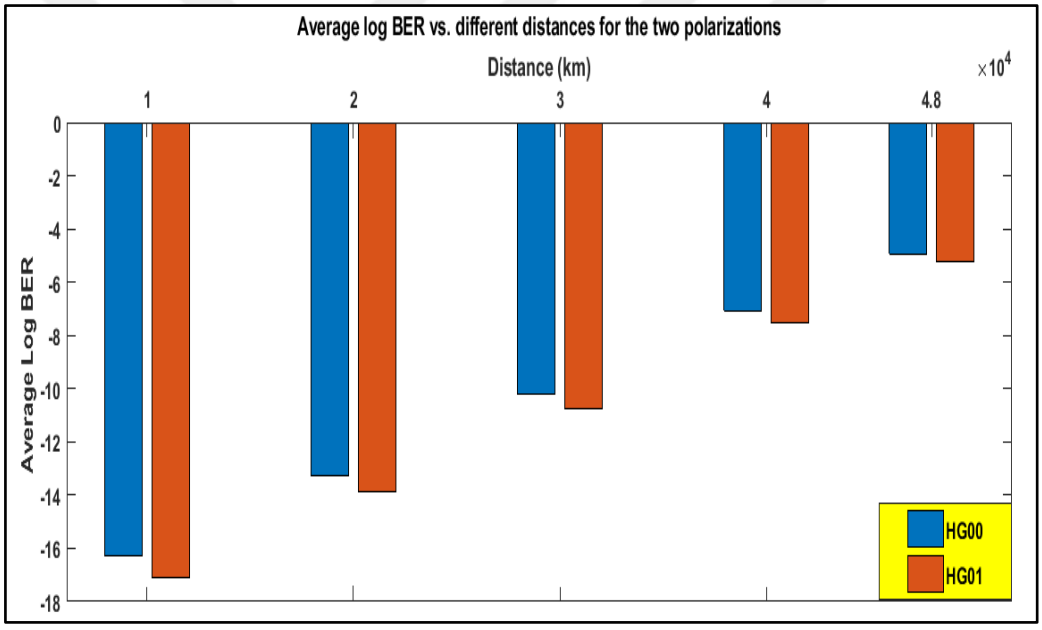

Figure 4.3: Averaged Log BER Vs. Different Distances For The Two Polarizations.

4.2.2 Results Based Min BER

This parameter is an alternative to the log BER which can be calculated from the log BER values obtained for the proposed system by setting the Min BER value equal to ten to power the log BER value. This thesis included the results of Min BER because some studies use it and base their studies on it. So, to make the proposed system reliable with all kinds of data to be further analyzed and compared with a large number of kinds of literature. The obtained results are listed in Table 4.4 and Table 4.5 for the two polarizations respectively. These

results indicate the direct relation between the Min BER and the distance as raising the distance will increase the impact of error in the sent data and thereby increase the data rate. To get a more accurate view of the proposed results of Min BER is achieved by obtaining the average Min BER concerning the two polarization and modes as listed in Table 4.6. These results confirm the reliability of the proposed system in achieving successful transmission up to 48,000 km as the average Min BER achieved for the p1 and p2 were and respectively. And these values were above the minimum threshold of 10^{-3}

Table 4.4: Min BER Results For The Proposed System With P1.

Channel	10,000 km		20,000 km		30,000 km		40,000 km		48,000 km	
	HG00	HG01	HG00	HG01	HG00	HG01	HG00	HG01	HG00	HG01
193.1	4.08E-18	9.19E-19	4.42E-15	2.03E-15	5.037E-12	2.707E-12	6.640E-09	4.814E-09	1.05E-06	9.61E-07
193.2	6.83E-18	1.25E-18	7.39E-15	2.76E-15	8.424E-12	3.679E-12	1.110E-08	6.542E-09	1.40E-06	1.04E-06
193.3	1.18E-17	1.07E-18	1.28E-14	2.37E-15	1.458E-11	3.164E-12	1.921E-08	5.627E-09	2.42E-06	1.12E-06
193.4	2.19E-17	1.29E-18	2.37E-14	2.85E-15	3.400E-11	3.798E-12	4.482E-08	6.754E-09	5.64E-06	1.35E-06
193.5	4.07E-17	2.96E-18	4.40E-14	6.53E-15	5.017E-11	8.714E-12	6.614E-08	1.550E-08	8.33E-06	3.09E-06
193.6	1.45E-16	2.60E-17	1.57E-13	2.87E-14	1.785E-10	3.831E-11	2.353E-07	6.812E-08	2.96E-05	1.36E-05
193.7	2.21E-16	6.32E-17	2.39E-13	6.99E-14	2.723E-10	9.326E-11	3.590E-07	1.658E-07	5.69E-05	3.31E-05
193.8	1.13E-15	3.82E-16	1.23E-12	4.22E-13	1.400E-09	5.633E-10	1.845E-06	1.002E-06	2.32E-04	1.42E-04

Table 4.5: Min BER Results For The Proposed System With P2.

Channel	10,000 km		20,000 km		30,000 km		40,000 km		48,000 km	
	HG00	HG01	HG00	HG01	HG00	HG01	HG00	HG01	HG00	HG01
193.1	4.67E-18	9.74E-19	5.05E-15	2.15E-15	5.759E-12	2.868E-12	7.592E-09	5.101E-09	1.20E-06	1.02E-06
193.2	8.42E-18	1.25E-18	9.10E-15	2.76E-15	1.038E-11	3.677E-12	1.368E-08	6.539E-09	1.72E-06	1.07E-06
193.3	1.95E-17	1.16E-18	2.11E-14	2.57E-15	2.406E-11	3.430E-12	3.171E-08	6.099E-09	3.99E-06	1.22E-06
193.4	2.27E-17	1.55E-18	2.45E-14	3.42E-15	4.435E-11	4.555E-12	5.847E-08	8.100E-09	7.36E-06	1.62E-06
193.5	8.25E-17	1.09E-17	8.92E-14	1.21E-14	1.017E-10	1.614E-11	1.341E-07	2.870E-08	1.69E-05	5.73E-06
193.6	1.92E-16	3.84E-17	2.07E-13	4.24E-14	2.362E-10	5.660E-11	3.114E-07	1.006E-07	3.92E-05	2.41E-05
193.7	4.30E-16	1.32E-16	4.65E-13	1.46E-13	5.300E-10	1.947E-10	6.987E-07	3.463E-07	1.24E-04	7.07E-05
193.8	1.80E-15	7.26E-16	1.94E-12	8.03E-13	2.217E-09	1.071E-09	2.922E-06	1.904E-06	4.63E-04	2.63E-04

Table 4.6: Averaged Min BER Vs. Different Distances For The Two Polarizations.

Channel	10,000 km		20,000 km		30,000 km		40,000 km		48,000 km	
	HG00	HG01	HG00	HG01	HG00	HG01	HG00	HG01	HG00	HG01
p1	1.98E-16	5.98E-17	2.14E-13	6.72E-14	2.45E-10	8.96E-11	3.23E-07	1.59E-07	4.22E-05	2.45E-05
p2	3.20E-16	1.14E-16	3.46E-13	1.27E-13	3.96E-10	1.69E-10	5.22E-07	3.01E-07	8.22E-05	4.60E-05

4.2.3 Results Based OSNR

OSNR is a very important parameter to evaluate the performance of the proposed system where several previous publications based their model system on the OSNR tolerance achieved by using different dedicated methods. Hence, this thesis will calculate the parameter of OSNR to evaluate the overall system concerning different other parameters such as the log BER. The OSNR values obtained from the proposed WDM Is-OWC system were based on the two polarization and the five cases of transmission distance as listed in Table 4.7 and as clarified in Figure 4.4 and Figure 4.5 for the two polarizations respectively. The obtained results indicate the reverse relation between the OSNR and the transmission distances as raising the distance will reduce the impact of OSNR which will influence the reliability of the proposed system. Thereby, higher OSNR indicates a much clearer signal.

Table 4.7: OSNR Values For Different Distances And The Two Polarizations.

Channel	OSNR value in (dB) for different distances				
	10,000 km	20,000 km	30,000 km	40,000 km	48,000 km
ch1/p1	78	76	73	70	68
ch1/p2	77	74	71	68	66
ch2/p1	74	72	69	66	64
ch2/p2	73	70	67	64	62
ch3/p1	71	68	65	62	60
ch3/p2	69	66	63	60	58
ch4/p1	67	64	61	58	56
ch4/p2	66	62	59	56	54
ch5/p1	64	60	57	54	52
ch5/p2	63	58	55	52	50
ch6/p1	59	56	53	50	48
ch6/p2	58	54	51	48	46
ch7/p1	57	52	49	46	44
ch7/p2	54	50	47	44	42
ch8/p1	51	48	45	42	40
ch8/p2	50	46	43	40	38

The error performance of the proposed system was studied concerning the analysis of log BER concerning the obtained OSNR. Which has been analyzed for the cases of five distances as seen in Figure 4.6. The case of 48,000 km confirms the reliability of the proposed system as achieving acceptable log BER above the FEC minimum threshold of -2.42 with OSNR requirements of 50.5 dB. It's worth mentioning that the proposed system proposed concerning Pe of 1 mard for the Tx and receiver side.

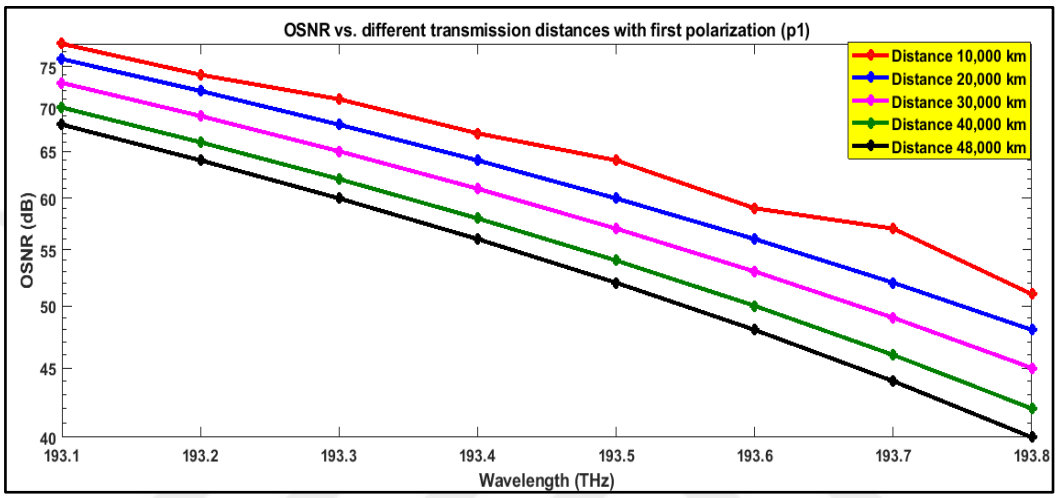

Figure 4.4: OSNR Vs. Different Transmission Distances For P1.

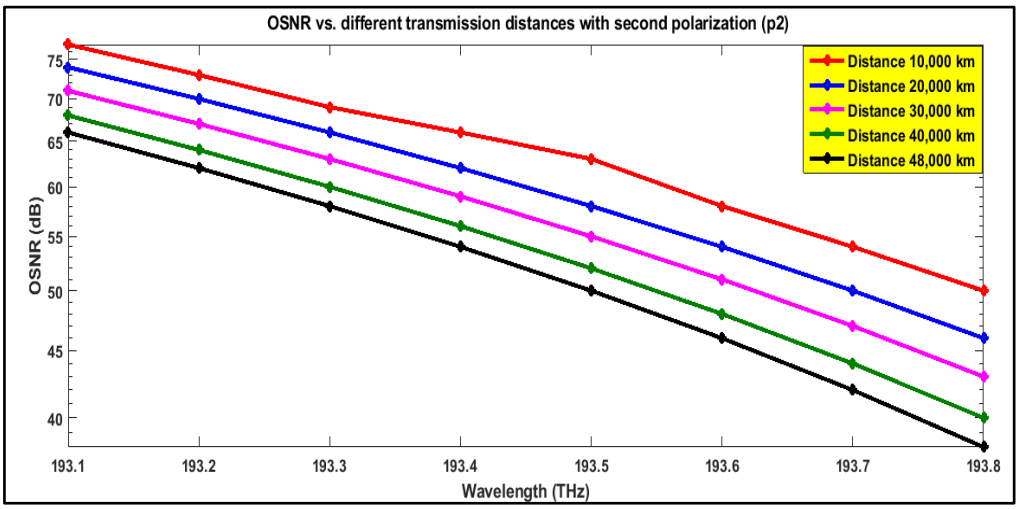

Figure 4.5: OSNR Vs. Different Transmission Distances For P2.

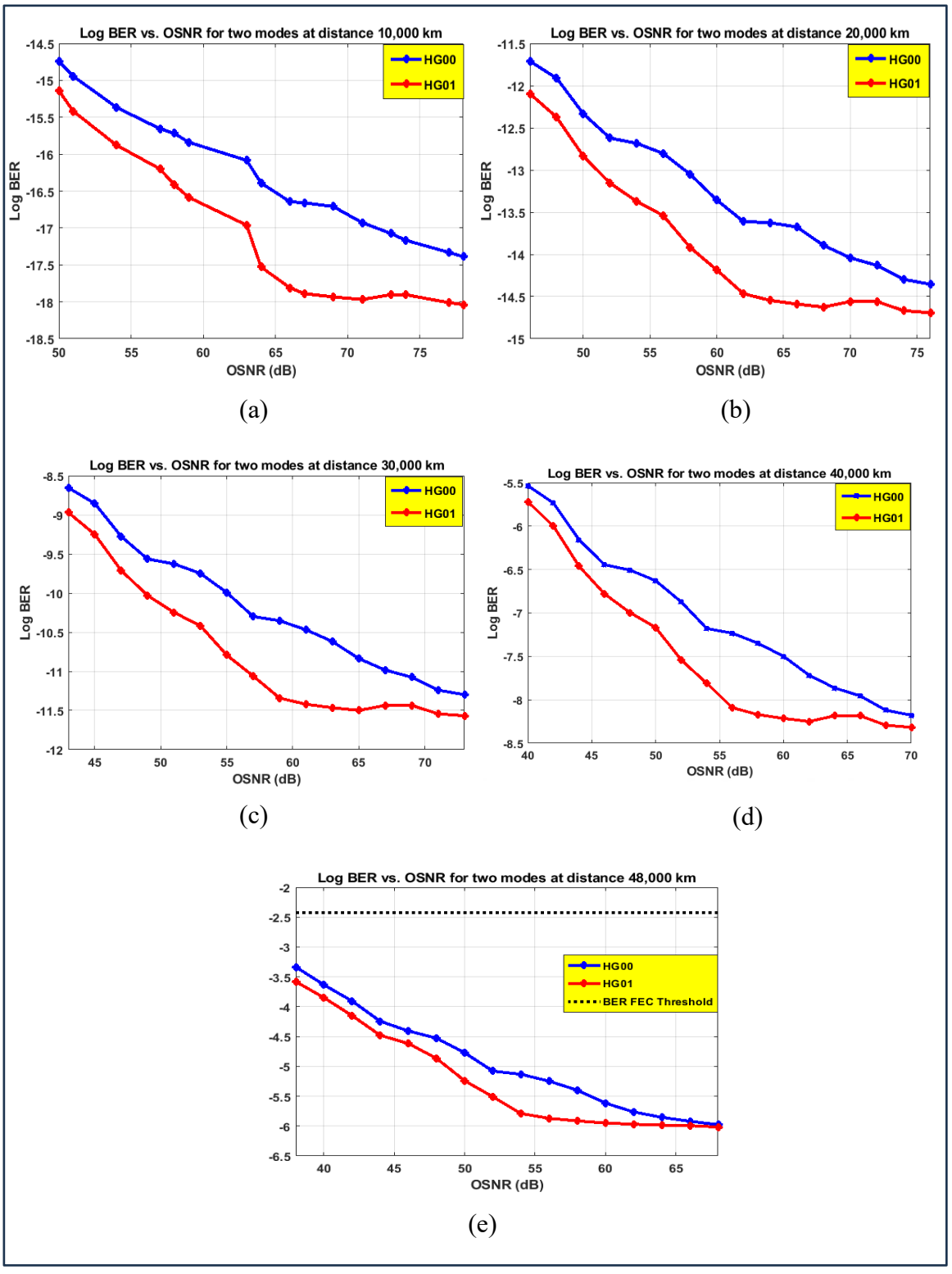

Figure 4.6: Log BER Vs. OSNR For Two Modes At A Distance a)10,000 Km, b) 20,000 Km, c) 30,000 Km, d) 40,000 Km, And e) 48,000 Km.

4.2.4 Results Based EVM

Error Vector Magnitude (EVM) may be computed from the constellation diagram at the received signal to quantify modulator or demodulator performance in nonlinear effects. From analyzing the impact of raising distance on the percentage of the EVM for the proposed system, Table 4.8 and Table 4.9 depict the obtained values for the two polarizations respectively. To visualize the impact of EVM obtained from each case of transmission distances Figure 4.7 withdrawn the impact of EVM from each mode and polarization with different transmission cases. It can be noticed as a direct relation as increasing transmission distance will raise EVM percentage due to noise, distortion, spurious signals, and Pe impact. Also, it can be noticed an EVM% was more in the HG00 or the case of p1 as compared to the HG01 or with the p2. The reason the HG01-based mode achieves the best results is that the HG01 is reaching the highest mode maximum power, which makes it more robust.

There is a connection between EVM and BER. When certain conditions are met, it is possible to estimate the BER of a system by measuring EVM and being familiar with the modulation scheme that is being used. A greater EVM often translates to a higher BER. EVM may be used in the operations of a real-world network to perform continuous monitoring of the quality of the service. Indicating problems in the network that need attention and making it possible to keep the quality of service at a high level are elevated EVM values. If the values of the EVM are found to be higher than the permitted levels, this acts as a warning sign that the gearbox system is not operating at its full potential. Because of this information, engineers and operators are better able to detect problems and take measures to fix them, hence improving the signal quality.

Table 4.8: EVM Values Obtained From System For The Two Modes Of The P1.

Channel	10,000 km		20,000 km		30,000 km		40,000 km		48,000 km	
	HG00	HG01	HG00	HG01	HG00	HG01	HG00	HG01	HG00	HG01
193.1	1.230	1.568	3.330	3.439	5.580	5.451	6.936	6.751	8.236	8.351
193.2	1.860	2.074	3.960	3.945	6.210	5.957	7.566	7.257	8.866	8.857
193.3	1.276	2.256	3.376	4.127	5.626	6.139	6.982	7.439	8.282	9.039
193.4	1.705	1.759	3.805	3.630	6.055	5.642	8.065	7.745	9.365	9.345
193.5	3.967	3.751	4.567	5.622	6.817	7.634	8.827	9.737	12.081	12.857
193.6	4.612	4.070	8.822	7.520	11.072	9.532	14.192	12.642	17.446	15.762
193.7	6.990	5.860	11.200	8.310	16.320	13.560	20.870	18.100	25.120	22.340
193.8	21.090	15.425	23.212	18.875	28.332	24.125	32.882	28.665	37.132	32.905

Table 4.9: EVM Values Obtained From System For The Two Modes Of The P2.

Channel	10,000 km		20,000 km		30,000 km		40,000 km		48,000 km	
	HG00	HG01	HG00	HG01	HG00	HG01	HG00	HG01	HG00	HG01
193.1	1.860	2.074	3.960	3.945	6.210	5.957	7.566	7.257	8.866	8.857
193.2	1.191	2.513	3.291	4.384	5.541	6.396	6.897	7.696	8.197	9.296
193.3	1.271	1.285	2.808	3.156	5.058	5.168	7.068	7.271	8.368	8.871
193.4	3.473	3.420	5.573	6.291	7.823	8.303	9.833	10.406	11.133	12.006
193.5	3.901	3.798	7.311	7.248	9.561	9.260	11.571	11.363	14.825	14.483
193.6	5.295	5.057	9.505	6.307	14.625	11.557	17.745	14.667	21.995	18.907
193.7	14.461	12.140	18.583	14.590	23.703	18.840	28.253	23.380	32.503	27.620
193.8	29.498	26.020	34.620	32.470	39.740	37.720	44.290	42.260	48.540	46.500

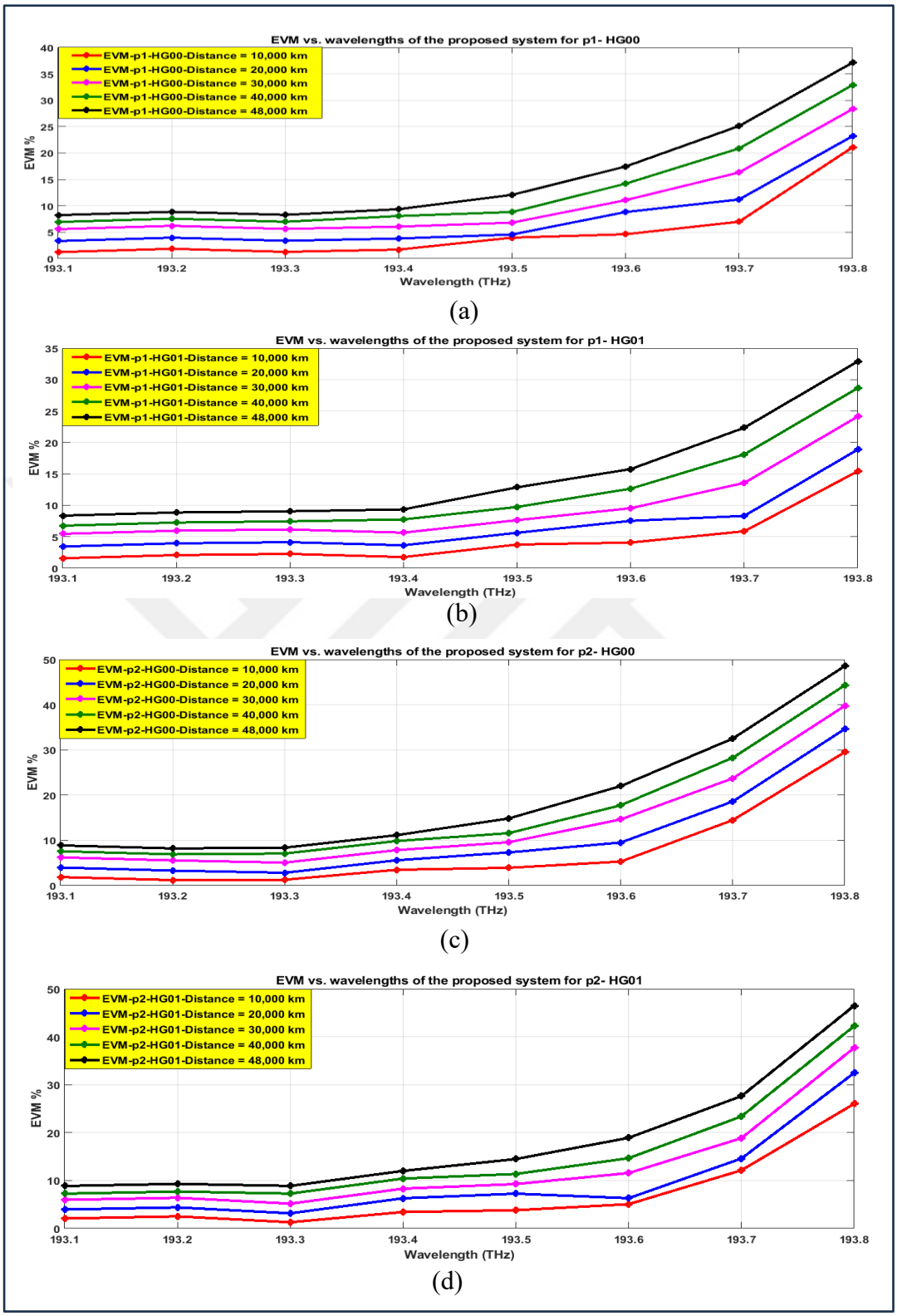

Figure 4.7: EVM Vs. Wavelengths Of The Proposed System With Different Distances For a) HG00-P1, b) HG01-P1, c) HG00-P2, And d) HG01-P2.

4.2.5 Results Based Received Power

This parameter studied to obtain the impact of the receiver sensitivity, where it has been studied the impact of received power in dBm vs. different transmission distances and for the two polarizations of the PDM techniques that were utilized to form the novelty of the proposed system as listed in Table 4.10 and Table 4.11 respectively. Additionally, Figure 4.8 analyze that relation, where it can be concluded a reverse relation as increasing the distance of transmission will result in more interference and noise for the transmitted signal and will have a significant impact on the receiver sensitivity.

Table 4.10: Received Power Vs. Transmission Distances For P1.

Channel	Received power in (dBm) for different Distance (km)				
	10,000	**20,000**	**30,000**	**40,000**	**48,000**
193.1	-17.480	-22.467	-27.899	-32.945	-37.324
193.2	-18.810	-23.797	-29.229	-34.275	-38.654
193.3	-20.179	-25.166	-30.598	-35.644	-40.023
193.4	-23.043	-28.030	-33.462	-37.751	-42.324
193.5	-25.882	-30.869	-36.301	-40.550	-45.123
193.6	-27.700	-32.687	-38.119	-42.665	-47.238
193.7	-32.215	-37.202	-42.634	-47.180	-51.753
193.8	-34.616	-39.603	-45.035	-49.581	-54.124

Table 4.11: Received Power Vs. Transmission Distances For P2.

Channel	Received power in (dBm) for different Distance (km)				
	10,000	**20,000**	**30,000**	**40,000**	**48,000**
193.1	-15.591	-20.578	-26.010	-31.056	-35.435
193.2	-17.142	-22.129	-27.561	-32.607	-36.986
193.3	-19.700	-24.687	-30.119	-35.165	-39.544
193.4	-22.911	-27.898	-33.330	-37.579	-41.958
193.5	-24.063	-29.050	-34.482	-38.751	-43.324
193.6	-26.964	-31.951	-37.383	-41.632	-46.205
193.7	-31.005	-35.992	-41.424	-45.970	-50.543
193.8	-34.005	-38.992	-44.424	-48.970	-53.543

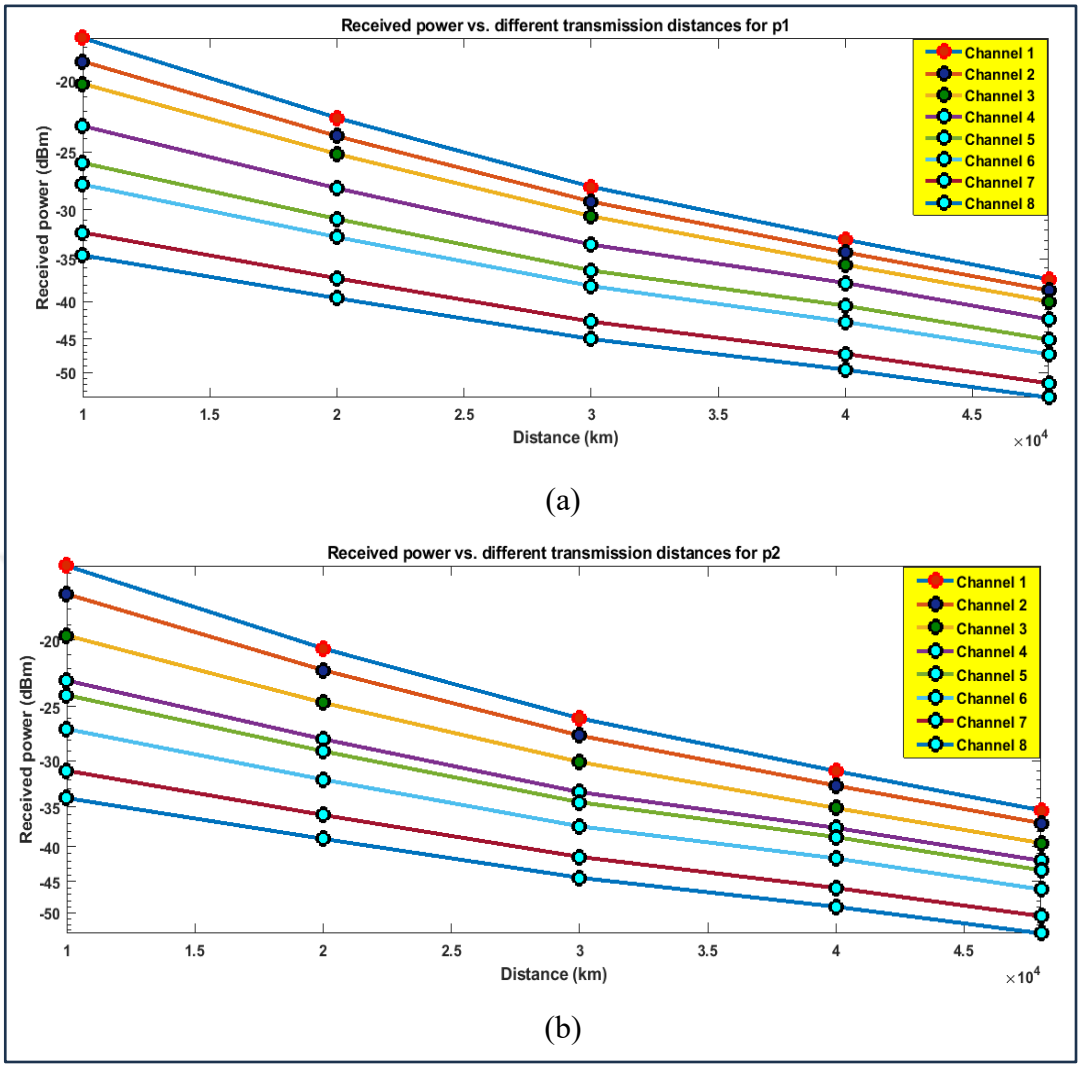

Figure 4.8: Received Power Vs. Different Distances For a) P1, And b) P2.

The significance of studying the receiver sensitivity is represented by analyzing its impact on the log BER parameter as shown in Figure 4.9. A reverse relation can be noticed as reducing the impact of bit error in the transmitted data will mean increasing the received power at the Rx side which will have a significant influence on the amount of the receiver sensitivity. Also, it can be noticed specifically for the case of 48,000 km that the achieved results were above the FEC threshold which confirms the reliability of the proposed OFDM 16 QAM Is-OWC-based system. The significance behind studying the relation between log BER and receiver sensitivity is to obtain the sensitivity tolerance when values reach the minimum FEC threshold.

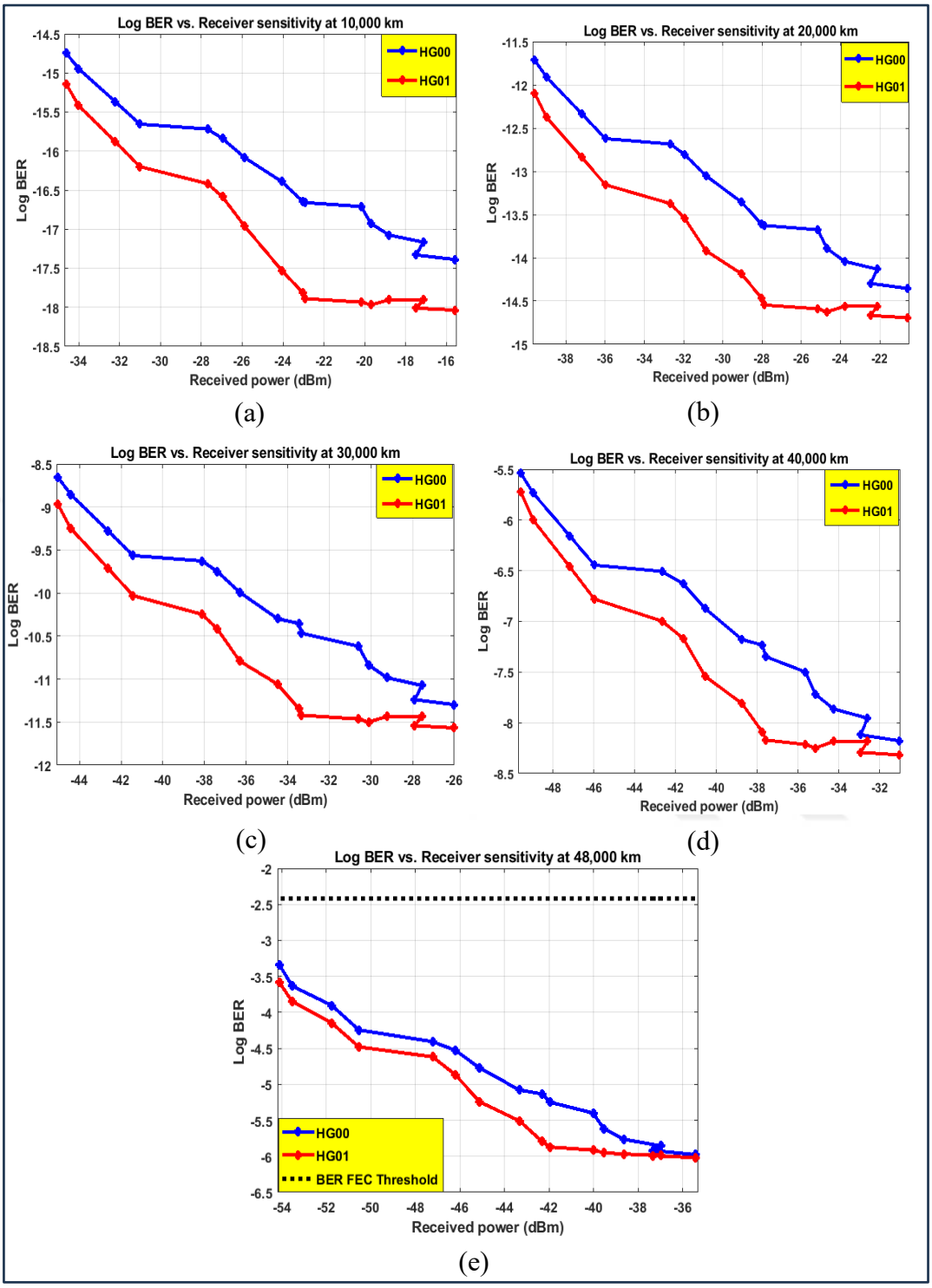

Figure 4.9: Log BER Vs. Receiver Sensitivity For Two Modes At Distance Of: a) 10,000 Km, b) 20,000 Km, c) 30,000 Km, d) 40,000 Km And e) 48,000 Km.

Furthermore, EVM % concerning the impact of Rx power was analyzed to indicate comprehensive analysis from the proposed system of this thesis where the five cases of distances were included in the investigation. Figure 4.10 demonstrate the mentioned relation where a reverse relation can be concluded as raising the EVM would result in a reduction in the received power.

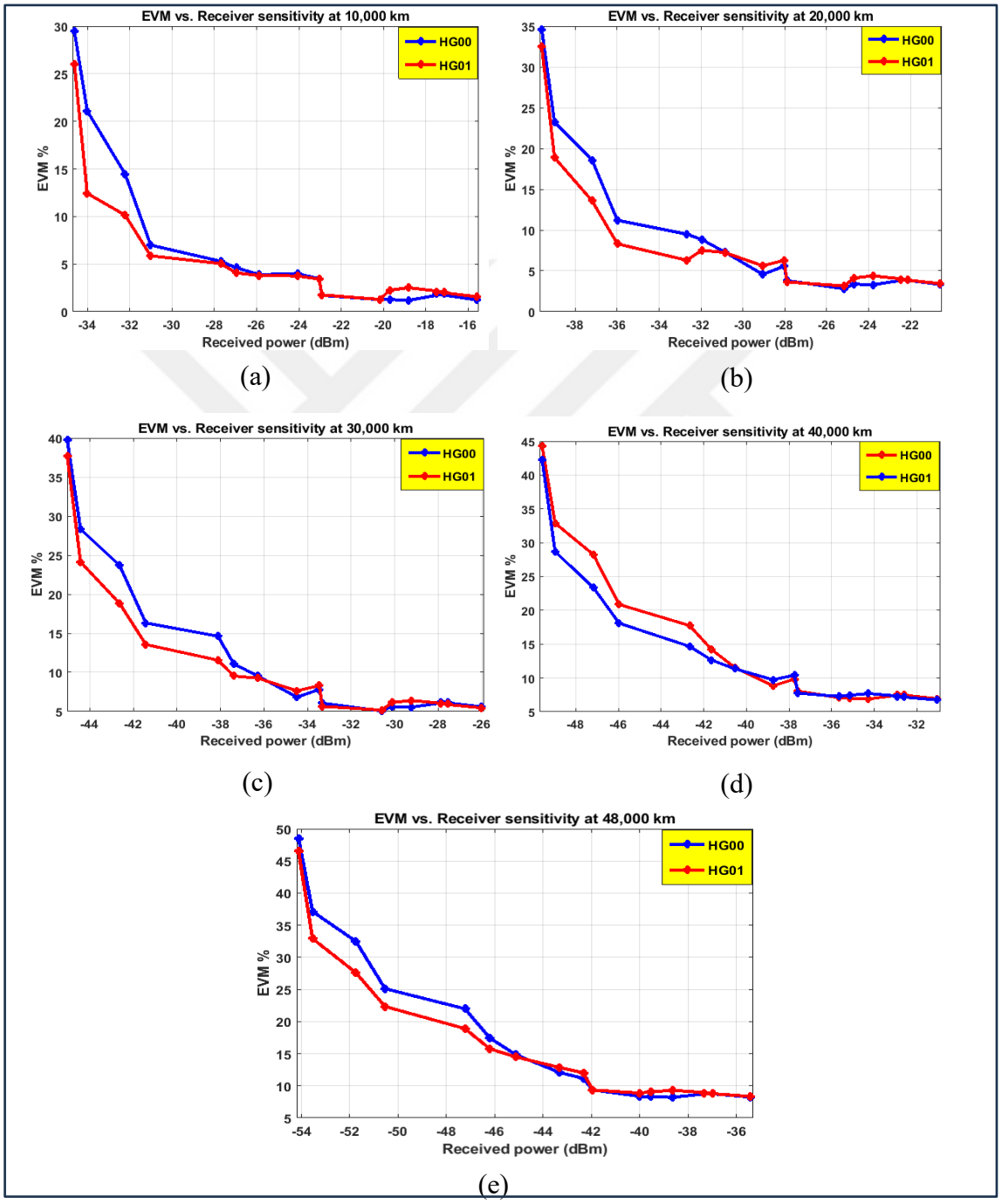

Figure 4.10: EVM% Vs. Receiver Sensitivity For Two Modes At Distance Of: a) 10,000 Km, b) 20,000 Km, c) 30,000 Km, d) 40,000 Km And e) 48,000 Km.

4.2.6 Results Based Constellation Diagram

Figures 4.11 and 4.12 show the constellation diagram for a distance of 48,000 km, along with three cases: one before Channel Estimation (CE), one after CE, and one after Carrier Phase Estimation (CPE). These cases pertain to two port modes, HG 00 and HG 01, and two polarizations, p1 and p2, for each mode relative to the channel.

a. where the left graphs illustrate the overlapping in points of the constellation before estimating the channels, The construction of the channel transfer function that adjusts for dispersion and polarization-based losses is accomplished via the use of training symbols. Before CE, the selection of a suitable modulation scheme for a certain communication case was accomplished via the use of constellation diagrams. The spectrum efficiency and error rate behaviours of various modulation systems might vary greatly from one another. A well-informed selection about which scheme to use may be made with the assistance of the constellation diagram by basing the decision on the anticipated channel conditions and the data rate needs.

b. After channel estimation in the middle graphs (b), rotating constellation points may be seen because of phase drift caused by the progression of time. It is anticipated that this phase drift will remain the same throughout a symbol period, and the channel transfer function will be updated using the pilot symbols that have been received. After CE, constellation diagrams aid equalisation and demodulation. Channel estimation minimises channel effects on transmitted signals. The predicted channel response may correct for channel imperfections and align the received signal with optimum constellation locations. Accurate symbol identification requires this alignment.

c. Figures in the right graphs, which were created after CPE, have a distinct 16 QAM constellation. It is necessary in circumstances in which the carrier phase of the received signal could be unknown or influenced by phase noise. Following CPE, the constellation diagram is used to assist in the phase shift compensation process. By making the necessary adjustments to the carrier phase, one may guarantee that the received signal is correctly aligned with the reference constellation, hence enhancing the accuracy of symbol recognition, and lowering the number of mistakes that occur.

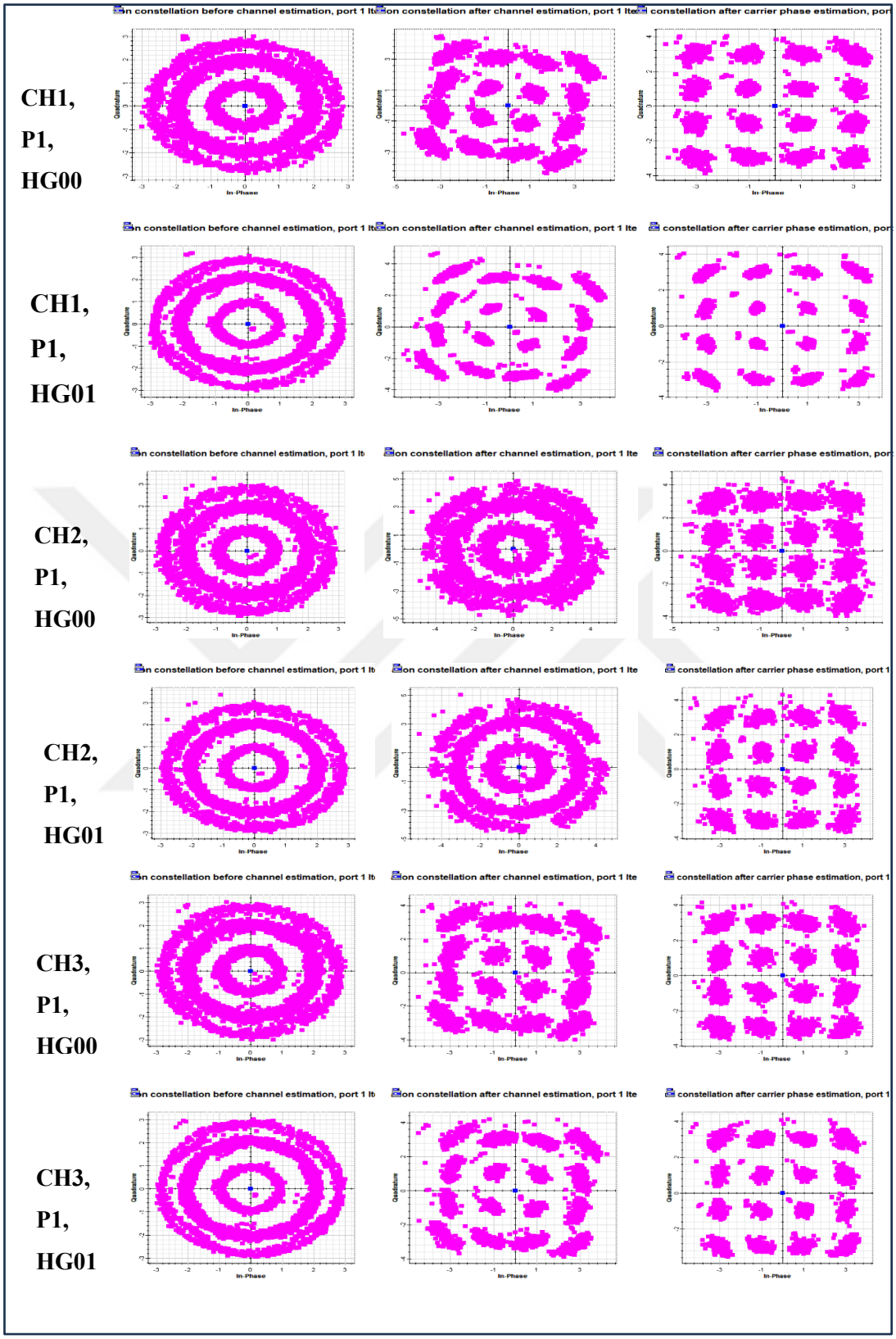

Figure 4.11: Constellation Diagram For P1 And Two Modes Where: (Left) Before CE, (Middle) After CE, And (Right) After CP "Figure Continued".

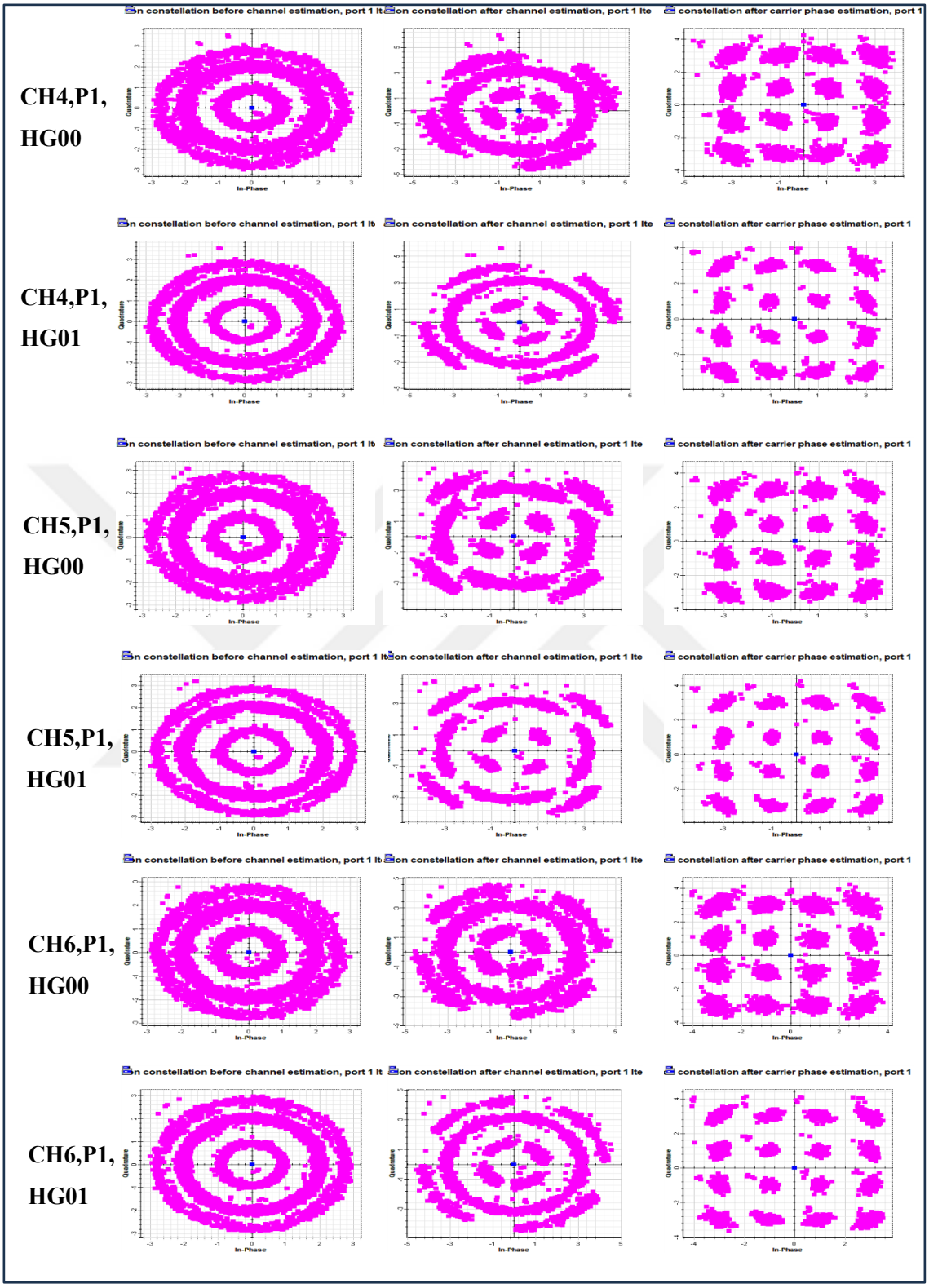

Figure 4.11: Constellation Diagram For P1 And Two Modes Where: (Left) Before CE, (Middle) After CE, And (Right) After CP "Figure Continued".

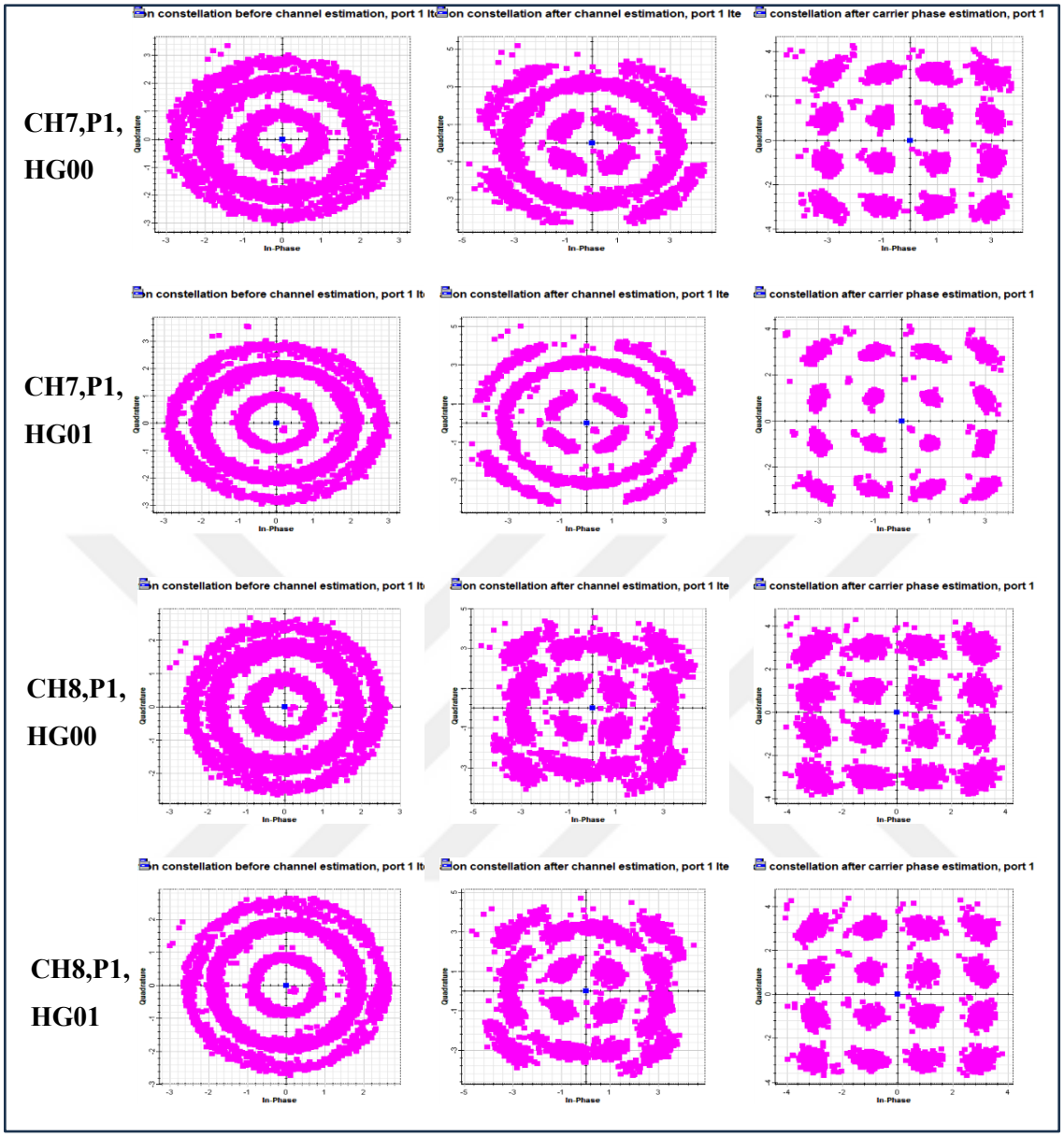

Figure 4.11: Constellation Diagram For P1 And Two Modes Where: (Left) Before CE, (Middle) After CE, And (Right) After CPE "Figure Continued".

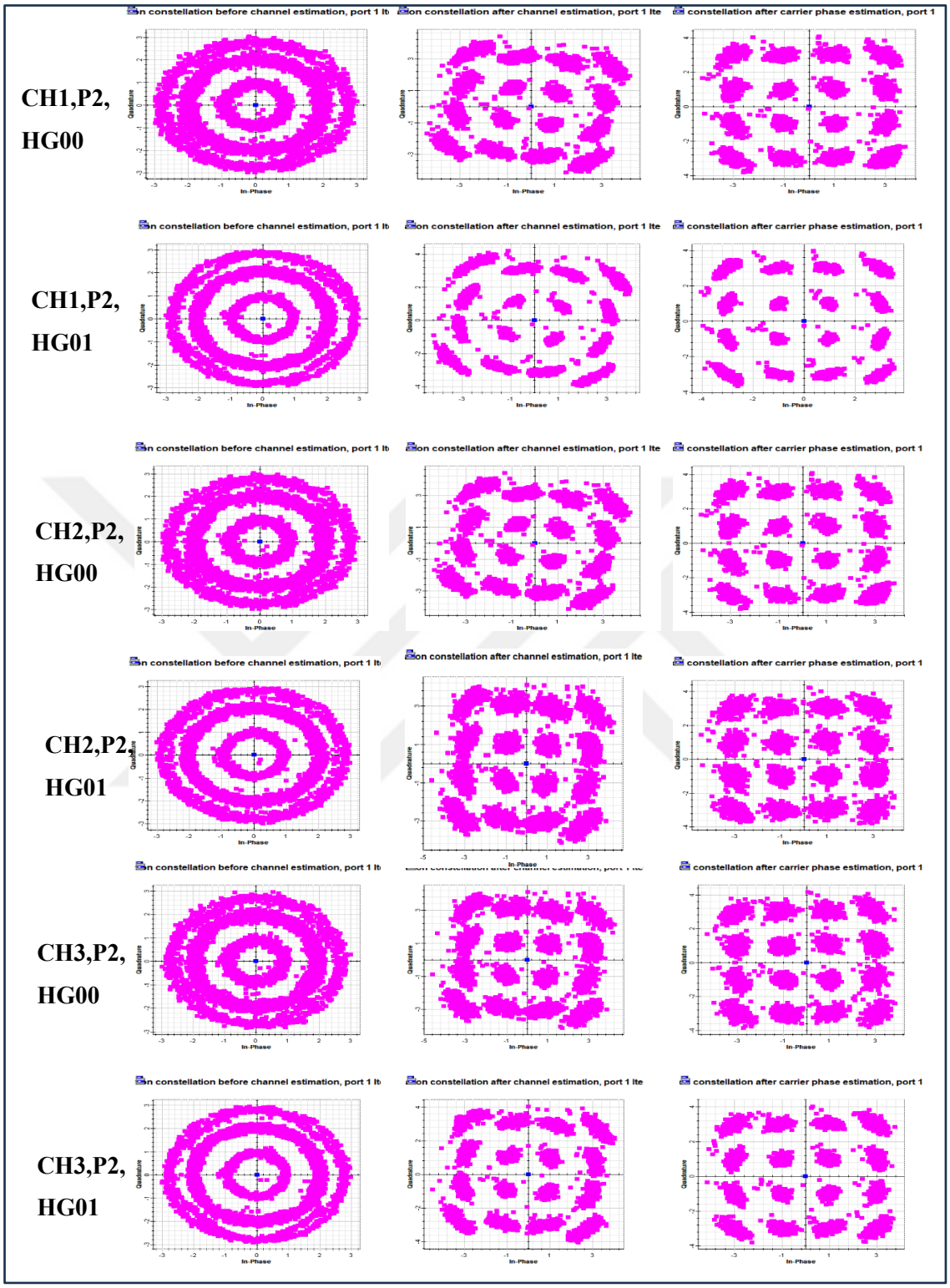

Figure 4.12: Constellation Diagram For P2 And Two Modes Where: (Left) Before CE, (Middle) After CE, And (Right) After CP.

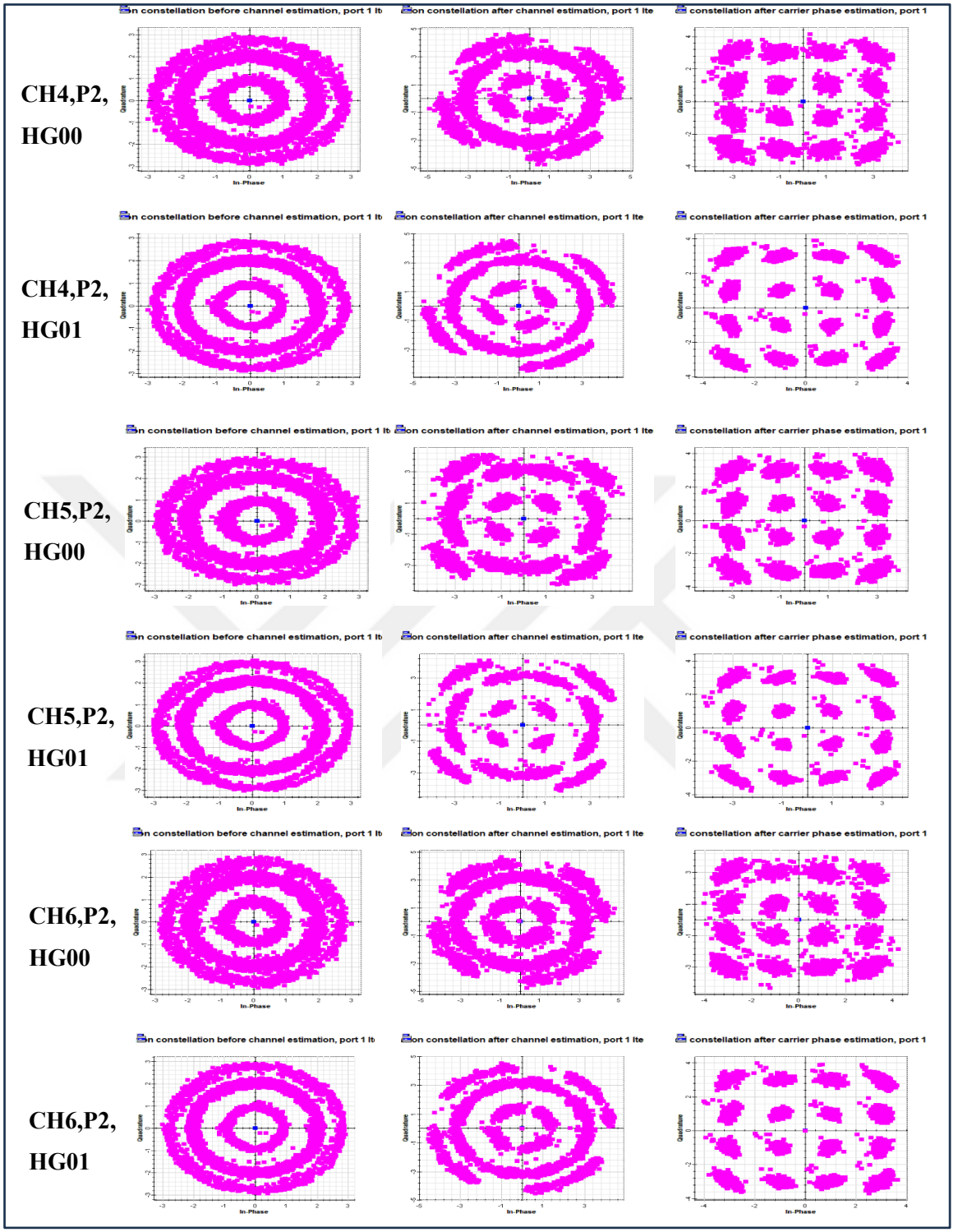

Figure 4.12: Constellation Diagram For P2 And Two Modes Where: (Left) Before CE, (Middle) After CE, And (Right) After CP "Figure Continued".

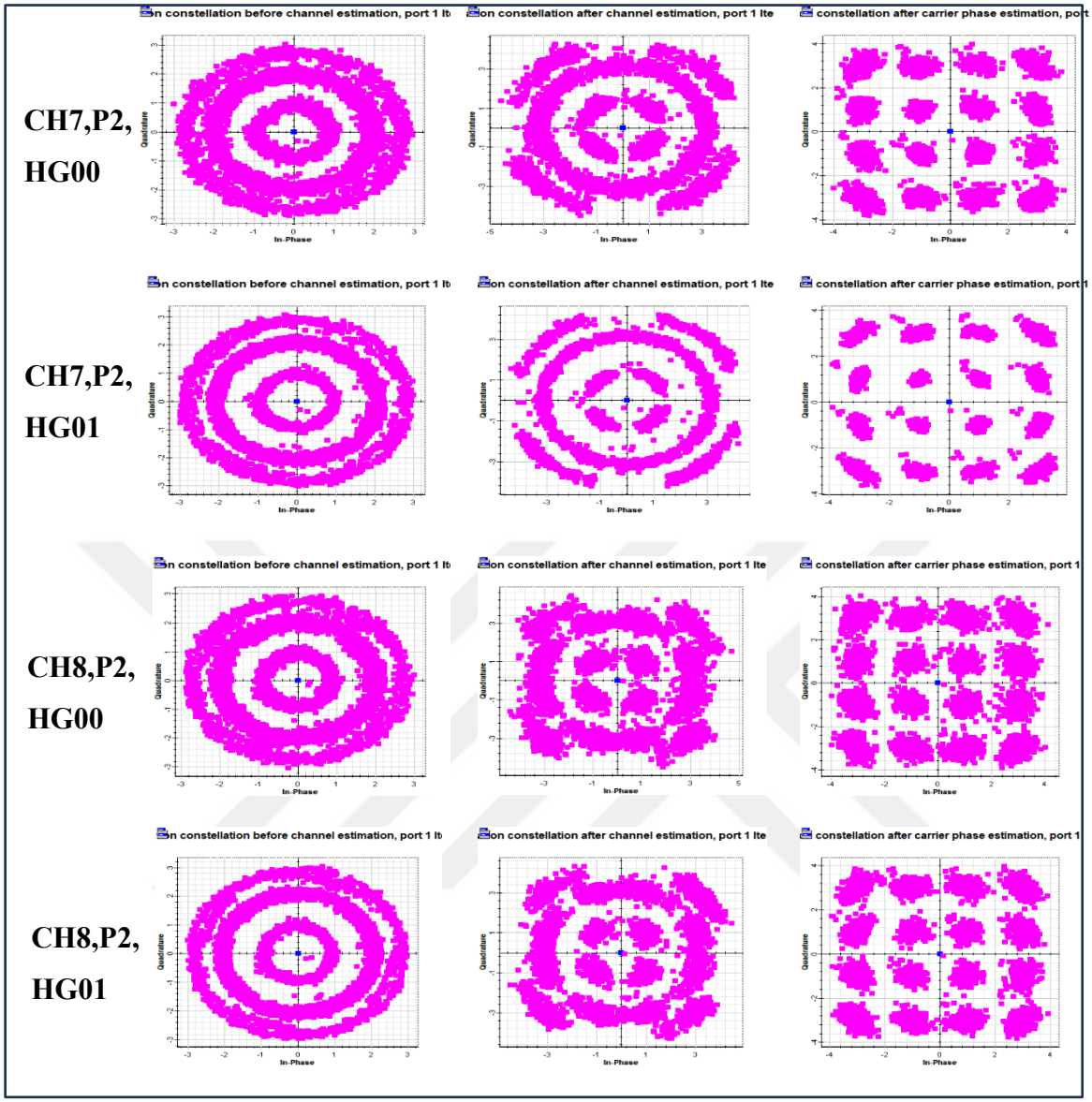

Figure 4.12: Constellation Diagram For P2 And Two Modes Where: (Left) Before CE, (Middle) After CE, And (Right) After CP "Figure Continued".

4.2.7 Results of Comparison with Alternative Satellite System

In this section, the second system is designed and implemented based on using other techniques of DP-DQPSK with 8 channel WDM technique system and using the direct detection-based method. The aim of designing a such system is to compare it and the proposed system of the thesis to demonstrate the significance of the novelty methodology proposed by using the technique of MDM-PDM. Also, the alternate system is designed by investigating two precoding techniques to demonstrate the optimum precoding scheme to boost the transmission of the alternate system to reach 48,000 km which is the targeted distance of the first objective of this thesis.

A complete account of the alternate approach that was suggested in Chapter 3. A comparison will be made between a few parameters. The log BER, a crucial metric for gauging the inaccuracy in transmitted bits over varying distances, was chosen as the comparing parameter. Table 4.12 shows the two precoding techniques used for all 8 channels, and Table 4.13 shows the two polarizations for each channel. Consequently, this parameter will be analyzed from both sources. Figures 4.13 and 4.14 show the two precoding's, and the findings will be dependent on the change of this parameter relating to distance rising. Since the incorrect data grows in direct proportion to the distance, a clear relationship is evident. By the same token, the Duobinary shows better performance when it comes to reducing transmission errors.

To compare the two precoding schemes, we will average and organize the data from each scheme as shown in Table 4.14 and Table 4.15, respectively. Figure 4.15 will show the results of our analysis. Based on the results, it seems that Duobinary precoding successfully decreased BER up to 20,000 km, but at longer distances approaching 48,000 km, the two techniques perform similarly. Furthermore, the suggested system may successfully transmit data up to 40,000 km when compared to the averaged results and the minimal FEC threshold of log BER, which is -2.42 as indicated.

Table 4.12: Log BER Parameter For DPSK Precoder Under Different Distances.

Log BER/ Distance		Distance (km)				
		10,000	**20,000**	**30,000**	**40,000**	**48,000**
Ch1	p1	-43.9176	-13.9511	-7.94973	-1.88174	-1.32104
	p2	-43.5435	-13.92619	-7.62251	-3.27954	-1.41739
ch2	p1	-42.9182	-12.3094	-6.11624	-3.03359	-1.56149
	p2	-42.8213	-12.2629	-5.98991	-2.91774	-1.56524
ch3	p1	-39.656	-10.6117	-6.47361	-3.3269	-1.29002
	p2	-37.6587	-10.5983	-6.40363	-3.37143	-1.28671
ch4	p1	-27.6157	-6.36354	-5.14576	-2.41217	-1.09508
	p2	-26.703	-6.15647	-5.02359	-2.3914	-1.06394
ch5	p1	-25.5646	-10.3792	-8.05165	-2.64254	-1.51122
	p2	-25.6427	-10.0813	-7.74007	-2.67317	-1.47819
ch6	p1	-23.3895	-9.35551	-6.42994	-2.93593	-1.26991
	p2	-21.6843	-9.36746	-6.25275	-2.81473	-1.27323
ch7	p1	-50.48	-10.359	-7.19486	-3.02317	-1.29393
	p2	-48.522	-10.0793	-7.34436	-2.86604	-1.27956
ch8	p1	-40.4934	-11.234	-7.99121	-3.42401	-1.52811
	p2	-41.5093	-11.2219	-7.92211	-3.47692	-1.51038

Table 4.13: Log BER Parameter For Duobinary Precoder Under Different Distances.

Log BER/ Distance		Distance (km)				
		10,000	**20,000**	**30,000**	**40,000**	**48,000**
Ch1	p1	-47.41448	-14.68142	-5.45783	-2.85086	-1.61164
	p2	-46.4867	-13.2057	-4.16068	-2.64773	-2.47476
Ch2	p1	-105.102	-10.9368	-3.58427	-2.96283	-2.81835
	p2	-105.4	-11.1441	-3.45462	-2.72997	-2.78297
Ch3	p1	-137.87	-15.5461	-4.74391	-2.80625	-2.04602
	p2	-138.532	-15.1991	-4.67941	-2.81631	-2.05966
Ch4	p1	-144.48	-16.2187	-4.34553	-2.70977	-1.91072
	p2	-146.35	-16.4017	-4.35824	-2.66014	-1.90803
Ch5	p1	-42.216	-13.335	-5.28869	-1.92455	-2.56738
	p2	-41.285	-12.9943	-5.28593	-1.9222	-2.61451
Ch6	p1	-33.8112	-11.6325	-4.07805	-1.92702	-2.46899
	p2	-33.2835	-11.655	-4.01299	-1.93995	-2.39685
Ch7	p1	-127.804	-16.2655	-2.77852	-2.26173	-1.82371
	p2	-115.165	-17.0538	-2.90913	-2.3018	-1.84877
Ch8	p1	-96.3785	-12.5156	-3.42278	-3.20776	-2.38235
	p2	-98.6621	-12.5574	-3.4374	-3.24079	-2.33786

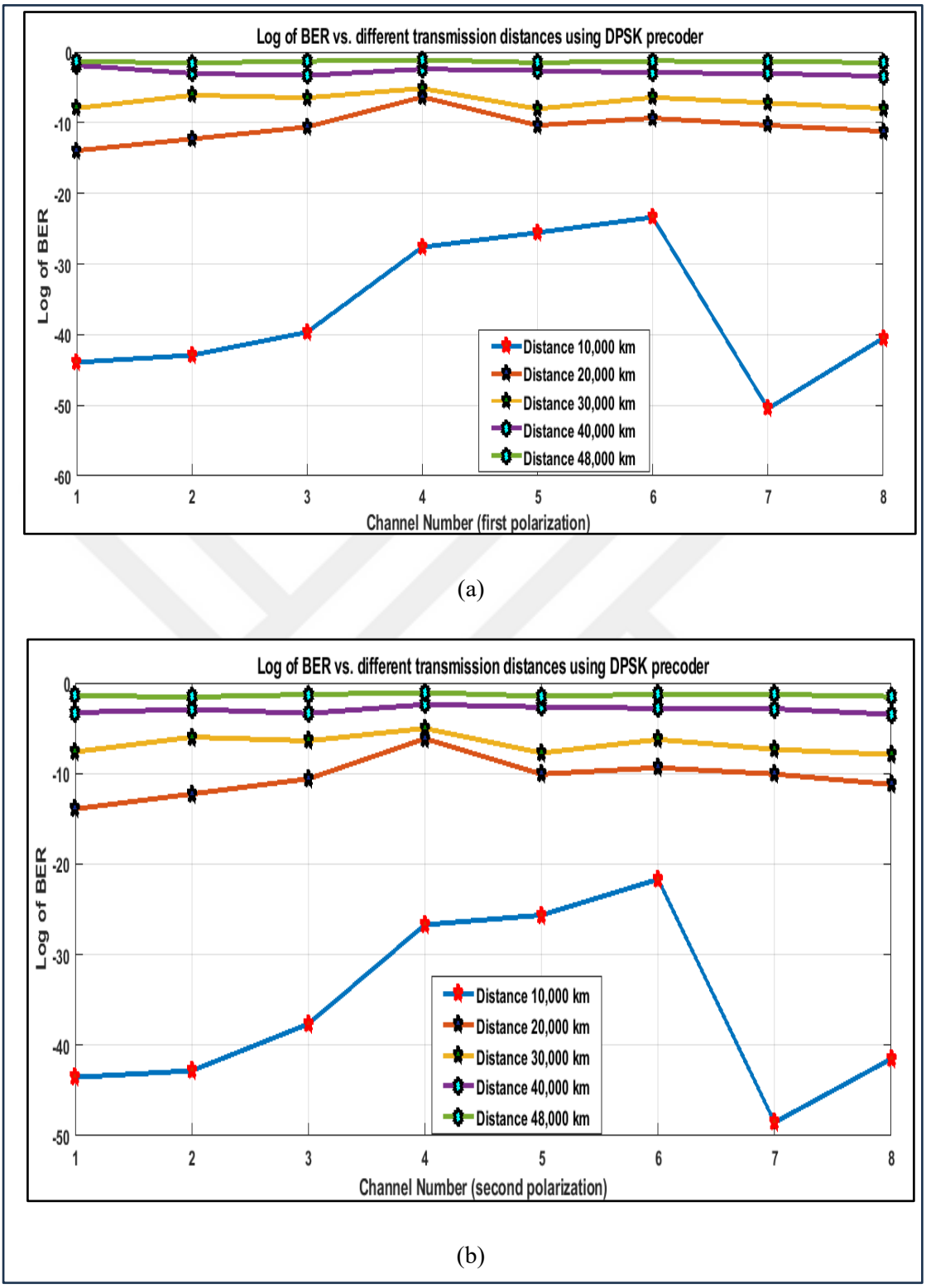

Figure 4.13: Log BER Vs. Different Distances For DPSK Precoder a) P1 And b) P2.

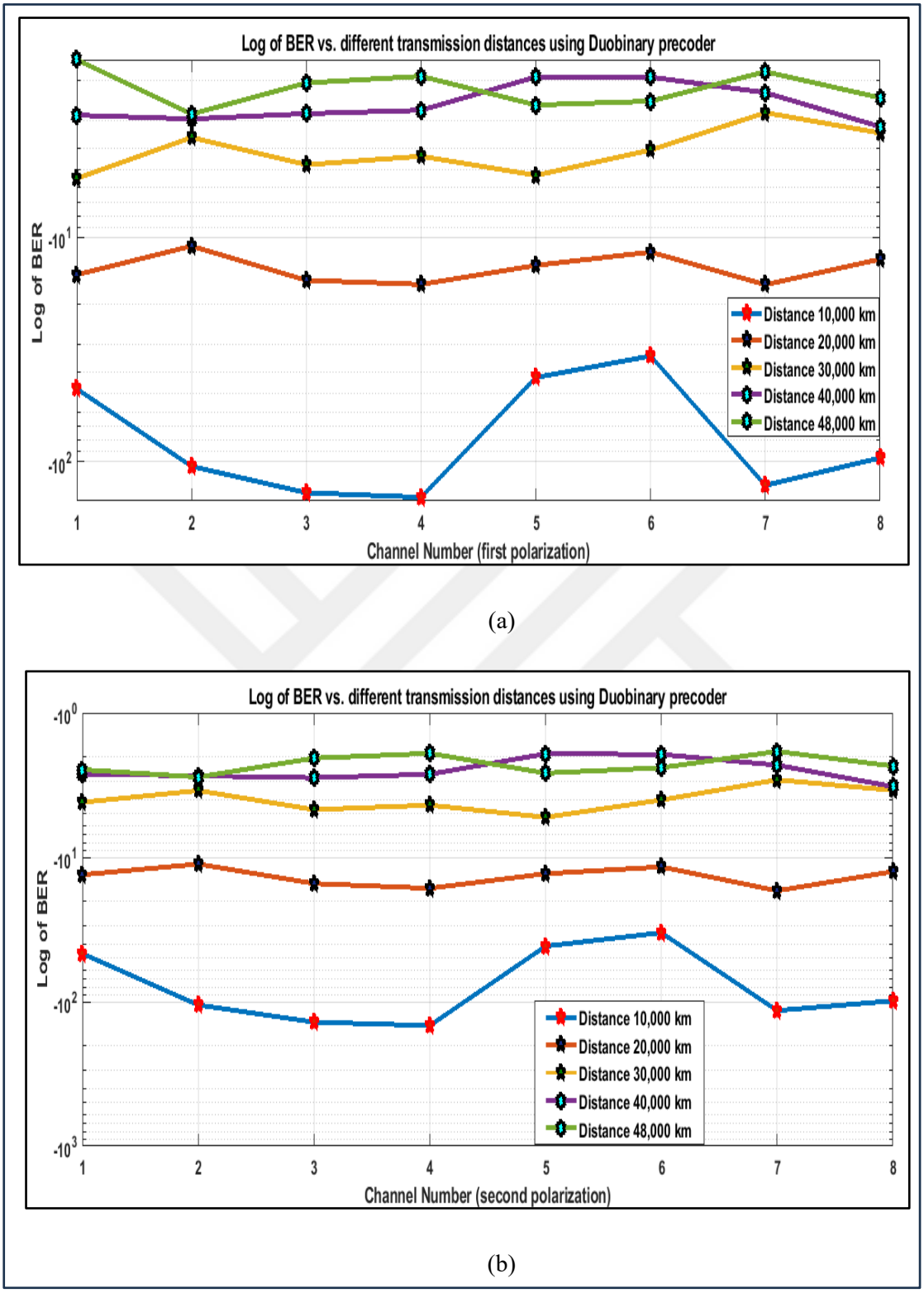

Figure 4.14: Log BER Vs. Different Distances For Duobinary Precoder a) P1 And b) P2.

Table 4.14: Averaged Log BER For Two-Polarization System Using DPSK Precoder.

Average log BER / Distance	Distance (km) – using DPSK precoder				
	10,000	**20,000**	**30,000**	**40,000**	**48,000**
p1	-36.7544	-10.5704	-6.91913	-2.83501	-1.35885
p2	-36.0106	-10.4617	-6.78737	-2.97387	-1.35933

Table 4.15: Averaged Log BER For The Two-Polarization System Using Duobinary Precoder.

Average log BER / Distance	Distance (km) – using Duobinary precoder				
	10,000	**20,000**	**30,000**	**40,000**	**48,000**
p1	-91.885	-13.891	-4.2124	-2.58135	-2.203645
p2	-90.646	-13.776	-4.0373	-2.53236	-2.30292625

Finally, the comparison between the major satellite system demonstrated by the thesis's first objective and the alternate system will be carried out based on comparing the log BER parameter between the two systems and as seen in Table 4.16 and analyzed as seen in Figure 4.15. From these results it can confirm the below points:

a. For distances up to 20,000 km using the DP-DQPSK-based method can achieve reliable results. However, keep in mind the tested system has not included the Pe impact. Such performance may be reduced when handling the Pe parameter.
b. For distances higher than 20,000 km up to 40,000 km, the proposed OFDM 16 QAM MDM-PDM system achieves the best performance with less BER impact as compared to the other system.
c. For distances over 40,000 km and up to 48,000 km, the DP-DQPSK system fails to perform successful transmission based on the minimum FEC threshold of -2.42.

It is worth mentioning, the results listed in Table 4.16 for the two systems include the average log BER obtained from the two polarization and then the two modes to get a final single value to achieve the comparison more realistically. Major comparisons from different prospects of view between the two systems are listed in Table 4.17.

Table 4.16: Comparison Of Average Log BER Between The Two Proposed Systems.

Distance (km) /system	OFDM 16 QAM system	DP-DQPSK DPSK precoder	DP-DQPSK Duobinary precoder
10,000	-16.69469	-36.38	-91.265
20,000	-13.57131	-10.52	-13.8339
30,000	-10.47094	-6.85	-4.12487
40,000	-7.285936	-2.90	-2.55685
48,000	-5.081405	-1.36	-2.25329

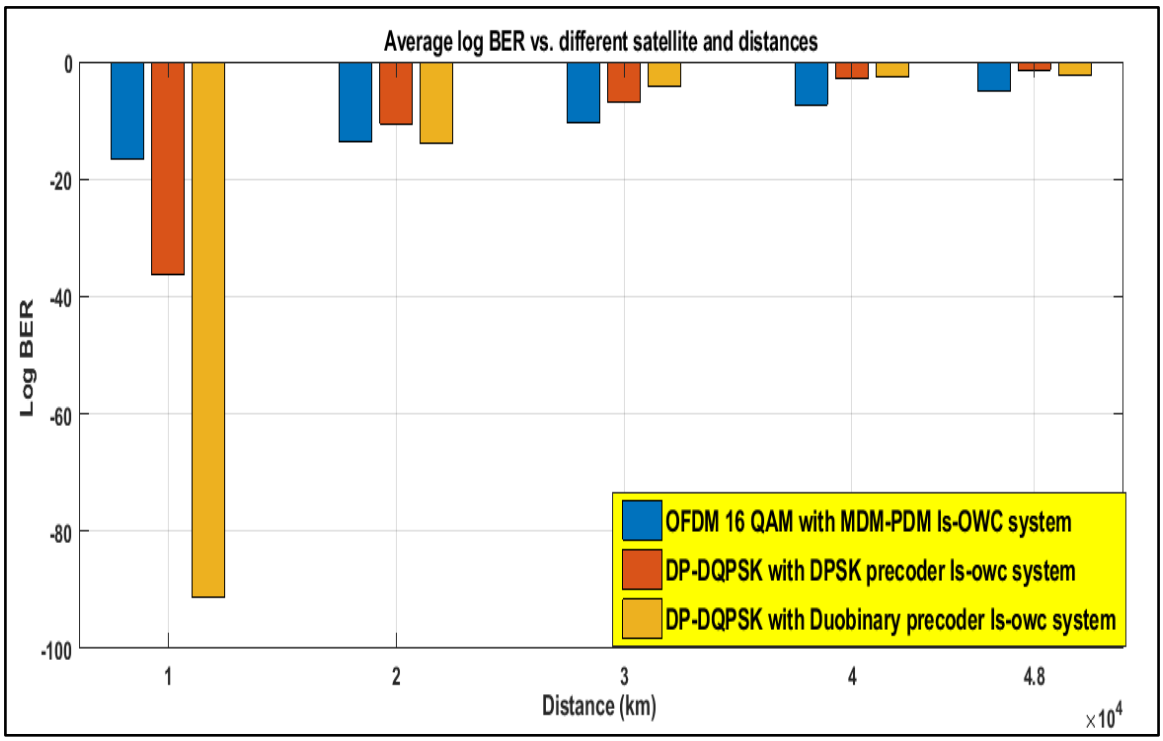

Figure 4.15: Average Log BER Vs. Different Satellite Systems And Distances.

Table 4.17: Comparison Between The Performance Of The Proposed Is-OWC MDM-PDM System And Is-OWC DP-DQPSK System.

Parameter	**DP-DQPSK-Is-OWC system**	**WDM-Is-OWC OFDM system [thesis]**	**Remark**
Number of channels	8	8	Same
Number of modes	-	2 (HG00 and HG01)	Using multimode technique
Number of Polarization	2 Dual polarization DQPSK	2 (PDM technique)	Same
Data rate/channel	15 Gbps	640 Gbps	Higher
Data rate/polarization	30 Gbps	320 Gbps	Higher
Transmission capability	40,000 km	48,000 km	Higher
Capability with transmission	For distances less than 20,000 km use (a duobinary precoder) and for distances between 20,000 km and 40,000 km (using a DPSK precoder is recommended).	Capable to perform all tested transmission	Reliable performance
Log BER at 48,000 km	DPSK (p1) = -1.35	HG00 (p1) = -5.02	Higher log BER performance indicates less error rate
	DPSK (p2) = -1.35	HG01 (p1) = -5.32	
	Duobinary (p1) = -2.20	HG00 (p2) = -4.83	
	Duobinary (p2) = -2.30	HG01 (p2) = -5.16	
Modulation method	Phase modulation (PSK)	Amplitude & phase	Advanced modulation scheme

Table 4.17: Comparison Between The Performance Of The Proposed Is-OWC MDM-PDM System And Is-OWC DP-DQPSK System "Table Continued".

Number of bits transmitted	2	4	Higher
Number of symbols transmitted	4	16	Higher
Total system capacity	240 Gbps	5.12 Tbps	Higher data rate
Division Multiplexing	WDM	OFDM with WDM	Orthogonal allocation
Tx Pe	Not included	1 mrad	Misalignment
Rx Pe	Not included	1 mrad	Misalignment
Frequency utilization	190.3 – 191 (THz)	193.1 – 193.8 (THz)	Reliable performance with less distortion and higher gain
Launched power	30 dBm	30 dBm	Same
Standard	ITU-T G.984.6	ITU-T G.694.1	Recommended standard

4.3 RESULTS-BASED SECOND OBJECTIVE

This part will demonstrate the results of the second objective mentioned in the first chapter of this thesis, which will include the result of investigating the performance of the proposed satellite system under the impact of Pe for both the Tx and Rx antenna sides. Pe variation will be analyzed concerning different parameters for performance evaluation.

4.3.1 Results-Based Rx Pointing Error

This part will demonstrate the performance evaluation of the proposed system concerning the Pe effect related to the Rx satellite. This investigation aims to provide a comprehensive analysis of the performance of the proposed system and its related capabilities under different pointing misalignments at the Rx antenna side. These results will be classified based on the studied parameters and as listed in the following.

4.3.1.1 Log BER-based results

The performance of the proposed OFDM 16 QAM system will be evaluated under different 5 cases of Rx Pe ranging, which are (1,1.5, 2, 2.5, and 3) mrad and analyzed for the two polarizations and per two modes of (HG00 and HG01) per each polarization. The analyzed data were listed in (Table 4.18 to Table 4.22) and (Figure 4.16 to Figure 4.20) for distances of 10,000 km, 20,000 km, 30,000 km, 40,000 km, and 48,000 km respectively. The analysis of the raising of Pe for the Rx can be listed in the below points:

a. A direct relation can be noticed between raising the Pe and the obtained log BER values. The influence is varied concerning the polarization and the mode per each polarization. And this influence is due to the variation impact of the utilized wavelengths with distortion.
b. HG00-based mode is more affected by the influence of raising Pe as compared to the HG01-based mode. Because the power intensity of the HG00 not reaching higher attached with maximum input power.
c. The proposed system showed successful performance under different Rx Pes for distances up to 30,000 km. And indicate acceptable performance with log BER not reaching the BER FEC threshold of -2.42. This confirms the reliability of the proposed system to handle effective transmission with Pes up to 3 mrad.

Further analysis can be carried out as shown in Table 4.23 by taking the average log BER from all the channels concerning all Pe values, different polarization, and different modes per polarization. This analysis aims to demonstrate the variation in log BER with raising the distance. It is found that for the distance of 10,000 km, the variation range in BER was between (-1.47 to -1.68), the distance of 20,000 km the variation range was between (-1.49 to -1.61). while, when raising the distance to 30,000 km variation reduced in the range between (-1.58 to -1.64) and the distance of 40,000 km recorded variation between (-1.58 to -1.62) and finally for 48,000 km the variance was very small due to series effect of raising distance and its correlation with raising Pe which was varied between (-1.17 to -1.21)

The last analysis of the obtained log BER values with different Pes was obtained as the averaged final value obtained from the four modes per the two polarizations. These data were listed in Table 4.23 and clarified in Figure 4.21. The final view indicates the superior performance of the proposed system with handling varied Pes. This can confirm the reliability of the system in handling Rx antenna misalignment for up to 3 mrad.

.

Table 4.18: Log BER Vs. Rx Pe At Distance Of 10,000 Km.

Log BER (p1)	Rx Pe at 10,000 km- p1- HG00				
	1 mrad	**1.5 mrad**	**2 mrad**	**2.5 mrad**	**3 mrad**
193.1	-17.3888	-17.0388	-16.6848	-16.3098	-15.9228
193.2	-17.1655	-16.7955	-16.4315	-16.0490	-15.6505
193.3	-16.9274	-16.5774	-16.1985	-15.8395	-15.4630
193.4	-16.6595	-16.2895	-15.9355	-15.5454	-15.1669
193.5	-16.3905	-16.0405	-15.6765	-15.2912	-14.9162
193.6	-15.8394	-15.4694	-15.0906	-14.7252	-14.3262
193.7	-15.6559	-15.3059	-14.9519	-14.5830	-14.2132
193.8	-14.9450	-14.5750	-14.2110	-13.8360	-13.4490
Log BER (p1)	Rx Pe at 10,000 km- p1- HG01				
193.1	-18.0365	-17.6665	-17.2905	-16.9048	-16.3198
193.2	-17.9033	-17.5533	-17.1847	-16.7862	-16.2078
193.3	-17.9687	-17.5987	-17.2401	-16.8600	-16.2902
193.4	-17.8895	-17.5395	-17.1635	-16.7813	-16.1963
193.5	-17.5288	-17.1588	-16.7902	-16.4045	-15.8075
193.6	-16.5857	-16.2357	-15.8771	-15.4786	-14.9188
193.7	-16.1993	-15.8293	-15.4533	-15.0732	-14.5234
193.8	-15.4182	-15.0682	-14.6996	-14.3174	-13.7324
Log BER (p2)	Rx Pe at 10,000 km - p2- HG00				
193.1	-17.3306	-16.9706	-16.6252	-16.2399	-15.8649
193.2	-17.0748	-16.7348	-16.3608	-15.9954	-15.5964
193.3	-16.7097	-16.3497	-15.9603	-15.5914	-15.2216
193.4	-16.6441	-16.3041	-15.9587	-15.5837	-15.1967
193.5	-16.0836	-15.7236	-15.3496	-14.9671	-14.5686
193.6	-15.7177	-15.3777	-14.9883	-14.6293	-14.2528
193.7	-15.3667	-15.0067	-14.6613	-14.2712	-13.8927
193.8	-14.7453	-14.4053	-14.0313	-13.6460	-13.2710
Log BER (p2)	Rx Pe at 10,000 km- p2- HG01				
193.1	-18.0114	-17.6514	-17.2528	-16.8770	-16.2800
193.2	-17.9035	-17.5585	-17.1988	-16.8234	-16.2636
193.3	-17.9337	-17.5737	-17.1871	-16.8130	-16.2632
193.4	-17.8105	-17.4655	-17.0669	-16.6987	-16.1137
193.5	-16.9611	-16.6011	-16.2415	-15.8657	-15.2873
193.6	-16.4162	-16.0712	-15.6846	-15.3092	-14.7394
193.7	-15.8796	-15.5196	-15.1210	-14.7469	-14.1619
193.8	-15.1393	-14.7943	-14.4346	-14.0664	-13.4814

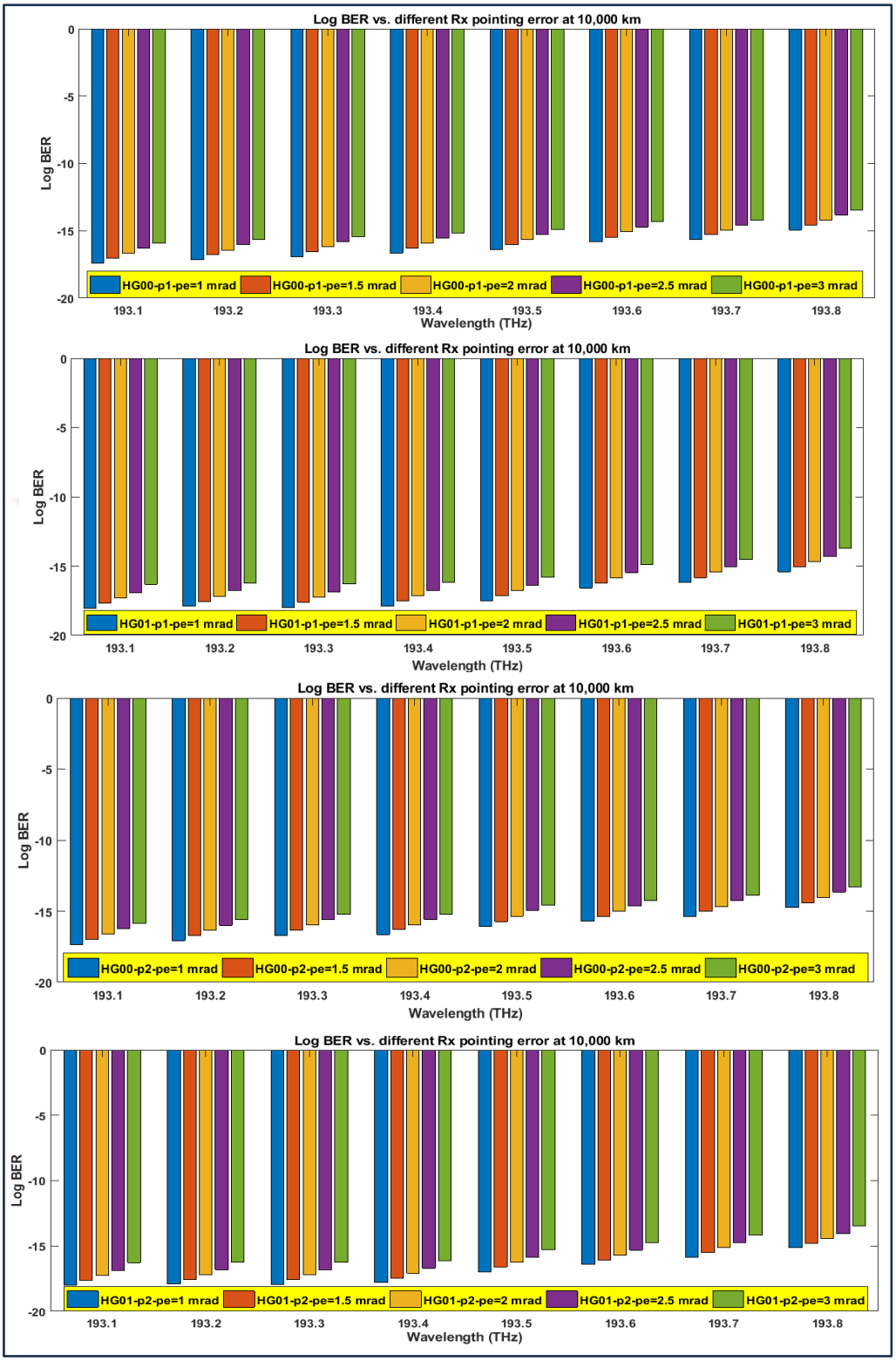

Figure 4.16: Log BER Vs. Rx Pe At 10,000 Km With a) HG00-P1, b) HG01-P1, c) HG00-P2, And d) HG01-P2.

Table 4.19: Log BER Vs. Rx Pe At Distance Of 20,000 Km.

Log BER (p1)	Rx Pe at 20,000 km- p1- HG00				
	1 mrad	**1.5 mrad**	**2 mrad**	**2.5 mrad**	**3 mrad**
193.1	-14.3548	-13.9878	-13.6338	-13.2468	-12.7618
193.2	-14.1315	-13.7565	-13.3791	-13.0140	-12.5155
193.3	-13.8934	-13.5264	-13.1362	-12.7471	-12.2713
193.4	-13.6255	-13.2505	-12.8965	-12.5167	-12.0317
193.5	-13.3565	-12.9895	-12.6121	-12.2341	-11.7356
193.6	-12.8054	-12.4304	-12.0403	-11.6825	-11.2067
193.7	-12.6219	-12.2549	-11.9009	-11.5324	-11.0474
193.8	-11.9110	-11.5360	-11.1586	-10.7716	-10.2731
Log BER (p1)	Rx Pe at 20,000 km- p1- HG01				
193.1	-14.6925	-14.4330	-14.0780	-13.6908	-13.1928
193.2	-14.5593	-14.2643	-13.9002	-13.5344	-13.0599
193.3	-14.6247	-14.3352	-13.9747	-13.5846	-13.1195
193.4	-14.5455	-14.2805	-13.9255	-13.5510	-13.0923
193.5	-14.1848	-13.8653	-13.5012	-13.1140	-12.6452
193.6	-13.5417	-13.2822	-12.9217	-12.5559	-12.1103
193.7	-13.1553	-12.8603	-12.5053	-12.1152	-11.6368
193.8	-12.3742	-12.0847	-11.7207	-11.3462	-10.8482
Log BER (p2)	Rx Pe at 20,000 km - p2- HG00				
193.1	-14.2966	-13.9426	-13.5772	-13.1992	-12.7122
193.2	-14.0408	-13.6918	-13.3138	-12.9560	-12.4873
193.3	-13.6757	-13.3217	-12.9718	-12.6033	-12.1444
193.4	-13.6101	-13.2611	-12.8957	-12.5087	-12.0217
193.5	-13.0496	-12.6956	-12.3176	-11.9525	-11.4838
193.6	-12.6837	-12.3347	-11.9848	-11.5957	-11.1368
193.7	-12.3327	-11.9787	-11.6133	-11.2335	-10.7465
193.8	-11.7113	-11.3623	-10.9843	-10.6063	-10.1376
Log BER (p2)	Rx Pe at 20,000 km- p2- HG01				
193.1	-14.6674	-14.4024	-14.0374	-13.6594	-13.1906
193.2	-14.5595	-14.2400	-13.8635	-13.4654	-13.0198
193.3	-14.5897	-14.3302	-13.9427	-13.5614	-13.0830
193.4	-14.4665	-14.1715	-13.8065	-13.4409	-12.9429
193.5	-13.9171	-13.6276	-13.2511	-12.8731	-12.3986
193.6	-13.3722	-13.1072	-12.7197	-12.3216	-11.8565
193.7	-12.8356	-12.5161	-12.1511	-11.7698	-11.3111
193.8	-12.0953	-11.8358	-11.4493	-11.0837	-10.6149

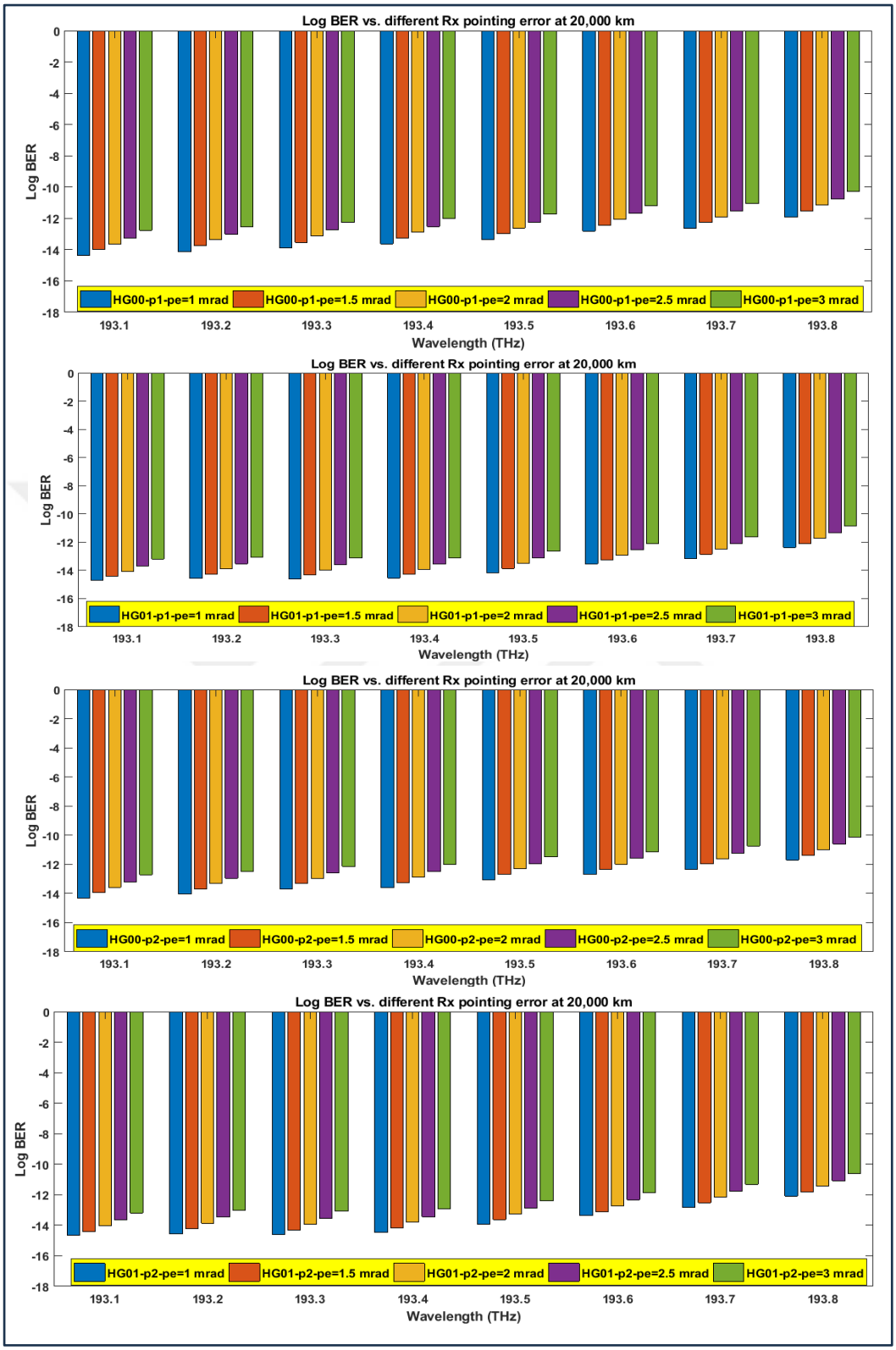

Figure 4.17: Log BER Vs. Rx Pe At 20,000 Km With a) HG00-P1, b) HG01-P1, c) HG00-P2, And d) HG01-P2.

Table 4.20: Log BER Vs. Rx Pe At Distance Of 30,000 Km.

Log BER (p1)	Rx Pe at 30,000 km- p1- HG00				
	1 mrad	**1.5 mrad**	**2 mrad**	**2.5 mrad**	**3 mrad**
193.100	-11.2978	-10.9408	-10.5948	-10.2103	-9.7133
193.200	-11.0745	-10.7248	-10.3591	-9.9606	-9.5022
193.300	-10.8364	-10.4837	-10.0941	-9.7120	-9.2362
193.400	-10.4685	-10.0915	-9.7455	-9.3694	-8.9036
193.500	-10.2995	-9.9115	-9.5458	-9.1700	-8.6960
193.600	-9.7484	-9.3914	-9.0018	-8.6320	-8.1622
193.700	-9.5649	-9.2152	-8.8692	-8.4911	-8.0040
193.800	-8.8540	-8.5013	-8.1356	-7.7511	-7.2541
Log BER (p1)	Rx Pe at 30,000 km- p1- HG01				
193.100	-11.5675	-11.2175	-10.8525	-10.4653	-9.9783
193.200	-11.4343	-10.8553	-10.4798	-10.0886	-9.6338
193.300	-11.4997	-11.1217	-10.7230	-10.3644	-9.8663
193.400	-11.4205	-11.0625	-10.6840	-10.2968	-9.8098
193.500	-11.0598	-10.6920	-10.3353	-9.9481	-9.4933
193.600	-10.4167	-10.0607	-9.6739	-9.2827	-8.7846
193.700	-10.0303	-9.6812	-9.3247	-8.9661	-8.4791
193.800	-9.2492	-8.8992	-8.5342	-8.1470	-7.6922
Log BER (p2)	Rx Pe at 30,000 km - p2- HG00				
193.1	-11.2396	-10.8626	-10.5050	-10.1292	-9.6552
193.2	-10.9838	-10.5958	-10.2380	-9.8682	-9.3984
193.3	-10.6187	-10.2617	-9.9050	-9.5269	-9.0398
193.4	-10.3531	-10.0034	-9.6458	-9.2613	-8.7643
193.5	-9.9926	-9.6399	-9.2821	-8.8836	-8.4252
193.6	-9.6267	-9.2497	-8.8930	-8.5109	-8.0351
193.7	-9.2757	-8.8877	-8.5301	-8.1540	-7.6882
193.8	-8.6543	-8.2973	-7.9395	-7.5637	-7.0897
Log BER (p2)	Rx Pe at 30,000 km- p2- HG01				
193.1	-11.5424	-11.1746	-10.8179	-10.4425	-9.9685
193.2	-11.4345	-11.0785	-10.6917	-10.3230	-9.8479
193.3	-11.4647	-11.1157	-10.7592	-10.3702	-9.8826
193.4	-11.3415	-10.9915	-10.6265	-10.0393	-9.5653
193.5	-10.7921	-10.4431	-10.0676	-9.6922	-9.2171
193.6	-10.2472	-9.8692	-9.4704	-9.1017	-8.6141
193.7	-9.7106	-9.3526	-8.9741	-8.5851	-8.1111
193.8	-8.9703	-8.6025	-8.2458	-7.6586	-7.1835

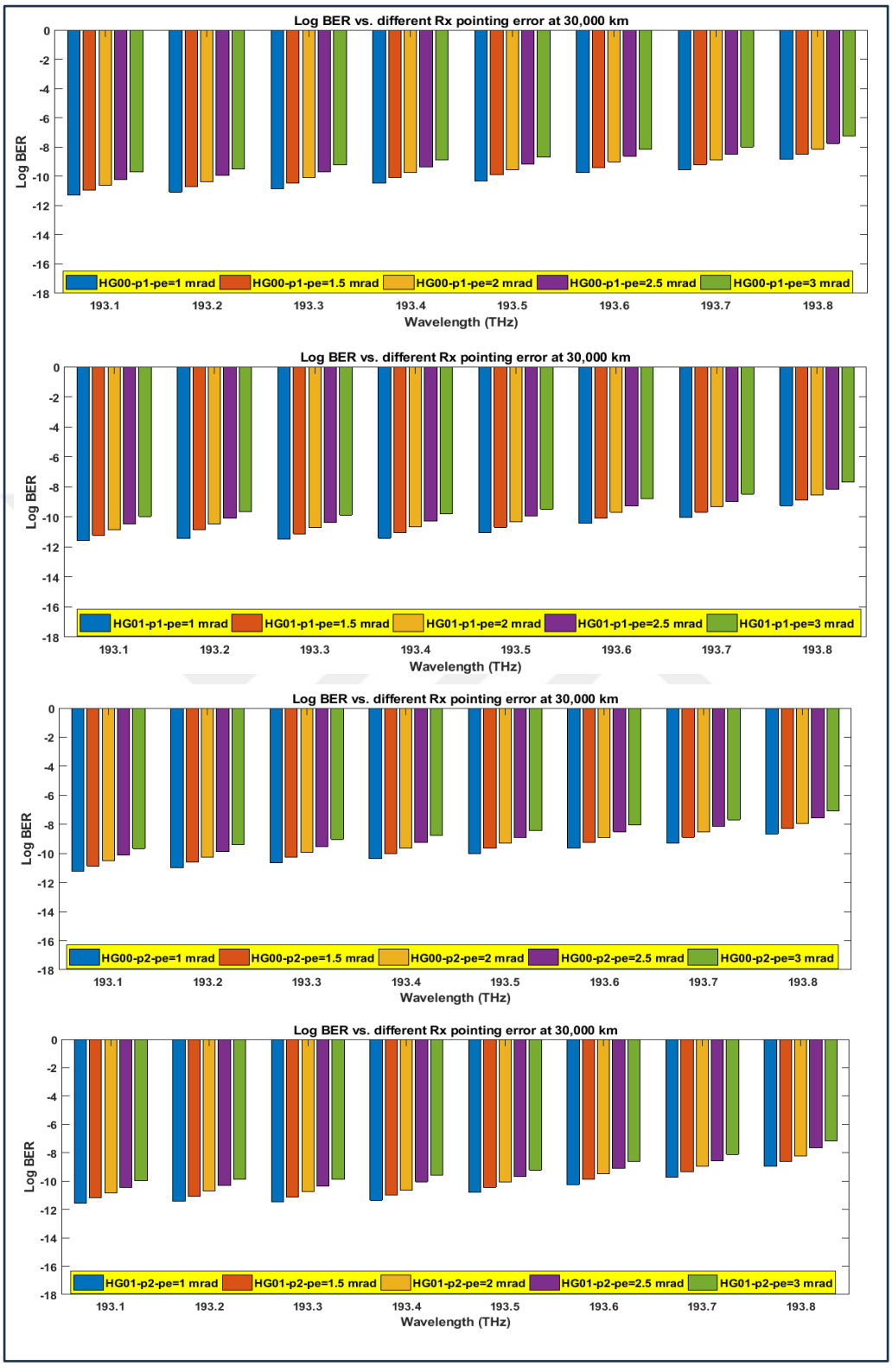

Figure 4.18: Log BER Vs. Rx Pe At 30,000 Km With a) HG00-P1, b) HG01-P1,c) HG00-P2, And d) HG01-P2.

Table 4.21: Log BER Vs. Rx Pe At Distance Of 40,000 Km.

Log BER (p1)	Rx Pe at 40,000 km- p1- HG00				
	1 mrad	**1.5 mrad**	**2 mrad**	**2.5 mrad**	**3 mrad**
193.1	-8.1778	-7.8128	-7.4528	-7.0653	-6.5783
193.2	-7.9545	-7.6065	-7.2525	-6.8938	-6.4340
193.3	-7.7164	-7.3420	-6.9608	-6.5921	-6.1167
193.4	-7.3485	-6.9615	-6.5763	-6.1916	-5.6955
193.5	-7.1795	-6.8230	-6.4580	-6.0705	-5.5835
193.6	-6.6284	-6.2634	-5.8882	-5.5295	-5.0697
193.7	-6.4449	-6.0969	-5.7316	-5.3629	-4.8875
193.800	-5.7340	-5.3597	-4.9997	-4.6150	-4.1189
Log BER (p1)	Rx Pe at 40,000 km- p1- HG01				
193.1	-8.3175	-7.9635	-7.5895	-7.2025	-6.7155
193.2	-8.1843	-7.8059	-7.4184	-7.0497	-6.5708
193.3	-8.2497	-7.8713	-7.5015	-7.1101	-6.6403
193.4	-8.1705	-7.8011	-7.4119	-7.0183	-6.5485
193.5	-7.8098	-7.4508	-7.0855	-6.6985	-6.2115
193.6	-7.1667	-6.8127	-6.4530	-6.0843	-5.6054
193.7	-6.7803	-6.4019	-6.0422	-5.6508	-5.1810
193.800	-5.9992	-5.6208	-5.2468	-4.8532	-4.3834
Log BER (p2)	Rx Pe at 40,000 km - p2- HG00				
193.1	-8.1196	-7.7326	-7.3676	-6.9931	-6.5191
193.2	-7.8638	-7.5073	-7.1321	-6.7607	-6.2742
193.3	-7.4987	-7.1337	-6.7684	-6.4106	-5.9657
193.4	-7.2331	-6.8851	-6.5251	-6.1593	-5.6639
193.5	-6.8726	-6.4982	-6.1442	-5.7697	-5.2957
193.6	-6.5067	-6.1197	-5.7385	-5.3671	-4.8806
193.7	-6.1557	-5.7992	-5.4140	-5.0562	-4.6113
193.8	-5.5343	-5.1693	-4.8043	-4.4385	-3.9431
Log BER (p2)	Rx Pe at 40,000 km- p2- HG01				
193.1	-8.2924	-7.9230	-7.5577	-7.1827	-6.6837
193.2	-8.1845	-7.8255	-7.4658	-7.0671	-6.5826
193.3	-8.2147	-7.8607	-7.5010	-7.1085	-6.6100
193.4	-8.0915	-7.7131	-7.3391	-6.9475	-6.4581
193.5	-7.5421	-7.1637	-6.7762	-6.4012	-5.9022
193.6	-6.9972	-6.6278	-6.2580	-5.8593	-5.3748
193.7	-6.4606	-6.1016	-5.7124	-5.3199	-4.8214
193.8	-5.7203	-5.3663	-5.0010	-4.6094	-4.1200

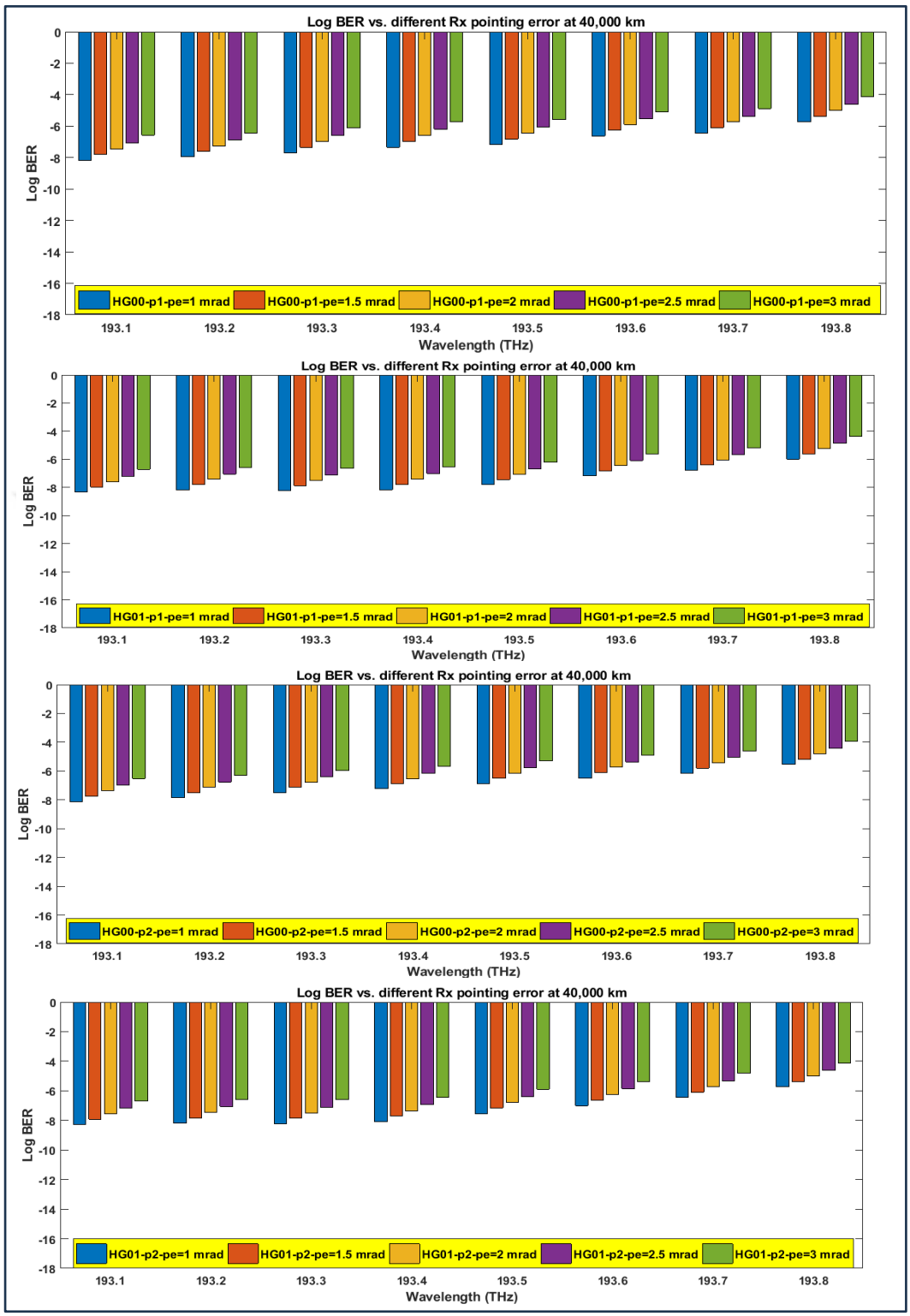

Figure 4.19: Log BER Vs. Rx Pe At 40,000 Km With a) HG00-P1, b) HG01-P1, c) HG00-P2, And d) HG01-P2.

Table 4.22: Log BER Vs. Rx Pe At Distance Of 48,000 Km.

Log BER (p1)	Rx Pe at 48,000 km- p1- HG00				
	1 mrad	**1.5 mrad**	**2 mrad**	**2.5 mrad**	**3 mrad**
193.100	-5.9778	-5.6648	-5.4108	-5.1898	-4.9898
193.200	-5.8545	-5.5302	-5.2544	-5.0004	-4.7004
193.300	-5.6164	-5.3001	-5.0122	-4.8112	-4.4532
193.400	-5.2485	-4.9422	-4.6610	-4.3770	-3.9890
193.500	-5.0795	-4.7642	-4.5002	-4.2222	-3.8642
193.600	-4.5284	-4.2154	-3.9258	-3.6938	-3.3058
193.700	-4.2449	-3.9206	-3.6496	-3.4086	-3.0506
193.800	-3.6340	-3.3177	-3.0637	-2.8252	-2.4372
Log BER (p1)	Rx Pe at 48,000 km- p1- HG01				
193.100	-6.0175	-5.7165	-5.4595	-5.2185	-4.9935
193.200	-5.9843	-5.6582	-5.3847	-5.1237	-4.8987
193.300	-5.9497	-5.6286	-5.3599	-5.1245	-4.7020
193.400	-5.8705	-5.5695	-5.3042	-5.0501	-4.5978
193.500	-5.5098	-5.1837	-4.9267	-4.6857	-4.2632
193.600	-4.8667	-4.5456	-4.2721	-4.0111	-3.5588
193.700	-4.4803	-4.1793	-3.9106	-3.6752	-3.2527
193.800	-3.8492	-3.5231	-3.2579	-3.0038	-2.5515
Log BER (p2)	Rx Pe at 48,000 km - p2- HG00				
193.1	-5.9196	-5.6133	-5.3493	-5.1173	-4.8673
193.2	-5.7638	-5.4485	-5.1589	-4.9179	-4.6059
193.3	-5.3987	-5.0857	-4.8147	-4.5762	-4.1792
193.4	-5.1331	-4.8088	-4.5548	-4.2648	-3.8298
193.5	-4.7726	-4.4563	-4.1805	-3.9595	-3.5625
193.6	-4.4067	-4.1004	-3.8125	-3.5585	-3.1235
193.7	-3.9057	-3.5904	-3.3092	-3.1082	-2.7112
193.8	-3.3343	-3.0213	-2.7573	-2.5363	-2.2388
Log BER (p2)	Rx Pe at 48,000 km- p2- HG01				
193.1	-5.9924	-5.6813	-5.3992	-5.1482	-4.9072
193.2	-5.9695	-5.6424	-5.3847	-5.1107	-4.7977
193.3	-5.9147	-5.6166	-5.3256	-5.0505	-4.6255
193.4	-5.7915	-5.4804	-5.2304	-5.0050	-4.6920
193.5	-5.2421	-4.9150	-4.6329	-4.3819	-3.9569
193.6	-4.6172	-4.3191	-4.0614	-3.7874	-3.4744
193.7	-4.1506	-3.8395	-3.5484	-3.2733	-2.8483
193.8	-3.5803	-3.2532	-3.0032	-2.7778	-2.4648

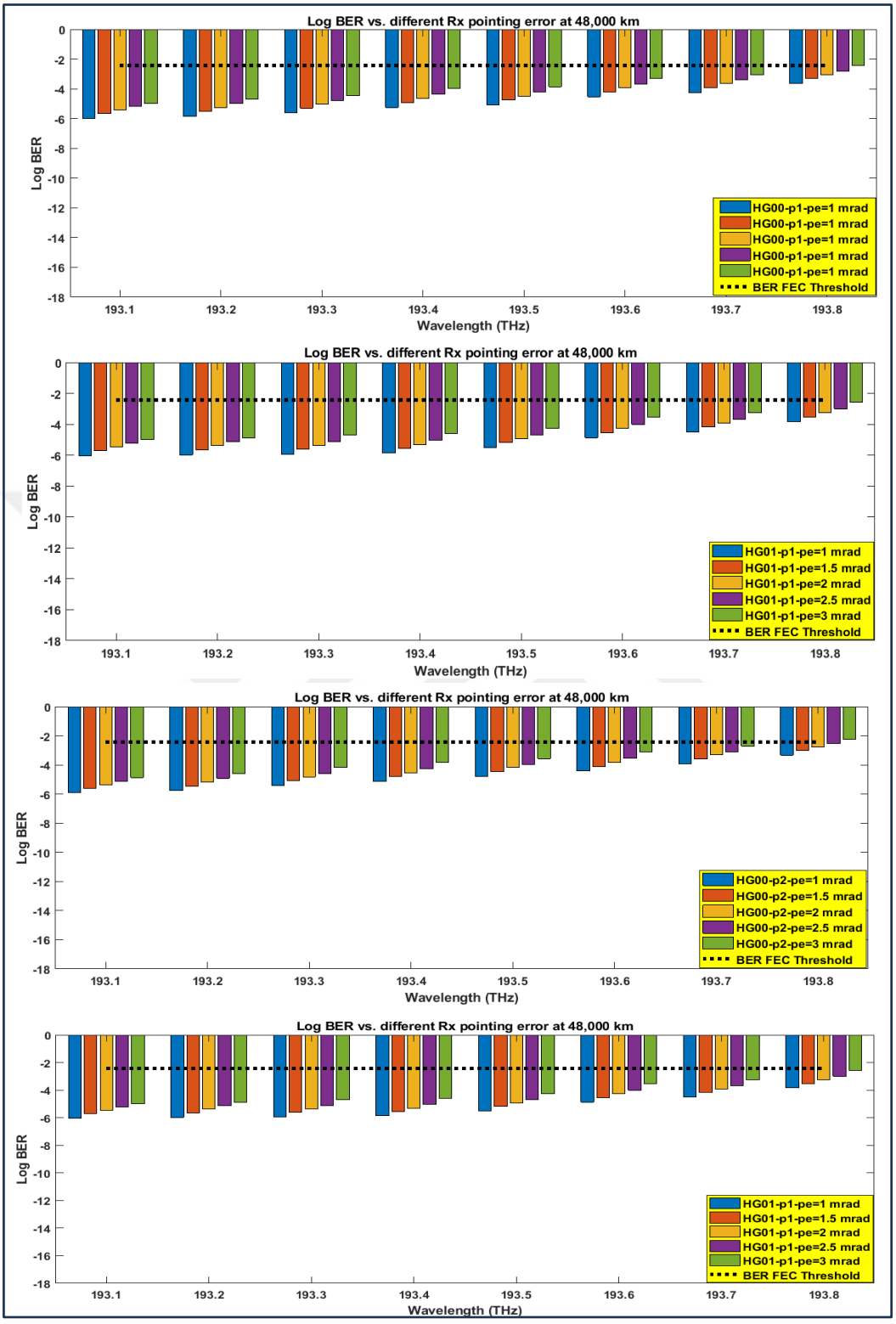

Figure 4.20: Log BER Vs. Rx Pe At 48,000 Km With a) HG00-P1, b) HG00-P2, c) HG01-P1, And d) HG01-P2.

Table 4.23: Averaged Log BER Under Influence Of Pe And Transmission Distances.

distance 10,000 km				
pe (mrad)	**HG00-p1**	**HG01-p1**	**HG00-p2**	**HG01-p2**
1	-16.372	-17.191	-16.209	-17.007
1.5	-16.01151	-16.83124	-15.85908	-16.65441
2	-15.64755	-16.46237	-15.49195	-16.27342
2.5	-15.2724	-16.07574	-15.11552	-15.90004
3	-14.88848	-15.49952	-14.7331	-15.32382
Log BER variance	-1.483	-1.692	-1.476	-1.683
distance 20,000 km				
1	-13.33751	-13.95974	-13.17508	-13.81291
1.5	-12.96651	-13.67568	-12.82358	-13.52885
2	-12.5947	-13.31591	-12.45732	-13.15266
2.5	-12.21816	-12.93651	-12.08191	-12.77192
3	-11.7304	-12.46312	-11.60879	-12.30218
Log BER variance	-1.60711	-1.496619	-1.566285	-1.510733
distance 30,000 km				
1	-10.26801	-10.83474	-10.09308	-10.68791
1.5	-9.907531	-10.44876	-9.724779	-10.32845
2	-9.543244	-10.07592	-9.367329	-9.956653
2.5	-9.162069	-9.694869	-8.987242	-9.526578
3	-8.683956	-9.217169	-8.512004	-9.048765
Log BER variance	-1.58405	-1.617574	-1.581075	-1.639149
distance 40,000 km				
1	-7.148006	-7.584744	-6.973079	-7.437914
1.5	-6.783231	-7.216001	-6.605661	-7.072729
2	-6.414994	-6.843601	-6.236798	-6.701417
2.5	-6.040094	-6.458426	-5.869423	-6.311967
3	-5.560519	-5.982051	-5.394223	-5.819117
Log BER variance	-1.587488	-1.602693	-1.578856	-1.618798
distance 48,000 km				
1	-5.02301	-5.31599	-4.82933	-5.15729
1.5	-4.70691	-5.00056	-4.5156	-4.84344
2	-4.43472	-4.73444	-4.24217	-4.57323
2.5	-4.19103	-4.48656	-4.00485	-4.31685
3	-3.84878	-4.10228	-3.63979	-3.97085
Log BER variance	-1.174225	-1.213711	-1.189538	-1.186435

Table 4.24: The Final Averaged Log BER Values Over Different Distances.

pe (mrad)	Distance (km)				
	10,000	**20,000**	**30,000**	**40,000**	**48,000**
1	-16.695	-13.571	-10.287	-7.286	-5.0814
1.5	-16.33906	-13.24865	-9.919084	-6.919406	-4.76663
2	-15.96882	-12.88015	-9.539238	-6.549202	-4.49614
2.5	-15.59092	-12.50212	-9.104082	-6.169977	-4.24983
3	-15.11123	-12.02612	-8.865474	-5.688977	-3.89043

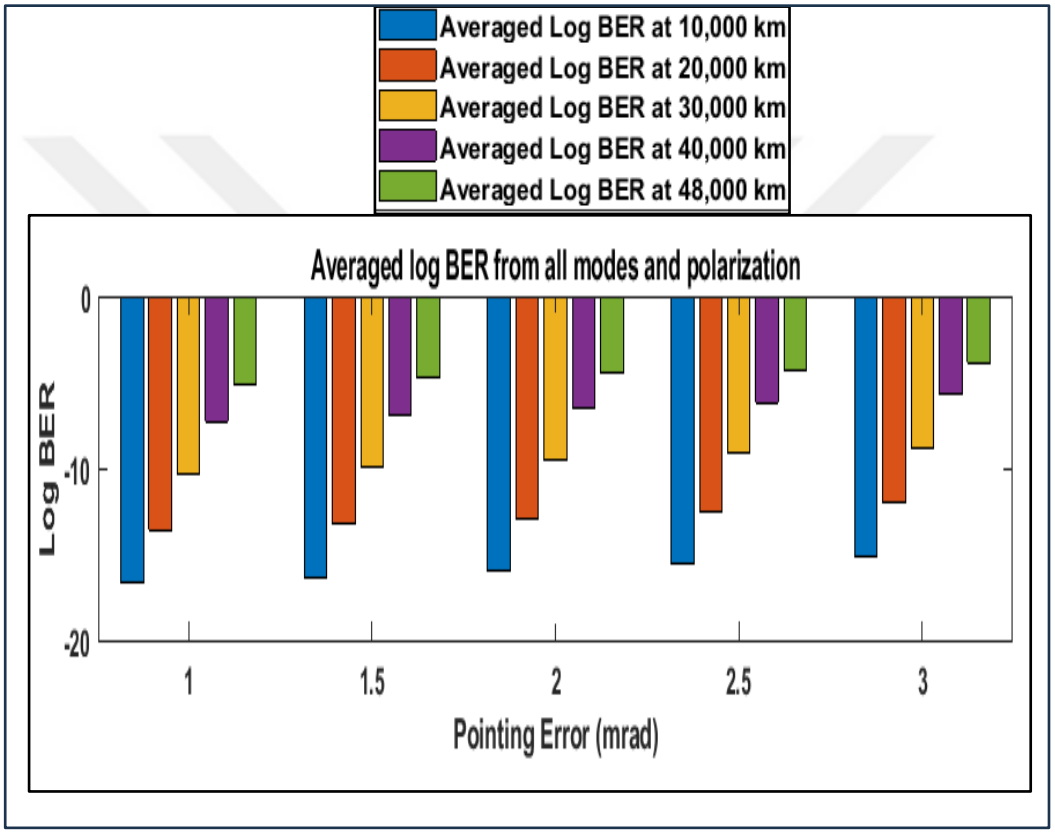

Figure 4.21: Averaged Log BER Vs. Different Pe For All Studied Distances.

4.3.1.2 OSNR- based results

The OSNR will be studied concerning different Rx Pes and for all the investigated distances to demonstrate the impact of raising the Pe on OSNR performance as listed in Table 4.25 and clarified in Figure 4.22. Results obtained will be analyzed concerning fixed and varied distances. For fixed distances, a reverse relation can be noticed as raising the Pe can reduce the OSNR performance for the proposed system. Where the variation for Pe up to 2 mrad was about 3 dB. While, when going for a higher Pe for the Rx to reach 3 mrad, the OSNR reduction was up to 5 dB. This may indicate the serious effect of the large antenna misalignment for the Rx satellite.

Analyzing the impact of OSNR for the five cases of distance variation, it can be noticed that OSNR influence for 1 mrad Pe was up to 3 dB, while for 1.5 mrad the influence was between (3-4) dB. And this influence is raised by increasing the Pe over 1.5 mrad to reach 3 mrad to be between (3-5) dB.

Table 4.25: OSNR From Different Channels Vs. Different Rx Pe At Different Distances.

Wavelength / OSNR	**1 mrad**	**1.5 mrad**	**2 mrad**	**2.5 mrad**	**3 mrad**
	OSNR (dB) at Distance = 10,000 km				
193.1	78	74	70	65	60
193.2	74	70	66	61	56
193.3	70	66	62	57	52
193.4	67	63	59	54	49
193.5	64	60	56	51	46
193.6	59	55	51	46	41
193.7	56	52	48	43	38
193.8	51	47	43	38	33
OSNR (dB) at Distance = 20,000 km					
193.1	75	71	67	62	57
193.2	71	67	63	58	53
193.3	67	63	59	54	49
193.4	63	59	55	50	45
193.5	59	55	51	46	41
193.6	55	51	47	42	37
193.7	51	47	43	38	33
193.8	47	43	39	34	29

Table 4.25: OSNR From Different Channels Vs. Different Rx Pe At Different Distances "Table Continued".

OSNR (dB) at Distance = 30,000 km					
193.1	72	67	62	57	52
193.2	68	63	58	53	48
193.3	64	59	54	49	44
193.4	60	55	50	45	40
193.5	56	51	46	41	36
193.6	52	47	42	37	32
193.7	48	43	38	33	28
193.8	44	39	34	29	24
OSNR (dB) at Distance = 40,000 km					
193.1	69	64	59	54	49
193.2	65	60	55	50	45
193.3	61	56	51	46	41
193.4	57	52	47	42	37
193.5	53	48	43	38	33
193.6	49	44	39	34	29
193.7	45	40	35	30	25
193.8	41	36	31	26	21
OSNR (dB) at Distance = 48,000 km					
193.1	67	62	57	52	47
193.2	63	58	53	48	43
193.3	59	54	49	44	39
193.4	55	50	45	40	35
193.5	51	46	41	36	31
193.6	47	42	37	32	27
193.7	43	38	33	28	23
193.8	39	34	29	24	19

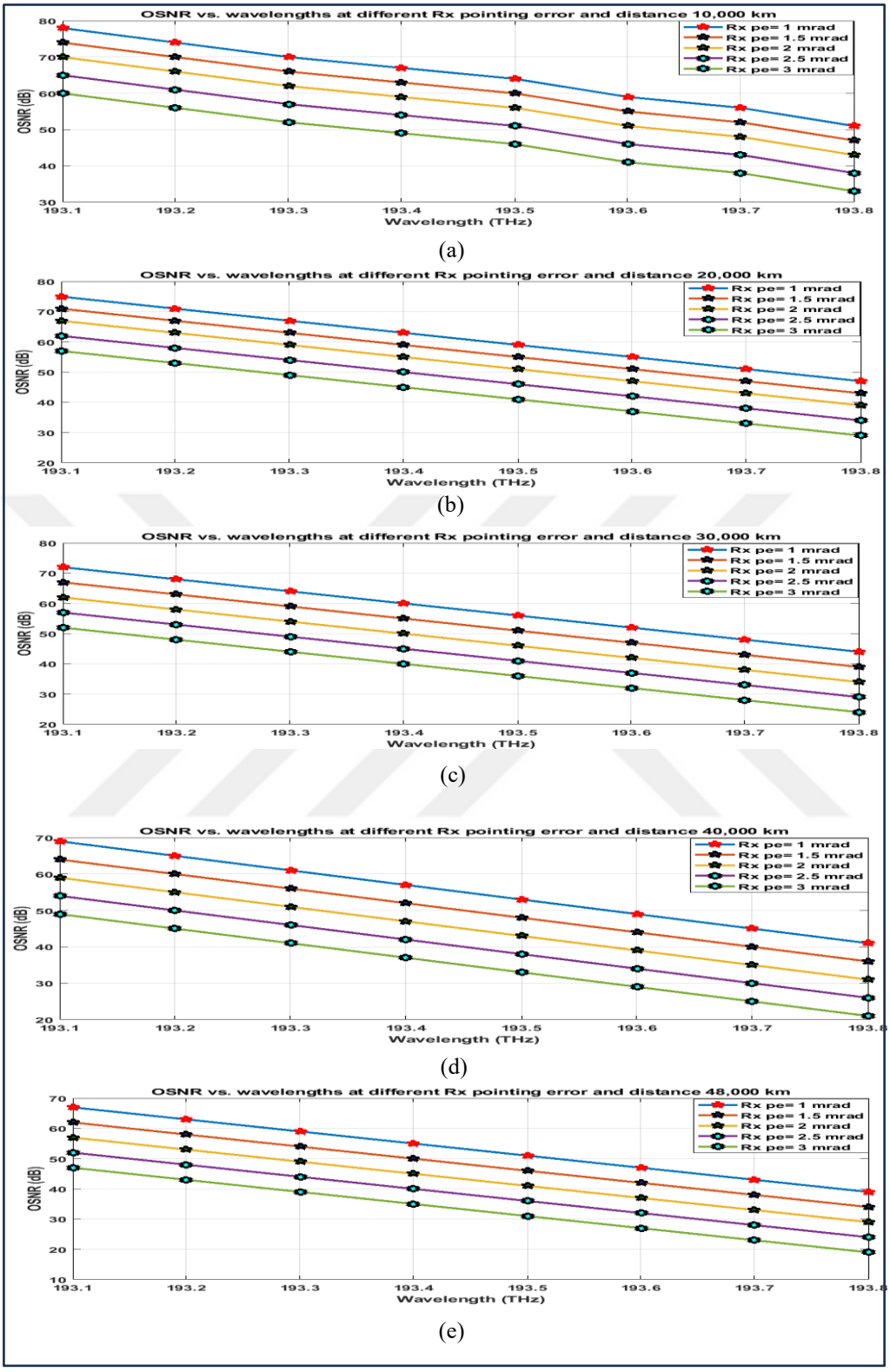

Figure 4.22: OSNR Vs. Wavelengths At Different Rx Pe For a) 10,000 Km, b) 20,000 Km, c) 30,000 Km, d) 40,000 Km, And e) 48,000 Km.

Specifically, the behaviour of the OSNR variation would be investigated in relation to the log BER performance for each of the five different transmission distances, as well as each of the Pe values for each of the two modes, as shown in Figures 4.23 to 4.27 for each of the five different transmission distances. It has been observed that HG01 provides superior performance in comparison to HG00, and this variation will be lessened if the Rx Pe values are increased. Considering this, it is necessary to verify the dependability of the OFDM 16 QAM system that has been presented to accomplish transmission at Rx Pe up to 3 mrad.

As a result of the significance of the optical signal-to-noise ratio (OSNR) as an important component that aids in the identification and troubleshooting of critical components, as well as the reduction of operating expenses and the capability to lead to increases in network potential, the OSNR is an essential component. Because of this, it is of the highest necessity to obtain the minimum OSNR value that can maintain the BER FEC threshold. The calculation of the averaged log BER from each mode scenario will be used to achieve this goal. This calculation will take into consideration all the distances and peer values that have been analyzed.

Subsequently, as seen in Figure 4.28, it is necessary to calculate the average of each of the two modes to merge them into a single value. Considering the Rx Pe values of 1 mrad, 1.5 mrad, 2 mrad, 2.5 mrad, and 3 mrad, it is feasible to arrive at the conclusion that the system offers an OSNR tolerance of 50.5 dB, 45.75 dB, 41.7 dB, 36.8 dB, and 31.9 dB, respectively.

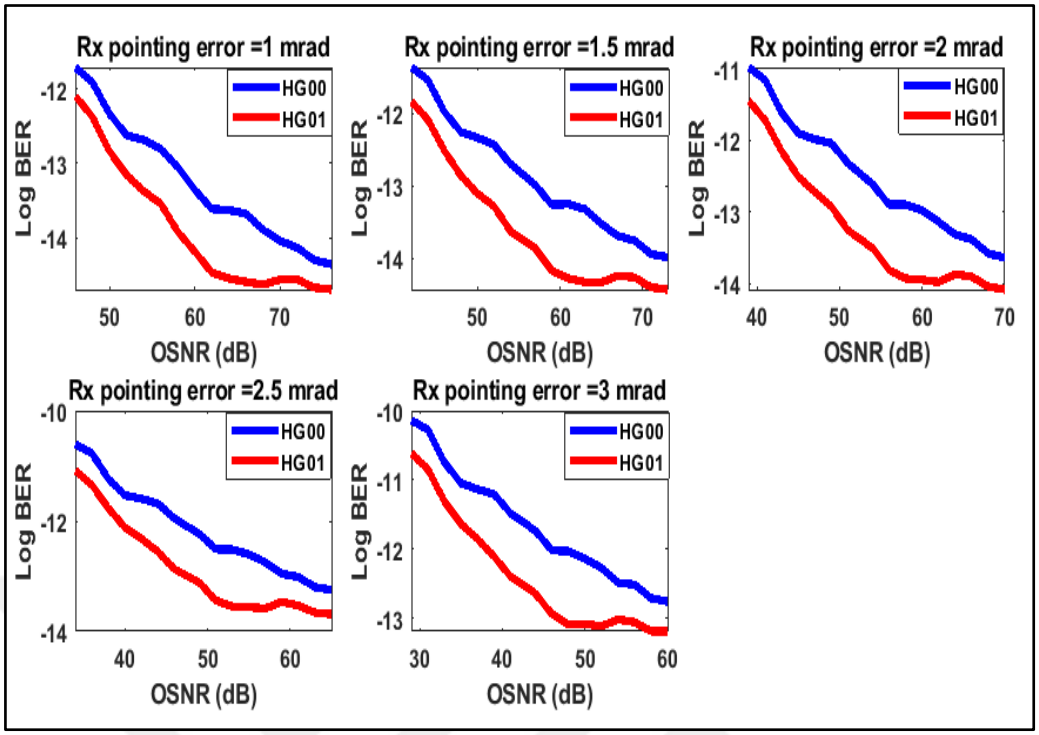

Figure 4.23: Log BER Vs. OSNR With Different Rx Pe At 10,000 Km Distance.

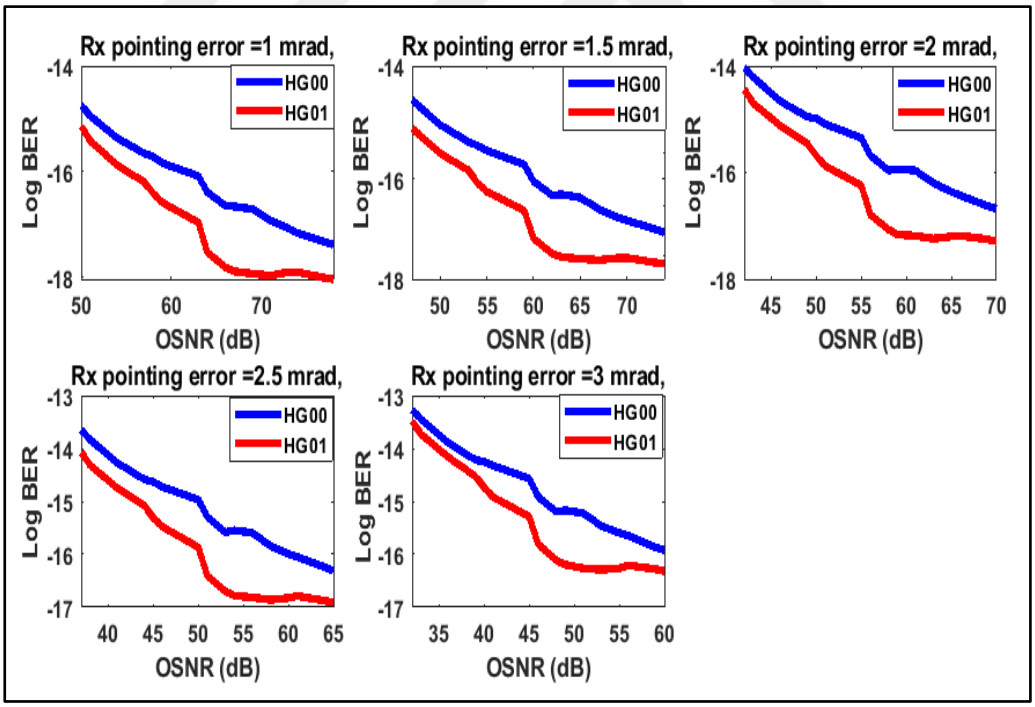

Figure 4.24: Log BER Vs. OSNR With Different Rx Pe At 20,000 Km Distance.

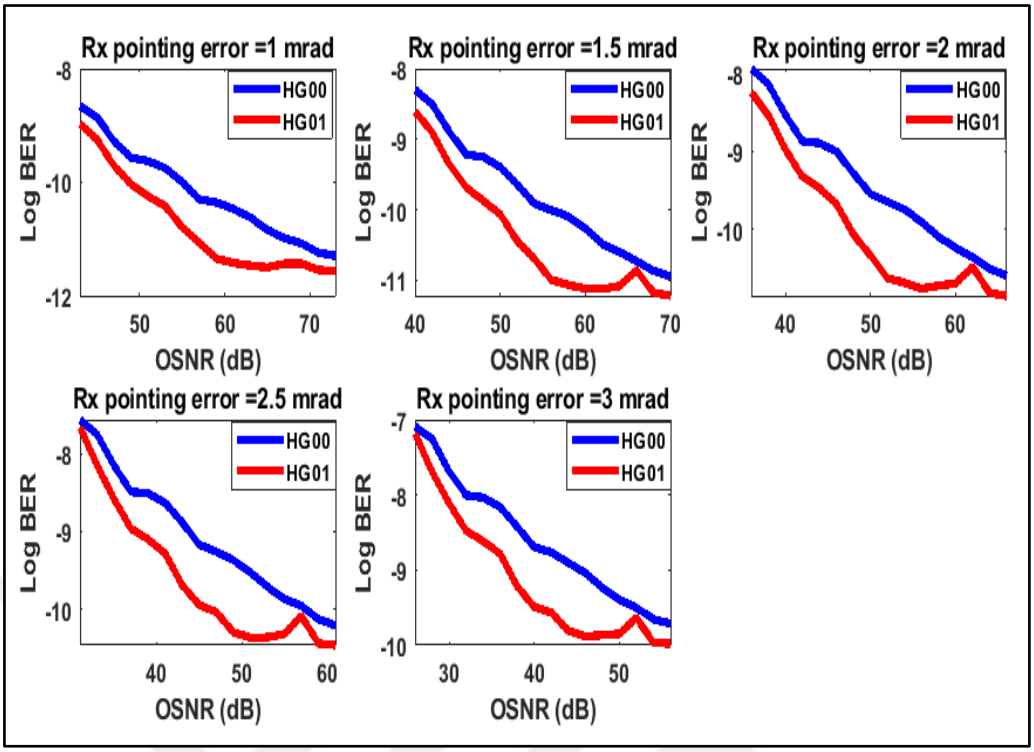

Figure 4.25: Log BER Vs. OSNR With Different Rx Pe At 30,000 Km Distance.

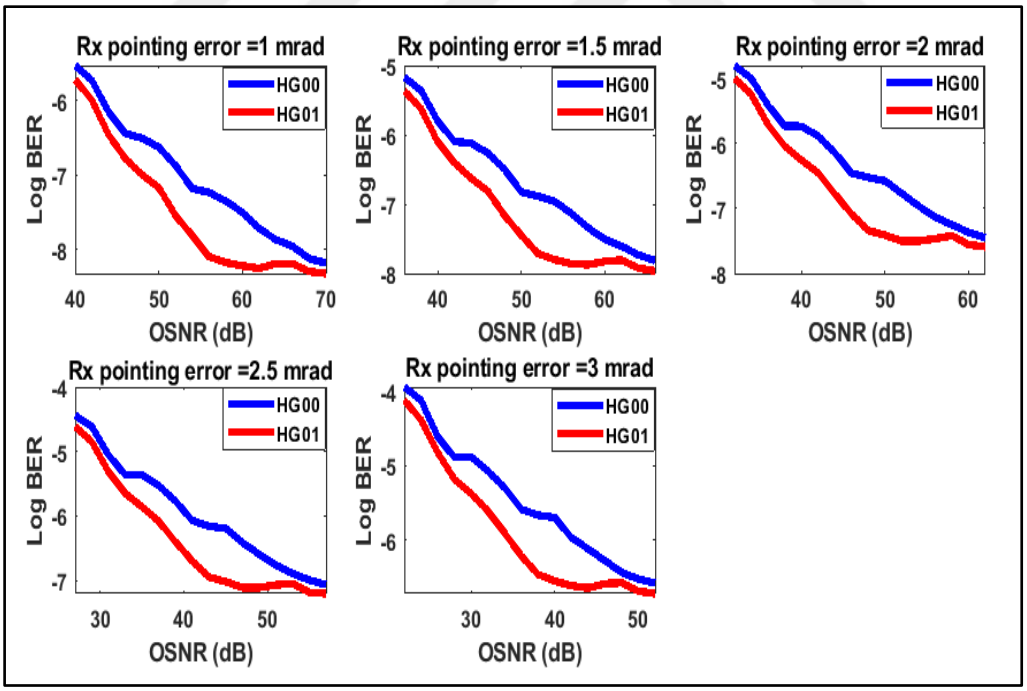

Figure 4.26: Log BER Vs. OSNR With Different Rx Pe At 40,000 Km Distance.

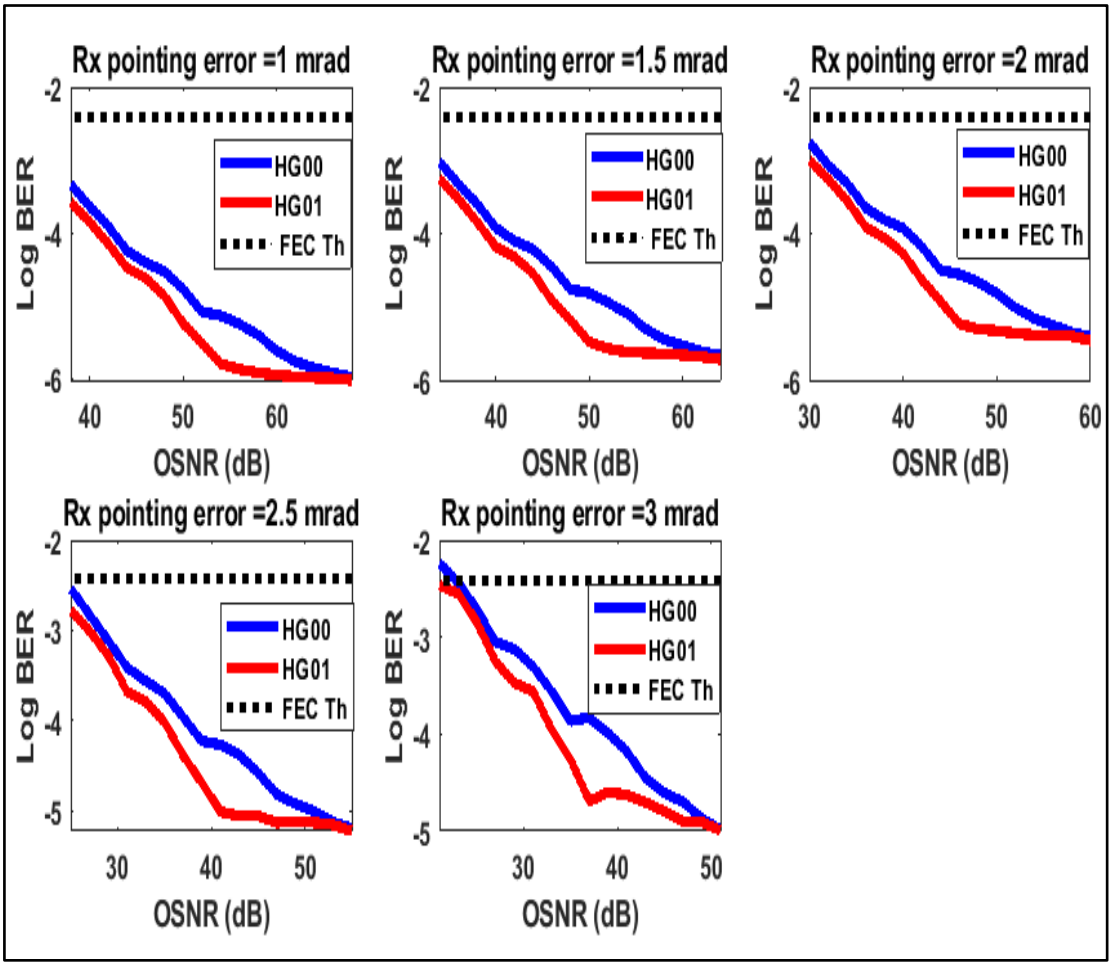

Figure 4.27: Log BER Vs. OSNR With Different Rx Pe At 48,000 Km Distance.

It is important to point out that the FEC threshold that is shown in these figures may be used to get a better understanding of the error level that the suggested system can manage to accomplish successful transmission without the need of performing retransmission. Additionally, the point at which the threshold is crossed with the value of the OSNR may be used to determine the OSNR tolerance as well as the performance of the proposed system.

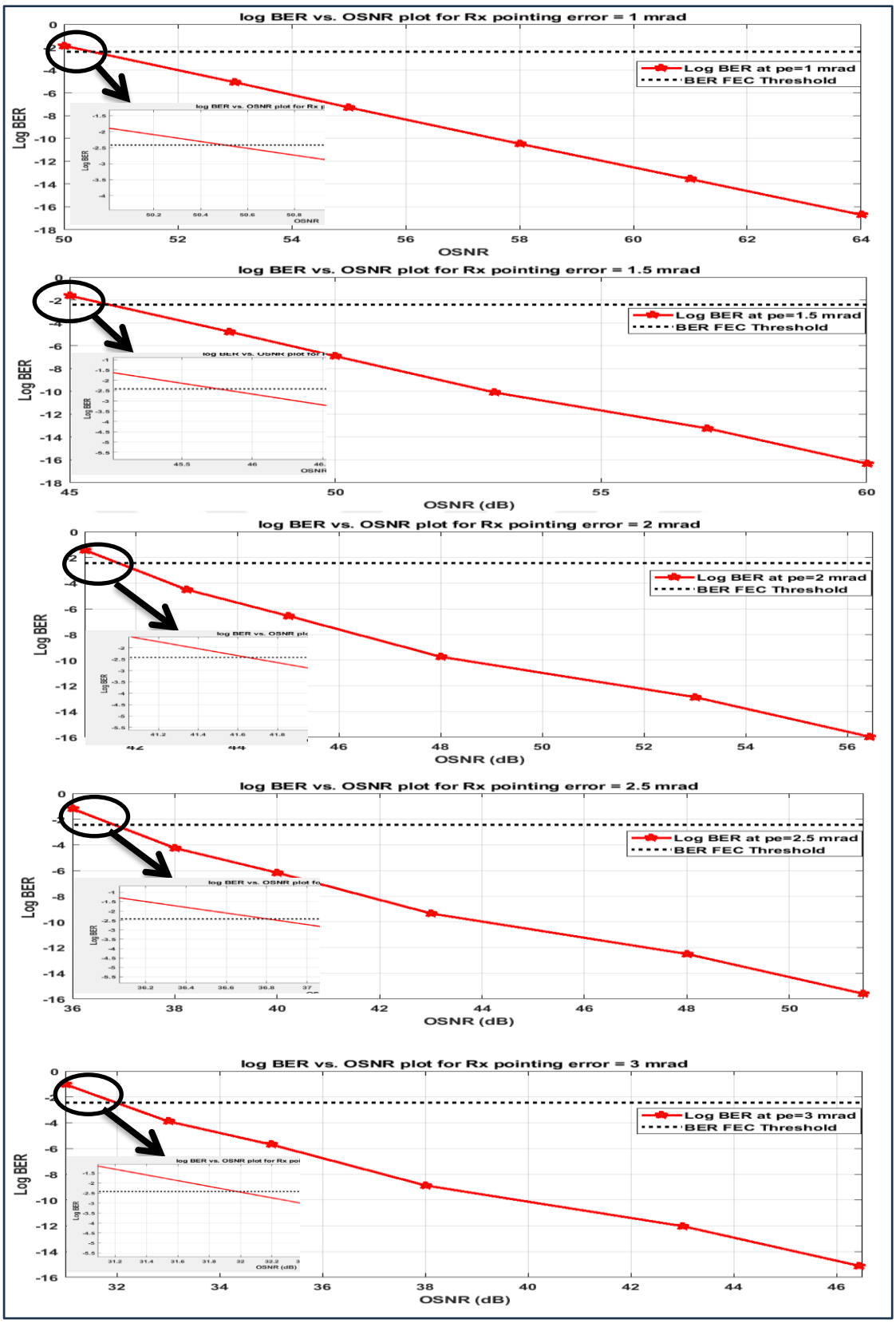

Figure 4.28: Average Log BER Vs. OSNR For Different Rx Pe.

4.3.2 Results-Based Tx Pointing Error

In this section, the variation of a Tx Pe from (1 to 5) mrad will be studied for the proposed system to quantify the reliability of the system and its capability of handling the Tx Pe and to give an indication for the OSNR requirements for the system to handle a successful transmission. The Tx Pe will be evaluated based on the studied parameters of log BER and OSNR as follows.

4.3.2.1 Log BER- based results

The performance of the proposed system was studied for various values of Tx Pe for the two modes of HG00 and HG01 and per the two polarizations of p1 and p2. These results were listed in (Table 4.26 to Table 4.30) and (Figure 4.29 to Figure 4.33) for the distances of 10,000 km, 20,000 km, 30,000 km, 40,000 km, and 48,000 km respectively. It can be noticed that using the distance of 10,000 km and 20,000 km the proposed system indicates superior performance for all cases of Tx Pe. Meanwhile, for 30,000 km the system gives a reliable performance, and when raising the distance to 40,000 km the system performance degradation due to the serious effects of several impairments on long transmission and large Pe impact. Finally, for the case of the targeted distance, it can be seen that the system fails in general to handle such distance, where the system gives potential performance for the case of 1 and 2 mrad of Tx Pe. Additionally, it can be noticed that the raising of the Tx Pe indicates direct relation with log BER.

To get a deeper point in analyzing the performance proposed system for different Tx Pes. The average log BER will be calculated from all channels per each case of Pe and for the two modes per each of the two utilized polarizations to be used to obtain the log BER variance when raising the distance from 10,000 km to 48,000. These results were calculated and listed as seen in Table 4.31, where it can be conducted that the variation for 10,000 km was between (-2.61 to -2.84) and for 20,000 km distance it was between (-2.79 to -2.93). When going for a larger distance represented by 30,000 km the variation reduced to be between (-2.99 to -3.6). Distance of 40,000 km gives log BER variation between (-3.27 to -3.33) Finally, the distance of 48,000 km gives a small amount of variation between (-3.11 to -3.13). The reduction in variation is reduced with increasing the transmission distance which may have a direct correlation with higher Tx Pe.

Table 4.26: Log BER Vs. Different Tx Pe At 10,000 Km.

Log BER (p1)	Tx Pe at 10,000 km- p1- HG00				
	1 mrad	**2 mrad**	**3 mrad**	**4 mrad**	**5 mrad**
193.1	-17.3888	-16.7788	-16.1288	-15.4288	-14.6788
193.2	-17.1655	-16.5555	-15.9055	-15.2055	-14.4555
193.3	-16.9274	-16.3174	-15.6674	-14.9674	-14.2174
193.4	-16.6595	-16.0495	-15.3995	-14.6995	-13.9495
193.5	-16.3905	-15.7805	-15.1305	-14.4305	-13.6805
193.6	-15.8394	-15.2294	-14.5794	-13.8794	-13.1294
193.7	-15.6559	-15.0459	-14.3959	-13.6959	-12.9459
193.8	-14.9450	-14.3350	-13.6850	-12.9850	-12.2350
Log BER (p1)	Tx Pe at 10,000 km- p1- HG01				
193.1	-18.0365	-17.4265	-16.7665	-16.0465	-15.3165
193.2	-17.9033	-17.2933	-16.6333	-15.9133	-15.1833
193.3	-17.9687	-17.3587	-16.6987	-15.9787	-15.2487
193.4	-17.8895	-17.2795	-16.6195	-15.8995	-15.1695
193.5	-17.5288	-16.9188	-16.2588	-15.5388	-14.8088
193.6	-16.5857	-15.9757	-15.3157	-14.5957	-13.8657
193.7	-16.1993	-15.5893	-14.9293	-14.2093	-13.4793
193.8	-15.4182	-14.8082	-14.1482	-13.4282	-12.6982
Log BER (p2)	Tx Pe at 10,000 km - p2- HG00				
193.1	-17.3306	-16.7206	-16.0706	-15.3706	-14.6206
193.2	-17.0748	-16.4648	-15.8148	-15.1148	-14.3648
193.3	-16.7097	-16.0997	-15.4497	-14.7497	-13.9997
193.4	-16.6441	-16.0341	-15.3841	-14.6841	-13.9341
193.5	-16.0836	-15.4736	-14.8236	-14.1236	-13.3736
193.6	-15.7177	-15.1077	-14.4577	-13.7577	-13.0077
193.7	-15.3667	-14.7567	-14.1067	-13.4067	-12.6567
193.8	-14.7453	-14.1353	-13.4853	-12.7853	-12.0353
Log BER (p2)	Tx Pe at 10,000 km- p2- HG01				
193.1	-18.0114	-17.4014	-16.7414	-16.0214	-15.2914
193.2	-17.9035	-17.2935	-16.6335	-15.9135	-15.1835
193.3	-17.9337	-17.3237	-16.6637	-15.9437	-15.2137
193.4	-17.8105	-17.2005	-16.5405	-15.8205	-15.0905
193.5	-16.9611	-16.3511	-15.6911	-14.9711	-14.2411
193.6	-16.4162	-15.8062	-15.1462	-14.4262	-13.6962
193.7	-15.8796	-15.2696	-14.6096	-13.8896	-13.1596
193.8	-15.1393	-14.5293	-13.8693	-13.1493	-12.4193

Table 4.27: Log BER Vs. Different Tx Pe At 20,000 Km.

Log BER (p1)	Tx Pe at 20,000 km- p1- HG00				
	1 mrad	**2 mrad**	**3 mrad**	**4 mrad**	**5 mrad**
193.1	-14.3548	-13.7248	-13.0548	-12.2748	-11.4648
193.2	-14.1315	-13.5015	-12.8315	-12.0515	-11.2415
193.3	-13.8934	-13.2634	-12.5934	-11.8134	-11.0034
193.4	-13.6255	-12.9955	-12.3255	-11.5455	-10.7355
193.5	-13.3565	-12.7265	-12.0565	-11.2765	-10.4665
193.6	-12.8054	-12.1754	-11.5054	-10.7254	-9.9154
193.7	-12.6219	-11.9919	-11.3219	-10.5419	-9.7319
193.8	-11.9110	-11.2810	-10.6110	-9.8310	-9.0210
Log BER (p1)	Tx Pe at 20,000 km- p1- HG01				
193.1	-14.6925	-14.0625	-13.3825	-12.5925	-11.7625
193.2	-14.5593	-13.9293	-13.2493	-12.4593	-11.6293
193.3	-14.6247	-13.9947	-13.3147	-12.5247	-11.6947
193.4	-14.5455	-13.9155	-13.2355	-12.4455	-11.6155
193.5	-14.1848	-13.5548	-12.8748	-12.0848	-11.2548
193.6	-13.5417	-12.9117	-12.2317	-11.4417	-10.6117
193.7	-13.1553	-12.5253	-11.8453	-11.0553	-10.2253
193.8	-12.3742	-11.7442	-11.0642	-10.2742	-9.4442
Log BER (p2)	Tx Pe at 20,000 km - p2- HG00				
193.1	-14.2966	-13.6666	-12.9966	-12.2166	-11.4066
193.2	-14.0408	-13.4108	-12.7408	-11.9608	-11.1508
193.3	-13.6757	-13.0457	-12.3757	-11.5957	-10.7857
193.4	-13.6101	-12.9801	-12.3101	-11.5301	-10.7201
193.5	-13.0496	-12.4196	-11.7496	-10.9696	-10.1596
193.6	-12.6837	-12.0537	-11.3837	-10.6037	-9.7937
193.7	-12.3327	-11.7027	-11.0327	-10.2527	-9.4427
193.8	-11.7113	-11.0813	-10.4113	-9.6313	-8.8213
Log BER (p2)	Tx Pe at 20,000 km- p2- HG01				
193.1	-14.6674	-14.0374	-13.3574	-12.5674	-11.7374
193.2	-14.5595	-13.9295	-13.2495	-12.4595	-11.6295
193.3	-14.5897	-13.9597	-13.2797	-12.4897	-11.6597
193.4	-14.4665	-13.8365	-13.1565	-12.3665	-11.5365
193.5	-13.9171	-13.2871	-12.6071	-11.8171	-10.9871
193.6	-13.3722	-12.7422	-12.0622	-11.2722	-10.4422
193.7	-12.8356	-12.2056	-11.5256	-10.7356	-9.9056
193.8	-12.0953	-11.4653	-10.7853	-9.9953	-9.1653

Table 4.28: Log BER Vs. Different Tx Pe At 30,000 Km.

Log BER (p1)	Tx Pe at 30,000 km- p1- HG00				
	1 mrad	**2 mrad**	**3 mrad**	**4 mrad**	**5 mrad**
193.100	-11.2978	-10.6278	-9.9278	-9.1078	-8.2278
193.200	-11.0745	-10.4045	-9.7045	-8.8845	-8.0045
193.300	-10.8364	-10.1664	-9.4664	-8.6464	-7.7664
193.400	-10.4685	-9.7985	-9.0985	-8.2785	-7.3985
193.500	-10.2995	-9.6295	-8.9295	-8.1095	-7.2295
193.600	-9.7484	-9.0784	-8.3784	-7.5584	-6.6784
193.700	-9.5649	-8.8949	-8.1949	-7.3749	-6.4949
193.800	-8.8540	-8.1840	-7.4840	-6.6640	-5.7840
Log BER (p1)	Tx Pe at 30,000 km- p1- HG01				
193.100	-11.5675	-10.8875	-10.1775	-9.3475	-8.4675
193.200	-11.4343	-10.7543	-10.0443	-9.2143	-8.3343
193.300	-11.4997	-10.8197	-10.1097	-9.2797	-8.3997
193.400	-11.4205	-10.7405	-10.0305	-9.2005	-8.3205
193.500	-11.0598	-10.3798	-9.6698	-8.8398	-7.9598
193.600	-10.4167	-9.7367	-9.0267	-8.1967	-7.3167
193.700	-10.0303	-9.3503	-8.6403	-7.8103	-6.9303
193.800	-9.2492	-8.5692	-7.8592	-7.0292	-6.1492
Log BER (p2)	Tx Pe at 30,000 km - p2- HG00				
193.1	-11.2396	-10.5696	-9.8696	-9.0496	-8.1696
193.2	-10.9838	-10.3138	-9.6138	-8.7938	-7.9138
193.3	-10.6187	-9.9487	-9.2487	-8.4287	-7.5487
193.4	-10.3531	-9.6831	-8.9831	-8.1631	-7.2831
193.5	-9.9926	-9.3226	-8.6226	-7.8026	-6.9226
193.6	-9.6267	-8.9567	-8.2567	-7.4367	-6.5567
193.7	-9.2757	-8.6057	-7.9057	-7.0857	-6.2057
193.8	-8.6543	-7.9843	-7.2843	-6.4643	-5.5843
Log BER (p2)	Tx Pe at 30,000 km- p2- HG01				
193.1	-11.5424	-10.8624	-10.1524	-9.3224	-8.4424
193.2	-11.4345	-10.7545	-10.0445	-9.2145	-8.3345
193.3	-11.4647	-10.7847	-10.0747	-9.2447	-8.3647
193.4	-11.3415	-10.6615	-9.9515	-9.1215	-8.2415
193.5	-10.7921	-10.1121	-9.4021	-8.5721	-7.6921
193.6	-10.2472	-9.5672	-8.8572	-8.0272	-7.1472
193.7	-9.7106	-9.0306	-8.3206	-7.4906	-6.6106
193.8	-8.9703	-8.2903	-7.5803	-6.7503	-5.8703

Table 4.29: Log BER Vs. Different Tx Pe At 40,000 Km.

Log BER (p1)	Tx Pe at 40,000 km- p1- HG00				
	1 mrad	**2 mrad**	**3 mrad**	**4 mrad**	**5 mrad**
193.100	-8.1778	-7.4778	-6.7178	-5.8178	-4.9078
193.200	-7.9545	-7.2545	-6.4945	-5.5945	-4.6845
193.300	-7.7164	-7.0164	-6.2564	-5.3564	-4.4464
193.400	-7.3485	-6.6485	-5.8885	-4.9885	-4.0785
193.500	-7.1795	-6.4795	-5.7195	-4.8195	-3.9095
193.600	-6.6284	-5.9284	-5.1684	-4.2684	-3.3584
193.700	-6.4449	-5.7449	-4.9849	-4.0849	-3.1749
193.800	-5.7340	-5.0340	-4.2740	-3.3740	-2.4640
Log BER (p1)	Tx Pe at 40,000 km- p1- HG01				
193.100	-8.3175	-7.6075	-6.8375	-5.9175	-5.0075
193.200	-8.1843	-7.4743	-6.7043	-5.7843	-4.8743
193.300	-8.2497	-7.5397	-6.7697	-5.8497	-4.9397
193.400	-8.1705	-7.4605	-6.6905	-5.7705	-4.8605
193.500	-7.8098	-7.0998	-6.3298	-5.4098	-4.4998
193.600	-7.1667	-6.4567	-5.6867	-4.7667	-3.8567
193.700	-6.7803	-6.0703	-5.3003	-4.3803	-3.4703
193.800	-5.9992	-5.2892	-4.5192	-3.5992	-2.6892
Log BER (p2)	Tx Pe at 40,000 km - p2- HG00				
193.1	-8.1196	-7.4196	-6.6596	-5.7596	-4.8496
193.2	-7.8638	-7.1638	-6.4038	-5.5038	-4.5938
193.3	-7.4987	-6.7987	-6.0387	-5.1387	-4.2287
193.4	-7.2331	-6.5331	-5.7731	-4.8731	-3.9631
193.5	-6.8726	-6.1726	-5.4126	-4.5126	-3.6026
193.6	-6.5067	-5.8067	-5.0467	-4.1467	-3.2367
193.7	-6.1557	-5.4557	-4.6957	-3.7957	-2.8857
193.8	-5.5343	-4.8343	-4.0743	-3.1743	-2.2643
Log BER (p2)	Tx Pe at 40,000 km- p2- HG01				
193.1	-8.2924	-7.5824	-6.8124	-5.8924	-4.9824
193.2	-8.1845	-7.4745	-6.7045	-5.7845	-4.8745
193.3	-8.2147	-7.5047	-6.7347	-5.8147	-4.9047
193.4	-8.0915	-7.3815	-6.6115	-5.6915	-4.7815
193.5	-7.5421	-6.8321	-6.0621	-5.1421	-4.2321
193.6	-6.9972	-6.2872	-5.5172	-4.5972	-3.6872
193.7	-6.4606	-5.7506	-4.9806	-4.0606	-3.1506
193.8	-5.7203	-5.0103	-4.2403	-3.3203	-2.4103

Table 4.30: Log BER Vs. Different Tx Pe At 48,000 Km.

Log BER (p1)	Tx Pe at 48,000 km- p1- HG00				
	1 mrad	**2 mrad**	**3 mrad**	**4 mrad**	**5 mrad**
193.100	-5.9778	-5.2778	-4.5478	-3.7478	-2.8878
193.200	-5.8545	-5.1545	-4.4245	-3.6245	-2.7645
193.300	-5.6164	-4.9164	-4.1864	-3.3864	-2.5264
193.400	-5.2485	-4.5485	-3.8185	-3.0185	-2.1585
193.500	-5.0795	-4.3795	-3.6495	-2.8495	-1.9895
193.600	-4.5284	-3.8284	-3.0984	-2.2984	-1.4384
193.700	-4.2449	-3.5449	-2.8149	-2.0149	-1.1549
193.800	-3.6340	-2.9340	-2.2040	-1.4040	-0.5440
Log BER (p1)	Tx Pe at 48,000 km- p1- HG01				
193.100	-6.0175	-5.3175	-4.5855	-3.7731	-2.9131
193.200	-5.9843	-5.2843	-4.5523	-3.7399	-2.8799
193.300	-5.9497	-5.2497	-4.5177	-3.7053	-2.8453
193.400	-5.8705	-5.1705	-4.4385	-3.6261	-2.7661
193.500	-5.5098	-4.8098	-4.0778	-3.2654	-2.4054
193.600	-4.8667	-4.1667	-3.4347	-2.6223	-1.7623
193.700	-4.4803	-3.7803	-3.0483	-2.2359	-1.3759
193.800	-3.8492	-3.1492	-2.4172	-1.6048	-0.7448
Log BER (p2)	Tx Pe at 48,000 km - p2- HG00				
193.1	-5.9196	-5.2196	-4.4896	-3.6896	-2.8296
193.2	-5.7638	-5.0638	-4.3338	-3.5338	-2.6738
193.3	-5.3987	-4.6987	-3.9687	-3.1687	-2.3087
193.4	-5.1331	-4.4331	-3.7031	-2.9031	-2.0431
193.5	-4.7726	-4.0726	-3.3426	-2.5426	-1.6826
193.6	-4.4067	-3.7067	-2.9767	-2.1767	-1.3167
193.7	-3.9057	-3.2057	-2.4757	-1.6757	-0.8157
193.8	-3.3343	-2.6343	-1.9043	-1.1043	-0.2443
Log BER (p2)	Tx Pe at 48,000 km- p2- HG01				
193.1	-5.9924	-5.2924	-4.5604	-3.7480	-2.8880
193.2	-5.9695	-5.2695	-4.5375	-3.7251	-2.8651
193.3	-5.9147	-5.2147	-4.4827	-3.6703	-2.8103
193.4	-5.7915	-5.0915	-4.3595	-3.5471	-2.6871
193.5	-5.2421	-4.5421	-3.8101	-2.9977	-2.1377
193.6	-4.6172	-3.9172	-3.1852	-2.3728	-1.5128
193.7	-4.1506	-3.4506	-2.7186	-1.9062	-1.0462
193.8	-3.5803	-2.8803	-2.1483	-1.3359	-0.4759

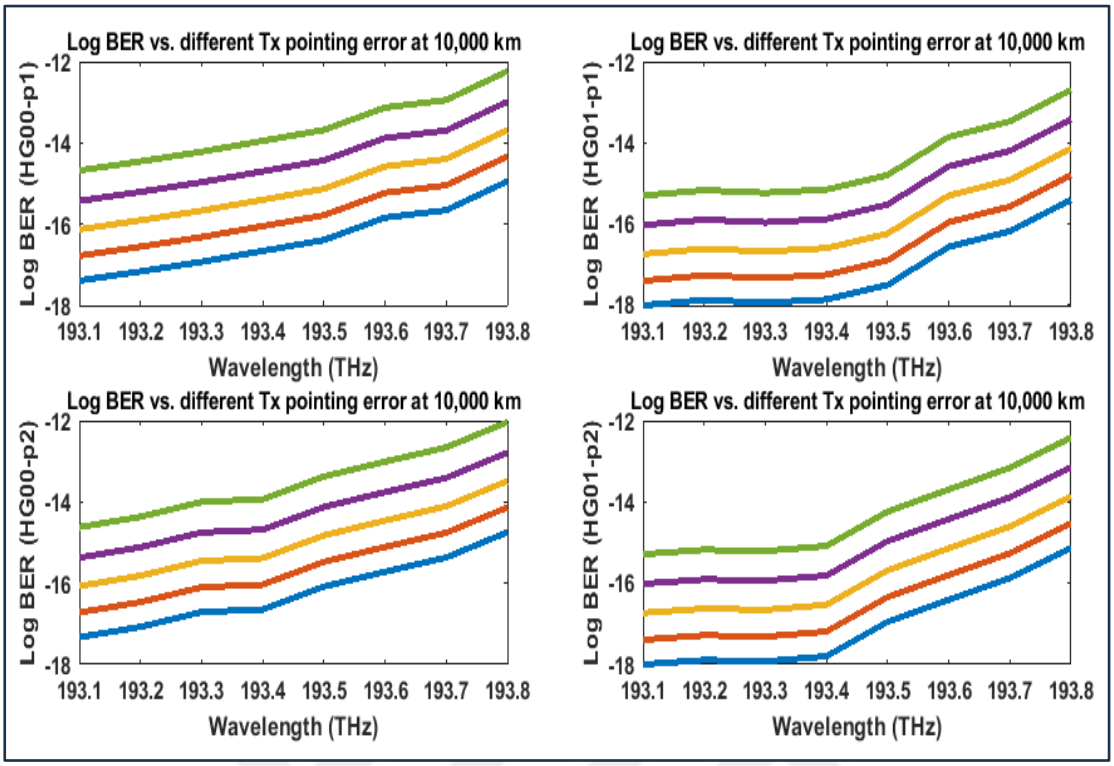

Figure: 4.29: Log BER Vs. Different Tx Pe At 10,000 Km.

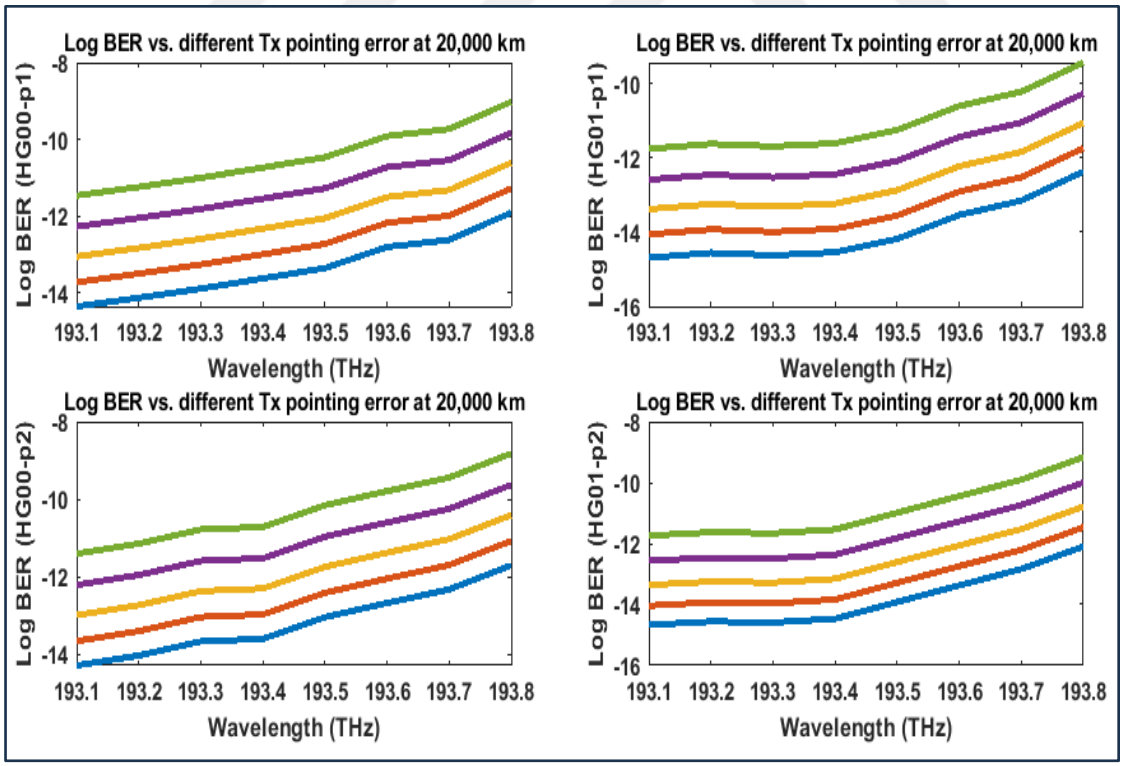

Figure: 4.30: Log BER Vs. Different Tx Pe At 20,000 Km.

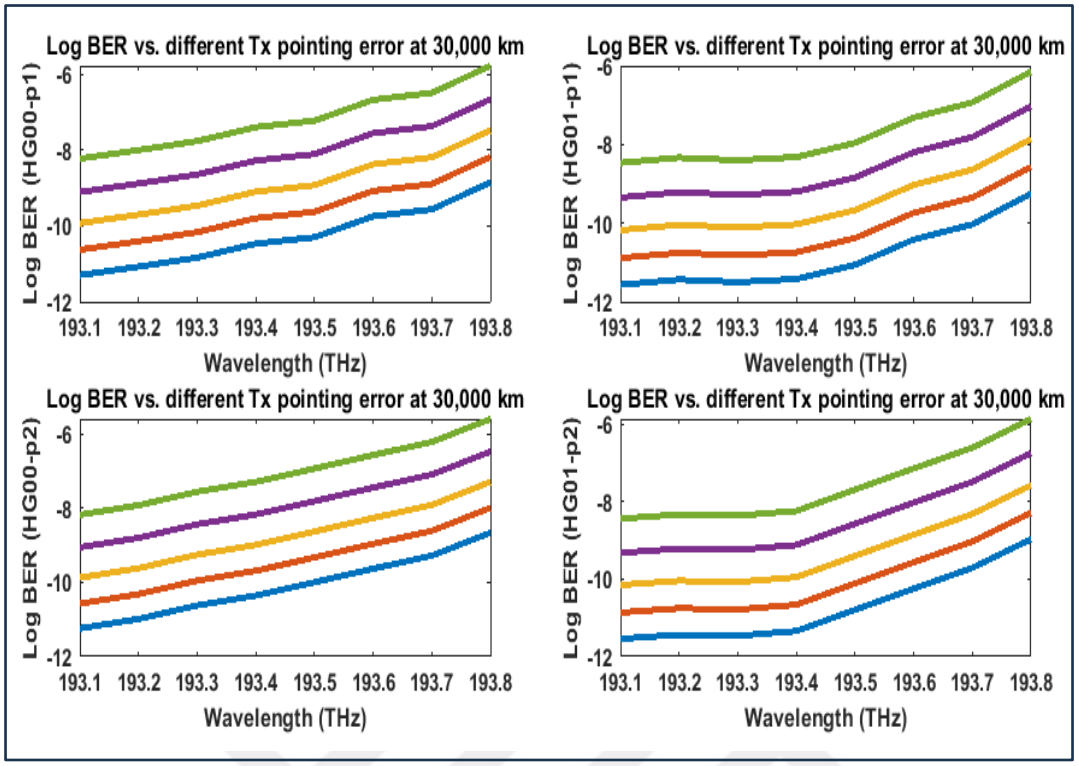

Figure: 4.31: Log BER Vs. Different Tx Pe At 30,000 Km.

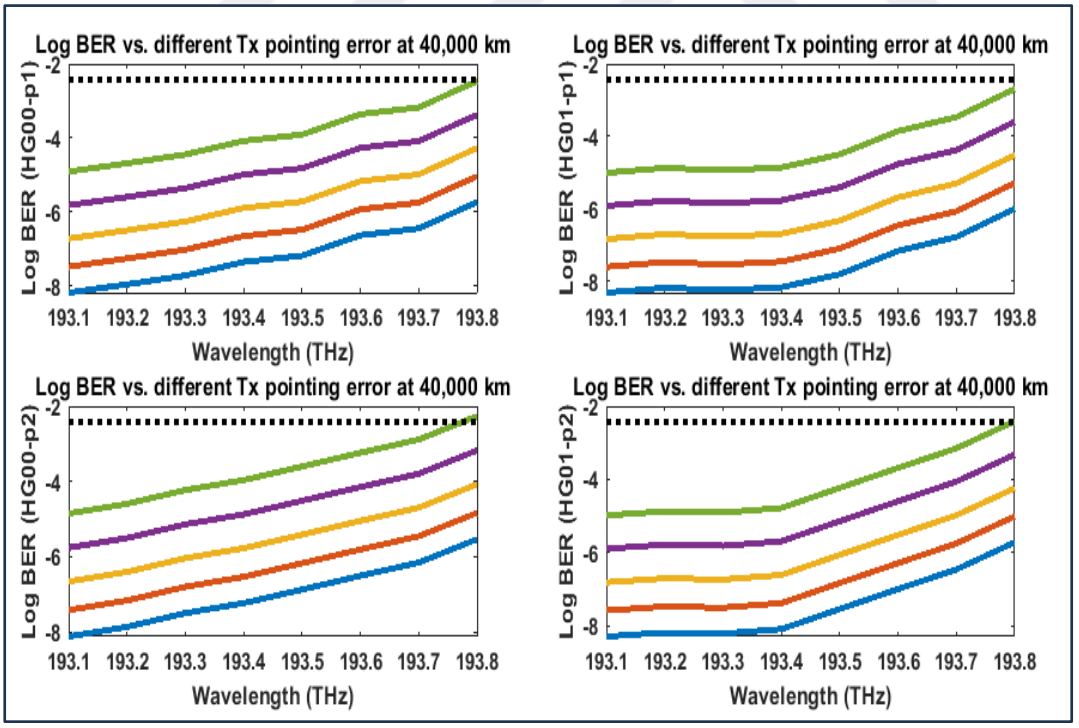

Figure: 4.32: Log BER Vs. Different Tx Pe At 40,000 Km.

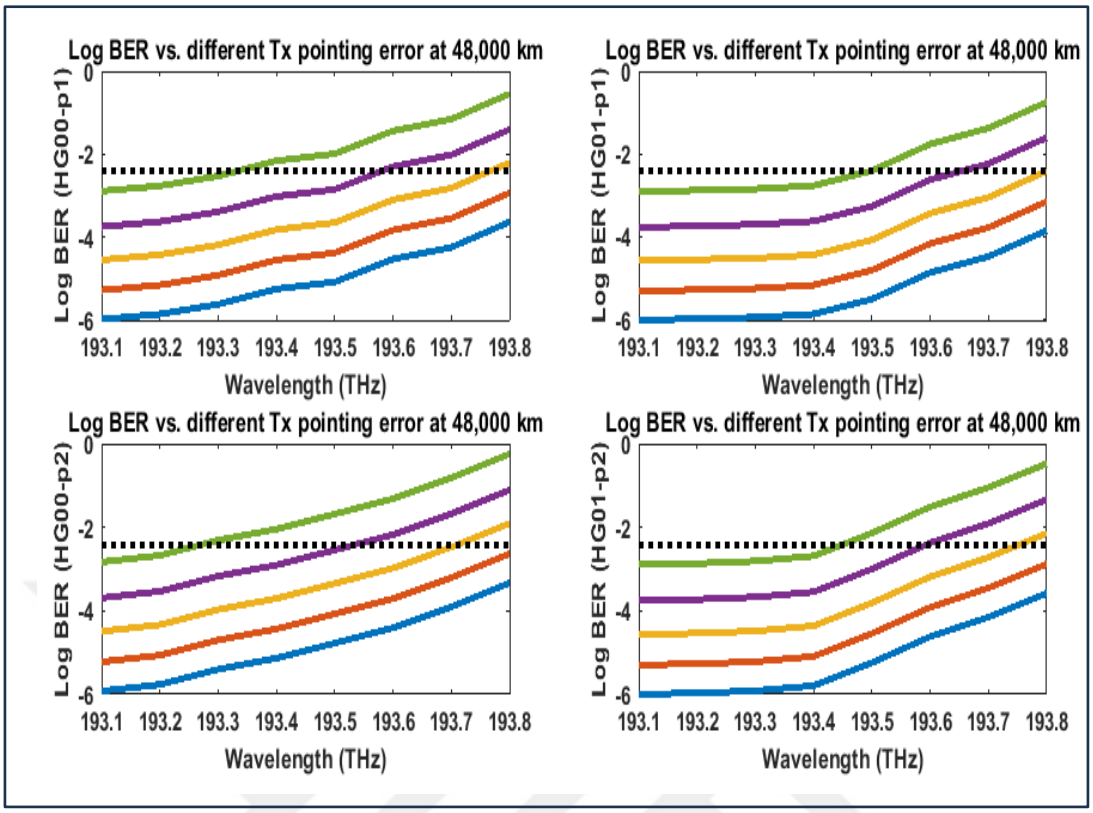

Figure: 4.33: Log BER Vs. Different Tx Pe At 48,000 Km.

In accordance with the information shown in Table 4.32, the final average log BER that was acquired from all the modes and polarization may be derived. which may provide a conclusive indication about the performance of the proposed system in managing various Pes, where it demonstrates that the system can perform effectively in all distances up to 40,000 kilometers, while for distances up to 48,000 kilometers, the system provides dependable performance for Tx Pe up to 4 meters.

It is important to keep in mind that the Rx Pe that was chosen was equivalent to 1 mrad for each of the different Tx Pe scenarios. In addition, there is a possibility that some channels may fail to meet the FEC threshold on their own. These channels can be managed by using specific techniques that are made specifically for the purpose of managing them independently.

Table 4.31: Averaged Log BER Vs. Different Tx Pe And Transmission Distances.

distance 10,000 km				
pe (mrad)	**HG00-p1**	**HG01-p1**	**HG00-p2**	**HG01-p2**
1	-16.072	-17.291	-16.209	-17.007
2	-15.76151	-16.38124	-15.59908	-16.39691
3	-15.11151	-15.92124	-14.94908	-15.73691
4	-14.41151	-15.20124	-14.24908	-15.01691
5	-13.46151	-14.45124	-13.49908	-14.18691
Log BER variance	-2.610	-2.840	-2.710	-2.820
distance 20,000 km				
1	-13.23751	-13.85974	-13.17508	-13.81291
2	-12.70751	-13.32974	-12.54508	-13.18291
3	-12.03751	-12.64974	-11.87508	-12.50291
4	-11.25751	-11.85974	-11.09508	-11.71291
5	-10.44751	-11.02974	-10.28508	-10.88291
Log BER variance	-2.79	-2.83	-2.89	-2.93
distance 30,000 km				
1	-10.18801	-10.93474	-10.06308	-10.87791
2	-9.598006	-10.15474	-9.423079	-10.00791
3	-8.898006	-9.444744	-8.723079	-9.297914
4	-8.078006	-8.614744	-7.903079	-8.467914
5	-7.198006	-7.734744	-7.023079	-7.287914
Log BER variance	-2.99	-3.2	-3.0	-3.6
distance 40,000 km				
1	-7.159006	-7.584744	-6.973079	-7.457914
2	-6.448006	-6.874744	-6.273079	-6.727914
3	-5.688006	-6.104744	-5.513079	-5.957914
4	-4.788006	-5.184744	-4.613079	-5.037914
5	-3.878006	-4.274744	-3.703079	-4.127914
Log BER variance	-3.28	-3.31	-3.27	-3.33
distance 48,000 km				
1	-5.05301	-5.34599	-4.84933	-5.18729
2	-4.32301	-4.61599	-4.12933	-4.45729
3	-3.59301	-3.88399	-3.39933	-3.72529
4	-2.79301	-3.07159	-2.59933	-2.91289
5	-1.93301	-2.21159	-1.73933	-2.05289
Log BER variance	-3.12	-3.1344	-3.11	-3.1344

Table 4.32: Total Averaged Log BER Vs. Tx Pe And Transmission Distances.

Average log BER		Distance (km)				
		10000	**20000**	**30000**	**40000**	**48000**
Tx pointing error (mrad)	1	-16.695	-13.571	-10.287	-7.287	-5.081
	2	-16.035	-12.94131	-9.795936	-6.580936	-4.381405
	3	-15.430	-12.26631	-9.090936	-5.815936	-3.650405
	4	-14.720	-11.48131	-8.265936	-4.905936	-2.844205
	5	-13.900	-10.66131	-7.310936	-3.995936	-1.984205

4.3.2.2 OSNR- based results

The OSNR parameters will be studied in the same way that follows in the investigation of Rx Pe, in which it will be obtained for the five cases of Tx Pe and for five cases of transmission distance. The aim of studying this parameter is to get a final view of how much the OSNR requirements for the proposed system to handle transmission for different distances for the influence of Tx Pe. To start with, The OSNR is calculated from all the cases of Tx Pe and all distances as listed in Table 4.33. A reverse relation can be noticed between the OSNR and raising the Tx Pe also same reason can be noticed with raising the transmission distances. The analysis of OSNR variation will be studied based on two cases of fixed and varied distance. Additionally,

Lastly, owing to the significance of OSNR as a vital aspect in detecting and troubleshooting essential components, it helps to decrease operating expenditures and may assist to increase network potential. As a result, it is critical to determine the minimal OSNR value that maintains the BER FEC threshold, which will be derived by averaging the log BER from each example of mode with all distances and researched Pe values. The average of the two modes is then used to represent a single value, as shown in Figure 4.34. The system provides an OSNR tolerance of 50.5 dB, 46.8 dB, 42.5 dB, 37.5 dB, and 30.5 dB for Tx pe of 1 mrad, 2 mrad, 3 mrad, 4 mrad, and 5 mrad, respectively. The item that can certify the proposed system's dependability about the OSNR criteria.

Table 4.33: OSNR From Different Channels Vs. Different Tx Pe At Different Distances.

Wavelength\ OSNR	distance 10,000 km				
	1 mrad	2 mrad	3 mrad	4 mrad	5 mrad
193.1	78	75	71	66	59
193.2	74	71	67	62	55
193.3	70	67	63	58	51
193.4	67	64	60	55	48
193.5	64	61	57	52	45
193.6	59	56	52	47	40
193.7	56	53	49	44	37
Wavelength\ OSNR	**distance 20,000 km**				
193.1	75	72	68	63	56
193.2	71	68	64	59	52
193.3	67	64	60	55	48
193.4	63	60	56	51	44
193.5	59	56	52	47	40
193.6	55	52	48	43	36
193.7	51	48	44	39	32
Wavelength\ OSNR	**distance 30,000 km**				
193.1	72	69	65	60	53
193.2	68	65	61	56	49
193.3	64	61	57	52	45
193.4	60	57	53	48	41
193.5	56	53	49	44	37
193.6	52	49	45	40	33
193.7	48	45	41	36	29
Wavelength\ OSNR	**distance 40,000 km**				
193.1	69	65	60	54	46
193.2	65	61	56	50	42
193.3	61	57	52	46	38
193.4	57	53	48	42	34
193.5	53	49	44	38	30
193.6	49	45	40	34	26
193.7	45	41	36	30	22
193.8	41	37	32	26	18
Wavelength\ OSNR	**distance 48,000 km**				
193.1	67	63	58	52	44
193.2	63	59	54	48	40
193.3	59	55	50	44	36
193.4	55	51	46	40	32
193.5	51	47	42	36	28
193.6	47	43	38	32	24

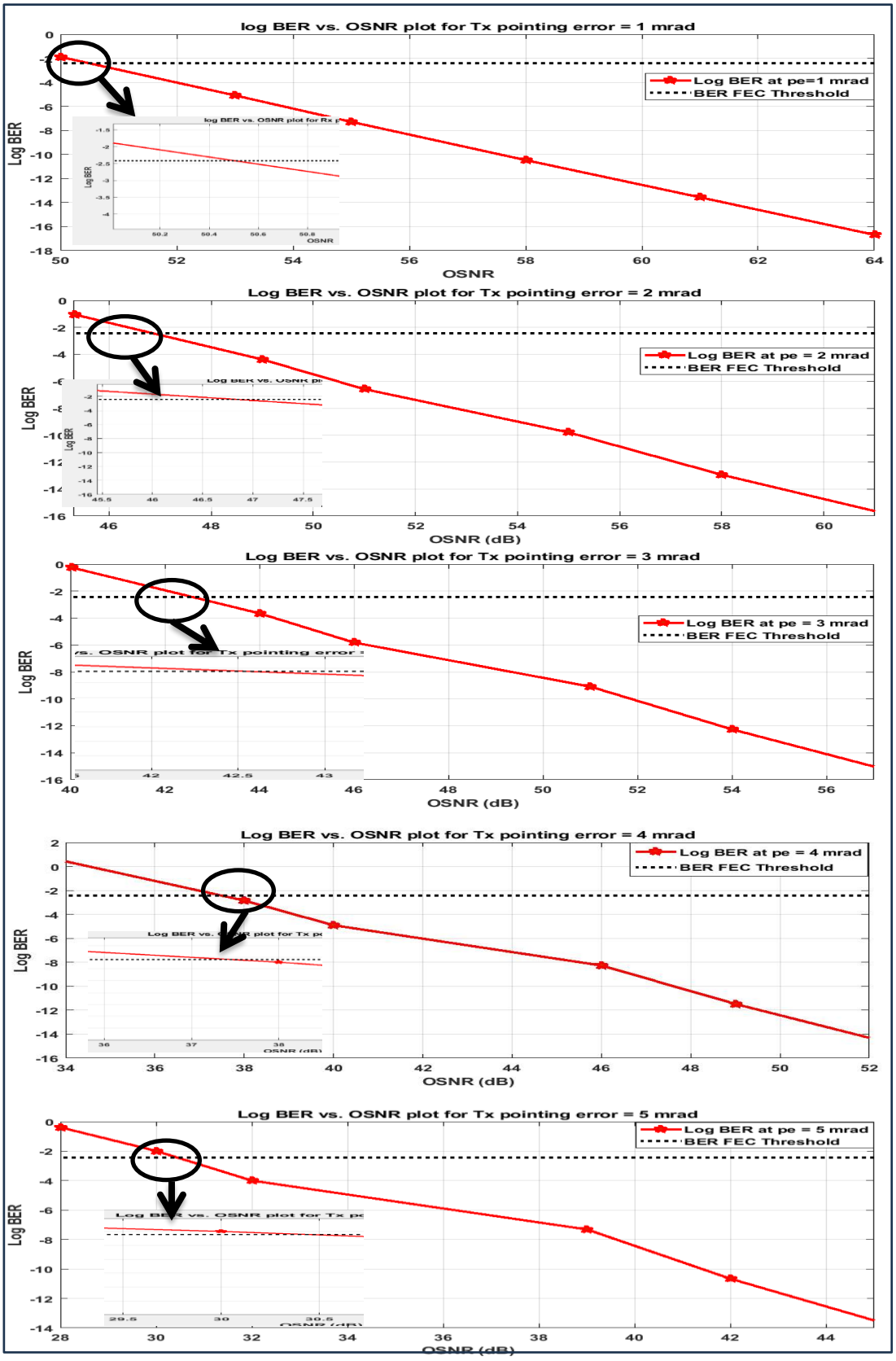

Figure 4.34: Average Log BER Vs. OSNR For Different Tx Pe.

4.4 RESULTS-BASED THIRD OBJECTIVE

This section will demonstrate the results of the investigation for the third objective carried in this thesis, which is related with evaluating the performance of the proposed system with respect to the variation of Tx and Rx aperture diameter. And their influence on the performance of the proposed Is-OWC MDM PDM WDM system.

4.4.1 Results Based Tx Aperture Diameter

The first part to be investigated related with the Tx part of satellite where different values of aperture diameter for the Tx antenna would be studied to quantify with the performance of the proposed system with various antenna diameters and with respect to different parameters for evaluating the system. It is worth to mention that the selected antenna diameter for the proposed system of this thesis was equal to 15 cm. The investigation will involve the variation of 5,10, 15 and 20 cm of Tx antenna aperture diameter. Additionally, in this investigation the value of Rx aperture diameter is fixed to be equal to 30 cm for all varied values of Tx diameters and with concerning to 1 mrad pointing error, which represent the original setting of the proposed system.

In this investigation, the log BER based parameter will be studied with respect to the selected antenna diameters and for the range between (10,000 km to 48,000 km). The values of the obtained log BER are calculated for the two polarization and two modes (HG00 and HG01) as seen in (Table 4.34 – Table 4.37). performance evaluation will be summarized by considering the averaged values of log BER obtained from each case of aperture diameter as expressed in Table 4.38 and as follows:

a. It can be seen at 5 cm diameter, the system capability was up to 40,000 km due to the small size of antenna diameter for Tx where the larger the aperture, the lighter the system gathers and the finer details it can see.
b. Raising diameter to 10 cm, can contribute to reach the transmission distance of 48,000 km, but not for all channels (channel 8 fails to reach the FEC threshold).
c. Setting the diameter equal to 15 cm represent the regular case of the proposed system, which indicate reliable performance for all the investigated distances with acceptable values and averaged values of log BER.

d. For the last case of 20 cm, it can be noticed that larger diameter means lower errors in the transmitted bit, and this is due to the reverse proportional between the attenuation (dB/Km) and the diameter of the Tx side. Even though, the significant of raising diameter in system performance however, there must be controlled so as not to converge to the size of the Rx diameter due to reasons related with increasing the noises.

Table 4.34: Log BER Values At Tx Aperture Diameter Of 5 Cm.

Channel	Log BER values at Tx aperture diameter = 5 cm									
	10,000 km		20,000 km		30,000 km		40,000 km		48,000 km	
	HG00	HG01	HG00	HG01	HG00	HG01	HG00	HG01	HG00	HG01
ch1/p1	-13.75	-14.40	-10.63	-10.97	-7.56	-7.83	-4.44	-4.57	*	*
ch1/p2	-13.70	-14.38	-10.58	-10.96	-7.50	-7.81	-4.38	-4.54	*	*
ch2/p1	-13.54	-14.28	-10.41	-10.85	-7.35	-7.71	-4.22	-4.44	*	*
ch2/p2	-13.45	-14.28	-10.32	-10.84	-7.26	-7.71	-4.13	-4.44	*	*
ch3/p1	-13.30	-14.34	-10.18	-10.92	-7.12	-7.78	-3.98	-4.50	*	*
ch3/p2	-13.08	-14.31	-9.96	-10.88	-6.90	-7.75	-3.76	-4.47	*	*
ch4/p1	-13.04	-14.27	-9.93	-10.85	-6.75	-7.71	-3.61	-4.42	*	*
ch4/p2	-13.03	-14.19	-9.91	-10.77	-6.64	-7.62	-3.50	-4.34	*	*
ch5/p1	-12.78	-13.92	-9.66	-10.50	-6.59	-7.35	-3.44	-4.06	*	*
ch5/p2	-12.47	-13.35	-9.35	-10.22	-6.29	-7.09	-3.14	-3.79	*	*
ch6/p1	-12.24	-12.99	-9.11	-9.86	-6.04	-6.71	-2.89	-3.42	*	*
ch6/p2	-12.11	-12.81	-8.99	-9.69	-5.92	-6.54	-2.77	-3.25	*	*
ch7/p1	-12.06	-12.61	-8.95	-9.49	-5.86	-6.32	-2.71	-3.03	*	*
ch7/p2	-11.77	-12.28	-8.66	-9.16	-5.57	-6.00	-2.42	-2.71	*	*
ch8/p1	-11.35	-11.82	-8.24	-8.71	-5.16	-5.55	-2.00	-2.25	*	*
ch8/p2	-11.15	-11.54	-8.04	-8.43	-4.96	-5.28	-1.80	-1.97	*	*

Table 4.35: Log BER Values At Tx Aperture Diameter Of 10 Cm.

Channel	Log BER values at Tx aperture diameter = 10 cm									
	10,000 km		20,000 km		30,000 km		40,000 km		48,000 km	
ch1/p1	-15.64	-16.28	-12.50	-12.84	-9.41	-9.68	-6.29	-6.43	-4.22	-4.26
ch1/p2	-15.58	-16.26	-12.45	-12.82	-9.36	-9.66	-6.24	-6.41	-4.17	-4.24
ch2/p1	-15.42	-16.16	-12.29	-12.72	-9.20	-9.56	-6.07	-6.30	-4.10	-4.23
ch2/p2	-15.33	-16.16	-12.19	-12.71	-9.11	-9.56	-5.98	-6.30	-4.01	-4.22
ch3/p1	-15.18	-16.22	-12.06	-12.79	-8.97	-9.64	-5.83	-6.37	-3.86	-4.20
ch3/p2	-14.97	-16.19	-11.84	-12.75	-8.76	-9.60	-5.62	-6.33	-3.65	-4.16
ch4/p1	-14.92	-16.15	-11.80	-12.72	-8.61	-9.56	-5.47	-6.29	-3.50	-4.12
ch4/p2	-14.91	-16.07	-11.79	-12.64	-8.49	-9.48	-5.35	-6.21	-3.38	-4.04
ch5/p1	-14.66	-15.80	-11.54	-12.36	-8.45	-9.21	-5.30	-5.93	-3.33	-3.76
ch5/p2	-14.36	-15.23	-11.22	-12.09	-8.14	-8.94	-4.99	-5.66	-3.02	-3.49
ch6/p1	-14.12	-14.87	-10.99	-11.73	-7.90	-8.56	-4.75	-5.28	-2.78	-3.11
ch6/p2	-13.99	-14.69	-10.87	-11.56	-7.77	-8.39	-4.62	-5.11	-2.65	-2.86
ch7/p1	-13.94	-14.49	-10.82	-11.35	-7.71	-8.18	-4.56	-4.90	-2.49	-2.73
ch7/p2	-13.65	-14.17	-10.53	-11.03	-7.42	-7.86	-4.27	-4.58	-2.15	-2.40
ch8/p1	-13.23	-13.70	-10.12	-10.58	-7.01	-7.41	-3.85	-4.12	-1.88	-2.10
ch8/p2	-13.03	-13.42	-9.92	-10.30	-6.81	-7.13	-3.65	-3.84	-1.58	-1.83

Table 4.36: Log BER Values At Tx Aperture Diameter Of 15 Cm.

Channel	Log BER values at Tx aperture diameter = 15 cm									
	10,000 km		20,000 km		30,000 km		40,000 km		48,000 km	
ch1/p1	-17.39	-18.04	-14.35	-14.69	-11.30	-11.57	-8.18	-8.32	-5.98	-6.02
ch2/p2	-17.07	-17.90	-14.04	-14.56	-10.98	-11.43	-7.86	-8.18	-5.76	-5.97
ch3/p1	-16.93	-17.97	-13.89	-14.62	-10.84	-11.50	-7.72	-8.25	-5.62	-5.95
ch3/p2	-16.71	-17.93	-13.68	-14.59	-10.62	-11.46	-7.50	-8.21	-5.40	-5.91
ch4/p1	-16.66	-17.89	-13.63	-14.55	-10.47	-11.42	-7.35	-8.17	-5.25	-5.87
ch4/p2	-16.64	-17.81	-13.61	-14.47	-10.35	-11.34	-7.23	-8.09	-5.13	-5.79
ch5/p1	-16.39	-17.53	-13.36	-14.18	-10.30	-11.06	-7.18	-7.81	-5.08	-5.51
ch5/p2	-16.08	-16.96	-13.05	-13.92	-9.99	-10.79	-6.87	-7.54	-4.77	-5.24
ch6/p1	-15.84	-16.59	-12.81	-13.54	-9.75	-10.42	-6.63	-7.17	-4.53	-4.87
ch6/p2	-15.72	-16.42	-12.68	-13.37	-9.63	-10.25	-6.51	-7.00	-4.41	-4.62
ch7/p1	-15.66	-16.20	-12.62	-13.16	-9.56	-10.03	-6.44	-6.78	-4.24	-4.48
ch7/p2	-15.37	-15.88	-12.33	-12.84	-9.28	-9.71	-6.16	-6.46	-3.91	-4.15
ch8/p1	-14.95	-15.42	-11.91	-12.37	-8.85	-9.25	-5.73	-6.00	-3.63	-3.85
ch8/p2	-14.75	-15.14	-11.71	-12.10	-8.65	-8.97	-5.53	-5.72	-3.33	-3.58

Table 4.37: Log Ber Values At Tx Aperture Diameter Of 20 Cm.

Channel	Log BER values at Tx aperture diameter = 20 cm									
	10,000 km		20,000 km		30,000 km		40,000 km		48,000 km	
	HG00	HG01	HG00	HG01	HG00	HG01	HG00	HG01	HG00	HG01
ch1/p1	-19.13	-19.78	-15.90	-16.25	-12.75	-13.02	-9.63	-9.77	-7.33	-7.36
ch1/p2	-19.07	-19.76	-15.85	-16.22	-12.69	-13.00	-9.57	-9.75	-7.27	-7.34
ch2/p1	-18.90	-19.64	-15.67	-16.10	-12.52	-12.88	-9.41	-9.64	-7.20	-7.32
ch2/p2	-18.81	-19.64	-15.58	-16.11	-12.43	-12.88	-9.32	-9.64	-7.11	-7.30
ch3/p1	-18.65	-19.69	-15.43	-16.16	-12.27	-12.93	-9.16	-9.69	-6.97	-7.29
ch3/p2	-18.43	-19.65	-15.22	-16.13	-12.06	-12.90	-8.94	-9.65	-6.75	-7.25
ch4/p1	-18.37	-19.60	-15.15	-16.07	-11.89	-12.84	-8.78	-9.60	-6.60	-7.20
ch4/p2	-18.36	-19.52	-15.13	-15.99	-11.78	-12.77	-8.66	-9.52	-6.48	-7.12
ch5/p1	-18.10	-19.24	-14.88	-15.70	-11.72	-12.47	-8.62	-9.25	-6.43	-6.82
ch5/p2	-17.80	-18.68	-14.56	-15.43	-11.41	-12.20	-8.31	-8.98	-6.12	-6.56
ch6/p1	-17.54	-18.29	-14.31	-15.05	-11.14	-11.82	-8.05	-8.59	-5.88	-6.18
ch6/p2	-17.42	-18.15	-14.19	-14.88	-11.02	-11.65	-7.93	-8.42	-5.76	-5.93
ch7/p1	-17.36	-17.90	-14.12	-14.65	-10.95	-11.42	-7.87	-8.20	-5.59	-5.78
ch7/p2	-17.07	-17.60	-13.83	-14.33	-10.67	-11.10	-7.58	-7.89	-5.26	-5.45
ch8/p1	-16.65	-17.13	-13.40	-13.86	-10.24	-10.63	-7.15	-7.41	-4.98	-5.15
ch8/p2	-16.45	-16.85	-13.18	-13.57	-10.04	-10.36	-6.95	-7.14	-4.68	-4.88

Table 3.38: Averaged Log BER At Various Tx Aperture Diameters.

aperture diameter	Averaged Log BER values at various Tx aperture diameter									
	10,000 km		20,000 km		30,000 km		40,000 km		48,000 km	
	HG00	HG01	HG00	HG01	HG00	HG01	HG00	HG01	HG00	HG01
5 cm	-12.68	-13.49	-9.56	-10.19	-6.47	-7.05	-3.32	-3.76	below	below
10 cm	-14.56	-15.37	-11.43	-12.06	-8.32	-8.90	-5.18	-5.63	-3.17	-3.48
15 cm	-16.29	-17.10	-13.26	-13.89	-10.18	-10.76	-7.06	-7.51	-4.93	-5.24
20 cm	-18.01	-18.82	-14.77	-15.41	-11.60	-12.18	-8.50	-8.95	-6.28	-6.56

4.4.2 Results Based Rx Aperture Diameter

The second aspect of the third objective is to investigate the Rx component of the satellite communication system. In this part of the investigation, various values of aperture diameter for the Rx antenna will be studied in order to quantify the performance of the proposed system with various antenna diameters and with respect to a variety of parameters for assessing the performance of the system. It is important to point out that the diameter of the antenna chosen for the system that is being suggested in this thesis was equivalent to 30 cm.

The aperture diameter of the Rx antenna will be varied at different intervals of 10, 20, and 30 cm during the research. In addition, the size of the Tx aperture diameter has been held constant throughout this inquiry at 15 cm, even though the Rx diameters have been altered, and the aiming error has been held at 1 mrad. These parameters constitute the initial settings of the proposed system.

The log BER based parameter will be explored in this inquiry regarding the specified antenna diameters and for the range between (10,000 km and 48,000 km). This investigation will focus on the range between (10,000 km and 48,000 km). The values of the acquired log BER are computed for the two polarizations and two modes (HG00 and HG01) as shown in (Table 4.39 – Table 4.41) for the three studied diameters accordingly. These values may be found for each of the investigated diameters. The results of the performance assessment will be summed up by considering the mean values of log BER that were acquired from each instance of aperture diameter, as stated in Table 4.42, and as follows:

a. For Rx aperture diameter of 10 cm, the proposed system of this thesis indicates regular performance for distance up to 30,000 km as some channels exceeded the min BER FEC threshold. For distances, higher than 30,000 km the system fails.
b. For the case of setting 20 cm aperture diameter for Rx side, the system capability of transmission was up to 40,000 km. The reason behind the failure of this diameter selection because of being converge to Tx diameter of 15 cm, which will increase the attenuation impact.
c. Raising the diameter to 30 cm can represent the best overall case which can achieve the required reliability of transmission towards 48,000 km. The diameter of the Rx aperture should be larger in size in comparison to the diameter of the Tx aperture. However, the Rx aperture should not be so big that it allows ambient light to mix in with the original signal and generate noise signals. Because of this, the diameter of the Rx aperture has to be increased in size in order to receive all of the information that is being conveyed by the optical carrier. However, increasing the size of the Rx aperture also increases the amount of noise caused by the surrounding light.

Table 4.39: Log BER Values At Rx Aperture Diameter Of 30 Cm.

Channel	Log BER values at Rx aperture diameter = 30 cm									
	10,000 km		20,000 km		30,000 km		40,000 km		48,000 km	
ch1/p1	-17.39	-18.04	-14.35	-14.69	-11.30	-11.57	-8.18	-8.32	-5.98	-6.02
ch1/p2	-17.33	-18.01	-14.30	-14.67	-11.24	-11.54	-8.12	-8.29	-5.92	-5.99
ch2/p1	-17.17	-17.90	-14.13	-14.56	-11.07	-11.43	-7.95	-8.18	-5.85	-5.98
ch2/p2	-17.07	-17.90	-14.04	-14.56	-10.98	-11.43	-7.86	-8.18	-5.76	-5.97
ch3/p1	-16.93	-17.97	-13.89	-14.62	-10.84	-11.50	-7.72	-8.25	-5.62	-5.95
ch3/p2	-16.71	-17.93	-13.68	-14.59	-10.62	-11.46	-7.50	-8.21	-5.40	-5.91
ch4/p1	-16.66	-17.89	-13.63	-14.55	-10.47	-11.42	-7.35	-8.17	-5.25	-5.87
ch4/p2	-16.64	-17.81	-13.61	-14.47	-10.35	-11.34	-7.23	-8.09	-5.13	-5.79
ch5/p1	-16.39	-17.53	-13.36	-14.18	-10.30	-11.06	-7.18	-7.81	-5.08	-5.51
ch5/p2	-16.08	-16.96	-13.05	-13.92	-9.99	-10.79	-6.87	-7.54	-4.77	-5.24
ch6/p1	-15.84	-16.59	-12.81	-13.54	-9.75	-10.42	-6.63	-7.17	-4.53	-4.87
ch6/p2	-15.72	-16.42	-12.68	-13.37	-9.63	-10.25	-6.51	-7.00	-4.41	-4.62
ch7/p1	-15.66	-16.20	-12.62	-13.16	-9.56	-10.03	-6.44	-6.78	-4.24	-4.48
ch7/p2	-15.37	-15.88	-12.33	-12.84	-9.28	-9.71	-6.16	-6.46	-3.91	-4.15
ch8/p1	-14.95	-15.42	-11.91	-12.37	-8.85	-9.25	-5.73	-6.00	-3.63	-3.85
ch8/p2	-14.75	-15.14	-11.71	-12.10	-8.65	-8.97	-5.53	-5.72	-3.33	-3.58

Table 4.40: Log BER Values At Rx Aperture Diameter Of 20 Cm.

Channel	Log BER values at Rx aperture diameter = 20 cm									
	10,000 km		20,000 km		30,000 km		40,000 km		48,000 km	
ch1/p1	-13.89	-14.54	-10.70	-11.04	-7.62	-7.89	-4.57	-4.67	*	*
ch1/p2	-13.84	-14.52	-10.75	-11.12	-7.59	-7.89	-4.51	-4.68	*	*
ch2/p1	-13.64	-14.38	-10.56	-10.99	-7.42	-7.78	-4.34	-4.57	*	*
ch2/p2	-13.62	-14.45	-10.51	-11.03	-7.34	-7.79	-4.25	-4.57	*	*
ch3/p1	-13.45	-14.49	-10.55	-11.28	-7.16	-7.82	-4.10	-4.64	*	*
ch3/p2	-13.31	-14.54	-10.22	-11.14	-6.93	-7.78	-3.89	-4.60	*	*
ch4/p1	-13.20	-14.43	-10.09	-11.01	-6.77	-7.72	-3.74	-4.56	*	*
ch4/p2	-13.31	-14.48	-10.08	-10.93	-6.73	-7.72	-3.62	-4.48	*	*
ch5/p1	-12.95	-14.09	-9.78	-10.61	-6.68	-7.44	-3.57	-4.20	*	*
ch5/p2	-12.61	-13.48	-9.55	-10.42	-6.33	-7.13	-3.26	-3.93	*	*
ch6/p1	-12.38	-13.13	-9.20	-9.94	-6.08	-6.74	-3.02	-3.55	*	*
ch6/p2	-12.22	-12.92	-9.07	-9.76	-5.95	-6.57	-2.89	-3.39	*	*
ch7/p1	-12.21	-12.76	-9.08	-9.61	-5.88	-6.34	-2.83	-3.17	*	*
ch7/p2	-11.94	-12.46	-8.81	-9.31	-5.42	-5.86	-2.54	-2.85	*	*
ch8/p1	-11.55	-12.02	-8.30	-8.76	-5.22	-5.62	-2.12	-2.39	*	*
ch8/p2	-11.29	-11.69	-8.05	-8.43	-5.00	-5.32	-1.92	-2.11	*	*

Table 4.41: Log BER Values At Rx Aperture Diameter Of 10 Cm.

Channel	Log BER values at Rx aperture diameter = 10 cm									
	10,000 km		20,000 km		30,000 km		40,000 km		48,000 km	
	HG00	HG01	HG00	HG01	HG00	HG01	HG00	HG01	HG00	HG01
ch1/p1	-10.01	-10.69	-6.83	-7.19	-3.84	-4.11	*	*	*	*
ch1/p2	-10.09	-10.77	-7.01	-7.38	-3.85	-4.15	*	*	*	*
ch2/p1	-9.84	-10.58	-6.83	-7.26	-3.67	-4.03	*	*	*	*
ch2/p2	-9.80	-10.62	-6.74	-7.26	-3.55	-4.00	*	*	*	*
ch3/p1	-9.64	-10.68	-6.75	-7.48	-3.37	-4.04	*	*	*	*
ch3/p2	-9.46	-10.69	-6.52	-7.44	-3.14	-3.99	*	*	*	*
ch4/p1	-9.36	-10.59	-6.34	-7.26	-2.97	-3.92	*	*	*	*
ch4/p2	-9.51	-10.68	-6.32	-7.18	-2.94	-3.93	*	*	*	*
ch5/p1	-9.09	-10.23	-5.91	-6.74	-2.90	-3.66	*	*	*	*
ch5/p2	-8.85	-9.73	-5.68	-6.55	-2.53	-3.33	*	*	*	*
ch6/p1	-8.58	-9.33	-5.46	-6.20	-2.26	-2.93	*	*	*	*
ch6/p2	-8.34	-9.04	-5.33	-6.02	-2.14	-2.76	*	*	*	*
ch7/p1	-8.45	-8.99	-5.43	-5.96	-2.04	-2.50	*	*	*	*
ch7/p2	-8.10	-8.61	-5.05	-5.55	-1.58	-2.01	*	*	*	*
ch8/p1	-7.71	-8.18	-4.44	-4.91	-1.49	-1.88	*	*	*	*
ch8/p2	-7.45	-7.84	-4.23	-4.61	-1.25	-1.56	*	*	*	*

Table 4.42: Averaged Log BER At Various Rx Aperture Diameters.

Diameter	Averaged log BER values at various Rx aperture diameter									
	10,000 km		20,000 km		30,000 km		40,000 km		48,000 km	
	HG00	HG01	HG00	HG01	HG00	HG01	HG00	HG01	HG00	HG01
10 cm	-9.02	-9.83	-5.93	-6.56	-2.72	-3.30	Below	Below	Below	Below
20 cm	-12.84	-13.65	-9.71	-10.34	-6.51	-7.09	-3.45	-3.90	Below	Below
30 cm	-16.29	-17.10	-13.26	-13.89	-10.18	-10.76	-7.06	-7.51	-4.93	-5.24

5. CONCLUSIONS

5.1 CONCLUSIONS BASED FIRST OBJECTIVE

a. This work proposes a novel 8-channel Is-OWC system by using the effective OFDM technique with 16 QAM modulation and by utilizing two division-based techniques represented by the MDM of two modes (HG00 and HG01) and PDM with two polarization (p1) and (p2). The targeted distance ranged between 10,000 km to 48,000 km.

b. A direct relation between the log BER and distance is concluded with achieved average log BER of (HG00= -5.02 and HG01= -5.32) for p1 and (HG00= -4.83 and HG01= -5.16) for p2 respectively at 48,000 km, which were above the BER FEC threshold of -2.42.

c. A reverse relation between the OSNR and the distance. For example, the OSNR tolerance was ≥ 50.5 dB with a selected Pe of 1 mrad for both the Tx and Rx, which confirm the reliability of the proposed system in achieving a data rate of 5.12 Tbps for distances satisfied with recent GEO-based applications.

d. The EVM raises with increasing the transmission distance, where the used mode of HG00 indicates a higher impact of EVM as compared to HG01. This is because the HG01 mode reaches a higher impact of maximum mode power as compared to HG00.

e. Reverse relation between the received power and the distance and indicating a robust receiver sensitivity at a Pe of 1 mrad for both the Tx and Rx, which may confirm the reliability of the proposed system in achieving a higher impact of data rate.

f. To confirm the reliability of the proposed system with the attached novel hybrid division techniques, an alternative 8-channel DP-DQPSK Is-OWC system with two precoding schemes (DPSK and duobinary) was designed and tested over the same range of distances. it is found that the effectiveness of the alternate system was up to 40,000 km and an overall capacity of 240 Gbps.

g. By comparing the performance of the two systems, the DP-DQPSK system was effective for only 10,000 km and showed superior performance by using the Duobinary precoder scheme at the receiver. While the proposed OFDM-based system indicates reliable performance overall studied distances which confirms its efficiency.

5.2 CONCLUSIONS BASED SECOND OBJECTIVE

a. The proposed system evaluated with respect to the capability of antenna misalignment (pe) for both the Tx and Rx antennas and for the same distances. For Rx pe, the system gives reliable performance for 3 mrad and indicate a direct relation with log BER. Additionally, HG00 mode has best outcomes as compared to HG01 mode due to its less influence by input power.

b. OSNR tolerance indicate reversal relation with raising the Rx pe with values of 50.5 dB, 45.75 dB, 41.7 dB, 36.8 dB, and 31.9 dB for the cases of 1 mrad, 1.5 mrad, 2 mrad, 2.5 mrad, and 3 mrad respectively.

c. It has been concluded that OSNR varied by 3 dB for Rx Pe up to 2 mrad and raising the pe values will increase the variation to 5 dB due to the serious effects of antenna misalignment on the Rx satellite side.

d. For Tx pe, the proposed novel system evaluates with values of 1 mrad, 2 mrad, 3 mrad, 4 mrad, and 5 mrad to demonstrate the system reliability. It can be concluded that the system performs well under all values of Tx pe for distance up to 40,000 km. Raising the distance, resulted in system capability to handle Tx pe of up to 4 mrad.

e. OSNR tolerance indicates reversal relation with raising the Tx pe with values of 50.5 dB, 46.8 dB, 42.5 dB, 37.5 dB, and 30.5 dB for Tx pe of 1 mrad, 2 mrad, 3 mrad, 4 mrad, and 5 mrad, respectively. The issue that can certify the proposed system's dependability about the OSNR criteria.

5.3 CONCLUSIONS BASED THIRD OBJECTIVE

a. The proposed system is evaluated with respect to the suitable diameter size for both the Tx and Rx antennas and for the same range of the investigated distances. Direct relation between the aperture diameter and the reached transmission distance can be concluded.

b. Reverse relation between both the (Tx and Rx) aperture diameter and the log BER, where raising the diameter can reduce the geometrical losses and attenuation thereby reducing the log BER for the estimated channels.

c. For Tx diameter investigation, the proposed system indicates that using 5 cm resulted in performance for distance up to 40,000 km, raising to 10 cm can contribute to reach the goal distance but not for all channels. Using diameter of 15 cm provides reliable performance. On the other way, using 20 cm can raise the performance of the proposed system, but trade-off between the Tx and Rx diameters to control the losses during transmission.

d. For Rx diameter investigation, the proposed system indicates that using 10 cm diameter can transmit data up to 30,000 km. Raising the diameter to 20 cm raises the capability of the transmission to reach 40,000 km. Finally, the setting of 30 cm represents the best case which can achieve the required transmission distance of 48,000 km.

e. As a conclusion reducing the impact of geometrical losses and attenuation will require setting the Rx aperture diameter to be larger than Tx aperture diameter and setting the appropriate diameters can have a direct impact on the specification of the antenna gain.

5.4 FUTURE WORK

For future studies several points can be studied as:

a. Propose novel methodology by using dedicated techniques of various MDM types or number of the utilized modes.

b. Investigate performance of Is-OWC system with different QAM bits.

c. Study the influence of different lens size for both the Tx and Rx antenna to reduce the impact of losses and attenuations.

REFERENCES

[1] C. Yu, L. Yu, Y. Wu, Y. He, and Q. Lu, "Uplink scheduling and link adaptation for narrowband internet of things systems," *IEEE Access*, vol. 5, pp. 1724–1734, 2017.

[2] W. Ejaz *et al.*, "Internet of things (IoT) in 5G wireless communications," *IEEE Access*, vol. 4, pp. 10310–10314, 2016.

[3] I. Alimi, A. Shahpari, V. Ribeiro, N. Kumar, P. Monteiro, and A. Teixeira, "Optical wireless communication for future broadband access networks," in *2016 21st European Conference on Networks and Optical Communications (NOC)*, 2016, pp. 124–128.

[4] G. Parca, A. Tavares, A. Shahpari, A. Teixeira, V. Carrozzo, and G. T. Beleffi, "FSO for broadband multi service delivery in future networks," in *2013 2nd International Workshop on Optical Wireless Communications (IWOW)*, 2013, pp. 67–70.

[5] Z. Ghassemlooy, W. Popoola, and S. Rajbhandari, *Optical wireless communications: System and channel modelling with MATLAB (R), second edition*, 2nd ed. London, England: CRC Press, 2019.

[6] B. G. Evans and Institution of Electrical Engineers, *Satellite Communication Systems*, 3rd ed. Stevenage, England: Institution of Engineering and Technology, 1999.

[7] B. Elbert, *Introduction to satellite communication, third edition*, 3rd ed. Norwood, MA: Artech House, 2008.

[8] J. Takei and J. Murai, "Satellite communication on the Internet: its history and the technology," in *2003 Symposium on Applications and the Internet Workshops, 2003. Proceedings*, 2003, pp. 3–7.

[9] J. N. Pelton, "History of Satellite Communications," in *Handbook of Satellite Applications*, New York, NY: Springer New York, 2013, pp. 27–66.

[10] J. N. Pelton, "The start of commercial satellite communications [History of communications]," *IEEE Commun. Mag.*, vol. 48, no. 3, pp. 24–31, 2010.

[11] G. Slocombe, “Satellites: Future roles for Australian industry in military satellite communications,” *Asia-Pacific Defence Reporter (2002)*, vol. 48, no. 1, pp. 12–14, 2022.

[12] R. De Gaudenzi, M. Luise, and L. Sanguinetti, “The open challenge of integrating satellites into (beyond-) 5G cellular networks,” *IEEE Netw.*, vol. 36, no. 2, pp. 168–174, 2022.

[13] L. J. Ippolito, *Satellite communications systems engineering: Atmospheric effects, satellite link design and system performance*, 2nd ed. Nashville, TN: John Wiley & Sons, 2017.

[14] M. Graydon and L. Parks, “‘Connecting the unconnected’: a critical assessment of US satellite Internet services,” *Media Cult. Soc.*, vol. 42, no. 2, pp. 260–276, 2020.

[15] G. Maral, M. Bousquet, and Z. Sun, *Satellite communications systems: Systems, techniques and technology*, 6th ed. Nashville, TN: John Wiley & Sons, 2020.

[16] G. A. Codding, *The future of satellite communications the future of satellite communications*. London, England: Routledge, 2019.

[17] I. del Portillo, B. G. Cameron, and E. F. Crawley, “A technical comparison of three low earth orbit satellite constellation systems to provide global broadband,” *Acta Astronaut.*, vol. 159, pp. 123–135, 2019.

[18] J. N. Pelton, S. Madry, and S. Camacho-Lara, Eds., *Handbook of Satellite Applications 2013*, 2013th ed. New York, NY: Springer, 2012.

[19] L. J. Ippolito, “Interference Mitigation in Satellite Communications,” in *Satellite Communications Systems Engineering*, Chichester, UK: John Wiley & Sons, Ltd, 2017, pp. 376–397.

[20] J. Gibson, *The Communications Handbook*, 2nd ed. Boca Raton, FL: CRC Press, 2002.

[21] ANZ-MEADOR, P. D., JN OPIELA, and D. Shoots, “History of on-orbit satellite fragmentations,” *FoC Space center*, 2018.

[22] I. Darwazeh, H. Ghannam, and T. Xu, “The first 15 years of SEFDM: A brief survey,” in *2018 11th International Symposium on Communication Systems, Networks & Digital Signal Processing (CSNDSP)*, 2018, pp. 1–7.

[23] M. M. A. Eid, F. M. A. M. Houssien, A. N. Z. Rashed, and A. E.-N. A. Mohammed, “Performance enhancement of transceiver system based inter satellite optical wireless channel (IS-OWC) for ultra long distances,” *J. Opt. Commun.*, vol. 0, no. 0, 2020.

[24] P. Sharma and S. Meena, “Performance analysis of inter-satellite optical wireless communication (is-OWC) system by using channel diversity technique,” in *2018 International Conference on Inventive Research in Computing Applications (ICIRCA)*, 2018, pp. 477–480.

[25] N. Kaur and G. Soni, “Performance analysis of inter-satellite optical wireless communication (IsOWC) system at 980 nm and 1550 nm wavelengths,” in *2014 International Conference on Contemporary Computing and Informatics (IC3I)*, 2014, pp. 1245–1250.

[26] M. Z. Chowdhury, M. T. Hossan, A. Islam, and Y. M. Jang, “A comparative survey of optical wireless technologies: Architectures and applications,” *IEEE Access*, vol. 6, pp. 9819–9840, 2018.

[27] M. Bero and I. Abu Kassem, “Investigation of the use of FXG gel dosimeter for UV radiation detection,” 2009.

[28] M. Richharia, *Mobile Satellite Communications: Principles and Trends*, 2nd ed. Nashville, TN: John Wiley & Sons, 2014.

[29] T. S. Rappaport, *Wireless communications: Principles and practice*, 1st ed. Piscataway, NJ: IEEE Publications, 1996.

[30] D. Roddy, *Satellite Communications*, 4th ed. New York, NY: McGraw-Hill Professional, 2006.

[31] J. E. Allnutt and T. Pratt, *Satellite Communications*, 3rd ed. Nashville, TN: John Wiley & Sons, 2019.

[32] R. P. Rajagopalan and N. Prasad, *Space India 2.0: Commerce, policy, security and governance perspectives*. Observer Research Foundation, 2017.

[33] A. K. Maini and V. Agrawal, *Satellite Technology: Principles and Applications*, 2nd ed. Standards Information Network, 2011.

[34] L. Shi, S. Du, Y. Miao, and S. Lan, "Modeling and performance analysis of satellite network moving target defense system with Petri nets," *Remote Sens. (Basel)*, vol. 13, no. 7, p. 1262, 2021.

[35] P. Kaur, A. Gupta, and M. Chaudhary, "Comparative analysis of inter satellite optical wireless channel for NRZ and RZ modulation formats for different levels of input power," *Procedia Comput. Sci.*, vol. 58, pp. 572–577, 2015.

[36] R. Kaur and H. Kaur, "Comparative analysis of chirped, AMI and DPSK modulation techniques in IS-OWC system," *Optik (Stuttg.)*, vol. 154, pp. 755–762, 2018.

[37] J. B. Padhy and B. Patnaik, "100 Gbps multiplexed inter-satellite optical wireless communication system," *Opt. Quantum Electron.*, vol. 51, no. 7, 2019.

[38] H. K. Gill, G. K. Walia, and N. S. Grewal, "Performance analysis of mode division multiplexing IS-OWC system using Manchester, DPSK and DQPSK modulation techniques," *Optik (Stuttg.)*, vol. 177, pp. 93–101, 2019.

[39] S. Chaudhary, A. Sharma, and V. Singh, "Optimization of high speed and long haul inter-satellite communication link by incorporating differential phase shift key and orthogonal frequency division multiplexing scheme," *Optik (Stuttg.)*, vol. 176, pp. 185–190, 2019.

[40] A. Grover and A. Sheetal, "A 2 × 40 gbps mode division multiplexing based inter-satellite optical wireless communication (IsOWC) system," *Wirel. Pers. Commun.*, vol. 114, no. 3, pp. 2449–2460, 2020.

[41] A. Sharma, J. Malhotra, S. Chaudhary, and V. Thappa, "Analysis of 2 × 10 Gbps MDM enabled inter satellite optical wireless communication under the impact of pointing errors," *Optik (Stuttg.)*, vol. 227, no. 165250, p. 165250, 2021.

[42] M. Singh and J. Malhotra, “Performance comparison of 2 × 20 gbit/s-40 GHz OFDM based RoFSO transmission link incorporating MDM of Hermite Gaussian modes using different modulation schemes,” *Wirel. Pers. Commun.*, vol. 110, no. 2, pp. 699–711, 2020.

[43] S. Chaudhary, L. Wuttisittikulkij, J. Nebhen, A. Sharma, D. Z. Rodriguez, and S. Kumar, “Terabyte capacity-enabled (10 x 400 Gbps) Is-OWC system for long-haul communication by incorporating dual polarization quadrature phase shift key and mode division multiplexing scheme,” *PLoS One*, vol. 17, no. 3, p. e0265044, 2022.

[44] S. Sharma, G. K. Walia, and H. Kaur, “A multichannel Hermite Gaussian (HG) intensity profiles based inter-satellite optical wireless communication (IsOWC) using transmitter diversity,” *Opt. Quantum Electron.*, vol. 55, no. 2, 2023.

[45] Optiwave, “Optisystem program,” *Optiwave Official website*. [Online]. Available: https://optiwave.com/optisystem-overview/.

[46] John, *Optical fiber communications: Principles and practice*, 3rd ed. Philadelphia, PA: Prentice Hall, 2008.

[47] World Web Technology, “CWDM and DWDM,” *Official website for World Web Technology website*, 2023. [Online]. Available: https://www.wwt.com/article/cwdm-or-dwdm-which-should-you-use-and-when. [Accessed: 01-Jul-2023].

[48] Official Website for Router Switch company, “DWDM and CWDM,” *Official Website for Router Switch company*, 2023. [Online]. Available: https://www.router-switch.com/faq/dwdm-vs-cwdm-optical-technologies-difference.html. [Accessed: 11-Jul-2023].

[49] H. J. R. Dutton, *Understanding Optical Communications*. Philadelphia, PA: Prentice Hall, 1998.

[50] D. K. Mynbaev and L. L. Scheiner, *Fiber-optic communications technology*. Upper Saddle River, NJ: Pearson, 2000.

[51] “Space -time and space -frequency coded orthogonal frequency division multiplexing transmitter diversity techniques,” *IEEE*, 2001.

[52] M. Morelli, C.-C. J. Kuo, and M.-O. Pun, “Synchronization techniques for orthogonal frequency division multiple access (OFDMA): A tutorial review,” *Proc. IEEE Inst. Electr. Electron. Eng.*, vol. 95, no. 7, pp. 1394–1427, 2007.

[53] X. Zhang, Z. Babar, P. Petropoulos, H. Haas, and L. Hanzo, “The evolution of optical OFDM,” *IEEE Commun. Surv. Tutor.*, vol. 23, no. 3, pp. 1430–1457, thirdquarter 2021.

[54] T. Hwang, C. Yang, G. Wu, S. Li, and G. Ye Li, “OFDM and its wireless applications: A survey,” *IEEE Trans. Veh. Technol.*, vol. 58, no. 4, pp. 1673–1694, 2009.

[55] M. El Jbari, M. Moussaoui, and N. Chahboun, “Coding and Modulation for Terahertz,” in *Terahertz Wireless Communication Components and System Technologies*, Singapore: Springer Singapore, 2022, pp. 59–79.

[56] R. Prasad, *OFDM for wireless communications systems*. Norwood, MA: Artech House, 2004.

[57] R. W. Chang, “Synthesis of band-limited orthogonal signals for multichannel data transmission,” *Bell Syst. Tech. J.*, vol. 45, no. 10, pp. 1775–1796, 1966.

[58] A. M. Jaradat, J. M. Hamamreh, and H. Arslan, “Modulation Options for OFDM-Based Waveforms: Classification, Comparison, and Future Directions,” *IEEE Access*, vol. 7, pp. 17263–17278, 2019.

[59] J. Ssimbwa, B. Lim, J.-H. Lee, and Y.-C. Ko, “A survey on robust modulation requirements for the next generation personal satellite communications,” *Front. Comms. Net.*, vol. 3, 2022.

[60] A. R. S. Bahai, B. R. Saltzberg, and M. Ergen, *Multi-Carrier Digital Communications: Theory and Applications of OFDM*, 2nd ed. New York, NY: Springer, 2004.

[61] J. Armstrong, “OFDM for Optical Communications,” *J. Lightwave Technol.*, vol. 27, no. 3, pp. 189–204, 2009.

[62] J. Singh, R. Garg, and I. K. Aulakh, “Effect of OFDM in cognitive radio: Advantages & issues,” in *2016 Second International Conference on Computational Intelligence & Communication Technology (CICT)*, 2016, pp. 554–558.

[63] R. F. Everything, “What is QAM or Quadrature Amplitude Modulation,” *everything RF*, 2023. [Online]. Available: https://www.everythingrf.com/community/what-is-qam-or-quadrature-amplitude-modulation. [Accessed: 01-Jul-2023].

[64] *Researchgate.net*. [Online]. Available: https://www.researchgate.net/profile/Suresh-Kumar-222/publication/329554648_A_Comprehensive_Review_of_QAM-OFDM_Optical_Networks/links/5ee30125a6fdcc73be739505/A-Comprehensive-Review-of-QAM-OFDM-Optical-Networks.pdf. [Accessed: 28-May-2023].

[65] Delson and I. Jose, “A survey on 5G standards, specifications and massive MIMO testbed including transceiver design models using QAM modulation schemes,” in *2019 International Conference on Data Science and Communication (IconDSC)*, 2019, pp. 1–7.

[66] “A Hybrid-Structure Offset-Qam Filter-Bank Multi-Carrier Mimo System,” 2022.

[67] G. C. Dogiamis *et al.*, “A 60-gbps 108-GHz 16-QAM dielectric waveguide interconnect with package integrated filters,” in *2022 IEEE/MTT-S International Microwave Symposium - IMS 2022*, 2022, pp. 556–559.

[68] M. Bilim, “Different QAM schemes analyses for ARS fading channels,” *Trans. Emerg. Telecommun. Technol.*, vol. 32, no. 1, 2021.

[69] E. Aydin, “A new hexagonal quadrature amplitude modulation aided media-based modulation,” *Int. J. Commun. Syst.*, vol. 34, no. 17, 2021.

[70] K. Chen, J. Zhang, Z. Nong, X. Cai, S. He, and L. Liu, “Compact multimode 3dB coupler for on-chip mode division multiplexing,” in *Optical Fiber Communication Conference*, 2017, p. W1B.4.

[71] C. P. Tsekrekos and D. Syvridis, “All-fiber broadband $\rm LP_02$ mode converter for future wavelength and mode division multiplexing systems,” *IEEE Photonics Technol. Lett.*, vol. 24, no. 18, pp. 1638–1641, 2012.

[72] “‘Research at CMMPE- Liquid crystals for telecommunications.’ CMMPE - ,” *University of Cambridge*, 2023. [Online]. Available: http://www-g.eng.cam.ac.uk/CMMPE/telecoms.html. [Accessed: 01-Jul-2023].

[73] N. Bai, “Mode-division multiplexed transmission in few-mode fibers,” University of Central Florida, 2013.

[74] M.-J. Li *et al.*, “Low delay and large effective area few-mode fibers for mode-division multiplexing,” in *2012 17th Opto-Electronics and Communications Conference*, 2012, pp. 495–496.

[75] A. E. Siegman, *Lasers*. Sausalito, CA: University Science Books, 1986.

[76] R. Paschotta, “Gouy phase shift,” *RP Photonics AG*, 20-May-2023. [Online]. Available: http://www.rp-photonics.com/gouy_phase_shift.html. [Accessed: 28-May-2023].

[77] G. Vallone, “On the properties of circular beams: normalization, Laguerre-Gauss expansion, and free-space divergence,” *Opt. Lett.*, vol. 40, no. 8, pp. 1717–1720, 2015.

[78] W. Paufler, “High-harmonic generation with Laguerre-Gaussian beams,” Friedrich-Schiller-Universität Jena, 2020.

[79] “Laser Spectroscopy, Quantum Electronics,” *sasada lab.*, 2023. [Online]. Available: http://www.phys.keio.ac.jp/faculty/hasegawa/sasada-lab/research/orbangmom-en.html. [Accessed: 01-Jul-2023].

[80] M. A. Bandres, J. C. Gutiérrez-Vega, and S. Chávez-Cerda, “Parabolic nondiffracting optical wave fields,” *Opt. Lett.*, vol. 29, no. 1, pp. 44–46, 2004.

[81] E. Karimi, G. Zito, B. Piccirillo, L. Marrucci, and E. Santamato, “Hypergeometric-Gaussian modes,” *Opt. Lett.*, vol. 32, no. 21, pp. 3053–3055, 2007.

[82] X. S. Yao, L.-S. Yan, B. Zhang, A. E. Willner, and J. Jiang, “All-optic scheme for automatic polarization division demultiplexing,” *Opt. Express*, vol. 15, no. 12, pp. 7407–7414, 2007.

[83] D. Ivanovich, S. B. Powell, R. D. Chamberlain, and V. Gruev, “Polarization division multiplexing for optical data communications,” in *Optical Interconnects XVIII*, 2018.

[84] A. She and F. Capasso, “Parallel polarization state generation,” *Sci. Rep.*, vol. 6, no. 1, p. 26019, 2016.

[85] Ghatak, A. K., and K. Thyagarajan, "Introduction to fiber optics," *Cambridge University*, 1998.

[86] E. G. Johnson, J. Stack, and C. Koehler, "Light coupling by a vortex lens intoGraded index fiber," *J. Lightwave Technol., JLT*, vol. 19, no. 5, p. 753, 2001.

[87] J. C. Cartledge, C. Rolland, S. Lemerle, and A. Solheim, "Theoretical performance of 10 Gb/s lightwave systems using a III-V semiconductor Mach-Zehnder modulator," *IEEE Photonics Technol. Lett.*, vol. 6, no. 2, pp. 282–284, 1994.

[88] S. Chaudhary, X. Tang, A. Sharma, B. Lin, X. Wei, and A. Parmar, "A cost-effective 100 Gbps SAC-OCDMA–PDM based inter-satellite communication link," *Opt. Quantum Electron.*, vol. 51, no. 5, 2019.

[89] P. Pinho, *Optical Communication Technology*. London, England: InTech, 2017.

[90] J. Jiao, H. Gao, S. Wu, and Q. Zhang, "Performance analysis of space information networks with backbone satellite relaying for vehicular networks," *Wirel. Commun. Mob. Comput.*, vol. 2017, pp. 1–13, 2017.

[91] U. Kumar, S. Banerjee, and A. V. R. Murthy, "Bit error rate performance of underwater optical wireless communication test bed simulating the seawater conditions," *Optik (Stuttg.)*, vol. 251, no. 168434, p. 168434, 2022.

[92] M. P. Ninos, H. E. Nistazakis, and G. S. Tombras, "On the BER performance of FSO links with multiple receivers and spatial jitter over gamma-gamma or exponential turbulence channels," *Optik (Stuttg.)*, vol. 138, pp. 269–279, 2017.

[93] A. Hossain and S. P. Majumder, "BER performance limitations due to inter-core crosstalk in a multi-core fiber-optic transmission system," *Optik (Stuttg.)*, vol. 232, no. 166582, p. 166582, 2021.

[94] P. Ge *et al.*, "A Low-complexity OSNR monitoring scheme based on amplitude variance analysis," *Optik (Stuttg.)*, vol. 246, no. 167788, p. 167788, 2021.

[95] A. E. Willner, Z. Pan, and C. Yu, "Optical performance monitoring," in *Optical Fiber Telecommunications V B*, I. P. Kaminow, T. Li, and A. E. Willner, Eds. San Diego, CA: Elsevier, 2008, pp. 233–292.

[96] H. R. A. O'Sullivan, "Fiber-Optic Measurement Techniques," *Academic Press*, 2022.

[97] "In-band OSNR measurements on 40 G polarization-multiplexed QPSK signals using a field-deployable , high-resolution OSA," *semantic scholar*, 2015.

[98] E. Acar, "How error vector magnitude (EVM) measurement improves your system-level performance," *Analog Devices Tech. Art*, pp. 1–6, 2021.

[99] O. O. Omomukuyo, "Orthogonal frequency division multiplexing for optical access networks," UCL (University College London), 2013.

[100] Balanis, C. A. (1992). Antenna theory: A review. Proceedings of the IEEE, 80(1), 7-23.

[101] Haslett, C. (2008). Essentials of radio wave propagation. Cambridge University Press.

[102] Mushtaq, M. T., Yasir, S. M., Khan, M. S., Wahid, A., & Iqbal, M. S. (2018). Analysis of internal design parameters to minimize geometrical losses in free-space optical communication link. Acta Phys. Polonica A, 134, 275-277.

APPENDIX A

DEMONSTRATION OF THE SATELLITE COMPANIES THAT USE KA-BAND (ITU REGULATION)

Company name	Satellite System	Description
Arabsat	Arabsat-5B, Arabsat 5C	Arabsat owns and operates six satellites, at 3 orbital positions, 20°, 26°, and 30.5° East: Arabsat-5C (20°E), BADR-4, BADR-5, BADR-6 and BADR-7 (26°E), Arabsat-5A (30.5°E).
Avanti	HYLAS-1 / HYLAS-2	Launched in 2012, HYLAS 2 uses high-throughput Ka-band technology. The spacecraft has 24 fixed beams and one steerable beam, addressing markets across Europe, the Middle East, the Caucasus, and Africa, location is 31˚E
Eutelsat	Eutelsat-W3 series, Ka-Sat, Hotbird	EUTELSAT's new generation of telecommunications satellites began to take over service from the EUTELSAT II series in 1998/1999. These new satellites operate at orbital positions other than 13 degrees East. They allow for the expansion of telecommunications services as well as supply some television services to other markets than those served from the 13 degrees East HOT BIRD position. The new satellites (ALCATEL space bus 3000) feature steerable antennas and an extended coverage of the Middle East. They are equipped with 24 transponders of 90 Watts (in comparison to 16 transponders of 50 Watts on the EUTELSAT II generation) and their minimum lifetime will be 12 years.
Hispasat	Spainsat, Hispasat-1E	On March 11, 2006, the Spainsat was launched into space from French Guiana, aboard the Ariane 5 ECA launcher. This second satellite belonging to HISDESAT Services Strategics, located at the 30º West orbital position, is added to the advanced program for governmental communications for the Spanish Ministry of Defense and the governments of allied and friendly countries.
Hughes	Spaceway-3 / Jupiter-1	Launched in July 2012 into its geostationary orbital slot 22,300 miles above the equator, JUPITER 1 (EchoStar XVII) is a fourth-generation Ka-band satellite providing HughesNet® high-speed internet services in North America. JUPITER 1 exponentially increased the capacity of its predecessor SPACEWAY 3 to 120 Gbps and delivered 100 times more capacity than conventional Ku-band satellites. This satellite has a multi-spot beam and bent-pipe Ka-band architecture and was the world's highest-capacity broadband satellite when it launched. Click here to watch the launch.
Intelsat	IAS-28 / Intelsat-20	In December 2003 the Board issued a revised IAS 28 with a new title—Investments in Associates. This revised IAS 28 was part of the Board's initial agenda of technical projects. Intelsat- 20 is a geostationary communications satellite that is operated by Intelsat. It was constructed by Space Systems/Loral and is based on the LS-1300 satellite bus.[1] It was launched on 2 August 2012 and replaced the Intelsat

		7 and Intelsat 10 spacecraft at 68.5° East longitude. It is fully operational since September 2012.
Ipstar	Ipstar	Thaicom 4 (IPSTAR) Satellite is currently under the operation of National Telecommunications Public Company Limited (NT). IPSTAR is the world's first high-throughput satellite (HTS) and is located at the orbital position of 119.5° East. It provides the telecom industry, businesses, and government administrations in Asia-Pacific with cost-effective satellite broadband capacity and services. The satellite's 2-way multiple Ku-band spot beams deliver cost-effective satellite broadband services to unserved and underserved areas.
Iridium	Iridium	The Iridium constellation consists of 75 satellites (66 operational and 9 in-orbit spares) that are cross-linked in space just 780 kilometers above Earth. Because Iridium is the largest constellation and orbits closer to Earth than other networks, Iridium users enjoy worldwide access to the phone, text, or data services with shorter network registration times and low communications latency.
JAXA/NICT	Winds	is a collaborative Japanese broadband communication technology mission within the "i-Space" project of JAXA/NICT (Japan Aerospace Exploration Agency/National Institute of Information and Communications Technology). The objective is to advance information and telecommunications and network technologies to a next-generation level by demonstrating in geostationary orbit technologies necessary to construct the spaceborne ultra-high-speed global fixed wireless communications networks (Ka-band). The i-Space initiative of JAXA and NICT is to explore various applications of satellite communications in a broader context, to maximize the space infrastructure of the next generation whose construction is in progress.
Nilesat	Nilesat 201	is an Egyptian communications satellite, which was launched on 4 August 2010. Nilesat 201 will enable the Egyptian satellite operator Nilesat to deliver digital Direct to Home (DTH) TV and radio broadcasting and high-speed data transmission services to North Africa and the Middle East starting in September 2010.[5] It was built by Thales Alenia Space in the Cannes Mande lieu Space Center and is based on the Space Bus 4000B2 satellite bus. It will be operated in geosynchronous orbit, at a longitude of 7° West.
SES	ASTRA 1H, ASTRA-1L, ASTRA-3B, ASTRA 4A, AMC-15, AMC-16, NSS-6	SES ordered its Hughes 601 satellites, in 1994 for Astra 1G; in 1995 for Astra 1H; and in 1996 for Astra 2A. In August 1999, SES ordered Astra 2C, another Hughes 601HP. The satellites enable SES to provide analog and digital television programs together. Most operate at 19.2 degrees East longitude. On Astra 1C, the 18 transmission frequencies can be selected on-orbit from 34 possibilities. On 1G, 1H, and 2A 56 possibilities are available, most in the BSS band. Because each spacecraft will provide an effective isotropic radiated power (EIRP) typically 51 dBW, these satellites deliver video and audio signals strong enough to be received by existing 60-cm dishes.
Spacecom	Amos 3	It was launched atop the maiden flight of the Zenit-3SLB launch vehicle, the first launch contracted by the Land Launch organization. The launch

		was originally scheduled to occur in 2007, and later in March 2008, however, this was delayed until 24 April 2008. The launch attempt on 24 April 2008 was scrubbed for "technical reasons".
Telesat Canada	Nimiq 4	is a Canadian geosynchronous communications satellite. It was launched aboard a Proton-M / Briz-M launch vehicle at 21:48:00 UTC on 19 September 2008. It was positioned at 82.0° West longitude and operated by Telesat Canada. The satellite was constructed by EADS Astrium, using a Eurostar-3000S bus. It is powered by two solar panels, with a span of 39 m (128 ft), producing 12 kW of power. The launch mass of the satellite is 4,850 kg (10,690 lb), with fuel. It carries 40 transponders, 32 of which operate in the Ku-band, and 8 which operate in the Ka-band. It provides digital HDTV to Canada and the United States.
ViaSat	ViaSat-1, Wildblue -1, Anik-F2	The ViaSat-1 launch occurred at the Baikonur Cosmodrome, Kazakhstan on October 19, 2011, ViaSat-1 became the record-holder for the highest-capacity satellite in the world at the time. The ViaSat-1 satellite broadband coverage included the continental United States, Alaska, Hawaii, and Canada.
Yahsat	Yahsat 1A (government) / Yahsat-1B	is a communications satellite constructed by EADS Astrium and Thales Alenia Space for Al Yah Satellite Communications Company (Yahsat). It was launched in April 2011 from Arianespace's Guiana Space Centre in Kourou French Guiana in a dual payload launch with Intelsat New Dawn atop an Ariane 5 ECA rocket. Yahsat Y1A is based on the Eurostar E3000 satellite bus and had a launch mass of about 6000 kg. It is intended to provide Ku, Ka, and C-band communications to the Middle East, Africa, Europe, and Southwest Asia.
ABS	ABS-7, ABS-2	is a geostationary communication satellite operated by ABS (formerly known as Asia Broadcast Satellite) which was designed and manufactured by Lockheed Martin on the A2100 platform. It featured 30 Ku-band and 3 Ka-band transponders to serve Afghanistan, the Middle East, and Pakistan operating from 116.1EL. In May 2010, the satellite was sold to ABS and renamed ABS-7. Its original name was Koreasat 3. The satellite was de-orbited from the geostationary arc and retired on February 16, 2022.
Arabsat	BADR 7	This also known as Arabsat 6B is a geostationary communications satellite manufactured by Airbus Defense and Space, with its Ku-band and Ka-band communications payload provided by Thales Alenia Space. From its final orbital perch at 26 degrees East longitude, Arabsat 6B will beam hundreds of television channels and broadband services across Africa, the Middle East, and Central Asia for a 15-year mission.
Avanti	HYLAS-3	Launched in August 2019, HYLAS 3 is a steerable cluster of 8 beams that can be steered to anywhere within the 31˚ E coverage zone, providing flexible and high throughput connectivity across EMA and part of Asia.
Eutelsat	W3C, EUTELSAT-3B	EUTELSAT 3B is a tri-band satellite for markets in Europe, Africa, the Middle East, Central Asia, and South America. Located at 3° East, the satellite is optimized for customers operating broadband, data, telecom, and video services in a vast footprint spanning from Brazil to Central Asia.

		With up to 51 transponders, EUTELSAT 3B offers satellite resources in Ku, C, and Ka-band connected to fixed and steerable antennas for maximum flexibility. This enables users to select the most relevant frequency band for different types of services.
Eutelsat / ictQATAR	ES'HAIL	is a Qatari satellite, launched aboard a SpaceX Falcon 9 rocket on November 15, 2018. Es'hail 2 was built by Japan's Mitsubishi Electric company and operates at 26° East longitude along a geostationary orbit to provide direct-to-home television services in the Middle East and North Africa region. The satellite features 24 Ku-band and 11 Ka-band transponders to provide direct broadcasting services for television, government, and commercial content distribution.
Hispasat	Hispasat AG1, Amazonas-3	Amazonas 3 is the first satellite that provides Ka-band to Latin America, which enables it to offer advanced, broadband services that respond to the increasing demand for Internet access solutions and the deployment of initiatives of universalization to difficult-to-access areas. With this new satellite, HISPASAT maintains its privileged leadership position in Brazil and Latin America as well as reinforces its position in the United States.
Inmarsat	Global Xpress F1/F2/F3	Inmarsat-7 is the seventh generation of satellites for the London-based global mobile satellite communications operator Inmarsat. The three satellites called GX7, 8 & 9 will have an improved fully reconfigurable Ka-band payload for the Global Xpress services.
ISRO	G-Sat 14	is an Indian communications satellite launched in January 2014. It replaced the GSAT-3 satellite, which was launched in 2004. GSAT-14 was launched by a Geosynchronous Satellite Launch Vehicle Mk.II, which incorporated an Indian-built cryogenic engine in the third stage.
Measat	Measat -5	MEASAT Satellite Systems Sdn. Bhd, formerly Binariang Satellite Systems Sdn. Bhd is a Malaysian communications satellite operator, which owns and operates the MEASAT (Malaysia East Asia Satellite) and AFRICASAT spacecraft.
NBN Co	NBN-1 / NBN-2	in February 2012 that it has been awarded a contract to provide two high-throughput communications satellites called NBN Co 1A and 1B, that will be used to deliver high-speed broadband service to rural and remote areas of Australia.
NewSat	Jabiru 1	abiru-1 is the first satellite in the series of the Jabiru satellite program, which is intended to provide new and raw capacity coverage to the high-demand communication market. The satellite is being manufactured by Lockheed Martin Commercial Space Systems (LMCSS) and is expected to be launched into the geostationary transfer orbit in the first half of 2015.
O3B Networks Limited	O3b Networks (MEO)	Our O3b MEO constellation operates in the non-geostationary satellite medium earth orbit delivering low-latency, high-performance connectivity worldwide. Our fiber-like managed service enables the delivery of MEF Carrier Ethernet cloud-ready enterprise services.
RSCC	Express AM5 & AM6 & AM7	The Express-AM5 satellite is manufactured on RSCC's order by the JSC "Academician M.F. Reshetnev "Information Satellite Systems" in cooperation with Radio Research and Development Institute (Russia) and MDA Corporation (Canada). The satellite was launched into orbit on

		December 26, 2013. The commercial operation of the satellite started on April 22, 2014.
SES	Astra 2E, ASTRA 2F, ASTRA 2G, ASTRA 4B, ASTRA 5B	in December 2009 SES ordered four multi-mission satellites from Astrium to provide a replacement as well as incremental capacity for its SES ASTRA and SES WORLD SKIES divisions. The new satellites, to be designated Astra 2E, Astra 2F, Astra 2G, and Astra 5B, will allow the release of the existing satellites at two orbital positions (28.2 and 31.5 degrees East) and add new capacity as well as fleet deployment flexibility for the SES group over the coming years. The satellites are scheduled for launch in several steps between 2012 and 2014. The design life of each satellite is 15 years.
Spacecom	Amos 4 & 6	AMOS-4 was initially operated from 67.25° East longitude for in-orbit testing. The satellite is positioned at 65° East longitude in geostationary orbit
Telenor	Thor-7	THOR 7 was launched in 2015. Equipped with Ka payload providing land-based and maritime services. Thor-7 is a commercial Geostationary Communications Satellite operated by Telenor, Norway, and built by Space Systems Loral, California. The satellite carries a Ku/Ka-Band payload to deliver broadband communications to European and surrounding regions.
Turksat	Turksat 4A / Turksat 4B	is a communication satellite in which Turkish technical personnel also took part in its construction. The production and tests of the TÜRKSAT-4B satellite were carried out at the satellite production center of the Japanese Mitsubishi Electric (MELCO) company in Kamakura.
Space X	Starlink	is a satellite internet constellation operated by SpaceX, providing satellite Internet access coverage to 45 countries. It also aims for global mobile phone service after 2023. SpaceX started launching Starlink satellites in 2019. As of December 2022, Starlink consists of over 3,300 mass-produced small satellites in low Earth orbit (LEO), which communicate with designated ground transceivers. In total, nearly 12,000 satellites are planned to be deployed, with a possible later extension to 42,000. SpaceX announced reaching more than one million subscribers in December 2022. The SpaceX satellite development facility in Redmond, Washington houses the Starlink research, development, manufacturing, and orbit control teams. The cost of the decade-long project to design, build, and deploy the constellation was estimated by SpaceX in May 2018 to be at least US$10 billion. SpaceX expects more than $30 billion in revenue by 2025 from its satellite constellation, while revenues from its launch business were expected to reach $5 billion in the same year.

APPENDIX B

CODE SCRIPT FOR THE DESIGNED MODEL USING VB LANGUAGE (FOR SINGLE CHANNEL) (PART OF CODE)

```
'Get Layout Manager.
Dim Lm
Set Lm = Document.GetLayoutMgr
'SCRIPT for Layout 1
'Get Current Layout.
Dim Layout1
Set Layout1 = Lm.GetCurrentLayout
Layout1.Name  = "Layout 1"
 'Set Total Sweep Iterations
Layout1.SetTotalSweepIterations(5)
 'Set Current Sweep Iteration
Layout1.SetCurrentSweepIteration(1)
'Get Current Canvas.
Dim Canvas1
Set Canvas1 = Layout1.GetCurrentCanvas
Canvas1.Height = 5000
Canvas1.Width = 5000
'SCRIPT for Layout global parameters.
Layout1.SetParameterMode "Simulation window", 0
Layout1.SetParameterValue "Simulation window", "Set bit rate"
Layout1.SetParameterValue "Reference bit rate", TRUE
Layout1.SetParameterMode "Bit rate", 0
Layout1.SetParameterValue "Bit rate", 10e+009
Layout1.SetParameterValue "Time window", 0.1024e-006
Layout1.SetParameterValue "Sample rate", 320e+009
Layout1.SetParameterMode "Sequence length", 0
Layout1.SetParameterValue "Sequence length", 1024
Layout1.SetParameterMode "Samples per bit", 0
Layout1.SetParameterValue "Samples per bit", 32
Layout1.SetParameterValue "Symbol rate", 10e+009
Layout1.SetParameterMode "Number of samples", 0
Layout1.SetParameterValue "Number of samples", 32768
Layout1.SetParameterUnit "Reference wavelength", "THz"
Layout1.SetParameterMode "Reference wavelength", 0
Layout1.SetParameterValue "Reference wavelength", 193.1
Layout1.SetParameterValue "Export results to file", FALSE
Layout1.SetParameterMode "Export results options", 0
Layout1.SetParameterValue "Export results options", "Save after each sweep iteration"
Layout1.SetParameterMode "Power unit", 0
Layout1.SetParameterValue "Power unit", "dBm"
Layout1.SetParameterMode "Frequency unit", 0
Layout1.SetParameterValue "Frequency unit", "THz"
'SCRIPT for each component in the Layout.
'SCRIPT for component CW Laser.
Dim Canvas1_Component1
Set Canvas1_Component1 = Canvas1.CreateComponent("CW Laser","{6DA31CEE-058F-11D4-93BD-0050DAB7C5D6}",100,360, 34, 34,0)
Canvas1_Component1.Name  = "CW Laser"
Canvas1_Component1.Cost  = 0.000000
'Set CW Laser parameters.
Canvas1_Component1.SetParameterMode "Frequency", 0
Canvas1_Component1.SetParameterUnit "Frequency", "THz"
Canvas1_Component1.SetParameterValue "Frequency", 193.2
Canvas1_Component1.SetParameterMode "Power", 0
Canvas1_Component1.SetParameterUnit "Power", "dBm"
Canvas1_Component1.SetParameterValue "Power", 14
Canvas1_Component1.SetParameterMode "Linewidth", 0
Canvas1_Component1.SetParameterValue "Linewidth", 0.1
Canvas1_Component1.SetParameterMode "Initial phase", 0
Canvas1_Component1.SetParameterValue "Initial phase", 0
Canvas1_Component1.SetParameterMode "Azimuth", 0
Canvas1_Component1.SetParameterValue "Azimuth", 45
Canvas1_Component1.SetParameterMode "Ellipticity", 0
Canvas1_Component1.SetParameterValue "Ellipticity", 0
Canvas1_Component1.SetParameterMode "Enabled", 0
Canvas1_Component1.SetParameterValue "Enabled", TRUE
Canvas1_Component1.SetParameterMode "Iterations", 3
Canvas1_Component1.SetParameterScript "Iterations", "Iterations"
Canvas1_Component1.SetParameterMode "Parameterized", 3
Canvas1_Component1.SetParameterScript "Parameterized", "Parameterized"
'SCRIPT for component Subsystem.
Dim Canvas1_Component2
Set Canvas1_Component2 = Canvas1.CreateComponent("Subsystem 1.0","{C83C8C01-53FD-11D4-9407-0050DAB7C5D6}",290,320, 162, 120,0)
Canvas1_Component2.Name  = "Subsystem"
Canvas1_Component2.Cost  = 0.000000
Canvas1_Component2.AddPort "Input", 2, 0, 0.204156
Canvas1_Component2.AddPort "Input", 2, 0, 0.412592
Canvas1_Component2.AddPort "Input", 2, 0, 0.742054
Canvas1_Component2.AddPort "Output", 3, 2, 0.381418
Canvas1_Component2.AddPort "Output", 3, 1, 0.170504
Canvas1_Component2.AddPort "Output", 3, 1, 0.279856
Canvas1_Component2.AddPort "Output", 3, 3, 0.170504
Canvas1_Component2.AddPort "Output", 3, 3, 0.306475
'Set Subsystem parameters.
Canvas1_Component2.SetParameterMode "Subsystem Representation", 0
Canvas1_Component2.SetParameterValue "Subsystem Representation", "Default Icon"
Dim Canvas1_2
Set Canvas1_2 = Canvas1_Component2.GetCanvas
Canvas1_2.Height = 1776
Canvas1_2.Width = 1390
Canvas1_Component2.SetPosition 290, 320, 452, 440
'SCRIPT for component OFDM Modulation.
Dim Canvas1_2_Component3
Set Canvas1_2_Component3 = Canvas1_2.CreateComponent("OFDM Modulation","{1CCD3D1F-8E82-4A3E-92B9-1C9C20572BB1}",310,180, 34, 34,0)
Canvas1_2_Component3.Name  = "OFDM Modulation"
Canvas1_2_Component3.Cost  = 0.000000
'Set OFDM Modulation parameters.
Canvas1_2_Component3.SetParameterMode "Maximum possible subcarriers", 0
Canvas1_2_Component3.SetParameterValue "Maximum possible subcarriers", 128
Canvas1_2_Component3.SetParameterMode "Symmetric spectrum", 0
Canvas1_2_Component3.SetParameterValue "Symmetric spectrum", FALSE
```

```
Canvas1_2_Component3.SetParameterMode "Cyclic prefix", 0
Canvas1_2_Component3.SetParameterValue "Cyclic prefix", "Symbol extension"
Canvas1_2_Component3.SetParameterMode "Number of prefix points", 0
Canvas1_2_Component3.SetParameterValue "Number of prefix points", 10
Canvas1_2_Component3.SetParameterMode "Average OFDM power", 0
Canvas1_2_Component3.SetParameterUnit "Average OFDM power", "dBm"
Canvas1_2_Component3.SetParameterValue "Average OFDM power", 15
Canvas1_2_Component3.SetParameterMode "Number of input ports (users)", 0
Canvas1_2_Component3.SetParameterValue "Number of input ports (users)", 1
Canvas1_2_Component3.SetParameterMode "Number of subcarriers per port", 0
Canvas1_2_Component3.SetParameterValue "Number of subcarriers per port", "80"
Canvas1_2_Component3.SetParameterMode "Subcarrier locations", 0
Canvas1_2_Component3.SetParameterValue "Subcarrier locations", "25-104"
Canvas1_2_Component3.SetParameterMode "Subcarrier phases", 0
Canvas1_2_Component3.SetParameterValue "Subcarrier phases", "0"
Canvas1_2_Component3.SetParameterMode "Equalize port powers", 0
Canvas1_2_Component3.SetParameterValue "Equalize port powers", TRUE
Canvas1_2_Component3.SetParameterMode "Dual polarization", 0
Canvas1_2_Component3.SetParameterValue "Dual polarization", TRUE
Canvas1_2_Component3.SetParameterMode "Polarization", 0
Canvas1_2_Component3.SetParameterValue "Polarization", "X"
Canvas1_2_Component3.SetParameterMode "Number of training symbols", 0
Canvas1_2_Component3.SetParameterValue "Number of training symbols", 10
'SCRIPT for component OFDM Modulation_1.
Dim Canvas1_2_Component4
Set Canvas1_2_Component4 = Canvas1_2.CreateComponent("OFDM Modulation","{1CCD3D1F-8E82-4A3E-92B9-1C9C20572BB1}",310,590, 34, 34,0)
Canvas1_2_Component4.Name  = "OFDM Modulation_1"
Canvas1_2_Component4.Cost  = 0.000000
'Set OFDM Modulation_1 parameters.
Canvas1_2_Component4.SetParameterMode "Maximum possible subcarriers", 0
Canvas1_2_Component4.SetParameterValue "Maximum possible subcarriers", 128
Canvas1_2_Component4.SetParameterMode "Symmetric spectrum", 0
Canvas1_2_Component4.SetParameterValue "Symmetric spectrum", FALSE
Canvas1_2_Component4.SetParameterMode "Cyclic prefix", 0
Canvas1_2_Component4.SetParameterValue "Cyclic prefix", "Symbol extension"
Canvas1_2_Component4.SetParameterMode "Average OFDM power", 0
Canvas1_2_Component4.SetParameterUnit "Average OFDM power", "dBm"
Canvas1_2_Component4.SetParameterValue "Average OFDM power", 15
Canvas1_2_Component4.SetParameterMode "Number of input ports (users)", 0
Canvas1_2_Component4.SetParameterValue "Number of input ports (users)", 1
Canvas1_2_Component4.SetParameterMode "Number of subcarriers per port", 0
Canvas1_2_Component4.SetParameterValue "Number of subcarriers per port", "80"
Canvas1_2_Component4.SetParameterMode "Subcarrier locations", 0
Canvas1_2_Component4.SetParameterValue "Subcarrier locations", "25-104"
Canvas1_2_Component4.SetParameterMode "Subcarrier phases", 0
Canvas1_2_Component4.SetParameterValue "Equalize port powers", TRUE
Canvas1_2_Component4.SetParameterMode "Dual polarization", 0
Canvas1_2_Component4.SetParameterValue "Dual polarization", TRUE
Canvas1_2_Component4.SetParameterMode "Polarization", 0
Canvas1_2_Component4.SetParameterValue "Polarization", "Y"
Canvas1_2_Component4.SetParameterMode "Number of training symbols", 0
Canvas1_2_Component4.SetParameterValue "Number of training symbols", 10
'SCRIPT for component Serial To Parallel Converter 1xN.
Dim Canvas1_2_Component5
Set Canvas1_2_Component5 = Canvas1_2.CreateComponent("Serial To Parallel Converter 1xN","{498E720E-4E63-48CA-BF47-0A19891A9A5F}",70,380, 34, 50,0)
Canvas1_2_Component5.Name  = "Serial To Parallel Converter 1xN"
Canvas1_2_Component5.Cost  = 0.000000
'Set Serial To Parallel Converter 1xN parameters.
Canvas1_2_Component5.SetParameterMode "Number of output ports", 0
Canvas1_2_Component5.SetParameterValue "Number of output ports", 2
'SCRIPT for component Polarization Splitter.
Dim Canvas1_2_Component6
Set Canvas1_2_Component6 = Canvas1_2.CreateComponent("Polarization Splitter","{F11D0C07-3C7D-11D4-93F0-0050DAB7C5D6}",460,390, 34, 34,0)
Canvas1_2_Component6.Name  = "Polarization Splitter"
Canvas1_2_Component6.Cost  = 0.000000
'Set Polarization Splitter parameters.
Canvas1_2_Component6.SetParameterMode "Device angle", 0
Canvas1_2_Component6.SetParameterUnit "Device angle", "deg"
Canvas1_2_Component6.SetParameterValue "Device angle", 0
Canvas1_2_Component6.SetParameterMode "Enabled", 0
Canvas1_2_Component6.SetParameterValue "Enabled", TRUE
'SCRIPT for component QAM Sequence Generator.
Dim Canvas1_2_Component7
Set Canvas1_2_Component7 = Canvas1_2.CreateComponent("QAM Sequence Generator","{4462750B-F858-42BB-A415-994DFE4D44BD}",170,190, 34, 34,0)
Canvas1_2_Component7.Name  = "QAM Sequence Generator"
'Set QAM Sequence Generator parameters.
Canvas1_2_Component7.SetParameterMode "Bits per symbol (b/sym)", 0
Canvas1_2_Component7.SetParameterValue "Bits per symbol (b/sym)", 4
Canvas1_2_Component7.SetParameterMode "Constellation type", 0
Canvas1_2_Component7.SetParameterValue "Constellation type", "Square/Rectangular"
Dim Canvas1_2_Component7_0100000705000005_arrCol(2)
Canvas1_2_Component7_0100000705000005_arrCol(0) = "Bit seq"
Canvas1_2_Component7_0100000705000005_arrCol(1) = "I (a.u.)"
Canvas1_2_Component7_0100000705000005_arrCol(2) = "Q (a.u.)"
Canvas1_2_Component7.SetParameterValueMxN "I-Q amplitudes (a.u.)", Canvas1_2_Component7_0100000705000005_arrMxN, Canvas1_2_Component7_0100000705000005_arrCol, 0
Canvas1_2_Component7.SetParameterMode "I-Q amplitudes file name", 0
Canvas1_2_Component7.SetParameterValue "I-Q amplitudes file name", "QAM_IQ.dat"
'SCRIPT for component QAM Sequence Generator_1.
Dim Canvas1_2_Component8
Set Canvas1_2_Component8 = Canvas1_2.CreateComponent("QAM Sequence Generator","{4462750B-F858-42BB-A415-994DFE4D44BD}",170,590, 34, 34,0)
Canvas1_2_Component8.Name  = "QAM Sequence Generator_1"
'Set QAM Sequence Generator_1 parameters.
Canvas1_2_Component8.SetParameterMode "Bits per symbol (b/sym)", 0
Canvas1_2_Component8.SetParameterValue "Bits per symbol (b/sym)", 4
Canvas1_2_Component8.SetParameterMode "Constellation type", 0
Canvas1_2_Component8.SetParameterValue "Constellation type", "Square/Rectangular"
Dim Canvas1_2_Component8_0100000805000005_arrCol(2)
Canvas1_2_Component8_0100000805000005_arrCol(0) = "Bit seq"
Canvas1_2_Component8_0100000805000005_arrCol(1) = "I (a.u.)"
Canvas1_2_Component8_0100000805000005_arrCol(2) = "Q (a.u.)"
Canvas1_2_Component8.SetParameterValueMxN "I-Q amplitudes (a.u.)", Canvas1_2_Component8_0100000805000005_arrMxN, Canvas1_2_Component8_0100000805000005_arrCol, 0
Canvas1_2_Component8.SetParameterMode "I-Q amplitudes file name", 0
Canvas1_2_Component8.SetParameterValue "I-Q amplitudes file name", "QAM_IQ.dat"
'SCRIPT for component Fork 1x2.
Dim Canvas1_2_Component9
Set Canvas1_2_Component9 = Canvas1_2.CreateComponent("Fork 1x2","{E138711F-3E0D-11D4-93F3-0050DAB7C5D6}",700,80, 32, 32,0)
Canvas1_2_Component9.Name  = "Fork 1x2"
Canvas1_2_Component9.Cost  = 0.000000
'Set Fork 1x2 parameters.
'SCRIPT for component LiNb Mach-Zehnder Modulator.
Dim Canvas1_2_Component10
Set Canvas1_2_Component10 = Canvas1_2.CreateComponent("LiNb Mach-Zehnder Modulator","{6DA31CEE-058F-11D4-93BD-0050DAB7C5D6}",820,80, 34, 34,0)
Canvas1_2_Component10.Name  = "LiNb Mach-Zehnder Modulator"
Canvas1_2_Component10.Cost  = 0.000000
'Set LiNb Mach-Zehnder Modulator parameters.
Canvas1_2_Component10.SetParameterMode "Extinction ratio", 3
```

```
Canvas1_2_Component10.SetParameterScript "Extinction ratio", "ER"
'SCRIPT for component Optical Null.
Dim Canvas1_2_Component11
Set Canvas1_2_Component11 = Canvas1_2.CreateComponent("Optical Null","{E138711F-3E0D-11D4-93F3-0050DAB7C5D6}",640,250, 16, 16,0)
Canvas1_2_Component11.Name  = "Optical Null"
Canvas1_2_Component11.Cost  = 0.000000
'Set Optical Null parameters.
Canvas1_2_Component11.SetParameterMode "Iterations", 3
Canvas1_2_Component11.SetParameterScript "Iterations", "Iterations"
'SCRIPT for component X Coupler.
Dim Canvas1_2_Component12
Set Canvas1_2_Component12 = Canvas1_2.CreateComponent("X Coupler","{F11D0C07-3C7D-11D4-93F0-0050DAB7C5D6}",700,190, 32, 32,0)
Canvas1_2_Component12.Name  = "X Coupler"
Canvas1_2_Component12.Cost  = 0.000000
'Set X Coupler parameters.
Canvas1_2_Component12.SetParameterMode "Coupling coefficient", 0
Canvas1_2_Component12.SetParameterValue "Coupling coefficient", 0.5
Canvas1_2_Component12.SetParameterMode "Additional loss", 0
Canvas1_2_Component12.SetParameterValue "Additional loss", 1
Canvas1_2_Component12.SetParameterMode "Conjugate", 0
Canvas1_2_Component12.SetParameterValue "Conjugate", TRUE
Canvas1_2_Component12.SetParameterMode "Cost", 0
Canvas1_2_Component12.SetParameterValue "Cost", 0
Canvas1_2_Component12.SetParameterMode "Order number", 0
Canvas1_2_Component12.SetParameterValue "Order number", ""
Canvas1_2_Component12.SetParameterMode "Description", 0
Canvas1_2_Component12.SetParameterValue "Description", ""
Canvas1_2_Component12.SetParameterMode "Include in bill of sale", 0
Canvas1_2_Component12.SetParameterValue "Include in bill of sale", TRUE
'SCRIPT for component Fork 1x2_1.
Dim Canvas1_2_Component13
Set Canvas1_2_Component13 = Canvas1_2.CreateComponent("Fork 1x2","{E138711F-3E0D-11D4-93F3-0050DAB7C5D6}",700,280, 32, 32,0)
Canvas1_2_Component13.Name  = "Fork 1x2_1"
Canvas1_2_Component13.Cost  = 0.000000
'Set Fork 1x2_1 parameters.
'SCRIPT for component LiNb Mach-Zehnder Modulator_1.
Dim Canvas1_2_Component14
Set Canvas1_2_Component14 = Canvas1_2.CreateComponent("LiNb Mach-Zehnder Modulator","{6DA31CEE-058F-11D4-93BD-0050DAB7C5D6}",820,290, 34, 34,0)
Canvas1_2_Component14.Name  = "LiNb Mach-Zehnder Modulator_1"
Canvas1_2_Component14.Cost  = 0.000000
'Set LiNb Mach-Zehnder Modulator_1 parameters.
Canvas1_2_Component14.SetParameterMode "Extinction ratio", 3
Canvas1_2_Component14.SetParameterScript "Extinction ratio", "ER"
'SCRIPT for component Electrical Gain.
Dim Canvas1_2_Component15
Set Canvas1_2_Component15 = Canvas1_2.CreateComponent("Electrical Gain","{1CCD3D1F-8E82-4A3E-92B9-1C9C20572BB1}",600,70, 16, 16,0)
Canvas1_2_Component15.Name  = "Electrical Gain"
Canvas1_2_Component15.Cost  = 0.000000
'Set Electrical Gain parameters.
Canvas1_2_Component15.SetParameterMode "Gain", 3
Canvas1_2_Component15.SetParameterScript "Gain", "Gain"
Canvas1_2_Component15.SetParameterMode "Enabled", 0
Canvas1_2_Component15.SetParameterValue "Enabled", TRUE
Canvas1_2_Component15.SetParameterMode "Cost", 0
Canvas1_2_Component15.SetParameterValue "Cost", 0
Canvas1_2_Component15.SetParameterMode "Order number", 0
Canvas1_2_Component15.SetParameterValue "Order number", ""
Canvas1_2_Component15.SetParameterMode "Description", 0
Canvas1_2_Component15.SetParameterValue "Description", ""
Canvas1_2_Component15.SetParameterMode "Include in bill of sale", 0
Canvas1_2_Component15.SetParameterValue "Include in bill of sale", TRUE
'SCRIPT for component Electrical Gain_1.
Dim Canvas1_2_Component16
Set Canvas1_2_Component16 = Canvas1_2.CreateComponent("Electrical Gain","{1CCD3D1F-8E82-4A3E-92B9-1C9C20572BB1}",610,320, 16, 16,0)
Canvas1_2_Component16.Name  = "Electrical Gain_1"
Canvas1_2_Component16.Cost  = 0.000000
'Set Electrical Gain_1 parameters.
Canvas1_2_Component16.SetParameterMode "Gain", 3
Canvas1_2_Component16.SetParameterScript "Gain", "Gain"
Canvas1_2_Component16.SetParameterMode "Enabled", 0
Canvas1_2_Component16.SetParameterValue "Enabled", TRUE
Canvas1_2_Component16.SetParameterMode "Cost", 0
Canvas1_2_Component16.SetParameterValue "Cost", 0
Canvas1_2_Component16.SetParameterMode "Order number", 0
Canvas1_2_Component16.SetParameterValue "Order number", ""
Canvas1_2_Component16.SetParameterMode "Description", 0
Canvas1_2_Component16.SetParameterValue "Description", ""
Canvas1_2_Component16.SetParameterMode "Include in bill of sale", 0
Canvas1_2_Component16.SetParameterValue "Include in bill of sale", TRUE
'SCRIPT for component Electrical Gain_2.
Dim Canvas1_2_Component17
Set Canvas1_2_Component17 = Canvas1_2.CreateComponent("Electrical Gain","{1CCD3D1F-8E82-4A3E-92B9-1C9C20572BB1}",780,170, 16, 16,0)
Canvas1_2_Component17.Name  = "Electrical Gain_2"
Canvas1_2_Component17.Cost  = 0.000000
'Set Electrical Gain_2 parameters.
Canvas1_2_Component17.SetParameterMode "Gain", 0
Canvas1_2_Component17.SetParameterValue "Gain", -1
Canvas1_2_Component17.SetParameterMode "Enabled", 0
Canvas1_2_Component17.SetParameterValue "Enabled", TRUE
Canvas1_2_Component17.SetParameterMode "Cost", 0
Canvas1_2_Component17.SetParameterValue "Cost", 0
Canvas1_2_Component17.SetParameterMode "Order number", 0
Canvas1_2_Component17.SetParameterValue "Order number", ""
Canvas1_2_Component17.SetParameterMode "Description", 0
Canvas1_2_Component17.SetParameterValue "Description", ""
Canvas1_2_Component17.SetParameterMode "Include in bill of sale", 0
Canvas1_2_Component17.SetParameterValue "Include in bill of sale", TRUE
'SCRIPT for component Electrical Gain_3.
Dim Canvas1_2_Component18
Set Canvas1_2_Component18 = Canvas1_2.CreateComponent("Electrical Gain","{1CCD3D1F-8E82-4A3E-92B9-1C9C20572BB1}",790,360, 16, 16,0)
Canvas1_2_Component18.Name  = "Electrical Gain_3"
Canvas1_2_Component18.Cost  = 0.000000
'Set Electrical Gain_3 parameters.
Canvas1_2_Component18.SetParameterMode "Gain", 0
Canvas1_2_Component18.SetParameterValue "Gain", -1
Canvas1_2_Component18.SetParameterMode "Enabled", 0
Canvas1_2_Component18.SetParameterValue "Enabled", TRUE
Canvas1_2_Component18.SetParameterMode "Cost", 0
Canvas1_2_Component18.SetParameterValue "Cost", 0
Canvas1_2_Component18.SetParameterMode "Order number", 0
Canvas1_2_Component18.SetParameterValue "Order number", ""
Canvas1_2_Component18.SetParameterMode "Description", 0
Canvas1_2_Component18.SetParameterValue "Description", ""
Canvas1_2_Component18.SetParameterMode "Include in bill of sale", 0
Canvas1_2_Component18.SetParameterValue "Include in bill of sale", TRUE
'SCRIPT for component X Coupler_1.
```

APPENDIX C

OPTISYSTEM COMPONENTS TERMINOLOGY (TOOLS USED TO FORM THE PROPOSED NOVEL SYSTEM)

Tool symbol	Tool name	Tool Function
	CW Laser	Generates a continuous wave (CW) optical signal.
	Dual Port MZ Modulator Measured	This component simulates a Mach-Zehnder modulator based on measured parameters.
	Electrical Gain	Ideal gain element.
	Fork 1x2	Copies the input signal into two output signals. This tool allows you to duplicate component output ports.
	Hermite Transverse Mode Generator	This component attaches Hermite-Gaussian transverse mode profiles to the input signal. It also converts single-mode signals into multimode signals.
	Ideal Mux	Multiplexers a user-defined number of inputs WDM signal channels. This model is equivalent to an ideal adder since there is no power splitting and filtering.
	Low Pass Rectangle Filter	Optical filter with a rectangle frequency transfer function.
	OFDM Modulation	This component modulates a digital signal into multiple orthogonal sub-carriers.
	Phase Shift	Adds a time phase advance/delay to the optical signal input.
	Polarization Combiner	Simulates a polarization combiner.
	Polarization Splitter	Simulates a polarization splitter.
	Power Splitter 1x2	Ideal power splitter — splits an optical input signal into two output signals.
	QAM Sequence Generator	Generates two parallel M-ary symbol sequences from binary signals using quadrature amplitude modulation (QAM).
	Serial To Parallel Converter 1xN	Converts the input sequence at bit rate R into N output sequences at R/N bit rate.
	WDM Mux	Multiplexes a user-defined number of input WDM signal channels.

	X Coupler	Cross coupler for combining or splitting optical signals.
	OWC Channel	This component models an optical wireless communication (OWC) channel. It is a subsystem of two telescopes and the wireless communication channel between them. It is best suited for the modeling of satellite-satellite and earth-satellite links
	Optical Amplifier	Allows pre-defined operational condition amplifier design, including EDFAs. Gain, noise figure, and amplifier output power can be predetermined.
	BER Test Set	This component generates a big bit sequence, transmits it to DUT, and compares the received bit sequence to the broadcast one.
	Electrical Amplifier	Electrical amplifier with additive thermal noise.
	Electrical Subtractor	Subtracts the input electrical signals.
	OFDM Demodulation Dual Polarization	This component demodulates the OFDM signal into a digital M-ary signal. It is specifically designed to be used for OFDM systems with dual polarization multiplexing.
	Optical Null	Generates a zero-value optical signal.
	Parallel To Serial Converter Nx1	Combine N input sequences at bit rate R into one output sequence at N x R bit rate.
	Photodiode PIN	The PIN Photodiode component is used to convert an optical signal into an electrical current based on the device‘s Responsivity.
	QAM Sequence Decoder	Decodes two parallel QAM M-ary symbol sequences to a binary signal.
	Spatial Demultiplexer	The Spatial Demultiplexer component first de-multiplexes a user-defined number of WDM spatial signal channels and then separates out all spatial modes associated with each channel
	WDM DEMUX	Demultiplexes a user-defined number of WDM signal channels.

APPENDIX D

PUBLICATIONS

1- Paper title "The channel WDM system incorporates of Optical Wireless Communication (OWC) hybrid MDM-PDM for higher capacity (LEO-GEO) inter satellite link" published in Optik Journal, SCI close access, free of charge, Elsevier, https://www.sciencedirect.com/science/article/abs/pii/S0030402622017077

2- Paper title "Implementation of 2D Ray SBR Modeling for different MIMO Antenna Array placement in Outdoor communication using Wireless InSite software" Published in research square, https://www.researchsquare.com/article/rs-2487125/v1

3- Paper title "Design and Analysis of 50 Channel by 40 Gbps DWDM-RoF System for 5G Communication Based on Fronthaul Scenario", published in Springer nature Lecture, Notes in Networks and Systems book series (LNNS, volume 479), https://link.springer.com/chapter/10.1007/978-981-19-3148-2_9

4- Book title "Satellite Communication for Different Orbits Allocation Steps to Design and Model an Is-OWC system", Scholars' Press, ISBN 978-620-5-52113-7, https://my.scholars-press.com/catalogue/details/gb/978-620-5-52113-7/satellite-communication-for-different-orbits-allocation.

5- Book title "Optisystem Program for Various Fiber Optic Modeling Learning Optisystem for Beginner", LAB publisher, ISBN 978-620-5-52784-9, https://www.lap-publishing.com/catalog/details//store/ru/book/978-620-5-52784-9/optisystem-program-for-various-fiber-optic-modeling

6- Paper title "The Utilization of Different AI Methods-based Satellite Communications: A Survey", published in AIP, 3rd International Conference on Engineering and Science, Scopus, Q3.

7- Paper title "Implementation of Two Polarization DQPSK WDM Is-OWC System with Different Precoding Schemes for Long-Reach GEO Inter Satellite Link", published in IET & IEEE explorer, International Conference on Green Energy, Computing and Intelligent Technology (GEn-CITy 2023), Malaysia, Scopus, Q3.